2002

SOLVENT-RESISTANT NANOFILTRATION MEMBRANES: SEPARATION STUDIES AND MODELING

Dharmesh S. Bhanushali
University of Kentucky, dsbhan0@uky.edu

ABSTRACT OF DISSERTATION

Dharmesh S. Bhanushali

The Graduate School

University of Kentucky

2002

SOLVENT-RESISTANT NANOFILTRATION MEMBRANES: SEPARATION STUDIES AND MODELING

ABSTRACT OF DISSERTATION

A dissertation submitted in partial fulfillment of the
requirements for the degree of Doctor of Philosophy in the
College of Engineering
at the University of Kentucky

By

Dharmesh S. Bhanushali

Lexington, Kentucky

Director: Dr. Dibakar Bhattacharyya, Alumni Professor of Chemical Engineering

Lexington, Kentucky

2002

ABSTRACT OF DISSERTATION

SOLVENT-RESISTANT NANOFILTRATION MEMBRANES: SEPARATION STUDIES AND MODELING

The primary focus of the research is to extend the principles of Nanofiltration (NF) to non-aqueous systems using solvent-resistant NF membranes. Several different levels of interaction are introduced when organic solvents are used with polymeric membranes and thus quantification of polymer-solvent interactions is critical. Pure solvent permeation studies were conducted to understand the mechanism of solvent transport through polymeric membranes. Different membrane materials (hydrophilic and hydrophobic) as well as different solvents (polar and non-polar) were used for the study. For example, hexane flux at 13 bar through a hydrophobic silicone based NF membrane was ~ 0.6×10^{-4} cm^3/cm^2. s. and that through a hydrophilic aromatic polyamide based NF membrane was ~ 6×10^{-4} cm^3/cm^2. s. A simple model based on a solution-diffusion approach which uses solvent physical properties (molar volume, viscosity) and membrane properties (surface energy, etc) is used for correlating the pure solvent permeation through hydrophobic polymeric membranes.

Solute transport studies were performed using organic dyes and triglycerides in polar and non-polar solvents. For example, the rejection of Sudan IV (384 MW organic dye) in n-hexane medium is about 25 % at 15 bar and that in methanol is about –10 % at about 20 bar for a hydrophobic (PDMS-based) membrane. However, for a hydrophilic polyamide based NF membrane, the direction of separation is reversed (86 % in methanol and 43 % in n-hexane). From our experimental data with two types of membranes it is clear that coupling of the solute and solvent fluxes cannot be neglected. Two traditional transport theories (Spiegler-Kedem and Surface Force-Pore Flow model) that consider coupling were evaluated with literature and our experimental solute permeation data. A model based on a fundamental chemical potential gradient approach has been proposed for explaining solute separation. The model uses solute, solvent and membrane physical properties and uses the Flory-Huggins and UNIFAC theories as activity coefficient models. This model has been used to obtain a correlation for the diffusion coefficients of solutes in hexane through a hydrophobic membrane. This correlation along with convective coupling can be used to predict separation behavior for different solutes and at different temperatures.

KEYWORDS: Nanofiltration, non-aqueous, convective coupling, solute transport

(Dharmesh S. Bhanushali)

September 15th 2002
(Date)

SOLVENT-RESISTANT NANOFILTRATION MEMBRANES: SEPARATION STUDIES AND MODELING

By

Dharmesh S. Bhanushali

D. Bhattacharyya
(Director of Dissertation)

D. Bhattacharyya
(Director of Graduate Studies)

September 15th 2002
(Date)

RULES FOR THE USE OF DISSERTATIONS

Unpublished theses submitted for the Doctor's degrees and deposited in the University of Kentucky Library are as a rule open for inspection, but are to be used only with due regard to the rights of the authors. Bibliographical references may be noted, but quotations or summaries of parts may be published only with the permission of the author, and with the usual scholarly acknowledgments.

Extensive copying or publication of the thesis in whole or in part also requires the consent of the Dean of the Graduate School of the University of Kentucky.

Name and Address	Date

DISSERTATION

Dharmesh S. Bhanushali

The Graduate School

University of Kentucky

2002

SOLVENT-RESISTANT NANOFILTRATION MEMBRANES: SEPARATION STUDIES AND MODELING

DISSERTATION

A dissertation submitted in partial fulfillment of the
requirements for the degree of Doctor of Philosophy in the
College of Engineering
at the University of Kentucky

By

Dharmesh S. Bhanushali

Lexington, Kentucky

Director: Dr. Dibakar Bhattacharyya, Alumni Professor of Chemical Engineering

Lexington, Kentucky

2002

ACKNOWLEDGEMENTS

Several people have been instrumental in my success as a Ph.D. student and I am extremely grateful for their support. First and foremost, I would like to thank my advisor, Dr. Dibakar Bhattacharyya for his guidance throughout the last four years. His enthusiasm for research kept me motivated and looking forward at all times during my stay as a graduate student. I would specially like to mention how important his encouragement to go to conferences and meet different people has helped me in shaping my personality. I would also like to thank the Kentucky Research Challenge Trust Fund for awarding me a fellowship during my first year as a graduate student at the University of Kentucky. I would also like to extend my gratitude towards Dr. Steve Kloos from Osmonics, Inc. and his research team in Minnetonka, MN. In particular I would like to mention Brian Rudie, C. J. Kurth, Patrick Levy and Ismail Ferrer for their support during my internship. I would also like to acknowledge NIST-ATP (Cooperative Agreement Number 70NANB8H4028), GlaxoSmithKline and NIEHS for their partial support to the research projects. On the personal level, I would like to thank all my colleagues past and present who have always made DB's lab a fun place to work. Last but not the least, I would like to extend my deepest gratitude to my parents and siblings for supporting me and having faith in me throughout my dissertation research.

TABLE OF CONTENTS

LIST OF TABLES

LIST OF FIGURES

LIST OF FILES

FILENAME	TYPE	SIZE (KB)
1. DISSERTATION	PDF	1,600

CHAPTER ONE

Introduction

Liquid separations are encountered commonly in the chemical, pharmaceutical and food industries. Unit-operations like distillation and liquid-liquid extraction are some of the popular traditional technologies employed in treating such liquid mixtures. However, increased energy and downstream processing costs have forced several industries to spend research dollars towards development of more efficient and less energy-intensive processes. This has led to the development and use of separation processes involving membranes which operate at much milder operating conditions as compared to traditional chemical engineering unit-operations. Such membrane-based processes can be classified into several categories depending on the type of driving force. The most common driving forces encountered are Pressure (Reverse Osmosis (RO), Nanofiltration (NF), Ultrafiltration (UF), Microfiltration (MF)); concentration (Pervaporation, Vapor Permeation, Gas Permeation, Dialysis) and electrical (Electrodialysis).

Reverse Osmosis (RO) is one of the most widely used membrane processes in the industry. It is a relatively new (1950s) separation technique compared to established technologies like distillation and extraction. The process dates back to the 50s when Loeb and Sourirajan made the first cellulose acetate RO membrane at UCLA [Sourirajan et al, 1985]. Since then, membrane manufacture has seen several modifications beginning from the classical asymmetric membrane structure to the modern thin film composite structure. Salt rejections (monolvalent ions, e.g. sodium chloride) for a typical

RO membrane would be in excess of 99.5 % (0.1 wt. % feed concentration) at operating pressures of > 1000 psi. Because of the extremely high separation efficiency, RO membranes are commonly employed in desalination applications and as a part of hybrid processes to treat process water. Typical materials used for RO membranes include cellulose acetate, aromatic polyamide etc. Several researchers have performed characterization studies on such RO membrane materials and have concluded that these membranes do not possess a well-defined pore structure, thus making species diffusion the most prevalent transport mechanism.

Nanofiltration (NF) is a recently evolved membrane process and has gained popularity as a treatment option for aqueous streams because of the versatile nature of its transport mechanisms (diffusion, convection and electromigration). NF membranes have higher surface charge density and slightly open membrane morphology as compared to dense RO membranes. As a result, the separation efficiency of such membranes is lower (for monovalent ions like Cl^-) as compared to RO membranes. The advantage, however, is that NF can be operated at much lower operating pressures to give similar fluxes. Typical membrane separation efficiency is reported in terms of divalent ion rejections in excess of 99 % at operating pressures of > 600 psi. The separation efficiency of NF is between RO and ultrafiltration (UF, separation mechanism is primarily size exclusion). Typical NF membrane materials include polyamide, polyethersulfone (PES), polypiperazine etc. Research efforts are being targeted towards surface modification of the base polymer to cause surface charge density variations which enhance water flux and improve the separation efficiency of such NF membrane materials.

Several transport models have been proposed for the aforementioned RO/NF processes and they can be classified into three broad categories: solution-diffusion based models, pore-flow based models and irreversible thermodynamics based models. The solution-diffusion based models [Lonsdale et al, 1965] are widely used in the literature and the premise of the model, as the name suggests, is a combination of "solution" of the species followed by diffusion through the membrane. The pore flow models, proposed by Sourirajan et al [1985], assume that the membrane is made of angstrom-diameter pores and the major species (water) preferentially moves (or diffuses) through the membrane. There are several modifications of this model proposed and used widely in literature [Mehdizadeh et al, 1991, 1993]. The third category involves the irreversible thermodynamics theory [Kedem and Katchalsky, 1958; Jagur-Grodzinski and Kedem, 1966] which considers the membrane as a black-box and uses phenomenological equations to explain solute and solvent transport.

RO and NF processes suffer from a major disadvantage: they can be employed only with dilute feed streams. Currently, RO/NF are being used exclusively for the purification of aqueous streams ranging from semiconductors to drinking water to food processing to pharmaceuticals. Several researchers [Sourirajan, 1964; Paul et al, 1970] envisioned using these processes for treating non-aqueous liquid mixtures. Extension of the principles of aqueous solutions to non-aqueous (organic) mixtures is not straightforward considering the enormity of the solvents that are employed in commercial applications. Organic solvents could range from alcohols to alkanes to ketones to esters. These solvents have varying levels of hydrophilicity and hydrophobicity which causes difficulty for the development of polymeric materials for their selective transport . One of

the major impediments that can be visualized for an extension of these processes to non-aqueous systems is the availability of solvent-resistant membrane materials. With the recent advancement in polymer chemistry and materials processing, it has become possible to synthesize and manufacture solvent-resistant membrane materials that can withstand harsh solution conditions. Such an extension holds tremendous potential for the food and pharmaceutical industries where stringent federal and environmental regulations require high purity of the final product. Use of membrane processes would also reduce the energy and downstream processing costs involved in distillation and extraction respectively. Thus, the current impetus is towards the development of such high flux-low pressure NF membrane materials which are more thermally and chemically resistant to significantly improve process applicability and economics.

Objectives:

With the aforementioned comments in mind, there is a strong motivation to extend the principles of these established membrane processes (RO/NF) to non-aqueous systems which will be the main focus of the research. The broad objectives can be outlined as follows:

a) Understand the separation characteristics of target organic solutes through solvent-resistant membranes in organic media.
b) Explore the extension of literature transport theories for aqueous systems and develop a comprehensive transport model to rationalize solute separation behavior in such membranes.

The research focused on a systematic approach towards the above broad objectives. The membranes used for the above study were mainly polyamide-based (hydrophilic) and polydimethyl siloxane-based (PDMS, hydrophobic). Some of the specific research objectives were as follows:

1. Understand the pure solvent permeation behavior through RO/NF polymeric membranes of different characteristics (hydrophilic, hydrophobic) using solvents with varying properties (polarity, size, viscosity).
2. Develop and experimentally verify a pure solvent permeation model based on a simple chemical potential gradient-based approach to predict the transport of pure solvents through hydrophobic polymeric membranes.
3. Extend the developed model to different types of membranes (polar and non-polar) using membrane properties measured from independent experiments.
4. Understand the solute transport behavior in non-aqueous medium using different organic marker molecules with varying degrees of hydrophilicity/hydrophobicity having solubility in the organic solvents of interest (polar and non-polar) for permeation studies.
5. Extend existing transport theories (e.g. Solution-Diffusion model, Spiegler - Kedem Model and pore model) to non-aqueous systems using literature and our experimental studies.
6. Develop a transport theory using a simple chemical potential gradient–based approach combined with suitable activity coefficient theories (Flory-Huggins, UNIFAC etc.) to rationalize the separation mechanism through polymeric membranes.

CHAPTER TWO

Theory and Background

Reverse Osmosis (RO) emerged as a separation technology in the mid 1960's and has matured over the past few decades as one of the most widely used process for water treatment. Since its conception, RO has come a long way and is being used in several hybrid processes for the removal of salts and organics present in dilute aqueous streams. Since RO membranes are considered as dense films (no pore structure), the primary mechanism of transport in dense RO membranes is diffusion and the principle of separation is the differences in the diffusion coefficients of the permeating species. Nanofiltration (NF) on the other hand uses membranes with a slightly open morphology as compared to dense RO membranes. NF membranes are typically charged and thus possess versatility in transport mechanisms (diffusion, convection and Donnan exclusion). The water permeability values for NF membranes are typically higher than RO. With NF, the selective separation possibilities (such as moderate MW organics from high concentration NaCl solution) are very advantageous over RO.

On the theoretical level, there have been several transport theories proposed for RO/NF processes over the past few years, however, there is little consensus about the universal applicability of one transport model. The models developed differ primarily in the physical interpretation of the transport mechanism, but fitted parameters are typically used to explain experimental observations. Most of the traditional transport theories were developed for a general solvent case, but since water was the most common solvent, these theories have been used for aqueous systems.

The possibility of extension of these principles to non-aqueous medium is going to be the focus of this work. In non-aqueous medium, several different levels of complexity are introduced to the problem because of the differences in the physical properties of the organic solvents. This section will concentrate on a systematic approach to extend the principles of RO/NF to non-aqueous systems beginning with some basic definitions of the reverse osmosis process. This section will also comprise of a brief review of traditional transport theories.

2.1 Definition of Reverse Osmosis:

The process of reverse osmosis can be visualized by comparing it with osmosis as shown in Figure 2.1. Figure 2.1a shows two solutions separated by a semi-permeable membrane. The left side contains, for example, a dilute salt solution in water indicated by the black dots and the right side contains a higher concentration of the same salt in water. This difference in salt concentration induces the driving force for the transport of water from the left-hand side to the right-hand side. After equilibration is allowed, the level of the solution on the right side rises by an amount equal to the osmotic pressure ($\Delta\pi$) of the salt solution. Figure 2.1b, on the other hand, illustrates the process of Reverse Osmosis (RO) which basically involves applying a pressure on the right hand side greater than the osmotic pressure of the solution to induce water flow from the concentrated salt solution to the dilute salt concentration side. Thus, reverse osmosis is defined as a pressure-driven membrane process that allows for the preferential transport of the major species (solvent) through the membrane causing separation of the minor species (solute).

A schematic for the process of RO can be shown in Figure 2.2. There are three streams of importance for any membrane process: viz. feed, permeate and retentate. For the case of RO/NF, since the driving force is pressure, there is a high-pressure side and a low-pressure side. The low-pressure side is the atmospheric pressure side or the permeate side. The retentate (or concentrate) is the stream that remains on the high-pressure side.

2.2 Terminologies and Variables:

The basic definitions and terminologies for the RO/NF system remain same regardless of aqueous or non-aqueous medium. For aqueous systems, pure water permeability and rejection are the two most common transport parameters used to characterize the membrane. Thus, for non-aqueous systems, the pure solvent (species i) permeability (A_i) and the rejection will be expressed in a similar way as:

$$A_i = \frac{J_i}{\Delta P} \qquad 2.1$$

The observed rejection of a solute in a solvent medium can be defined as:

$$R = 1 - \frac{c_p}{c_f} \qquad 2.2$$

c_p = solute concentration of the permeate

c_f = solute concentration of the feed solution

2.2.1 Variables:

The process of RO when extended to non-aqueous medium can introduce several variables to the system. Some of these variables can be identified as follows:

2.1(a)

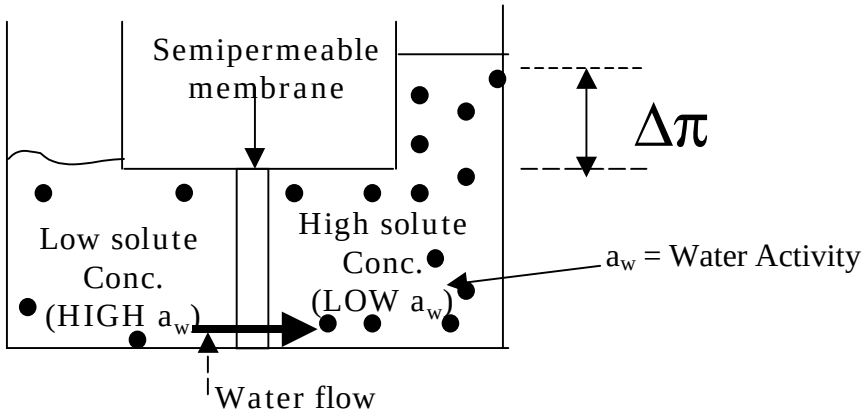

2.1(b)

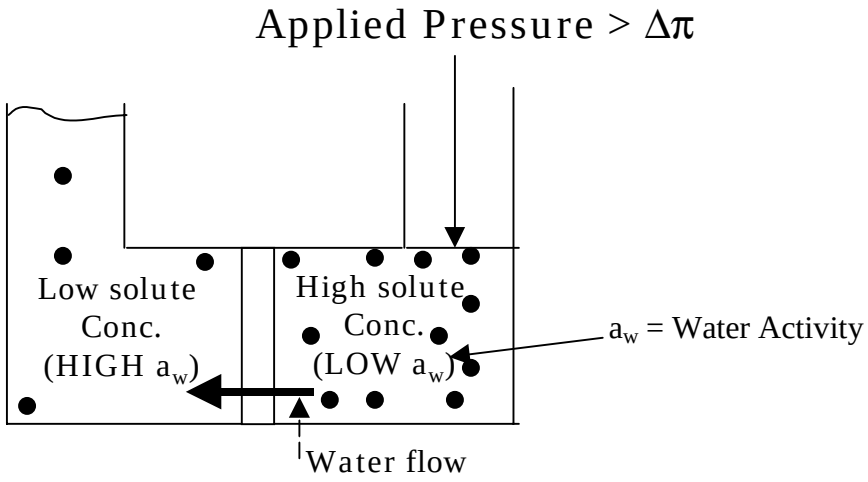

Figure 2.1: Schematic of Osmosis (2.1(a)) and Reverse Osmosis (2.1(b))

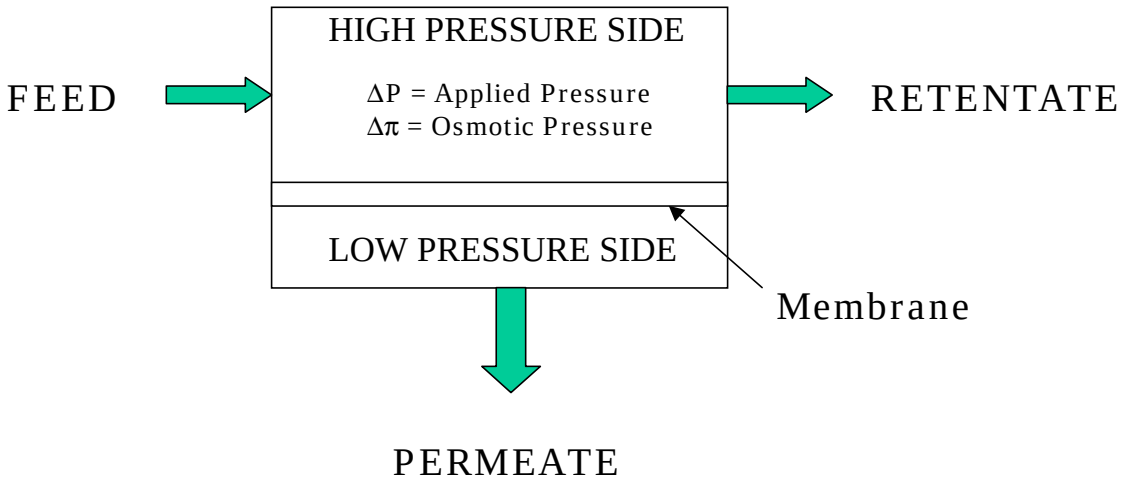

Figure 2.2: Schematic of the process of Reverse Osmosis

2.2.1.1 System Variables

2.2.1.1.1 Solvent Properties:

a) Polarity of the solvent

b) Viscosity of the solvent

c) Solvent Molar Volume (Size)

2.2.1.1.2 Solute Properties

a) Solute Molar volume (size)

b) Solute solubility in solvent (measure of solute-solvent affinity) and in membrane

2.2.1.1.3 Membrane Properties:

a) Surface Energy (analogous to the surface tension for a liquid) of the membrane

b) Type of interaction with solvent (Hydrophilicity/hydrophobicity)

c) Degree of crosslinking of the membrane (resistance to swelling)

2.2.1.2 Process Variables:

a) Feed temperature

b) Applied Pressure

c) Feed Concentration

2.3 Pure Solvent Transport through Polymeric Membranes:

Traditionally, RO/NF processes have been applied to aqueous systems primarily for the purposes of water purification applications. Typical membranes used for such operations include aromatic polyamide, polysulfone, cellulose acetate etc. These membrane materials have both hydrophilic and hydrophobic domains in their structure. The process of permeation of water through such membranes is typically an activated

diffusion process through the abundance of hydrophilic sites. In the case of NF membranes, residual charged groups (e.g. carbonyl) present on the polymer enhance the transport of water via their enhanced water sorption capability. Also, in the presence of other solutes, water is preferentially transported through these hydrophilic domains thus causing high permeation rates and better separation. However, for most non-aqueous systems, the flux through such membranes containing hydrophilic sites would be considerably lower than water as expected due to the limited (alcohols) and no (alkanes) hydrogen bonding capability of the organic solvents. As a result, the compatibility of the solvent and the membrane material become critical which makes it essential to establish the pure solvent transport through polymeric membranes.

2.3.1 Review of Literature Results for Pure Solvent Transport:

Understanding pure solvent transport is critical to extend the principles of RO/NF to non-aqueous medium targeted for specific applications. Thus, a brief review of the literature data reported in this area will be presented here.

Loeb and Sourirajan developed the first cellulose acetate-based dense RO membrane by phase inversion at UCLA which triggered the development of RO as a preferred treatment technology for aqueous systems. Since then Sourirajan and Matsuura have contributed tremendously to this field by proposing several transport theories including the Preferential sorption-capillary flow model and the Surface Force-Pore flow models. They envisioned the application of RO to non-aqueous systems in their classical articles in the mid 60s [Sourirajan, 1964]. The research primarily focussed on using cellulose acetate membranes with a vast variety of organic solvents (aliphatic and

aromatic, polar and non-polar). For example, cellulose acetate membranes were used for studying the separation characteristics of the xylene-ethanol and the n-heptane-ethanol solutions [Kopecek and Sourirajan, 1970]. They found that ethanol was transported preferentially through the membrane. However, when the membrane was coated with a hydrophobic layer, the direction of separation was reversed. Based on their observations, they proposed that the transport mechanism for non-aqueous systems studied by them was preferential sorption and transport of one of the species through the membrane. Paul *et al* [1970; 1975a; 1975b; 1976a; 1976b] performed experimental studies on rubbery membrane materials in the early and mid 70's to understand the transport characteristics for different organic solvents. The solvents used for their study were primarily organic solvents, aliphatic and aromatic, polar and non-polar. The membranes were lightly crosslinked natural rubber membranes and thus had a tendency to swell in the presence of organic solvents and undergo compaction at high feed pressures. Typical flux behaviors observed with pressure were linear at low pressures and leveling off at higher pressures of operation. The saturation flux values and the corresponding pressures were dependent on the type of solvent used. For example, the iso-octane flux saturated at about 15 bar with a corresponding flux of about 0.43×10^{-4} cm^3/cm^2 s. To explain this non-linear behavior, volume fractions of the solvents in the membrane (solvent uptake) were used as a driving force instead of the conventional pressure gradient [Paul *et al*, 1976a] thus pointing out the importance of polymer-solvent interactions. Aminabhavi *et al* [1991; 1993; 1995] on the other hand have published extensive results on the sorption and diffusion of organic solvents through rubbery films which can be used to understand permeation behavior in dense NF membranes. The importance of several parameters like

crosslinking density and the effects of temperature on the sorption and diffusion of organic solvents were the focus of the study. Importance of hydrogen-bonding capacity of polymers containing hydrophilic groups, which enhances the solvent-uptake capacity for polar solvents was reiterated. Koseoglu *et al* [1990] and Schmidt *et al* [1998] have published several results on the stability of some commercially available membranes towards organic solvents. From their findings, it can be substantiated that solvent-resistance is one of the key issues in solvent-resistant membrane development.

Machado *et al* [1999a; 1999b] and Whu *et al* [1999, 2000] have published articles recently using commercial NF (Koch) membranes for their transport and separation properties. Machado *et al* [1999a] used several polar and non-polar solvents to understand the role of the type of solvent on its permeation properties through commercial polymeric membranes (Koch MPF-50). They have proposed a resistance in series approach for explaining pure solvent transport through polymeric membranes [Machado *et al*, 1999b]. The parameters used for the prediction are viscosity and surface tension. Whu *et al* [1999,2000] have expressed the scope for the use of membranes in certain pharmaceutical applications and have published results pertaining to water and methanol transport through Koch MPF-series of membranes.

To summarize the above literature data, it can be concluded that polymer-solvent interactions are critical in understanding the transport behavior in non-aqueous systems. Special considerations for membrane swelling in the presence of organic solvents need to be made to understand the transport behavior in totality. Also, the solvent-resistance of the membrane material becomes critical as has also been pointed out by certain investigators.

2.3.2 Solvent Resistance:

Stability of the membrane material towards the feed solvent(s) is very critical for the applicability of RO/NF in non-aqueous medium. Results published in literature by Koseglu *et al*, 1990 and Schmidt *et al*, 1998 highlight the solvent-resistance of some commercial membranes and their permeation properties (Figure 2.3). From the plots, an immediate conclusion that can be drawn is that many currently available commercial membranes have low stability for non-polar hydrocarbons (e.g. hexane). Some polyvinylidene fluoride (PVDF) based membranes are also destroyed by hexane [Koseglu *et al*, 1990; Schmidt *et al*, 1998], presumably because of the incompatibility of the membrane backing material with hexane. The understanding of polymer-solvent interactions is thus critical for the development of membrane materials suited for specific applications in non-aqueous medium.

2.3.3 Polymer-Solvent Interactions:

The understanding of solvent interactions with membrane materials is crucial for membrane design, performance evaluation and prediction. Factors influencing interactions could be solvent polarity, degree of cross-linking of the polymer and nature of the polymer. For separation of aqueous mixtures (containing solvents), permeability behavior could be completely different as compared to results obtained for pure solvents. Therefore, increased knowledge of solvent-material characteristics is imperative for the improvement of membrane applications. An estimate of these interactions can provide valuable information for both predictions and also for the selection of a particular polymer system for a desired separation. There have been various ways of obtaining the

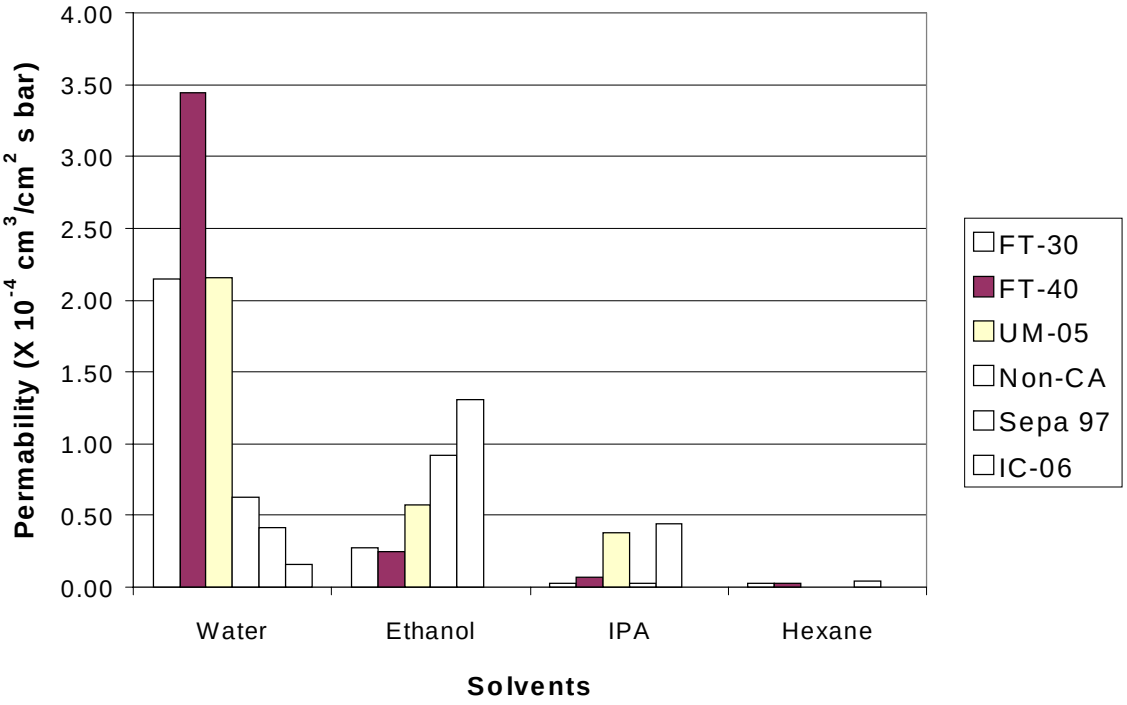

Membrane Commercial Name	Manufacturer	Molecular Weight Cut Off	Stability Towards Hexane	Material
FT-30	FilmTec	300	Stable	Aromatic Polyamide
FT-40	FilmTec	200	Stable	Aromatic Polyamide
UM-05	Koch	500	Destroys	Not Available
YC-05	Koch	300-400	Destroys	Not Available
Non-CA	Koch	200-1000	Destroys	Not Available
Sepa 97	Osmonics	150-200	Stable	Cellulose Acetate
IC-06	Microfiltration Systems	500	Destroys	Not Available

Figure 2.3: Solvent Permeability Data for some commercial RO Membranes (data taken from Koseoglu et al, [1990])

polymer-solvent interactions since its introduction in the Flory-Huggins theory for polymer solutions. Some of the parameters that can be used to semi-quantitatively represent such interactions will be discussed in this section.

2.3.3.1 Flory-Huggins Interaction Parameter (χ):

One of the foremost parameters to represent polymer-solvent interactions is the Flory-Huggins parameter or the χ (chi) parameter. Polymer solutions have unique thermodynamic properties and one of the first theories to account for such differences was the Flory-Huggins theory [Danner *et al*, 1993]. The activity of the penetrant inside the polymer for a binary system according to the Flory-Huggins theory can be given as [Mulder *et al*, 1997]:

$$ln\, a_i = ln\, \phi_i + \left(1 - \frac{V_m}{V_p}\right)\phi_p + \chi \phi_p{}^2 \qquad 2.3$$

Where, a_i is the activity of the penetrant molecule, ϕ_i is the volume fraction of the species and V_m is the molar volume of the solvent, V_p is the molar volume of the polymer. The χ parameter gives a qualitative estimate of the type of interactions possible between the polymer and the solvent. Some guidelines proposed for the χ values are as follows [Danner *et al*, 1993]: A value of χ which is > 2 is considered large and in this case the magnitude of interactions are small between the chosen pair of polymer and the solvent. On the other hand for χ values between 0.5 and 2, the interactions are high between the polymer and the solvent and high permeabilities exist. However, for χ values < 0.5, the interactions are very large and the polymer and the solvent are compatible often leading to solvation between the two. Thus for the permeation of such solvents, a high degree of

cross-linking would be required to cause maximum interaction without extensive swelling of the polymeric membrane.

2.3.3.1.1 Determination of Chi Parameter:

Several methods have been used in literature to obtain the chi parameters between polymer-solvent systems. Some of the methods are using Hildebrand solubility parameter approach, Flory-Rehner type of approach, Inverse Gas Chromatography, Precipitation values determined during membrane formation etc. A few of the above methods will be described here in brief with their salient features.

2.3.3.1.1.1 Hildebrand Solubility Parameter Approach:

Chi parameter can be obtained from Hilderbrand solubitlity parameters as follows [Danner *et al*, 1993]

$$\chi_{12} = \chi_s + \frac{V_m}{RT}(\delta_1 - \delta_2)^2 \qquad 2.4$$

The entropic contribution, (χ_s), is generally the inverse of the coordination number for the lattice structure, which is found to be between 0.3 and 0.4 [Danner *et al*, 1993]. The δ's are the Hildebrand Solubility parameters and these can be determined from group contribution methods [Sourirajan *et al*, 1985] for the solvent (1) and the polymer (2). Similar solubility parameters indicate a good compatibility of the polymer and the solvent.

The Hildebrand solubility parameter approach is a very simple one-parameter model for predicting the interaction parameter. Figure 2.4 shows the comparison of experimental [Gundert *et al*, 1997] and predicted data for the Polydimethylsiloxane

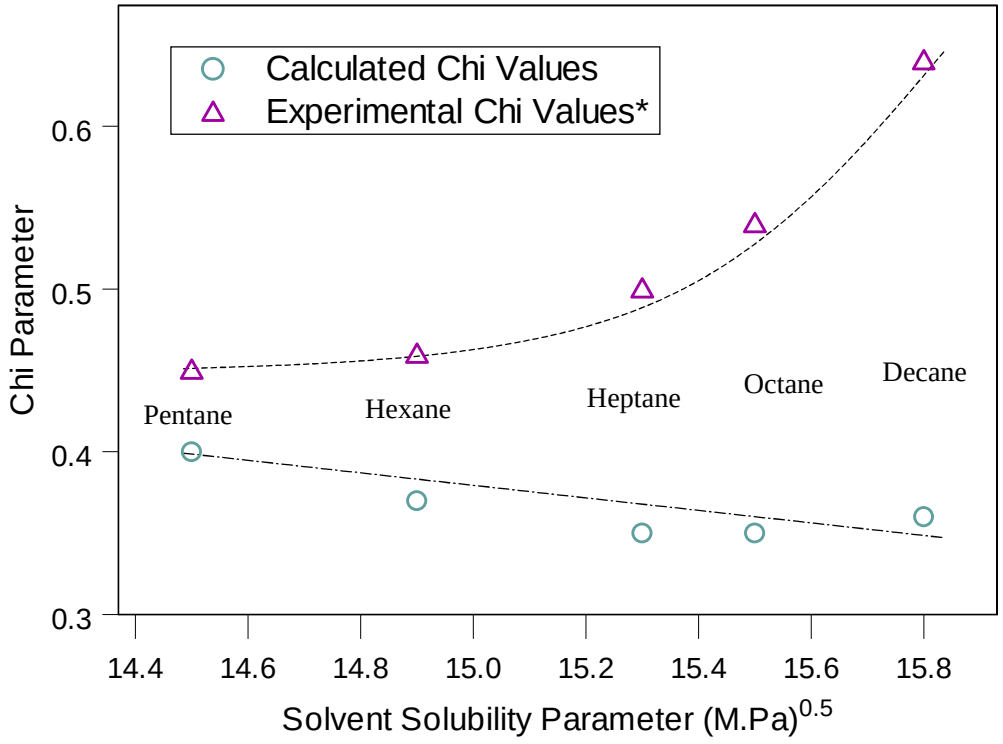

Figure 2.4: Comparison of chi values obtained from Hildebrand Solubility Parameter approach and literature data for the alkane-PDMS system (* Experimental chi values obtained from Gundert et al, [1997] and were reported using Inverse Gas Chromatography)

(PDMS) - alkane systems. From the figure, it can be seen that the method gives the opposite trend for the interaction parameter variation. However, it does predict the right magnitude of interaction for the PDMS alkane system (χ < 0.5). Another flaw in the method is that it predicts that the χ parameter for polysulfone with alcohols has a value much lower than that for alkanes. This implies that the polymer should interact more with the alcohols than with the alkanes, which is contrary to the nature of the groups present in the polysulfone backbone. Experimental values reported for water and IPA are shown in Figure 2.5. The nature of interaction predicted for IPA using the Hildebrand approach is opposite to that observed and reported in literature [Radovanovic *et al*, 1992]. The method also does not consider temperature dependence of the χ value.

2.3.3.1.1.2 Flory-Rehner Approach to determine chi parameter values.

Sorption capacity of the polymer for a solvent can be directly related to its interaction with the solvent. This is the approach of the Flory-Rehner theory to determine the χ parameter. Kim *et al* [1997] have discussed the application of the Flory Rehner theory to calculate the interaction parameter from the observed sorption data for the water-Polysulfone system. The equation used for this approach can be derived simply from using the Flory-Huggins theory for binary systems (Equation 2.3) and setting the activity of the solvent equal to unity (pure solvent). The resulting equation can be given by:

$$\chi = -\frac{\left[\left(ln\left(1-\upsilon_p\right)+\upsilon_p\right)\right]}{{\upsilon_p}^2} \qquad 2.5$$

In the above formula the ν_p is the volume fraction of the polymer and can be obtained by using sorption experiments. Kim *et al* [1997] have compared the values obtained by sorption studies to values obtained in literature. For example, the measured value for Polysulfone-water system was 4.0 and that obtained using the Flory-Rehner approach was about 3.7. Thus, it can be seen that there is good agreement between the values thus validating the method.

2.3.3.1.1.3 Precipitation values determined during membrane formation

Cloud point measurements [Wang *et al*, 1993] have been used to obtain a relatively rough estimate of the chi parameter. Membrane preparation by the phase inversion process involves a ternary system and essentially phase separation occurs when a non-solvent is used to partition out a solvent selectively from a polymer solution. The precipitation value can be defined as [Wang *et al*, 1993] the amount of non-solvent that needs to be added to a solution containing 100 gm of solvent and 2 gm of polymer to cause visual turbidity. The amount of non-solvent that is required to cause the precipitation of the polymer could provide a rough estimate of the interaction parameter. Wang *et al* [1993] use the precipitation values obtained for a ternary system of a polymer-solvent and a non-solvent system and use the magnitude of these values to explain the phase separation behavior depending on the interactions. They use polysulfone and several solvent non-solvent combinations to get the precipitation values.

Other methods that have been used for determining chi parameters are inverse gas chromatography (IGC) which uses a GC column prepared from the polymer of interest. Solvent is passed in a dilute quantity using a carrier gas and amount of solvent picked up

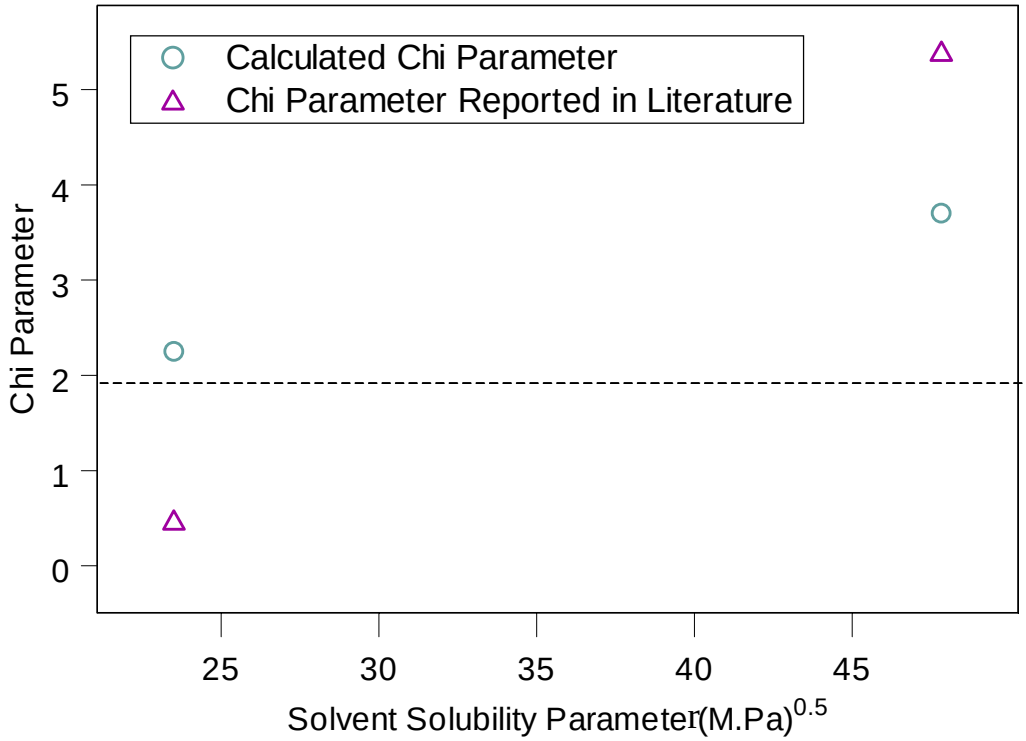

Figure 2.5: Comparison of the chi values determined from Hildebrand Solubility Parameter Approach and literature values reported for Polysulfone (Literature data taken from Radavanovic et al, 1992; Kim et al, 1997)

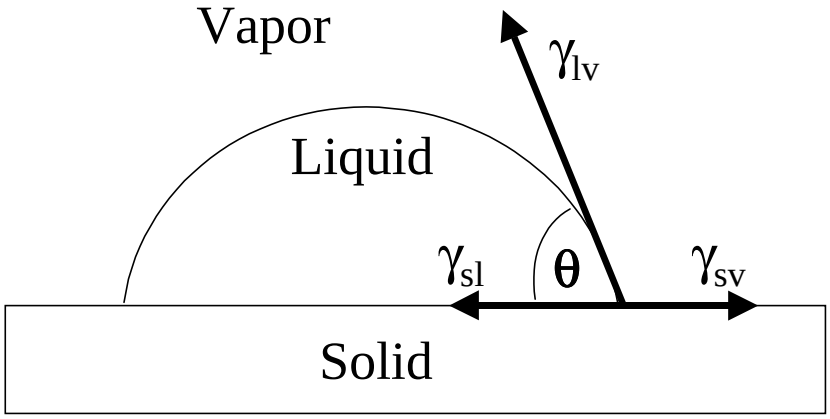

γ_{sl}: solid-liquid surface tension
γ_{sv}: solid-vapor surface tension
γ_{lv}: liquid-vapor surface tension

Figure 2.6: Schematic and Definition of contact angle

by the polymer is related to the interaction parameter. Surana *et al* [1998] have demonstrated the use of this method to obtain interaction parameters as well as partition coefficients. Approximate determination of the chi parameter would allow choice of suitable polymer material towards solvent compatibility as well as transport.

2.3.3.2 Membrane Surface Energy:

Polymer-solvent interactions can be accounted for by using the chi parameters or the solvent-uptake values as has been shown above. However, an indirect measure of the level of interaction can also be obtained by using certain membrane properties. Surface Energy, γ_{sv} for a membrane/polymer (analogous to the surface tension of a solvent), for example, can be used as an indirect measure of the hydrophilicity/hydrophobicity of the membrane material. Such values for a membrane or any solid surface can be measured using indirect techniques such as direct force measurements, contact angles and capillary penetration [Kwok and Neumann, 1999]. Use of contact angles is an extremely common method employed for measuring the membrane surface energy. Young's equation can be utilized to relate the contact angle to the three surface tension values of the system viz. the solid-liquid surface tension (γ_{sl}), the solid-vapor surface tension (γ_{sv}) and the liquid-vapor surface tension (γ_{lv}). Figure 2.6 shows the definition of contact angle along with those for the individual surface tension. It is evident that the contact angle is definitely a function of the membrane and solvent type. The Young's equation relates the three values as:

$$\gamma_{lv} \cos\theta = \gamma_{sv} - \gamma_{sl} \qquad 2.6$$

θ = Advancing contact angle between the solid and the liquid.

Among these three values, the liquid-vapor surface tension values can be easily obtained through curvature analysis of pendant drops. The solid-liquid surface tension values, γ_{sl} can be estimated through the use of several available theories, but the solid vapor value, γ_{sv} which is essentially a constant needs to be determined from a series of contact angle measurements for various liquids. Qualitatively, one can say that the lower is the contact angle, the higher is the wetting ability of the solvent for the membrane. The relevant equations based on the equation of state approach that can be used to calculate the membrane surface energies are [Kwok *et al*, 1999]:

$$\cos\theta = -1 + 2\sqrt{\frac{\gamma_{sv}}{\gamma_{lv}}}\, e^{-\beta(\gamma_{sl}-\gamma_{sv})^2} \qquad 2.7$$

Where, β is basically an adjustable parameter which is used for the iterative procedure. Kwok *et al* [1999] found a value of β of approximately 0.0001 to be true for a series of polymers and solvents that were used for measuring the surface energy. Contact angles can be obtained for a given polymer with several solvents and with known values for γ_{lv} the constant γ_{sv} can easily be determined. It needs to be pointed out that the γ_{sl} values can be estimated for liquids which do not completely wet the membrane. One could easily visualize the use of such interfacial tension values between the solvent and the polymeric material as a measure of the interaction, however, a finite contact angle needs to be obtained for the estimation. For example, for a hexane - PDMS system, the measurement of a contact angle is difficult since hexane has a high level of interaction with the polymer and completely wets it, which makes this an inherent disadvantage of the technique.

2.3.4 Transport Theories for Pure Solvent Transport:

As can be seen from the brief review of literature data presented in Section 2.3.1 above, the solvent and membrane type can significantly affect permeation behavior of the solvent. Understanding pure solvent transport thus is critical for predicting the transport behavior for different solute-solvent systems and hence will be discussed briefly in this section. There have been several transport theories proposed for reverse osmosis and nanofiltration for use in aqueous systems. Soltanieh and Gill [1981] provide an excellent review of the models that have been used for the prediction of transport properties for RO/NF membranes. Each model proposed has its own sphere of validity and several assumptions have been made in order to explain observed behavior of the system of interest. However, there can be three broad classifications of the models that have been proposed, i.e.

1. Solution-Diffusion-based models
2. Irreversible Thermodynamics-based models
3. Pore Flow-based Models

The first goal is to extend existing transport theories for aqueous systems to non-aqueous systems to explain pure solvent transport. The solution-diffusion-based models will be discussed in a little more detail in this section, since they use solvent physical properties to predict solvent transport. Thus, a brief discussion of the assumptions and some salient features of the solution-diffusion class of models will be presented here. The irreversible thermodynamics-based models and the pore flow-based models are typically used to interpret separation behavior and will be discussed in a later section with respect to solute separation.

2.3.4.1 Solution-Diffusion Based Models:

Typical solution-diffusion based models use the generalized approach:

$$Permeability \propto Diffusivity \times Solubility \qquad 2.8$$

If the solubility and the diffusivity of the solvent in the membrane are obtained from independent experiments, then the solvent permeability can be obtained using Equation 2.8. For example, Reddy *et al* [1996] have used the following equation to obtain the solubility of the penetrant molecule, S_i, through the membrane as:

$$S_i = \frac{B}{\left[(\delta_p - X)^2 + (\delta_h - Y)^2 + (\delta_d - Z)^2\right]} \qquad 2.9$$

Where, B is a constant, X, Y and Z are the polar, hydrogen-bonding and the dispersion solubility parameters respectively for the membrane material and δ_p, δ_h and δ_d are the polar, hydrogen-bonding and the dispersion solubility parameters respectively for the solvent. They have used Equation 2.9 to obtain the solubility parameters for the membrane material used for their study. There can be other ways to obtain the solubility of the species in the membrane, however, most of the times, researchers resort to indirect measurements for determination of the solubility.

Diffusion of a solvent molecule through a polymeric network depends on several parameters, some important ones being the polymer type (polar or non-polar), the crosslinking of the polymer network, solvent type and structure, the solution temperature etc. For aqueous systems, water is the major penetrant through the polymeric network. The molar volume of water (a measure of the size) is 18 cc/mole. When compared with that of some non-polar solvents such as hexane, which has a molar volume of 131 cc/mole, it can be seen that there is at least a 7-fold increase in the effective size of the

molecule. Also, as stated, the membrane polymer chemistry has an immense impact on the solvent permeation. Thus, measurement or prediction of true diffusion coefficients through the membrane matrix is not trivial.

Because of the above limitations of direct measurement and prediction of solubility and diffusivity, researchers have adopted an indirect route to develop transport theories based on the solution-diffusion approach. Most of the diffusion-based models revolve around the first model proposed by Lonsdale *et al* [1965], the Solution-Diffusion model. This is one of the most popular models that has been widely used in literature to explain the flux behavior for RO/NF and Pervaporation type of membrane processes. The key assumptions made in this model are [Wijmans *et al*, 1995]:

a) Both solute and solvent dissolve in the non-porous and homogeneous surface layers of the membrane
b) Each species diffuses across the membrane in an uncoupled manner due to its own chemical potential gradient, which is the result of the concentration and pressure differences across the membrane.
c) The pressure within a membrane is uniform and that the chemical potential gradient across the membrane is essentially due to a concentration gradient. This can be illustrated by Figure 2.7.
d) The chemical potentials on either side of the membrane are same as their bulk values.

Figure 2.8 illustrates the essential visualization of the transport mechanism for Solution-Diffusion-based models for pure solvent transport. The driving force for the transport of solvent through the membrane is due to a chemical potential gradient across the thickness of the membrane. Thus,

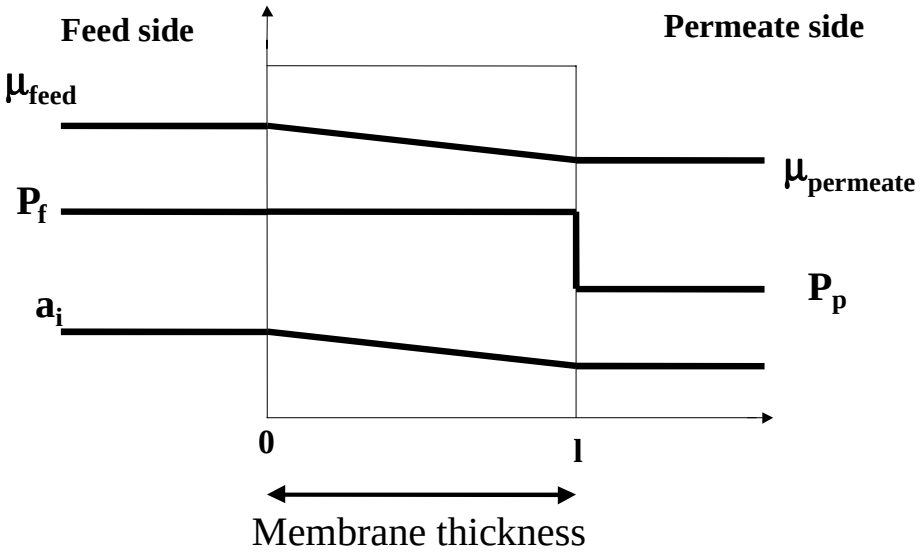

Figure 2.7: Driving Force for the solution-diffusion-based models.

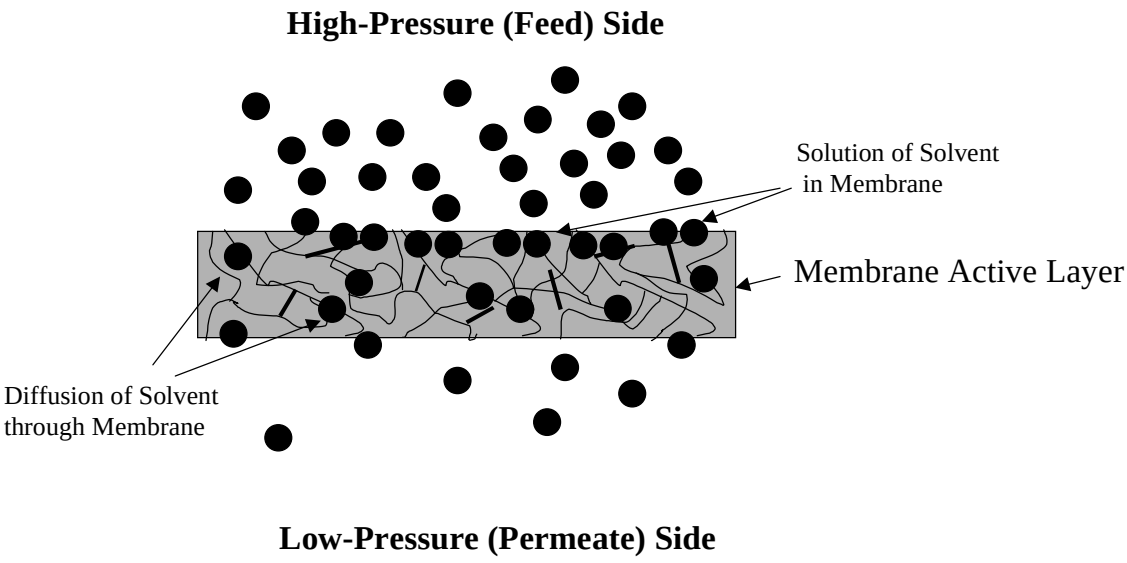

Figure 2.8: Visualization of the Solution-Diffusion process for pure solvent transport.

$$J_i = -L_i \frac{d\mu_i}{dz} \qquad 2.10$$

Where, J_i is flux of species i, L_i is a proportionality constant, μ_i is chemical potential of species i, z is the length dimension. The chemical potential can be expressed in terms of the activity and the pressure as:

$$d\mu_i = R_g T d(\ln a_i) + V_i dP \qquad 2.11$$

Where, a_i = activity of species i, V_i is the partial molar volume of the component i, P is the transmembrane applied pressure

Thus,

$$\mu_i = \mu^0{}_i + R_g T \ln a_i + V_i (P - P^0) \qquad 2.12$$

Where μ_i^0 is the standard chemical potential of species i, P^0 is the reference pressure.

Expressing the activity in terms of the concentration and also assuming that the pressure inside the membrane is the same as the applied pressure, one can get the following

$$J_i = -D_i \frac{dc_i}{dz} \qquad 2.13$$

where D_i is the diffusion coefficient of the species i. The concentrations on either side of the membrane at the interface can be denoted as $c_{if(m)}$ and $c_{ip(m)}$. Using a simple chemical potential balance at the membrane interface on the feed and the permeate side, one can get:

$$\mu_{if} = \mu_{if(m)}; \mu_{ip} = \mu_{ip(m)} \qquad 2.14$$

Using this assumption, the concentrations on the membrane surface can be expressed as a function of the bulk values on both the feed and the permeate side to obtain the value for $c_{if(m)}$

$$c_{if(m)} = K_i c_{if} \tag{2.15}$$

A similar treatment on the permeate side gives the following equations.

$$c_{ip(m)} = K_i c_{ip}\, exp\left(\frac{-V_i(P_f - P_p)}{R_g T}\right) \tag{2.16}$$

Thus the final flux equations can be written as,

$$J_i = -\frac{D_i K_i}{l}\left[c_{if} - c_{ip}\, exp\left(\frac{-V_i(P_f - P_p)}{R_g T}\right)\right] \tag{2.17}$$

Incorporating the definition of osmotic pressure into the final flux equation, one can finally obtain the equation (details can be obtained from Wijmans *et al*, [1995])

$$J_i = A_i(\Delta P - \Delta\pi) \tag{2.18}$$

Where A_i = permeability of the species i

$$A_i = \frac{D_i K_i c_{if} V_i}{l R_g T} \tag{2.19}$$

In case of pure solvent flux, the model simplifies to

$$J_i = A_i(\Delta P) \tag{2.20}$$

Some disadvantages of the model are that it is applicable for membranes with relatively small water content. For membranes which have a tendency to swell, a modified model was developed by Paul *et al* [1976]. Another aspect of the solution-diffusion model that needs attention is the following assumption [Wijmans *et al*, 1995]:

$$1 - exp\left(\frac{-V_i(\Delta P - \Delta\pi)}{R_g T}\right) = \frac{-V_i(\Delta P - \Delta\pi)}{R_g T} \tag{2.21}$$

Such an approximation was made for aqueous systems where the molar volume of water was 18 cc/mol. However, it may not be valid for the case of solvent systems.

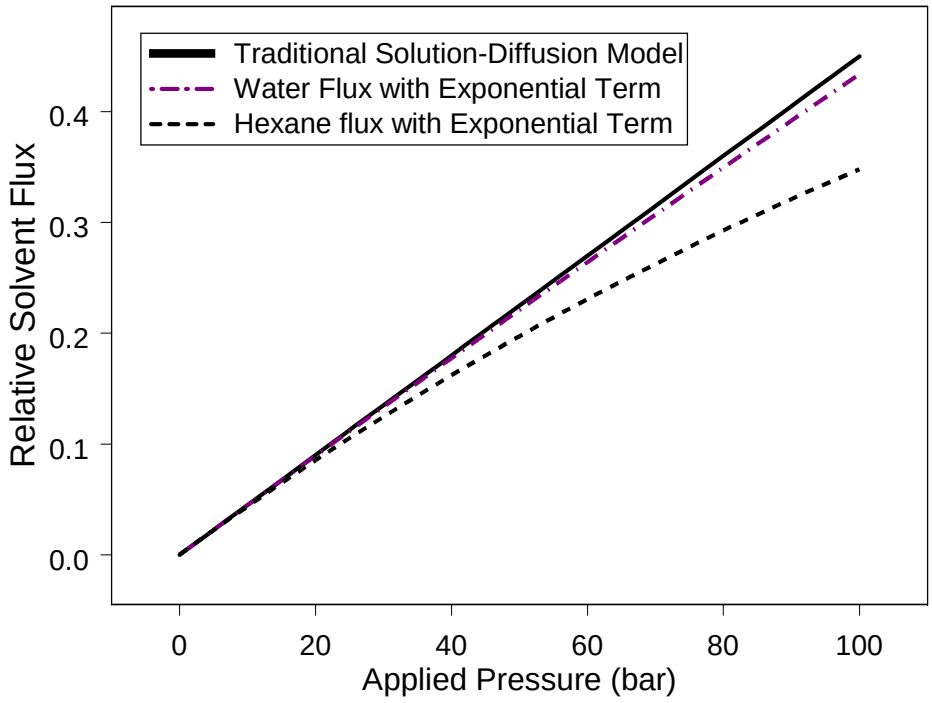

Figure 2.9: Effect of Pressure and Molar Volume on Flux variation simulated using the Solution-Diffusion model equations modified for the case of pure solvent

Table 2.1: Contribution of the exponential term in Solution-Diffusion Model

Solvent	**Molar Volume (V_i, cc/mol)**	**Applied Pressure (ΔP, bar)**	**x**	**1 – exp(-x)**	**% Deviation**
Water	18	50	0.04	0.04	1.85
Hexane	131.6	50	0.27	0.24	14.06
Decane	195.1	50	0.40	0.33	21.27

$$x = \frac{-V_i(\Delta P - \Delta\pi)}{RT}, \text{ for pure solvents } \Delta\pi = 0$$

Table 2.1 gives the relative errors that may occur because of this approximation calculated at an applied pressure of 50 bar. It can be seen that for large hydrocarbons like decane, the error can be quite significant (~ 21 % for decane). Figure 2.9 gives a simulation plot showing the relative contributions of the exponential term for pure water and pure systems with $\Delta\pi = 0$. Also, the error term may propagate at higher pressures. Thus application of the above set of equations to non-aqueous systems needs considerable experimental verification and thorough evaluation of the assumptions.

2.4 Solute Transport in Non-Aqueous Medium:

The prediction of separation behavior requires understanding of mechanisms of both solute and solvent transport. Since there are several transport theories proposed in literature for aqueous systems, the first goal is to highlight the essential similarities/differences between aqueous and non-aqueous systems.

2.4.1 Aqueous Systems:

Most of the models proposed in literature have been used to explain the flux behavior of several solute species in water through polymeric membranes. In most cases, the membrane material has strong affinity for water which results in its preferential transport. Water also has a very high hydrogen bonding ability and thus transports preferentially across the membrane using the hydrophilic groups present in the active layer of the polymeric material. Transport of solute species primarily occurs in such membranes by a combination of diffusion and Donnan exclusion. In cases where there is stronger interaction of the solutes with the membrane material there have been observations of negative rejections, for example, phenol with cellulose acetate [Matsuura

and Sourirajan, 1972 and 1973; Burgoff *et al*, 1980]. There is experimental proof in such cases that the solute strongly adsorbs onto the membrane material causing higher flux through the membrane which eventually results in negative rejections. Thus, solute molecular size and charge along with membrane surface charge are important parameters that govern the RO/NF rejection in aqueous systems

2.4.2 Non-Aqueous systems and difference from aqueous systems:

As mentioned above, transport mechanisms and experimental observations for aqueous systems have been well studied and documented in literature. As has already been pointed out from the section on Pure Solvent Transport, the type of solvent and membrane can significantly affect the permeation characteristics. For example, alcohols are polar compounds and also have hydrophobic segments and the length of these segments varies in a particular homologous series. In the case of propanol, for instance, the hydrophobic propyl group will interact strongly with the hydrophobic segments of the polymeric chain, and the hydroxyl group interacts with the hydrophilic parts of the polymer. For a binary system of a solute and a solvent, the solute affinity for the solvent as well as the membrane material thus become critical.

2.4.3 Selected Literature Results for Solute Transport in Non-Aqueous Medium:

The above comments regarding the dependence of solute separation on solvent and membrane type can be further substantiated using literature data reported in non-aqueous medium . Some of the earliest work on solute transport in non-aqueous medium dates back to the mid-70s with the work of Paul *et al* [1976b] who studied the diffusion

characteristics of Sudan IV (384 MW organic dye) in various solvents through uncrosslinked natural rubber membranes. As expected, the role of solvent was quite profound. For example, the diffusivity of Sudan IV with hexane as solvent was 200 times higher than that observed in ethanol and subsequently, the permeability in hexane = 76 times that in ethanol. They explained the results using the solution-diffusion model taking into account the role of membrane swelling. One of their findings was that for the same swelling ratio (similar solvent-uptakes), there is a direct correlation between the measured solute diffusion coefficient through the membrane and its bulk solution phase diffusion coefficient. This implies that the solute transports through the solvent domains in swollen membranes. On the other hand, Farnand *et al* [16] studied the transport behavior of polar organic solutes (dimethyl aniline, acetonitrile etc.) in methanol medium and used the Surface Force-Pore Flow model to explain the results. They compared the separation behavior obtained for cellulose acetate membranes in methanol and water medium. For example, they reported a rejection of *tert*-butylbenzene in methanol to be about 27 % and that in water to be about 81 % under similar operating conditions. The pore flow model uses the potential function as a measure of the interaction between the solute and the membrane material. The mathematical calculations showed that the constant in the potential function is dependent on the type of solvent implying different attractive/repulsive forces with the membrane material.

Cheryan *et al* [1996a; 1996b; 1999] have reported several findings relating to the use of polymeric solvent-resistant membranes for separation in non-aqueous medium. These membranes were used for solvent recovery and partial deacidification of vegetable oil, soybean oil and rice bran oil. They expressed the importance of membrane resistance

to organic solvents such as n-hexane. They evaluated several commercial polymeric membranes and proposed an alternative treatment technique which was economically competitive with existing treatment technologies. For example, during the single stage separation of a 200 gm/l solution of triglyceride (vegetable oil) in hexane in the feed, the membrane used was able to obtain a rejection of > 90 %. Yang *et al* [2001] studied and reported the separation behavior of three organic solutes (Safranine O, orange II dye and solvent blue 35) in water, methanol, ethyl acetate and toluene using several commercial membranes. Koops *et al* [2001] performed similar studies in ethanol and hexane medium using cellulose acetate membranes prepared in their own laboratory. The solutes used for their study include organic acids and alkanes. The extension of non-aqueous systems to inorganic NF membranes was reported by Tsuru *et al* [2001]. They have used silica-zirconia membranes (pore size 1 – 4nm) to study the rejection characteristics of PEG molecules in methanol and ethanol medium at high temperature (50 ^{o}C). The critical role of solvent was further demonstrated by studying PEG600 rejection values in water and methanol solvents. The rejection in methanol was reported to be 74 % in contrast to negligible rejection with water as the solvent medium.

From most of the literature data, the common conclusion that can be drawn for RO/NF applications in non-aqueous medium is that solvent and membrane type can significantly affect the solute separation behavior. Table 2.2 summarizes the recently reported results obtained by Koops *et al* [2001], Yang *et al* [2001] and also contains classical CA data from [Sourirajan and Matsuura, 1985]. Some qualitative conclusions can be drawn from the literature data reported for both aqueous and non-aqueous systems:

a) When the solute has higher affinity for the membrane material than the solvent, the rejection is considerably lower. This is evident from the ternary systems of docosanoic acid – hexane – cellulose acetate [Koops *et al*, 2001] and phenol – water – cellulose acetate [Sourirajan *et al*, 1985], where the rejection of docosanoic acid (-35 %) and phenol (-10 %) are considerably low.

b) When membrane-solvent interaction >> membrane-solute interaction, the rejection is high. For example, the rejection of tetracosane and docosanoic acid in ethanol medium for the cellulose acetate membrane is 80 % and 90 %, respectively [Koops *et al*, 2001].

c) When both the solvent and the solute have high/low affinity for the membrane material, the rejection is governed by the species with the higher relative affinity. For example, when the solute has higher affinity (phenol – water – cellulose acetate), the permeate is enriched with the solute. In addition it should be noted that high solute-solvent affinity (for ex. Solvent Blue 35 solubility in ethyl acetate >> in methanol) leads to lower rejection. This can be seen in Table 2.2 through the results for tetracosane and Solvent Blue 35.

Table 2.2 also shows the data on hydrophobic MPF 60 membrane which clearly illustrates the charge effect in methanol medium showing that the rejection of the neutral solute (Solvent blue 35) is a lot lower than the charged species (Orange II and Safranine O) [Yang *et al*, 2001]. All the three solutes studied with the MPF 60 membrane have similar molecular weight (about 350).

Table 2.2: Comparison of affinity of solute and solvent type for the membrane material and its impact on rejection for aqueous and non-aqueous systems (literature data)

Membrane Material	Solute	Solvent	Rejection (%)
CA*	Tetracosane	Ethanol	80
CA*	Tetracosane	Hexane	55
CA*	Docosanoic Acid	Ethanol	90
CA*	Docosanoic Acid	Hexane	-35
CA**	Phenol	Water	-10
CA**	p-chlorophenol	Water	-8
MPF60***	Orange II	Methanol	94
MPF60***	Safranin O	Methanol	92
MPF60***	Solvent Blue 35	Methanol	81
MPF60***	Solvent Blue 35	Ethyl Acetate	66

* Data taken from Koops et al [2001]; ** Data taken from Sourirajan et al [1985]; *** Data taken from Yang et al [2001]

Note:

CA: Cellulose Acetate;

MPF 60: hydrophobic membrane (Koch Membrane Systems)

Koops et al [2001] used laboratory made CA membranes with NaCl rejection of 85.5 % (2000mg/l, Pressure = 4 Mpa, Temperature = 31 deg C, water flux = 8.0 l/m^2 h)

2.4.4 Evaluation of Traditional Transport Models for Solute Transport in Non-Aqueous Medium:

From the literature data, it is further substantiated that the dependence of the solute separation behavior on the solvent and membrane type cannot be neglected. A brief review of the models as they apply to pure solvent transport has already been discussed in a previous section. For non-aqueous solvents, in addition to various interaction parameters, special considerations regarding the membrane swelling may also be needed. Convective coupling aspects for solute transport thus need to be considered for the development of a unified transport theory. This section will primarily concentrate on the extension of existing transport theories to solute transport with special emphasis on the theories that consider convective coupling of the solvent and solute fluxes.

2.4.4.1 Solution-Diffusion-based models:

For solute transport, the traditional solution-diffusion model uses a simple concentration gradient across the membrane thickness as the driving force [Lonsdale *et al*, 1965; Wijmans *et al*, 1995]. Also, the primary assumption made in the model development is that the flux of the solute and the solvent are independent of each other. The basic flux equation for solute transport is:

$$J_{solute} = J_{solvent} C_p = B_{SD}\left(C_f - C_p\right) \qquad 2.22$$

where C_f is the bulk feed solute concentration (no concentration polarization) in the feed stream, C_p is the solute concentration in the permeate stream and B_{SD} is the solute transport parameter

The simplified solute transport parameter, B_{SD}, is related to the solute properties as:

$$B_{SD} = \frac{D_{solute} \times K_{solute}}{l} \qquad 2.23$$

D_{solute} is the solute diffusion coefficient, K_{solute} is the solute partition coefficient (and thus a function of solute-polymer interactions) and l is the membrane thickness. The partition coefficient of a particular solute is dependent on the type of membrane material and also on the type of solvent present in the system. One of the primary assumptions in the Solution-Diffusion model is that the solvent and solute species transport across the membrane independently and that there is no coupling. From the brief literature data presented on solute transport in non-aqueous medium, it is apparent that such an assumption cannot be valid. Thus, the applicability of this model to non-aqueous systems for solute transport is questionable. Also, this model can be mainly applied to systems where experimental data is available and prediction of data for different systems from existing data is cumbersome.

Other models based on the solution-diffusion approach, which consider convective coupling, were developed to account for membrane imperfections. For example, Sherwood *et al* [1967] developed the Solution-Diffusion Imperfection model to include pore flow along with the solution-diffusion process to recognize the presence of small defects in the membrane. The disadvantage of this model was that it incorporated an additional parameter into the Solution-diffusion model which required the use of non-linear regression analysis. Burgoff *et al* [1980] developed the Extended Solution diffusion model to explain negative rejections obtained for phenol - Cellulose Acetate

systems. They included the pressure dependent term in the chemical potential of the solute.

2.4.4.2 Irreversible Thermodynamics-Based models:

The key assumption in models based on the concept of irreversible thermodynamics (IT) is that the membrane is not far from equilibrium. The basic premise of this model is that the flux of the components is affected by the other permeating components. Thus,

$$J_i = -\sum_j L_{ij} \frac{d\mu_j}{dz} \qquad 2.24$$

Kedem and Katchalsky [1958] proposed one of the early models based on this approach. They assumed that solvent and the solute fluxes were linked by a coupling coefficient called the Staverman reflection coefficient.

$$J_{solvent} = L_p(\Delta P - \sigma \Delta \pi) \qquad 2.25$$

$$J_{solute} = \omega \Delta \pi + (1 - \sigma) \times C \times J_{solvent} \qquad 2.26$$

where, L_p and ω are phenomenological coefficients, C is the average solute concentration and σ is the Staverman reflection coefficient. The inherent disadvantage of this model is that the phenomenological coefficients were concentration dependent. To avoid this dependence, the Spiegler-Kedem model [Jagur-Grodzinski and Kedem, 1966] was developed which also considered the convective coupling aspects of the solute transport. The Spiegler-Kedem model assumes that the solute flux is a combination of diffusion and convection [Jagur-Grodzinski and Kedem, 1966; Gilron *et al*, 2001; Burghoff *et al*, 1980]. Figure 2.10

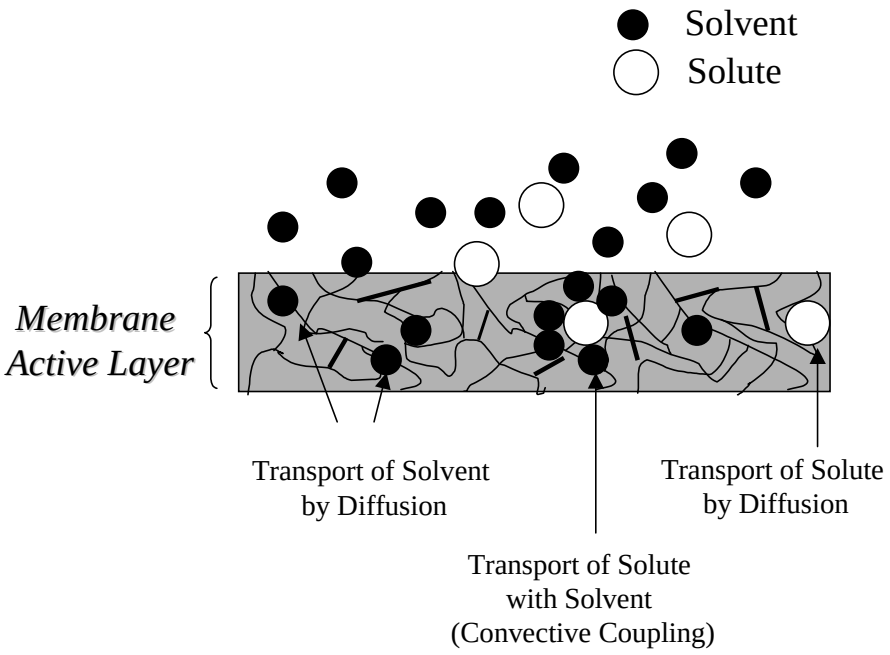

Figure 2.10: Physical Interpretation of the Spiegler-Kedem model for solute transport.

depicts the physical interpretation of the Spielger-Kedem Analysis. The relevant equation for the Spiegler-Kedem model is:

$$J_{solute} = \overline{P}\frac{dc}{dz} + J_v C(1-\sigma) \qquad 2.27$$

where, $\overline{P}$ is the local solute permeability coefficient (similar to the B_{SD} in the solution-diffusion model), C is the average concentration of the solute in the membrane, J_v is the total volume flux and σ is the reflection coefficient. To obtain the two parameters, the following equations can be used:

$$R \equiv 1 - \frac{C_p}{C_b} = \frac{(1-F)\sigma}{1-\sigma F} \qquad 2.28$$

$$\text{where, } F = exp\left[\frac{-J_v(1-\sigma)}{P_s}\right] \text{ and } P_s = \frac{\overline{P}}{\Delta x} = \text{permeance} \qquad 2.29$$

The two parameters, $\overline{P}$ and σ can be obtained using the permeation/rejection data for the solvent and the solute. In cases where independent diffusive flux data are available, the $\overline{P}$ values can be obtained from the slopes of concentration versus time curves. These values can then be used to calculate the approximate contribution of convection and diffusion to the solute transport, thus giving more insight into the transport mechanism. Obviously, the convective contributions will be dominant when the asymptotic solute rejection values are low. This has been also pointed out by Gilron *et al* [2001] in their recent work and they suggest that the convective transport of the solute in such cases cannot be neglected. Thus, the above treatment can be easily extended to non-aqueous systems. The $\overline{P}$ and σ values can be correlated with the different solute/solvent properties and can then be used as a predictive tool for extending it to different systems.

2.4.4.3 Pore Models:

Sourirajan *et al* were the first proponents of the pore flow-based models. The basic assumption underlying the models based on pore flow is that the membrane consists of several angstrom-dimension pores. The main aspect differentiating the pore flow-based models from solution-diffusion type models is that the solvent activity across the membrane is assumed to be a constant and the pressure is assumed to vary across the thickness of the membrane (Figure 2.11). The first theory in this category is the preferential sorption capillary flow model [Sourirajan *et al*, 1985]. The forces acting on the solvent/solute molecule in the presence of other components and the pore wall are considered to explain the transport behavior. Matsuura and Sourirajan [1985] developed an elegant model based on the pore flow analysis, the Surface Force-Pore Flow (SFPF) model for membrane transport and will be discussed in detail in this section.

The SFPF model was developed by Sourirajan *et al* in the early 1980's and has been modified [Mehdizadeh and Dickson, 1991; 1993] since. However, the original model itself has been used for explaining several reverse osmosis data collected by several research groups in the past couple of decades [Bhattacharyya *et al*, 1986]. The basic assumption is that the solvent preferentially wets the membrane pore and allows for the transport of the solute through the pore. Figure 2.12 gives a physical interpretation of the pore-flow models. The frictional force balance used for the basic derivation as a starting point can be given by [Sourirajan *et al*, 1985]:

$$F_A(r,z) = F_{AB}(r,z) + F_{AM}(r,z) \qquad 2.30$$

where, $F_A(r,z)$ is the driving force (i.e. chemical potential gradient) for solute A, $F_{AM}(r,z)$ is the friction force between solute A and the membrane wall M and $F_{AB}(r,z)$ is the

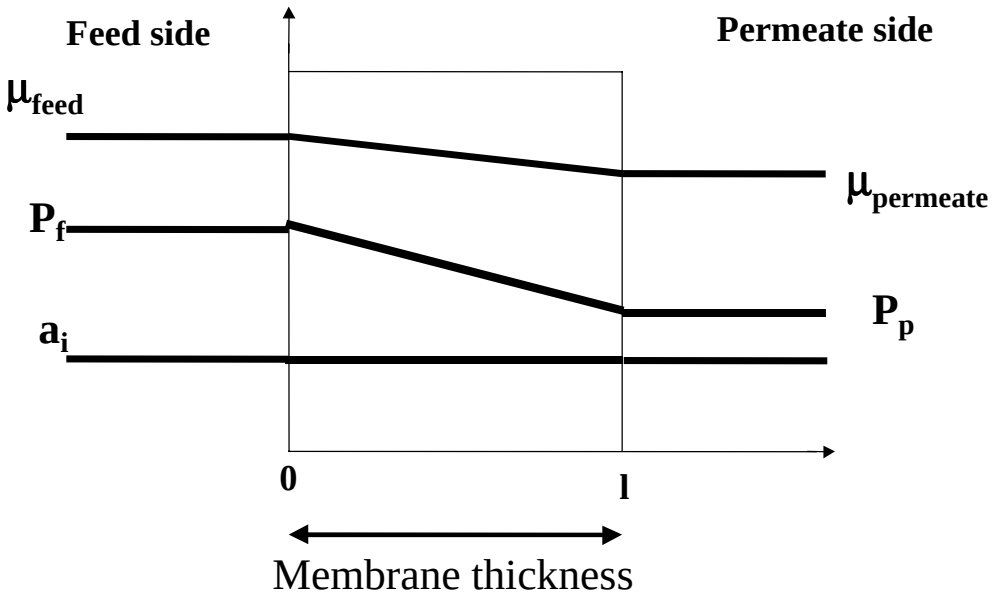

Figure 2.11: Driving Force for the Pore Flow-based models.

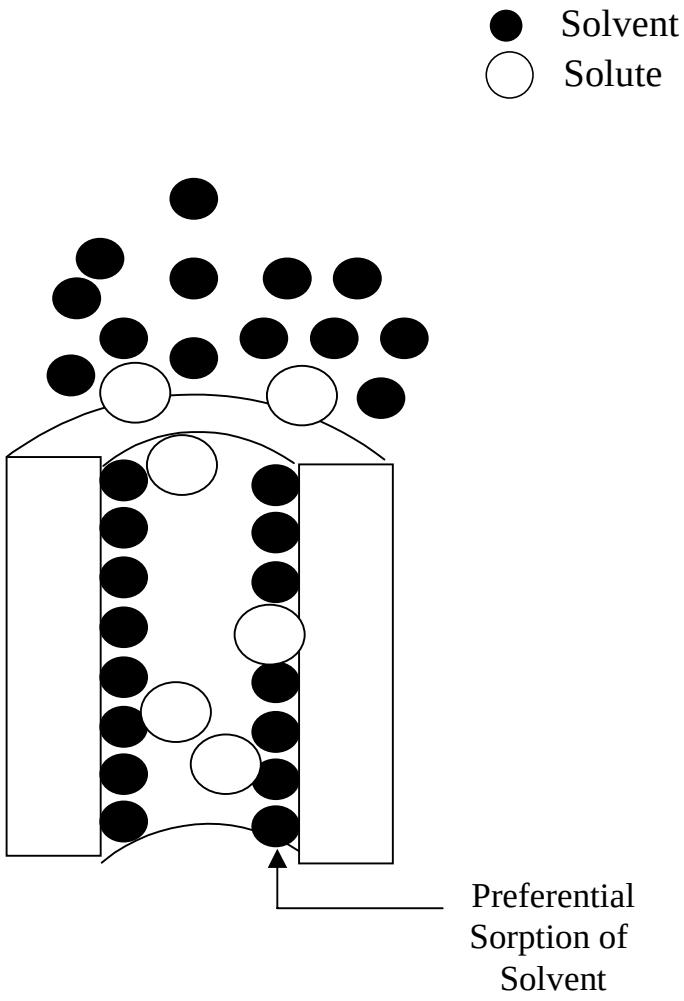

Figure 2.12: Physical Interpretation of the Pore-Flow-based model for solute transport.

friction force between the solute A and solvent B. As can be seen from the model development, the dependence of solute separation on solvent and membrane type have been considered here. Further development of the model relates to expressing the forces in terms of the molar fluxes and concentrations of the permeating species. After several mathematical manipulations (outlined in [Sourirajan *et al*, 1985]), the final expression for the apparent rejection (rejection based on the wall concentration) is given by:

$$R' = 1 - \frac{\int_0^{R_b} \left(\frac{\exp\left(\frac{u_B(r) l X_{AB}}{RT} \right) \times (u_B(r)) r dr}{1 + \exp\left(\frac{b(r) RT}{-\varphi(r)} \right) \times \left\{ \exp\left(\frac{u_B(r) l X_{AB}}{RT} \right) - 1 \right\}} \right)}{\int_0^{R_b} u_B(r) r dr} \qquad 2.31$$

where, $u_B(r)$ is the velocity of the solvent B as a function of r, l is the membrane thickness, $\varphi(r)$ is the potential function between the solute and membrane, R' is the rejection based on wall concentration, R_b is the radius of the pore, b(r) is the overall friction coefficient and X_{AB} is the proportionality constant relating the friction force to the velocity gradient.

Sourirajan *et al* also expressed the radial velocity profile, $u_B(r)$, as a function of r using momentum balances in the cylindrical pore. The above equation in dimensionless quantities can be given by [Sourirajan and Matsuura, 1985]:

$$R' = 1 - \frac{\int_0^1 \left(\frac{exp(\alpha(x)) \times \alpha(x) x dx}{1 + exp\left(\frac{b(x)}{-\varphi(x)} \right) \times \{exp(\alpha(x)) - 1\}} \right)}{\int_0^1 \alpha(x) x dx} \qquad 2.32$$

where,

$\alpha(x) = \frac{u_B(r) l X_{AB}}{R_g T}$ = dimensionless velocity

$\varphi(x) = \frac{\varphi(r)}{R_g T}$ = dimensionless potential function

$x = \frac{r}{R_b}$ = dimensionless distance

For ease of application of the model, several simplifications can be made to make the equation numerically integrable. For example, the radial velocity profile can be assumed to be parabolic in nature, or a constant average velocity can be used. Such assumptions lead to approximate prediction of the rejection behavior. If the velocity profile is assumed to be parabolic within the pore, the dimensionless velocity, α can be given by [Hance, 1987]:

$$\alpha(x) = \frac{\beta_2}{4\beta_1}(1 - x^2) \qquad 2.33$$

where,

$$\beta_1 = \frac{\mu \times D_{ab}}{R_g \times T \times R_a{}^2 \times C_f} \text{ and } \beta_2 = \frac{\Delta P}{R_g \times T \times C_f} \qquad 2.34$$

This is a simple Hagen-Poiseuille Equation used for pipe flow. ΔP is the applied pressure on the feed side; C_f is the feed concentration of the solute A and μ is the solvent viscosity. The above assumption makes the equation integrable numerically and can be used to fit the existing literature data to the model. Also,

$$R_a = R_b - r_{solvent} \qquad 2.35$$

R_a is the effective radius of the pore available for solute transport. Radius of the solvent can be calculated by assuming a spherical molecule. However, some data is available in literature for the molecular dimensions of certain solvents like water (0.87 A°). The overall friction coefficient (b(r)) can be determined from the work of Faxen and Satterfield [Sourirajan *et al*, 1985] using the ratio of the Stokes Radius and the Pore radius, R_b.

Sourirajan and Matsuura [1985] expressed the solute characteristics and interaction through the potential function, $\phi(x)$. In dimensionless quantities, $\phi(x)$ for non-ionized organic solutes can be given as

$$\varphi(x) = \frac{\varphi(r)}{R_g T} = -\frac{\dfrac{B_{SFPF}}{R_a{}^3}}{\left(\dfrac{R_b}{R_a} - x\right)^3} \qquad 2.36$$

where, R_a is the effective radius of the membrane pore after preferential solvent wetting, R_b is the radius of the membrane pore and x is the dimensionless pore distance. B_{SFPF} is a measure of the resultant short-range van der Waals forces between the solute and the membrane. Its sign can be positive or negative. A positive value of B_{SFPF} implies attractive force at the membrane interface and thus a negative value implies a repulsive force. The parameter B_{SFPF} can be obtained by simplifying the equations suitably and can

be used as a measure of the interaction between the solute and the membrane material. The radius of the membrane pore (R_b), the overall friction coefficient (b(r)) and radius of the solvent ($r_{solvent}$) are all determined making several assumptions. For example, the assumption of spherical molecules for solute and solvent species, and a parabolic velocity profile (to simplify the model) all lead to approximations. Experimental data obtained for non-aqueous medium can be easily fit to the SFPF model and B_{SFPF} values for the potential function can be obtained and can be compared with those obtained for aqueous system. Also, Sourirajan *et al* [1985] proposed using a pore size distribution function to make the model more realistic and thus more complex in its prediction. The SFPF model without the above simplifications needs special solving techniques which involve complex computer programming.

CHAPTER THREE

Proposed Models for Solvent and Solute Transport

The previous chapter summarized some findings in literature relating to transport studies in non-aqueous medium through polymeric membranes. This chapter will concentrate on outlining our proposed transport models for solute and solvent transport through polymeric membranes in non-aqueous medium.

3.1 Proposed Model for Solvent Transport:

Development of sound theories for solvent transport from a fundamental point of view is critical. One of the objectives of this research is to take into account polymer-solvent interactions and develop a unified semi-empirical model to explain pure solvent transport through solvent-resistant polymeric membranes. The solution-diffusion model uses physical properties of the solvent (such as the diffusion coefficients and the molar volume, for example) and hence will be used as a basis for explaining pure solvent transport [Bhanushali *et al*, 2001].

There have been few attempts in literature to explain pure solvent transport through polymeric membranes. Machado *et al* [1999a, 1999b] have used a resistance-in-series model to explain their pure solvent permeation data. They divided the membrane into three different transport zones viz. the NF surface layer, the UF sublayer and the porous support. They represent their solvent permeation model as:

$$J_{solvent} = \frac{\Delta P}{R_s^0 + R_\mu^1 + R_\mu^2} \qquad 3.1$$

Where, R_s^0, R_μ^1, R_μ^2 are the resistances at the surface of the NF skin layer, through the NF skin layer and through the UF sublayer respectively. The resistance at the skin layer has been related to the mean pore diameter of the membrane and the difference in the surface energy of the membrane and the surface tension of the solvent. The other two resistances however have been related to the pore diameters of the respective sublayers using a typical Hagen-Poiseuille kind of viscous flow approach. The final equation developed by Machado *et al* [1999b] for the solvent flux can be represented as:

$$J_i = \frac{\Delta P}{k_1[(\gamma_c - \gamma_{lv}) + f_1\mu] + f_2\mu} \qquad 3.2$$

Where, f_1 and f_2 are solvent independent parameters characterizing the NF and the UF sublayers and k_1 is a solvent parameter. The best fit values reported by Machado et al, [1999b] for the MPF-50 membrane with several organic solvents were 7.6 m/s and 71.8 m^{-1} respectively. γ_c is the critical surface tension of the membrane material and γ_{lv} is the surface tension of the solvent. The parameters f_1 and f_2 were determined from experimental data as well as from some surface tension measurements.

The model developed by Machado *et al* considers solvent and membrane properties to explain the permeation behavior, however, it uses two adjustable parameters to fit the experimental data. On the other hand, the Solution-Diffusion model can also be used as a basis for explaining pure solvent transport through polymeric membranes. A_i is the pure solvent permeability coefficient (analogous to the pure water permeability in aqueous systems) and is a function of several variables (D_i, c_{if}, V_i, T, K_i) as shown in Equation 2.19. As a first approximation, one can relate the solvent diffusivity in the membrane matrix (D_i) to an easily measurable physical property, the viscosity of the solvent as:

$$\frac{D_i}{T} \propto \frac{1}{\mu} \qquad 3.3$$

Several researchers have used such an approximation. When combined with the original form of the solvent permeability coefficient (Equation 2.19), and using the pure solvent molar volume, V_m, (instead of the partial molar volume, V_i) one can obtain the following equation:

$$J_{solvent} \propto A_i \propto \frac{V_m}{\mu} \qquad 3.4$$

To extend the correlation relating the molar volume and viscosity to the solvent permeability of all the membranes (hydrophobic and water-permeating), incorporation of polymer-solvent interactions is critical. It has already been shown that the Flory-Huggins interaction parameter, the sorption value and the membrane surface energy can be used to express such an interaction. For example, somewhat hydrophilic polymers like aromatic polyamide posses relatively high surface energy (38 to 43 dyne /cm surface energy) as compared to hydrophobic polymeric materials like siloxanes which are considerably low-energy materials (14-18 dyne /cm surface energy). Thus it would be expected that non-polar solvents (alkanes) would be preferentially transported over the polar solvents (alcohols) through low-energy membrane materials. In fact, Paul *et al* [1970] have demonstrated this by using uncrosslinked natural rubber membranes. They reported the n-hexane flux to be four times that of methyl iso-butyl ketone (MIBK) at 6.7 bar through a hydrophobic low-energy material (natural rubber). Low energy membranes can give higher solvent permeation rates than that of water as has been pointed out earlier. Thus a general comment about the relation of the flux of organic solvents with the surface energy can be made as follows:

$$J_{solvent} \propto A_i \propto \frac{1}{\gamma_{sv}} \qquad 3.5$$

Eventually, when combined with the other properties of the system (Equation 2.19 and 2.25), one could relate the solvent permeability for different membranes as:

$$J_{solvent} \propto A_i \propto \left(\frac{V_m}{\mu}\right) \times \left(\frac{1}{\gamma_{sv}}\right) \qquad 3.6$$

As one would expect, γ_{sv} by itself does not provide complete information on polymer-solvent interactions. Also, orientation of the polymer groups on the surface can influence the performance of the membrane. However, those changes would be reflected in the variations in the contact angles for the solvents used and consequently the surface energy of the membrane. Relevant correlation plots with the above variables and model verification plots will be discussed in the Results and Discussion section.

3.2 Proposed Model for Solute Transport:

The literature-based models used widely for aqueous systems contain adjustable parameters (usually lumped) which have little physical significance and can be used to fit the experimental data. The Solution-Diffusion model, for example, fails to consider the dependence of the solute flux on the type of solvent thus neglecting the convective coupling. The Spiegler-Kedem model gives more insight into the convective and diffusive components of the solute flux, but cannot be used as a predictive tool. The pore flow models suffer from a major disadvantage that several assumptions are questionable and complex programming is required in order to fit the experimental data. Most of the above models fail to incorporate the physical properties of the solvent and solute in their

3.1 (a)

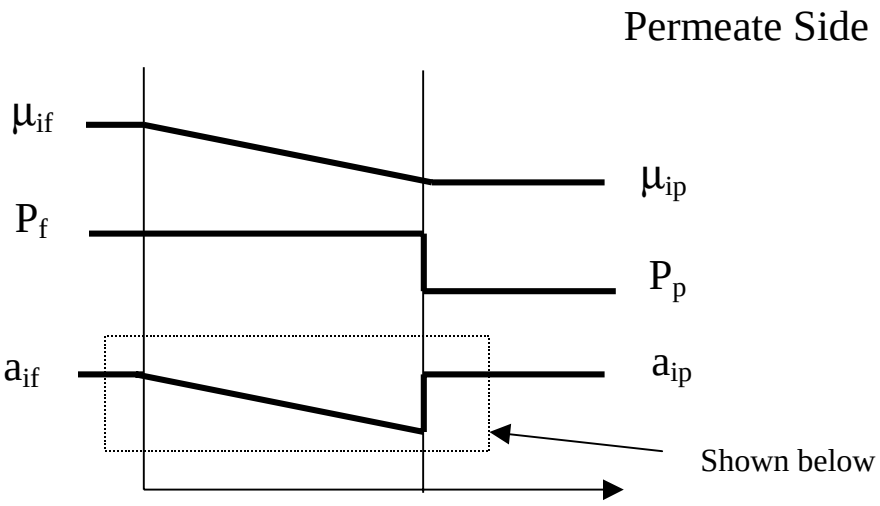

3.1 (b)

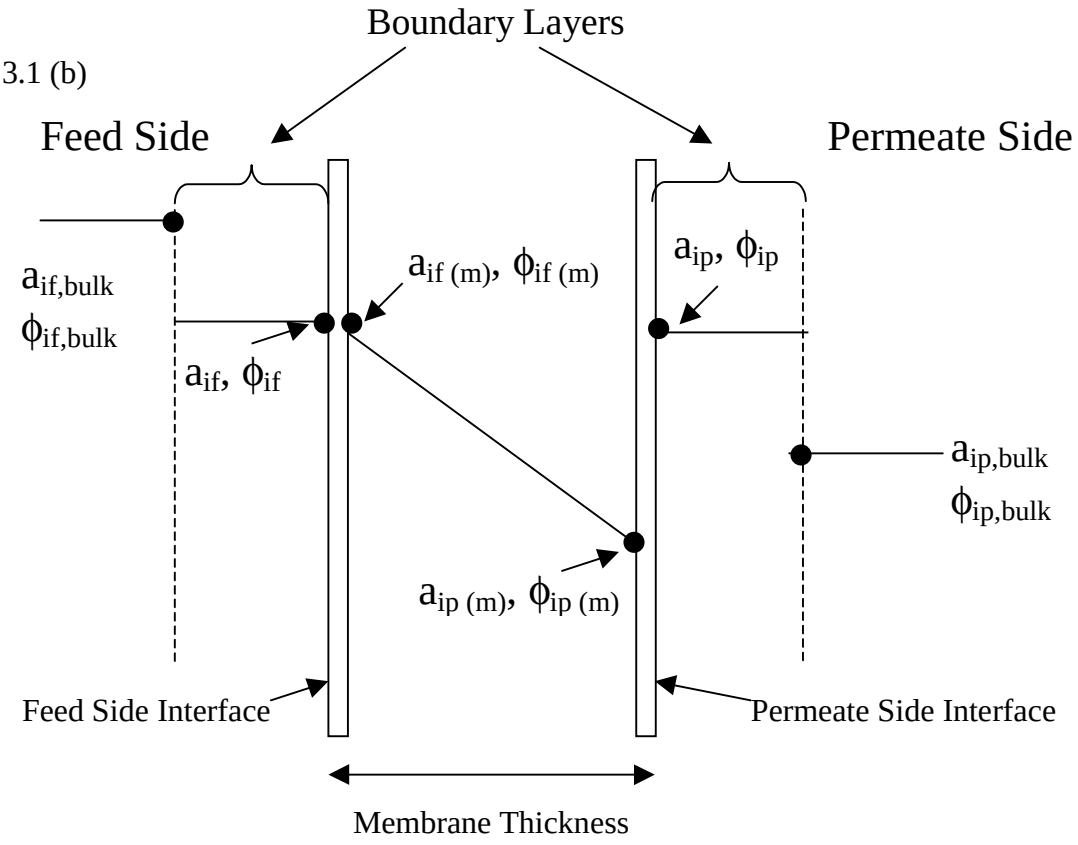

Figure 3.1: Schematic for the proposed solute transport model (3.1(a)) and definitions of the various species activity and species volume fractions (3.1(b)).

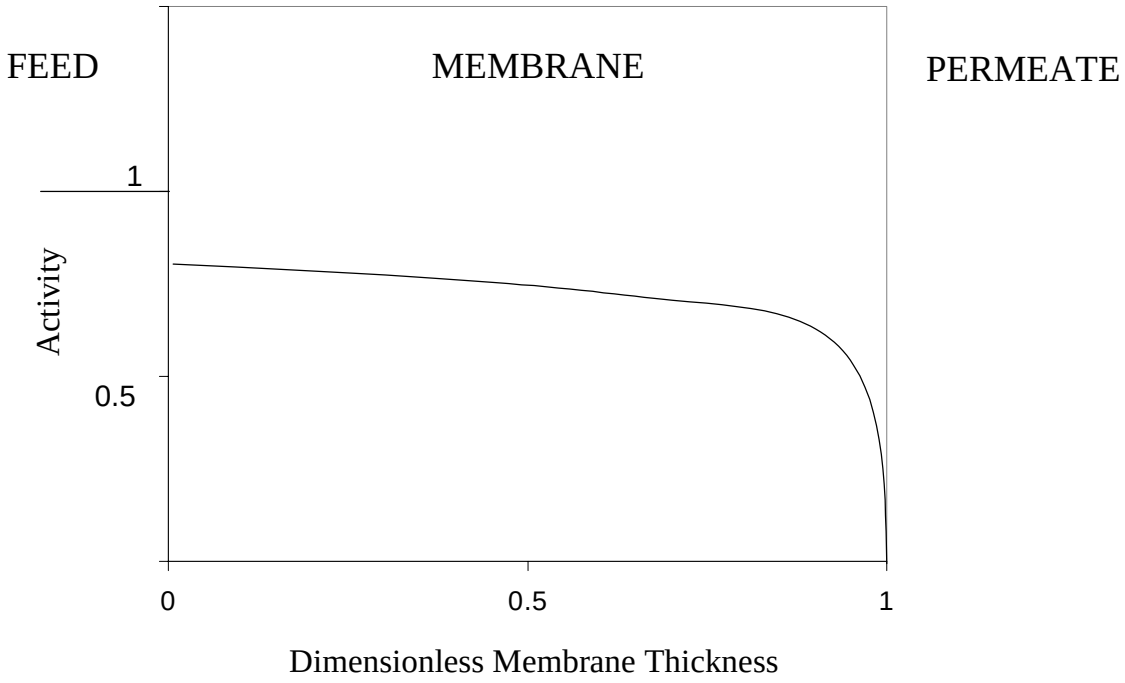

Figure 3.2: Activity Profile for the binary system ethanol-cellulose acetate (taken from Mulder et al [1985])

overall modeling effort. Since one of the primary research goals is to develop a unified transport theory to explain solute transport, a simple model based on a chemical potential gradient is proposed here. This model can be solved with relative ease using the numerical techniques for solving systems of differential equations. The model contains two adjustable parameters, the solvent and the solute diffusion coefficients through the membrane, and can be used as a predictive tool if the values of these parameters can be related to the solvent/solute properties. Figure 3.1a shows a visualization of the proposed model. The activity and volume fractions shown in the figure are all at the membrane interfaces and not the bulk solution. Towards the development of this model, the following assumptions are made:

a. The pressure across the membrane is a constant and is assumed to be equal to the applied pressure on the feed side (similar to the Solution-Diffusion-based models). This implies that there is a discontinuous boundary condition on the permeate side interface since the permeate side is essentially at atmospheric pressure.

b. The species present in the feed solution partition into the membrane phase from the bulk phase. These partitioning values are specified as volume fractions at the interface and can be obtained from experimental measurements or from theoretical calculations. This allows for elimination of any boundary resistances. For example, Mulder *et al*, [1985] have proved from theoretical measurements and calculations that boundary resistances can cause a discrepancy in the activities of the species. Figure 3.2, for example, compares the activity variation for an ethanol-cellulose acetate binary system under pervaporative driving force. Although the system is a pervaporative system, the feed side is not under any vacuum and pure ethanol liquid

is in contact with the cellulose acetate membrane. It can be clearly seen that the bulk activity of ethanol (which is essentially equal to unity) is not the same as that on the membrane surface. This analogy can be extended to a pressure-driven operation, since both the feed and permeate sides are in liquid phase. Thus to avoid such a discrepancy, the partitioning values for the two species will be imposed on both the feed and permeate side membrane interfaces and these values will then be used to determine the activity gradient for separation.

c. Feed solutions are dilute in the solute concentration and hence the diffusion coefficients are assumed to be independent of concentration.

Using the chemical potential gradient of the species as the driving force for transport, one can get a simple Fick's Law type equation which can be given by [Mulder and Smolders, 1984]:

$$J_i = -\phi_i B_i \frac{d\mu_i}{dz} \qquad 3.7$$

where, J_i is the flux of species i, B_i is the mobility of species i, μ_i chemical potential of species i and ϕ_i Volume fraction of species i. The chemical potential can be easily related to the activity of the species across the membrane and since the pressure across the membrane is assumed to be constant and equal to the applied pressure, one can obtain,

$$J_i = -\phi_i B_i R_g T \frac{d \ln a_i}{dz} \qquad 3.8$$

To account for coupling of the species fluxes, the activity of the species can be made dependent on that of the other in solution. Thus,

$$a_i = f(\phi_i, \phi_j) \qquad 3.9$$

The general flux equation for the species 1 then can be written as:

$$J_1 = -\phi_1 B_1 R_g T \left(\frac{\partial \ln a_1}{\partial \phi_1} \times \frac{d\phi_1}{dz} + \frac{\partial \ln a_1}{\partial \phi_2} \times \frac{d\phi_2}{dz} \right) \qquad 3.10$$

Similar equation for the species 2 can also be written as:

$$J_2 = -\phi_2 B_2 R_g T \left(\frac{\partial \ln a_2}{\partial \phi_1} \times \frac{d\phi_1}{dz} + \frac{\partial \ln a_2}{\partial \phi_2} \times \frac{d\phi_2}{dz} \right) \qquad 3.11$$

Rearranging the above set of equations, one can get two differential equations for the variation of the volume fractions across the membrane thickness.

$$\frac{d\phi_1}{dz} = \frac{\phi_1 (B_1 R_g T) \frac{\partial \ln a_1}{\partial \phi_2} J_2 - \phi_2 (B_2 R_g T) \frac{\partial \ln a_2}{\partial \phi_2} J_1}{\phi_1 \phi_2 (B_1 R_g T)(B_2 R_g T) \left(\frac{\partial \ln a_1}{\partial \phi_1} \frac{\partial \ln a_2}{\partial \phi_2} - \frac{\partial \ln a_1}{\partial \phi_2} \frac{\partial \ln a_2}{\partial \phi_1} \right)} \qquad 3.12$$

$$\frac{d\phi_2}{dz} = \frac{\phi_2 (B_2 R_g T) \frac{\partial \ln a_2}{\partial \phi_1} J_1 - \phi_1 (B_1 R_g T) \frac{\partial \ln a_1}{\partial \phi_1} J_2}{\phi_1 \phi_2 (B_1 R_g T)(B_2 R_g T) \left(\frac{\partial \ln a_1}{\partial \phi_1} \frac{\partial \ln a_2}{\partial \phi_2} - \frac{\partial \ln a_1}{\partial \phi_2} \frac{\partial \ln a_2}{\partial \phi_1} \right)} \qquad 3.13$$

The above set of equations can be normalized with respect to membrane thickness for ease of comparison. A similar treatment has been used for explaining the transport results for pervaporation polymeric membranes by Shah, [2001]. The next step is to use suitable activity coefficient theories to relate the activity of the species to its volume fraction.

3.2.1 Activity Coefficient Models:

The activities of the solute and solvent species in the above equations are in the membrane phase and have to be related to their respective volume fractions. There are several theories that can be used to relate the activity of species to the volume fraction in

a polymer-solvent-solute system. In this section, the classical Flory-Huggins theory and the modern group contribution UNIFAC model will be discussed in a little more detail. The reason for using the UNIFAC theory is because it has been established as a sophisticated group-contribution model which can be extended to polymeric solutions and can be used for systems where experimental equilibrium data is not available.

3.2.1.1 Flory-Huggins Theory:

Flory-Huggins theory was one of the first theories developed to explain the thermodynamics of polymer solutions [Danner *et al*, 1993]. The application of this theory to obtain polymer-solvent interactions has already been expressed in a previous section [Section 2.3.3.1]. For ternary systems, the Flory-Huggins theory can be used as a first approximation to the problem. One of the distinct advantages of choosing this theory is that it takes into account the interaction between all the three components of the ternary system involving the solvent (1), solute (2) and the polymer (3). The relevant equations for this theory can be given by [Mulder and Smolders, 1984]:

$$\ln a_1 = \ln\phi_1 + (1-\phi_1) - \phi_2\left(\frac{V_1}{V_2}\right) - \phi_3\left(\frac{V_1}{V_3}\right) + (\chi_{12}\phi_2 + \chi_{13}\phi_3)\times(\phi_3+\phi_2) - \chi_{23}\left(\frac{V_1}{V_2}\right)\phi_2\phi_3 \qquad 3.14$$

$$\ln a_2 = \ln\phi_2 + (1-\phi_2) - \phi_2\left(\frac{V_2}{V_1}\right) - \phi_3\left(\frac{V_2}{V_3}\right) + \left(\chi_{12}\phi_2\left(\frac{V_2}{V_1}\right) + \chi_{23}\phi_3\right)\times(\phi_3+\phi_1) - \chi_{13}\left(\frac{V_2}{V_1}\right)\phi_1\phi_3 \qquad 3.15$$

where, χ_{mn} are the Flory-Huggins interaction parameters between species m and n, V_i is the molar volume of species i, a_i is the activity of species i, ϕ_i is the volume fraction of

species i. Another advantage of using the above theory is that it embeds solvent and solute physical properties such as molar volume for the calculation of the activity. This enables extension of the model to various solvents, solutes and membranes which may lead to different interactions.

Evaluating the partial derivatives and using Equation 3.12 and Equation 3.13, two differential equations for the variation of the volume fractions across the membrane thickness can be obtained:

$$\frac{d\phi_1}{dz} = \frac{k_{2,2} \times J_1 - k_{1,2} \times J_2}{k_{1,1} \times k_{2,2} - k_{2,1} \times k_{1,2}} \tag{3.16}$$

$$\frac{d\phi_2}{dz} = \frac{k_{2,1} \times J_1 - k_{1,1} \times J_2}{k_{2,1} \times k_{1,2} - k_{1,1} \times k_{2,2}} \tag{3.17}$$

where,

$$k_{1,1} = -\phi_1 B_1 R_g T \left[2\chi_{13}\phi_1 + \left(\chi_{13} - \chi_{12} + \chi_{23} \frac{V_1}{V_2} \right) \phi_2 - 1 - 2\chi_{13} + \frac{1}{\phi_1} \right] \tag{3.18}$$

$$k1,2 = \phi_1 B_1 R_g T \left[\left(\chi_{13} - \chi_{12} + \chi_{23} \frac{V_1}{V_2} \right) \phi_1 + \left(\chi_{23} \frac{V_1}{V_2} \right) \phi_2 + \chi_{12} - \chi_{13} - \chi_{23} \frac{V_1}{V_2} - \frac{V_1}{V_2} \right] \tag{3.19}$$

$$k_{2,1} = -\phi_2 B_2 R_g T \left[\left(\chi_{13} + \chi_{13} \frac{V_1}{V_2} \right) \phi_1 + \left(\chi_{23} + \chi_{13} - \chi_{12} \frac{V_2}{V_1} \right) \phi_2 - \frac{V_2}{V_1} + \chi_{12} \frac{V_2}{V_1} - \chi_{23} - \chi_{13} \right] \tag{3.20}$$

$$k_{2,2} = -\phi_2 B_2 R_g T \left[2\chi_{23}\phi_2 + \left(\chi_{23} + \chi_{13} - \chi_{12} \frac{V_2}{V_1} \right) \phi_1 + 1 - 2\chi_{13} + \frac{1}{\phi_2} \right] \tag{3.21}$$

3.2.1.2 UNIFAC Group Contribution Activity Coefficient Models:

The introduction and success of the concept of "local composition" through the Wilson equation to correlate vapor-liquid equilibrium data triggered the development of several models such as NRTL (Non-Random Two Liquid) theory and the UNIQUAC (UNIversal QUAsi Chemical) group contribution theory [Smith and Van Ness, 1987]. The UNIQUAC equation was proposed by Abrams and Prausnitz [1975] and treats the excess free energy as a combination of two parts; a "combinatorial" part (to consider molecular size and shape differences) and a "residual" part (to account for molecular interactions) [Poling *et al*, 2001].

$$g^E = g^E(combinatorial) + g^E(residual) \qquad 3.22$$

In terms of the activity coefficient, the UNIQUAC equation can be given as [Poling *et al*, 2001]:

$$ln\,\gamma_i = ln\,\gamma_i^C + ln\,\gamma_i^R \qquad 3.23$$

where,

$$ln\,\gamma_i^C = ln\frac{\phi_i}{x_i} + \frac{z}{2} q_i\, ln\frac{\Theta_i}{\phi_i} + l_i - \sum_j \phi_i \frac{r_i}{r_j} l_j \qquad 3.24$$

$$ln\,\gamma_i^R = q_i\left[1 - ln\left(\sum_j \Theta_j \tau_{ji}\right) - \sum_j \frac{\Theta_j \tau_{ij}}{\sum_k \Theta_k \tau_{kj}}\right] \qquad 3.25$$

$$l_i = \frac{z}{2}(r_i - q_i) - (r_i - 1) \qquad 3.26$$

$$\Theta_i = \frac{\phi_i \left(\frac{q_i}{r_i} \right)}{\sum_j \phi_j \left(\frac{q_j}{r_j} \right)} \qquad 3.27$$

In the above set of equations, z is the co-ordination number (usually 10), ϕ_i and Θ_i are the volume and surface fractions defined for species i and τ_{ij}'s are the binary interaction parameters. The parameters r_i and q_i are measures of van der Waals volume and molecular surface areas respectively and can be obtained from literature. The binary interaction parameters are two adjustable parameters and are typically obtained from vapor-liquid or liquid-liquid equilibrium data. Heintz and Stephan [1994] have applied the UNIQUAC equation to a pervaporation system of two solvents and a membrane to predict the mixture solubilities in the active layer of the dense membranes used. The membranes used for their studies were poly(vinyl alcohol) based and they were successful in obtaining the UNIQUAC binary interaction parameters for the system studied. However, an extension of the UNIQUAC treatment to systems for which literature data is not available, it becomes necessary to use the UNIFAC model which allows for the computation of the interactions between species based on a functional group approach.

The UNIFAC method (UNIQUAC Functional group Activity Coefficient) is based on the UNIQUAC equation but is used for systems where experimental data is not available as has been mentioned above. The UNIFAC method uses the combinatorial part of the UNIQUAC equation (Equation 3.24) directly and the parameters r_i and q_i are obtained as a sum of the group volume and area parameters, R_k and Q_k respectively [Poling *et al*, 2001].

$$r_i = \sum_{k\ groups} v_k^{(i)} R_k \qquad 3.28$$

$$q_i = \sum_{k\ groups} v_k^{(i)} Q_k \qquad 3.29$$

The group parameters R_k and Q_k are calculated using the van der Waals group volume and surface areas and can be obtained from literature. The residual part of the activity coefficient for UNIFAC can be given by [Poling *et al*, 2001]:

$$\ln \gamma_i^R = \sum_k v_k^{(i)} \left(\ln \Gamma_k - \ln \Gamma_k^{(i)} \right) \qquad 3.30$$

where Γ_k is the group residual activity coefficient and $\Gamma_k^{(i)}$ is the residual activity coefficient of group k in a reference solution containing molecules of type i. These group residual activity coefficients can be obtained from the following equation:

$$\ln \Gamma_k = Q_k \left[1 - \ln \left(\sum_m \theta_m \Psi_{mk} \right) - \sum_m \frac{\theta_m \Psi_{km}}{\sum_n \theta_n \Psi_{nm}} \right] \qquad 3.31$$

where Ψ_{mn} is the group interaction parameter (similar to the τ_{ij} in UNIQUAC equation) and can be given by [Poling *et al*, 2001]:

$$\varnothing_{mn} = exp\left(- \frac{U_{mn} - U_{nm}}{R_g T} \right) = exp\left(- \frac{a_{mn}}{T} \right) \qquad 3.32$$

The a_{mn} values can be obtained from several databases available for a large number of groups and the basis of the method is that it can be applied to a particular system by breaking the species involved into subgroups. Fredenslund [1989] has summarized the advances in the UNIFAC method since its conception by Abrams and

Prausnitz in the mid 70s. It has been applied for design of chemical processes, flash calculations etc. because of the vast availability of reliable group interaction parameters.

3.2.2 Solution Technique:

Figure 3.1 shows the schematic for the proposed model. The first step is to obtain the boundary conditions for solving the differential equations developed for the variation of the volume fractions.

3.2.2.1 Calculation of the Boundary Conditions:

Figure 3.1b shows the definitions of the activities and the volume fractions used for the model. It needs to be reiterated that a primary assumption used in the calculation of the boundary conditions is that the membrane partitioning for the permeating species remains the same on the feed side and the permeate side membrane interfaces (shown as boundary layers). These species volume fractions at the membrane interfaces on the feed and permeate side are the partitioning values and these volume fractions need to be specified, as discussed in the model assumptions, thus making $\phi_{if} = \phi_{ip}$. It needs to be noted that these values are NOT the bulk phase values ($\phi_{if,bulk}$ and $\phi_{ip,bulk}$) and are used to eliminate boundary resistance effects. The essential driving force is induced by the difference in the activities within the membrane, i.e. $a_{if\,(m)}$ (thus $\phi_{if\,(m)}$) and $a_{ip\,(m)}$ (thus $\phi_{ip\,(m)}$). The goal is to obtain the volume fractions of the solute and the solvent on the membrane side at the permeate-membrane interface (i.e. $\phi_{ip(m)}$). Since there is no pressure gradient at the feed side interface, the two activity values are essentially equal. Thus,

$$a_{if} = a_{if(m)} \qquad 3.33$$

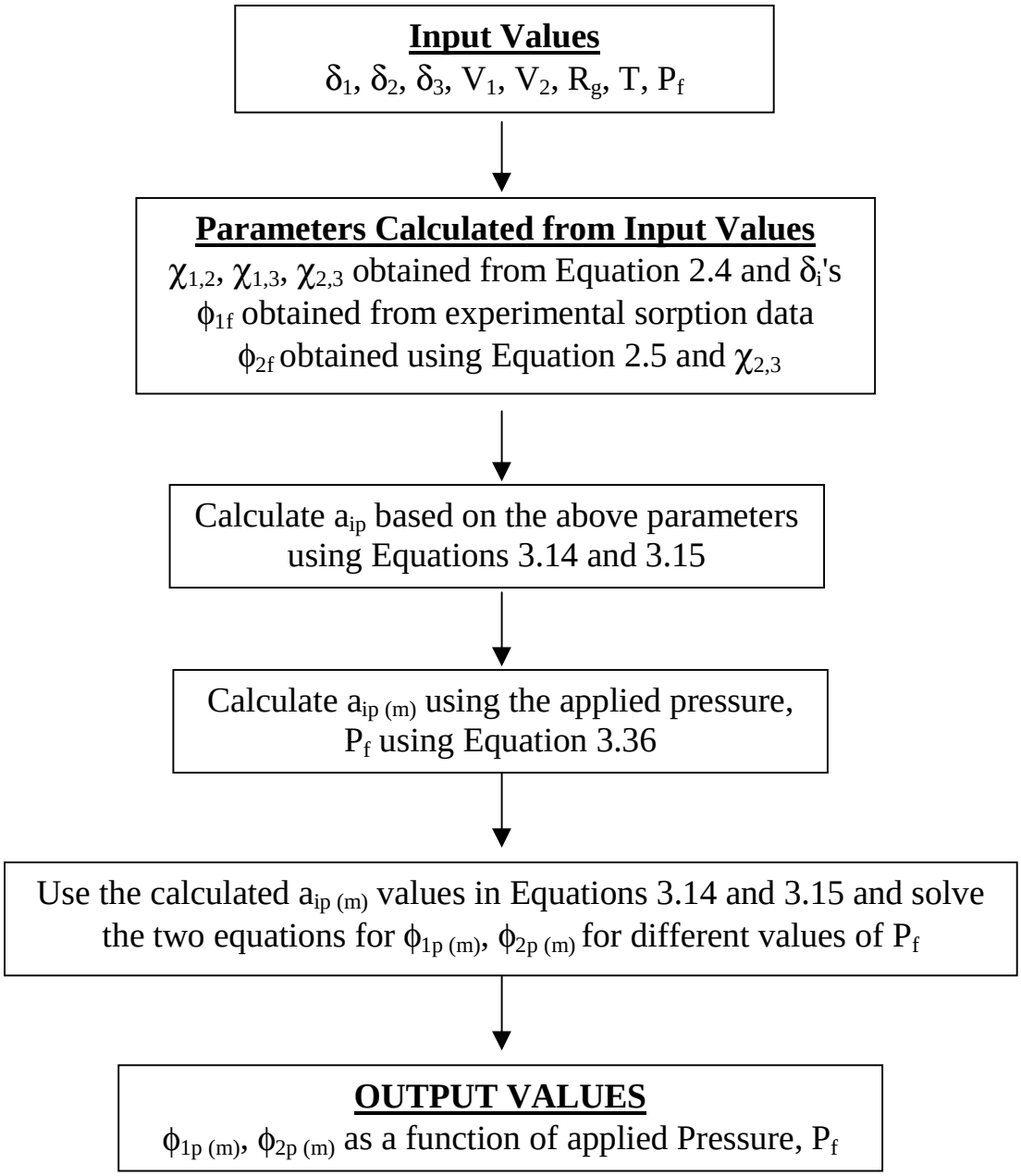

Figure 3.3: Algorithm used for obtaining boundary conditions using the Flory-Huggins Theory

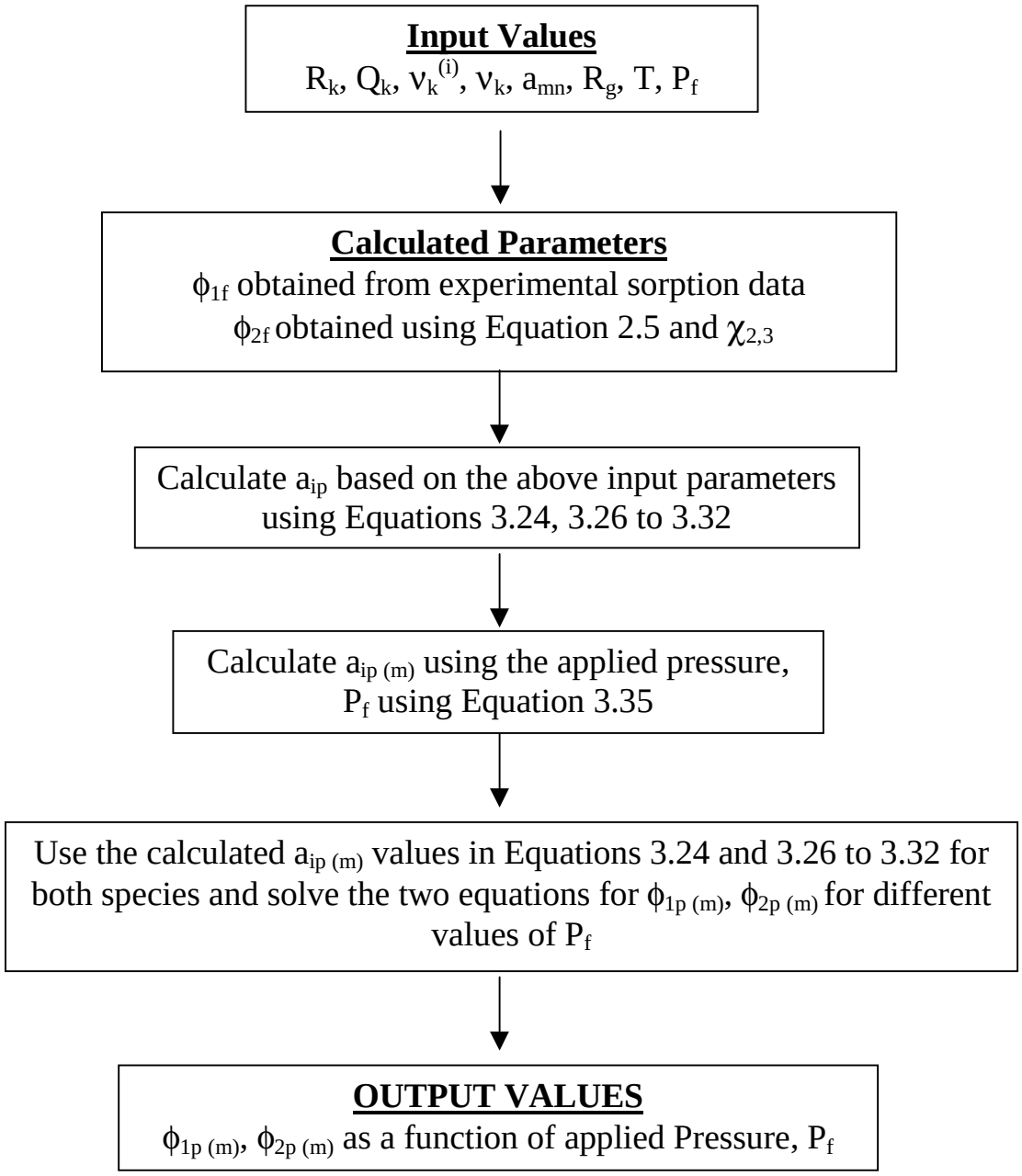

Figure 3.4: Algorithm used for obtaining boundary conditions using the UNIFAC Theory

This implies that in terms of the volume fractions, $\phi_{if} = \phi_{if\,(m)}$. However, on the permeate side, because of the discontinuity in the pressure, the following equation applies:

$$\mu^0{}_i + R_g T \ln a_{ip} + V_i\left(P_p - P^0\right) = \mu^0{}_i + R_g T \ln a_{ip(m)} + V_i(P_f - P^0) \qquad 3.34$$

where μ_i^0 is the standard chemical potential of species i at reference pressure P^0 and temperature T. For the case of the solvent species, the standard state can be defined as the pure solvent. For the solute case, there are two possible standard states that can be defined: the pure solute state at reference pressure P^0 and temperature T, or the infinite dilution state under the reference conditions. Under the infinite dilution state, a new activity coefficient needs to be defined so that the modified activity coefficient approaches unity as the solute concentration approaches zero [Tester and Modell, 1996]. Thus,

$$a_{ip(m)} = exp\left[\ln a_{ip} + \frac{V_i}{R_g T}\left(P_p - P_f\right)\right] \qquad 3.35$$

Figure 3.3 and Figure 3.4 show the algorithms used to obtain the boundary conditions for the Flory-Huggins theory and the UNIFAC-based theory. The following additional assumptions are made:

a. The solvent volume fraction value, ϕ_{1f} can be obtained using experimental sorption data. In the absence of experimental sorption values, the Flory-Rehner approach (Equation 2.5) can be used.
b. For the case of solutes also, the Flory-Rehner approach (Equation 2.5) can be used to obtain the values for $\phi_{2f\,(m)}$.

For simplicity, the species have been numbered as solvent = 1; solute = 2 and membrane = 3. The essential steps involved in the algorithm for the Flory-Huggins approach are as follows (Figure 3.3):

1. The input values for this approach are the species solubility parameters (δ_i's), R_g, temperature (T), the species molar volumes (V_1, V_2) and feed side applied pressure (P_f).
2. The Hildebrand Solubility Parameter approach (Equation 2.4) can been used to obtain the interactions parameters ($\chi_{1,2}$, $\chi_{1,3}$, $\chi_{2,3}$) using the solute, solvent and membrane solubility parameters (δ_i's). Although some discrepancies of the one-parameter Hildebrand approach have been pointed out in Section 2.3.3.1.1.1, it has been used successfully for hydrophobic materials and non-polar solvents. Experimental values for the interaction parameters can be used directly if available.
3. Use the specified volume fractions (partitioning values) on the permeate side to calculate the species activities (a_{ip}) from the Flory-Huggins equations (Equations 3.14 and 3.15).
4. Use Equation 3.35 with the desired applied pressure (P_f) and calculate the activity at the permeate side membrane interface, $a_{ip,m}$.
5. Solve the two activity equations for the Flory-Huggins theory (Equations 3.14 and 3.15) simultaneously using numerical techniques to obtain $\phi_{1p,m}$ and $\phi_{2p,m}$.

The algorithm used for the UNIFAC approach is similar to the Flory-Huggins approach but differs in the input parameters. The steps involved are as follows:

1. For the UNIFAC theory, the required input parameters are: the group area and volume parameters (R_k, Q_k respectively), the number of groups of type k in species i

($\nu_k^{(i)}$), the total number of groups of type k present in the system (ν_k) and the group interaction parameter (a_{mn}).

2. Use the specified volume fractions (partitioning values) on the permeate side to calculate the species activities (a_{ip}) from the UNIFAC equations (Equations 3.24 and Equations 3.26 to 3.32).
3. Use Equation 3.35 with the desired applied pressure (P_f) and calculate the activity at the permeate side membrane interface, $a_{ip,m}$.
4. Solve the two activity equations for the UNIFAC theory (Equations 3.24 and Equations 3.26 to 3.32) simultaneously using numerical techniques to obtain $\phi_{1p,m}$ and $\phi_{2p,m}$.

3.2.2.2 Calculation of Solute Separation:

The parameter B_iR_gT has been used as the species diffusivity (D_i) by several researchers [Mulder *et al*, 1984] and can be determined from independent experiments. However, in this study, the solute and solvent diffusion coefficients will be used as adjustable parameters to fit the experimental data. Using the diffusion coefficients obtained from this exercise, a correlation relating the solute diffusivity to its properties can be developed which can further be used for obtaining solute diffusion coefficients for which experiments were not performed. This would enable the use of the model as a predictive system. The algorithm for the prediction of the solute transport is shown in Figure 3.5.

1. The input values required for the boundary conditions need to be used for the solute separation. The input parameters for solute separation are the experimental solvent

flux (obtained from permeation data) and the experimental solute flux (obtained from permeation data).

2. Assume values for D_1 (solvent diffusion coefficient) and D_2 (solute diffusion coefficient)
3. Calculate $\phi_{1p,m}$ and $\phi_{2p,m}$ using the two differential equations (Equation 3.12 and Equation 3.13).
4. Compare the $\phi_{1p,m}$ and $\phi_{2p,m}$ values calculated from Step 3 with the boundary conditions (for a given Activity Coefficient Theory) for the chosen applied pressure. If the values match (within accuracy limits) then the correct solute diffusion coefficient and solvent diffusion coefficient have been reached and the iteration should be terminated. If the values do not match, goto Step 2 and repeat the calculation.

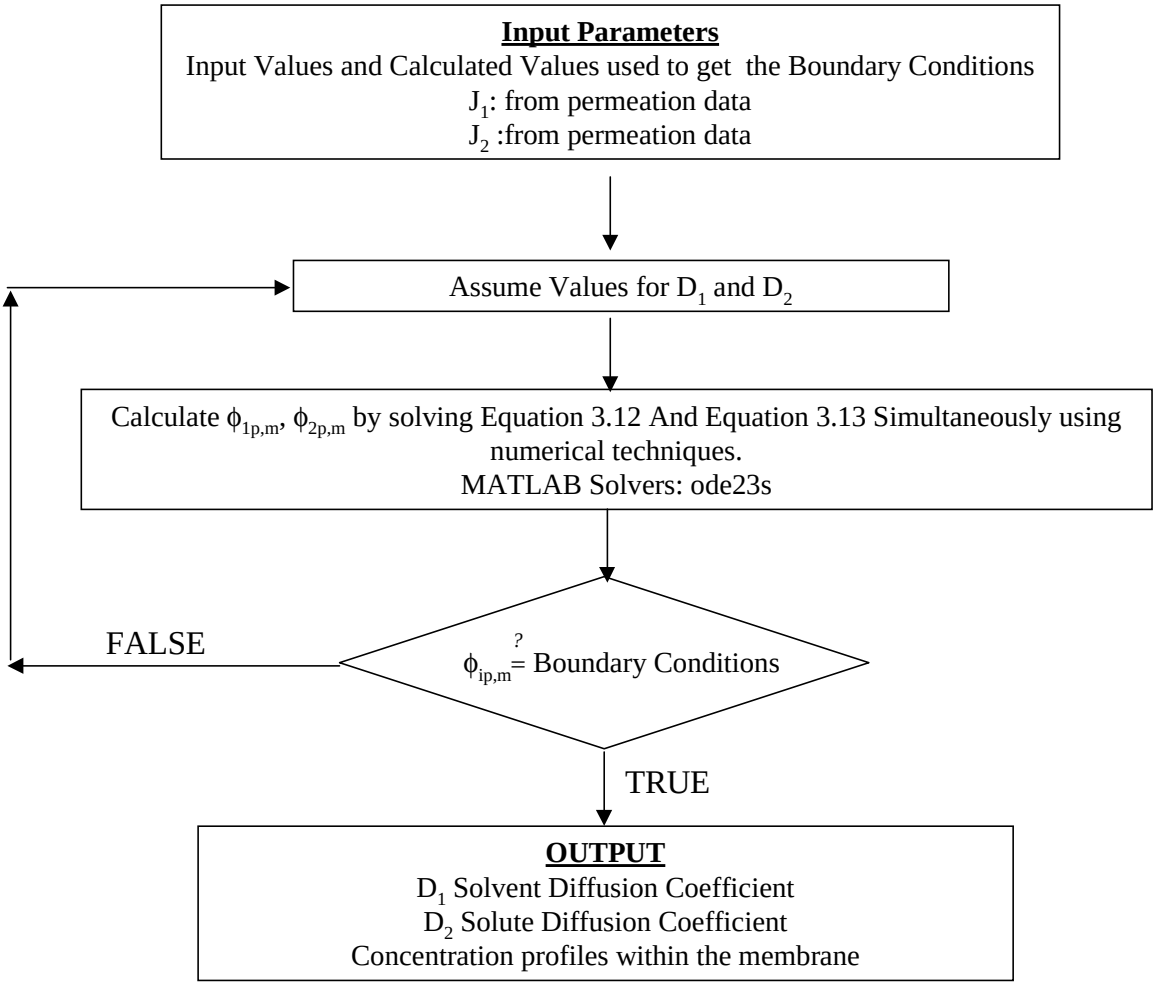

Figure 3.5: Algorithm used for predicting the solute separation using the boundary conditions obtained using the algorithms in Figure 3.3 and 3.4

CHAPTER FOUR

Experimental Methods and Analysis

Reverse Osmosis/Nanofiltration (RO/NF) experiments were performed using different solute-solvent-membrane systems. Since one of the research goals is to understand pure solvent transport, several organic solvents with different polarities were tested with various commercial and developmental polymeric membranes. Solutes for separation and diffusion studies were selected on the basis of solubility in the solvents of interest and ease of analysis. This section will cover the details of the solvent-solute-membrane systems studied, experimental protocols for solute and solvent transport studies, details of the diffusion cell measurements and the analytical techniques used.

4.1 Materials:

4.1.1 Solvents:

The solvents used for the study were alcohols and alkanes. Among the alcohols, methanol, ethanol and isopropanol were used. Pentane, hexane, octane and decane were the non-polar alkanes that were used. All solvents were analytical grade (99+ %) and were supplied by Mallinckroft, Sigma-Aldrich or Fischer Scientific.

4.1.2 Solutes:

The solutes used in the studies were organic in nature having reasonable solubility in organic solvents mentioned above. For solute rejection studies four compounds were used. The first is a 380 MW dye called Sudan IV (Figure 4.1a). Sudan IV has aromatic

4.1(a)

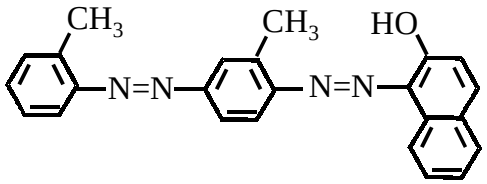

4.1(b)

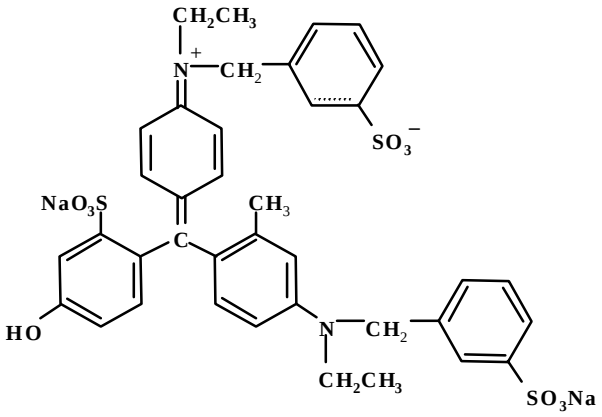

4.1(c)

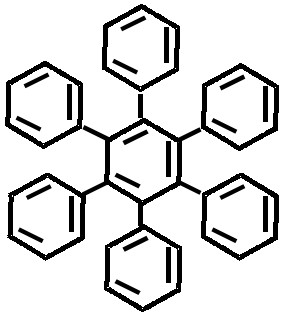

4.1(d)

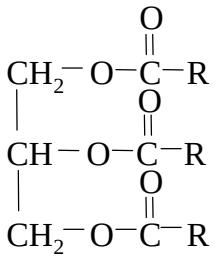

Figure 4.1: Structures of organic solutes used for solute separation studies (a) Sudan IV (384 MW organic dye); (b) Fast Green FCF (808 MW organic dye); (c) Hexaphenyl benzene (534 MW); (d) General Structure of Triglyceride

Table 4.1: Physical Properties of the solutes used for our study (Solubility Parameters were calculated using group contribution methods highlighted in [Sourirajan et al, 1985])

Solute	Molecular Weight	Solubility Parameter (M. Pa)$^{0.5}$
Organic solutes		
Sudan IV	384	22.3
Hexaphenyl Benzene	534	19.4
Fast Green FCF	808	16.4
Triglycerides		
C 10 (Tricaprin)	554	19.23
C 12 (Trilaurin)	639	18.98
C 14 (Trimyristin)	723	18.81
C 16 (Tripalmitin)	807	18.66
C 18 (Tristearin)	890	18.55

groups and also azo groups which impart it solubility in a wide range of solvents. The dye has a red color in all the solvents and it absorbs in the visible range at a wavelength of 510 nm. Due to the organic nature of the dye, low concentrations (~10 to 20 mg/l) of the dye were used because of solubility constraints.

The second is an 800 MW dye called Fast Green FCF (Figure 4.1b). The dye has several hydrophilic groups and is charged due to the presence of sulfonic acid groups along with aromatic groups. It has a strong green color at low concentration in polar solvents and has an absorbance peak at 610 nm in the visible range.

The third compound used was Hexaphenyl Benzene (534 MW) and was chosen because of its rigid structure (Figure 4.1c). It has a limited solubility in hexane, but gives a strong absorbance in the UV range at about 249 nm.

Along with these organic solutes, triglycerides were also used for rejection studies. Triglycerides are available in molecular weights from 218 MW (C2) and higher. The primary reason for selecting triglycerides was to establish the dependence of molecular size on the rejection behavior with non-polar solvents. The triglycerides used for the study were C10, C12, C14, C16 and C18. Figure 4.1d shows the general structure of the triglycerides.

Apart from the above-mentioned solutes, sodium chloride, benzocaine and phenol were also used for the diffusion studies. All the above mentioned solutes were obtained from Sigma-Aldrich Co. Table 4.1 summarizes the properties of the solutes used for the separation and diffusion studies. The solubility parameters for the solutes were obtained using the group contribution method outlined in Sourirajan et al [1985].

Table 4.2: Membranes used and their properties

Commercial Name	Remarks
DS 11 AG (Osmonics)	• Commercially available composite polyamide based RO membrane. • 2000 ppm NaCl rejection > 99%
Membrane D (Osmonics)	• Developmental composite dimethylsilicone NF membrane
PS 18 (Osmonics)	• Developmental composite dimethylsilicone NF membrane • Higher hexane flux than Membrane D
MPF 50 (Koch)	• Silicone based NF membrane • Erythromycin (MW 734) rejection in ethyl acetate > 90 %
YK (Osmonics)	• AP based charged NF membrane • MgSO4 rejection > 99%

4.1.3. Membranes:

Membranes used for the study ranged from traditional reverse osmosis and nanofiltration membranes used for aqueous systems to some developmental membranes suited for non-aqueous systems supplied by Osmonics, Inc. and Koch Membrane Systems. Table 4.2 summarizes the membranes and their properties. Most of the experimental results were obtained with the Osmonics Membrane D and Osmonics YK membrane. Few experiments were also performed with the PS 18 membrane which was developed by Osmonics. This membrane had a higher flux of n-hexane as compared to Membrane D. As shown in the table, the membrane D is a siloxane-based developmental membrane supplied by Osmonics. Thus, characterization procedures for this membrane had to be developed for this work and will be discussed in a later section. Figure 4.2 shows the Scanning Electron Microscope (SEM) image of the Membrane D cross-section. From the SEM image, it can be seen that the membrane is a composite membrane with a thickness of about 0.6 microns. The DS-11 AG and the YK membranes are solvent-resistant membranes suitable for aqueous systems and have been characterized using salt rejections in aqueous medium.

4.2 Apparatus:

4.2.1 Membrane Permeation Cells:

There were three cells on which permeation data was obtained. The system however consisted of pressurizing the cells using nitrogen gas. Zero grade nitrogen was used for the experiments. The first cell used a membrane area of 143 cm^2 and had a solution capacity of about 2 liters. The second cell is a Sepa ST® cell supplied by

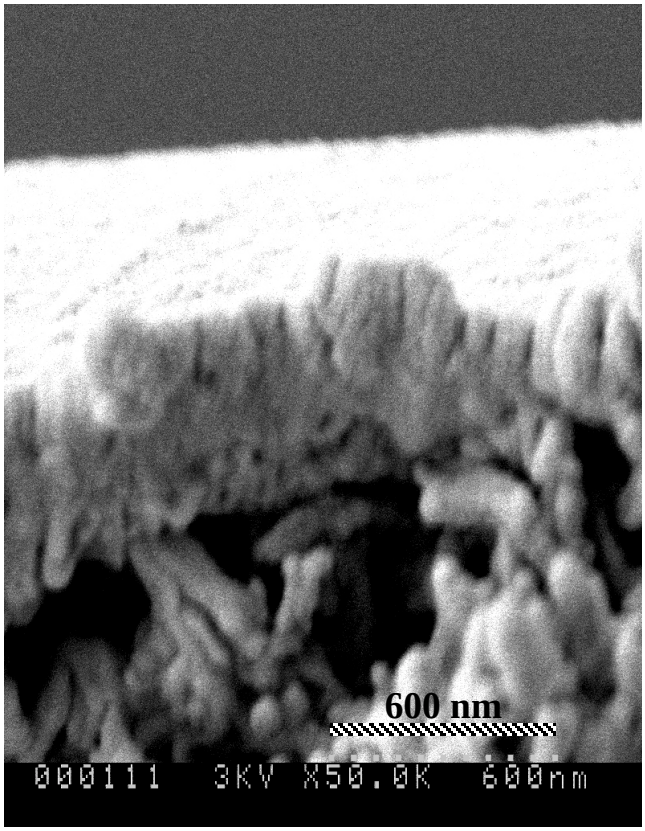

Figure 4.2: SEM picture of Membrane D cross-section

4.3 (a)

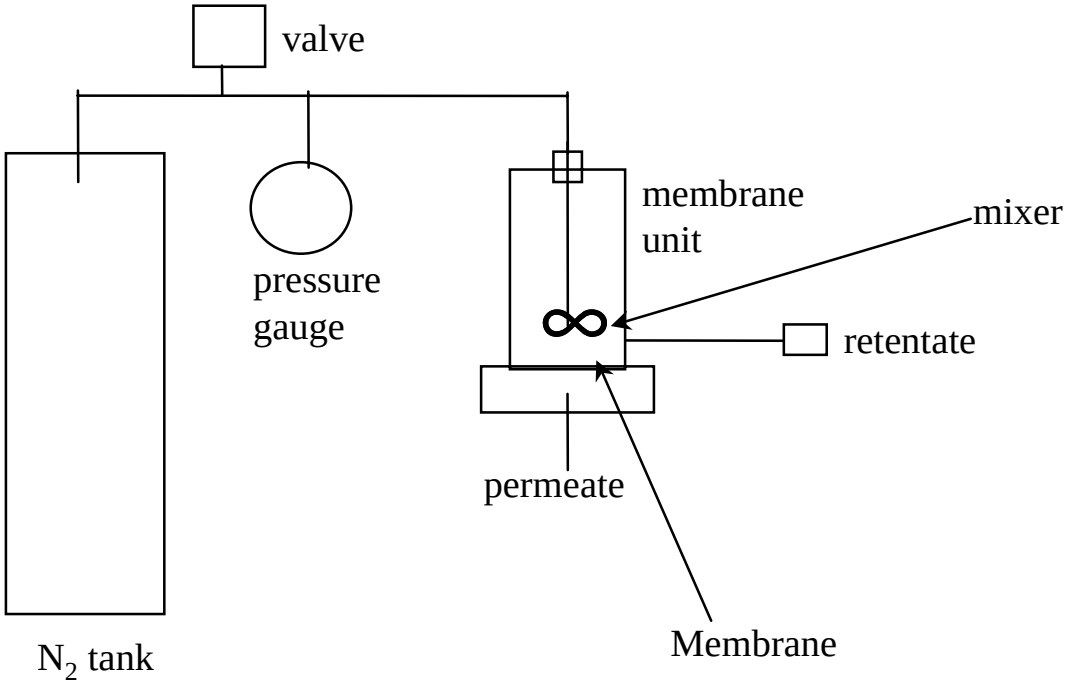

4.3 (b)

Figure 4.3: (a) Schematic of the Permeation set-up and (b) Sepa ST cell used for the experiments (Picture taken from www.osmonics.com)

Osmonics, Inc. The cell holds a membrane area of 13.2 cm^2 and has a solution capacity of about 300-ml. High-temperature experiments with n-hexane were carried out in a Sepa CF® cell which used a membrane area of 126 cm^2. Suitable O-rings were used for the permeation set-up to ensure solvent compatibility. Figure 4.3 shows the schematic of the permeation set-up and a picture of Sepa ST permeation cell which was used for most of the permeation studies [http://www.osmonics.com]. For the Sepa ST® cell, there is a magnetic stirrer assembly inside the cell feed chamber which allows the use of magnetic stir plates for the mixing. For the Sepa CF® cells, reasonable cross flow velocities were used to ensure proper mixing.

4.2.2 Diffusion Cell:

Solute diffusion measurements were carried out in a diffusion cell with 500-ml capacity chambers on either sides of the membrane. The dimensions of the cell used were 11.5-cm length, 5.5-cm width and 10.5 cm height. Magnetic stir bars were used in two chambers to ensure adequate agitation. Figure 4.4 shows a schematic of the diffusion cell set-up used. The membrane diameter used for diffusion studies is 3.2 cm which gives an effective membrane area of about 8 cm^2. The reason for the diffusion measurements is to obtain quantitative information about the contribution of diffusion to the total solute flux according to the Spiegler-Kedem Analysis. Also, the dependence of the solvent and membrane type can be analyzed by using these independent diffusion measurements. The solutes used for diffusion studies included Sudan IV, hexaphenyl benzene, phenol and Benzocaine. These solutes were dissolved in hexane, methanol and

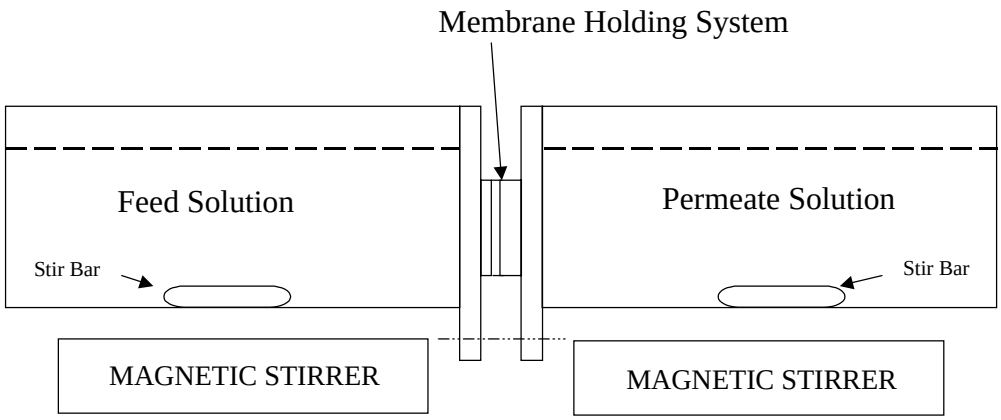

Figure 4.4: Schematic of the Diffusion Cell Apparatus.

ethanol medium and studied for diffusion properties through Membrane D, YK membrane and PS 18 membrane.

4.3 Experimental Procedures:

4.3.1 Membrane Characterization Procedures:

A list of membranes used and information about manufacturers and other data provided is listed in Table 4.2. For the water permeating membranes, pure water flux and salt rejections with suitable salts (sodium sulfate/ sodium chloride) were carried out after all the experiments were completed. Osmonics, Inc. also provided standard salt rejection data for their membranes. Pure solvent studies were performed using various polar (methanol, ethanol, isopropanol) and non-polar solvents (pentane, hexane, octane, decane). In most of the cases, pure solvent fluxes themselves were used as a characterization tool to ensure the reproducibility of the membranes. In some cases, the 380 MW organic dye, Sudan IV obtained from Aldrich was used.

The surface energy values were measured by Osmonics for the membranes used. They measured the values using contact angle measurements with a Kruss DSA10 goniometer. Typical solvents used for contact angle measurements were water, glycerol, thiodiethanol, diiodomethane, ethylene glycol and diethylene glycol. The surface energy values (γ_{sv}) used for the calculation are as follows: Membrane D - 16.6 dyne/cm, YK - 52 dyne/cm.

4.3.2 Membrane Pretreatment:

Unlike most aqueous systems, the membranes used for studies of non-aqueous systems need to undergo pretreatment to exchange any residual solvents present in the membrane after the manufacturing process. Common solvents used for membrane manufacture are glycerol, water etc. Presence of such residual solvents may affect the permeation of other organic solvents through the membrane. Thus exchange of these residual solvents is desirable using suitable pretreatment methods.

Most of the experimental results were performed with the silicone-based Membrane D and the polyamide-based YK membrane manufactured by Osmonics. A common pretreatment protocol was adopted to allow for suitable solvent exchange. The procedure used can be summarized as follows: The membrane was soaked in distilled water for 30 minutes to exchange traces of glycerol and then soaked in isopropanol for 30 minutes. To ensure complete wetting for the case of non-polar solvents, the membrane was then soaked in a mixture of 50-50-volume % isopropanol-n-hexane for 30 minutes followed by soaking in pure n-hexane for 30 minutes. The membranes were then loaded in the cell and permeation experiments were started with n-hexane. While changing from alkanes to alcohols, suitable solvent exchange procedures were used. For example, after a hexane run, the cell was loaded with ethanol and flushed until at least 120 ml of ethanol. The cell was then loaded with alcohols for permeation measurement. Similar procedures were used for other membranes used during the study. Membrane pretreatment has been an issue of importance and has been reported in several literature data. Thus it will be discussed in the Results and Discussion section in greater detail.

4.3.3 Procedures Adopted For Permeation Studies:

The solvents and solutes used for the permeation studies have been highlighted in Section 4.1.1 and Section 4.1.2. The protocols used for permeation and diffusion studies will be discussed here.

4.3.3.1 Solvent Permeation Studies:

Most of the solvent permeation experiments were performed using the Sepa ST ® cell. Experiments were carried out in a batch mode and at ambient temperatures. Pressure was varied in most cases from ~ 3.5 bar to ~ 27 bar and in some cases upto ~ 54 bar. A spout was used on the permeate side for collection of the sample. Graduated volumetric cylinders were used for measurement of the volumetric flow-rate. The high temperature experiments for alcohols were performed using the same experimental set-up and a glycerol temperature bath was used to control the temperature of the feed solution. Hexane permeation studies at high temperature were performed on Sepa CF® cells, with an active membrane area of 126 cm^2. Temperature- control for the CF cell was ensured by using a hot-water bath. Suitable time for steady state was allowed before samples were taken.

4.3.3.2 Solute Permeation Studies:

Table 4.3 summarizes all the experimental systems used for this work. Solute transport studies were carried out in both the Osmonics Sepa ST® (dead end) and Sepa CF® (cross-flow) cells. Most of the triglyceride permeation studies were performed on the Sepa CF® cells at different applied pressures and temperatures. Since triglycerides are highly soluble in n-hexane, 500 mg/l solutions were be used for rejection studies. The

Table 4.3: Summary of our experiments with Membrane D and YK.

Membrane Material	Solute	Solvent used	T (°C)	ΔP range (bar)
D	Sudan IV	Hexane	23	5-20
D	Tricaprin (554 MW)	Hexane	30, 45	5-40
D	Hexaphenyl Benzene	Hexane	23	5-14
D	Tripalmitin (807 MW)	Hexane	30, 45	5-40
D	Sudan IV	Methanol	23	5-40
D	Sudan IV	Ethanol	23	5-40
D	Fast Green FCF	Methanol	23	10-20
D	Fast Green FCF	Ethanol	23	10-20
YK	Sudan IV	Methanol	23	5-25
YK	Sudan IV	Hexane	23	10

dye permeation studies were carried out on the Sepa ST® cell. Due to the limited solubility of the organic dyes in the alcohols and alkanes, low concentrations (~10 to 20 mg/l) were used. Complete mixing was ensured in both the types of cells (insignificant concentration polarization). Sufficient time was allowed to reach steady state.

4.3.3.3 Diffusion Measurements:

Diffusion measurements were carried out for certain solute-solvent systems in the set-up mentioned in Section 4.2.2. Although the cell capacity was 500 ml, most of the diffusion measurements were carried out using volumes between 300 and 400 ml. Both the cell sides were sealed using Parafilm layers to ensure minimum loss of sample due to evaporation. Temperature was maintained at ambient condition (25 ± 2 ° C) during the diffusion measurements. Typically, samples (4 ml) were withdrawn at regular time intervals for analysis and returned back to the chambers as soon as the analysis was completed.

4.4 Analysis:

The analytical instruments used for the analysis of permeation and diffusion experiments are summarized in Table 4.4. The table contains the type of instrument, typical range of feed concentrations, wavelength and the % errors in the analysis. Calibration curves were obtained for each system and linear behavior was ensured in the range of operation.

Table 4.4: Instruments used to analyze the solutes and their parameters.

Solute	**Instrument**	**Feed Concentration (mg/l.)**	**Wavelength (nm)**	**% error**
Sodium Chloride	Conductivity	2000	NA	< 1 %
Sudan IV	UV-Visible	10 – 20	510	< 0.1 %
Hexaphenyl benzene	UV-Visible	10 – 20	249	< 0.5 %
Fast Green FCF	UV-Visible	10 – 20	610	< 0.1 %
Triglycerides	LC-MS (direct injection)	500 – 1000	NA	< 3 %

4.4.1 Liquid Chromatography – Mass Spectrometer (LC/MS)

For analysis of triglycerides the ThermoQuest / Finnigan Liquid Chromatography-Mass Spectrometer (LCQ) was used. The LCQ is an advanced analytical instrument that includes a mass spectrometer (MS) detector, a syringe pump and a data system. The advantage of using this instrument is that the LC and the MS parts can be run independently. Since most of our analysis involved using binary systems, the samples were shot directly into the MS unit to give solute peaks. The solvent flow through the LC had to be maintained and since hexane was the solvent medium, it was also used as the carrier liquid. The MS detector consists of an Atmospheric Pressure Ionization (API) source, ion optics, mass analyzer and ion detection system. These parts are enclosed in a vacuum manifold. Ionization of the samples occurs in the API source and the ions produced are transmitted by the ion optics into the mass analyzer. The LCQ can be operated in two ionization modes: the Electrospray Ionization (ESI) mode and the Atmospheric Pressure Chemical Ionization (APCI) mode. The ESI mode can be used to analyze any polar compound that makes a preformed ion in solution. The APCI mode is used to analyze compounds of medium polarity and was used in this study for the analysis of the triglycerides, which have medium polarity.

A typical spectrum output from the Mass Spectrometer for the analysis of Tripalmitin (807 MW C16 triglyceride) is shown in Figure 4.5. The spectrum peak visible in this case at 551.5 m/z can be explained as follows. A triglyceride molecule has three chains in its structure and thus each chain has a molecular weight of 269. The 551.5 MW peak can be rationally explained by the breaking of the triglyceride molecule

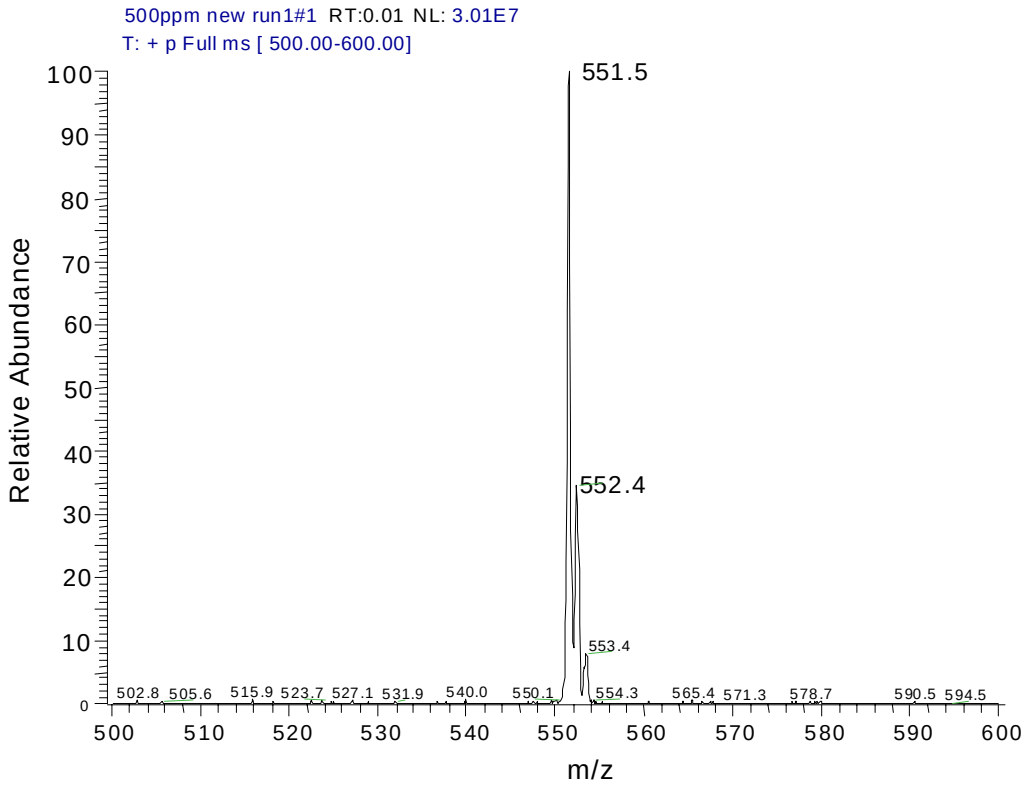

Figure 4.5: Typical Mass spectrum for Tripalmitin (807 MW triglyceride) obtained using the LCQ/MS instrument

into several fragments, one containing two chains of the triglyceride along with one $–CH_2$ group which adds up to a total of 552 MW (269×2 + 14). The peak is distinct and a characteristic of the triglyceride molecule. This type of breaking of the molecule was typical since other triglycerides analyzed also gave the most abundant peak with a similar analogy as for Tripalmitin. The total ion count was used for calibrating this peak obtained by the triglyceride. Typically, 3 samples were shot independently and the average of the total ion counts was taken for analysis. The sample volume shot in the MS detector ranged from 5 to 20 μL and the flow rate of the sample into the MS could be controlled using the computer interface.

4.4.2 Ultraviolet-Visible Spectrophotometer:

The UV-Visible spectrophotometer was primarily used for determination of solute concentrations for both separation and diffusion experiments. The instruments used were Hewlett Packard 8463 and Cary 300 Bio. The principle of the analysis is the simple Beer-Lambert's law, which states that the absorbance is directly proportional to the solute concentration. The Cary 300 Bio was used for most of the analysis and has an excellent PC interface which allows for setting up the instrument. A multi-cell holder was used for the analysis and each sample was analyzed three times. The number of replicates can be changed, if desired, and suitable calibration curves can be stored for analysis. The instrument error is typically less than 0.1 % (for triplicates) and the detection limits is about 0.05 mg/l. Analysis for most of the organic dyes, phenol, benzocaine and hexaphenyl benzene was carried out using the UV-Vis instrument.

4.4.3 Conductivity:

The instrument used for conductivity measurements is a Conductivity Meter (Fisher Accumet AB 30) and Probe (Cell Constant = 0.1) manufactured by Fisher Scientific. Conductivity was used to analyze the salt concentrations in aqueous medium for both characterization of hydrophilic membranes (sodium chloride and sodium sulfate rejection) and for diffusion measurements. The probe used had an optimum conductivity range of 10 to 2000 μSiemens. Typical concentrations used for rejection studies ranged from 500 to 2000 mg/l which correspond to a conductivity reading of about 3000 μSiemens. For diffusion measurements, lower concentrations were used. Suitable calibration curves were made to ensure linearity in the range of operation.

CHAPTER FIVE

Results and Discussion

The overall objective of the research is to extend the principles of Reverse Osmosis/Nanofiltration to non-aqueous systems. A systematic approach to the problem has already been highlighted in the Theory and Background Chapter. This section will primarily concentrate on reporting the results obtained from experimental studies and some transport modeling aspects. The overall goal is to develop a comprehensive transport theory which can be used to explain separation behavior for different solvent-solute-membrane systems. However, as discussed, understanding pure solvent permeation behavior is extremely critical for developing any unified transport theory for non-aqueous systems.

5.1 Pure Solvent Transport:

The primary aim of this section is to develop and verify a simplified transport model, which has a sound theoretical basis, to predict the pure solvent flux through dense polymeric membranes and not for UF/MF type membranes. Since pure water permeability is an important parameter in assessing the effectiveness of hydrophilic polymeric membranes, it becomes equally essential to estimate the pure solvent flux behavior for solvent-resistant polymeric membranes. As has been discussed before, there are several factors which influence this behavior viz. membrane material, solvent polarity, solvent physical properties, etc. Also the interaction between the solvent and the membrane material can be an important factor in determining membrane performance. In

order to develop a comprehensive theory to understand pure solvent transport, it is essential to experimentally establish the effects of the following parameters on solvent permeation:

a) Solvent polarity
b) Solvent viscosity
c) Solvent size
d) Membrane hydrophilicity/hydrophobicity
e) Solvent-membrane affinity

Solvents and membranes were carefully chosen for this particular study using the above system variables. The alcohol and alkane homologous series was studied since it incorporates most of the above solvent variables of interest. Traditional water-permeating membranes and developmental solvent permeating membranes were studied to understand the role of membrane type on pure solvent permeation. The methods and the apparatus used for these studies have been described in the Chapter Four. Results obtained in each class of membranes are discussed below. Table 5.1 summarizes the physical properties of the solvents employed in this study.

5.1.1 Experimental Observations:

5.1.1.1 Pure Solvent Permeation Studies through Hydrophilic Membranes:

The hydrophilic membranes tested for the study included a brackish water RO membrane, DS-11 AG and a negatively charged NF membrane, YK. Both the membranes are polyamide-based and were supplied by Osmonics. Figure 5.1 shows the effect of pressure on the pure solvent transport through the polyamide-based DS 11 AG

Table 5.1: Physical Properties of the solvents used

Solvent	Molar Volume (cm^3/mol)	Viscosity (cP)	δ_h $(MPa)^{0.5}$	δ_d $(MPa)^{0.5}$	δ_p $(MPa)^{0.5}$	Solubility Parameter $(MPa)^{0.5}$
Methanol	40.7	0.55	22.2	15.1	12.3	29.6
Ethanol	58.5	1.10	19.4	15.8	8.8	26.5
IPA	76.9	2.00	16.4	15.8	6.1	23.5
Propanol	75.2	2.00	17.4	16.0	6.8	24.5
Butanol	91.5	2.53	15.8	16.0	5.7	23.2
Pentanol	108.2	3.27	13.9	16.0	4.5	21.6
Acetone	74.0	0.30	7.0	15.5	10.4	20.0
Pentane	116.2	0.23	0	14.5	0	14.5
Hexane	131.6	0.32	0	14.9	0	14.9
Octane	163.5	0.54	0	15.5	0	15.5
Decane	195.5	0.90	0	15.8	0	15.8

Solubility Parameters and Molar Volumes obtained from [Barton et al, 1991], Viscosity values obtained from [Viswanath et al, 1989]

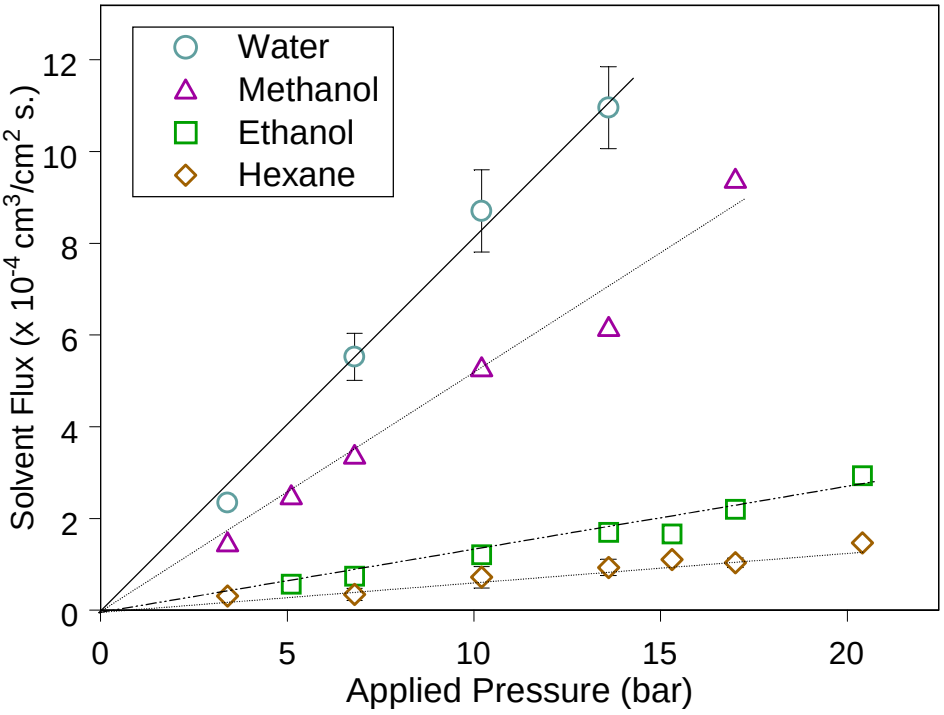

Figure 5.1: Effect of Pressure on the solvent flux through the Osmonics DS-11 AG membrane (brackish water RO membrane)

membrane. Two observations can be made from the figure: the solvent flux increases in a linear fashion with applied pressure for all the solvents studied (including water) unlike the observations of Paul *et al* [1970, 1972] and as expected, the flux of polar solvents is significantly higher than non-polar solvents. For example for the DS 11 AG membrane, the methanol flux obtained at ~ 13 bar was ~ 5 x 10^{-4} cm^3/ cm^2 s as opposed to the hexane flux through the same membrane being ~ 0.7 x 10^{-4} cm^3/ cm^2 s at the same pressure. Figure 5.2 shows a bar plot of solvent permeabilities for the DS-11 AG membrane. As expected the water flux for this membrane was the highest with a value of ~ 11 x 10^{-4} cm^3/ cm^2 s at ~ 13 bar. The mechanism of water transport through a traditional RO membrane is through activated diffusion because of the charged groups present in the polymer structure. In solvent medium, charge is considerably suppressed which results in lower fluxes for the alcohols and hexane. Figure 5.3 shows the permeation results for a polyamide-based negatively charged NF membrane (YK). The observed flux values for methanol, ethanol and hexane at about 10 bar are ~ 10 x 10^{-4} cm^3/ cm^2 s, ~ 2.5 x 10^{-4} cm^3/ cm^2 s and ~ 1 x 10^{-4} cm^3/ cm^2 s, respectively. Again, it can be seen that the solvent flux for all cases increases linearly with applied pressure which is consistent with water transport through such membranes. It can also be observed that the solvent permeability values for the NF membrane are slightly higher compared to the DS 11 AG RO membrane. For example, the methanol permeability through the polyamide-based YK membrane is ~ 1x 10^{-4} cm^3/ cm^2 s bar compared to ~ 0.4 x 10^{-4} cm^3/ cm^2 s bar. This is expected because NF membranes have a much open morphology as compared to dense RO membranes.

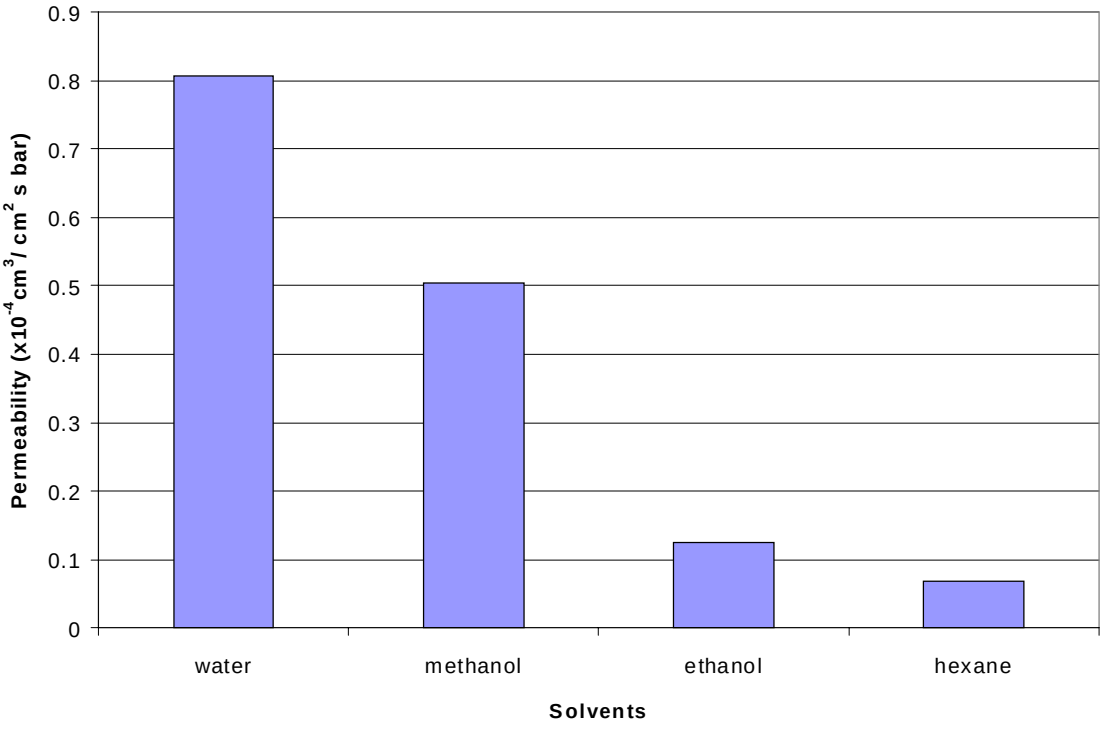

Figure 5.2: Bar plot showing permeabilities of various solvents through the Osmonics DS-11 AG membrane (brackish water RO membrane)

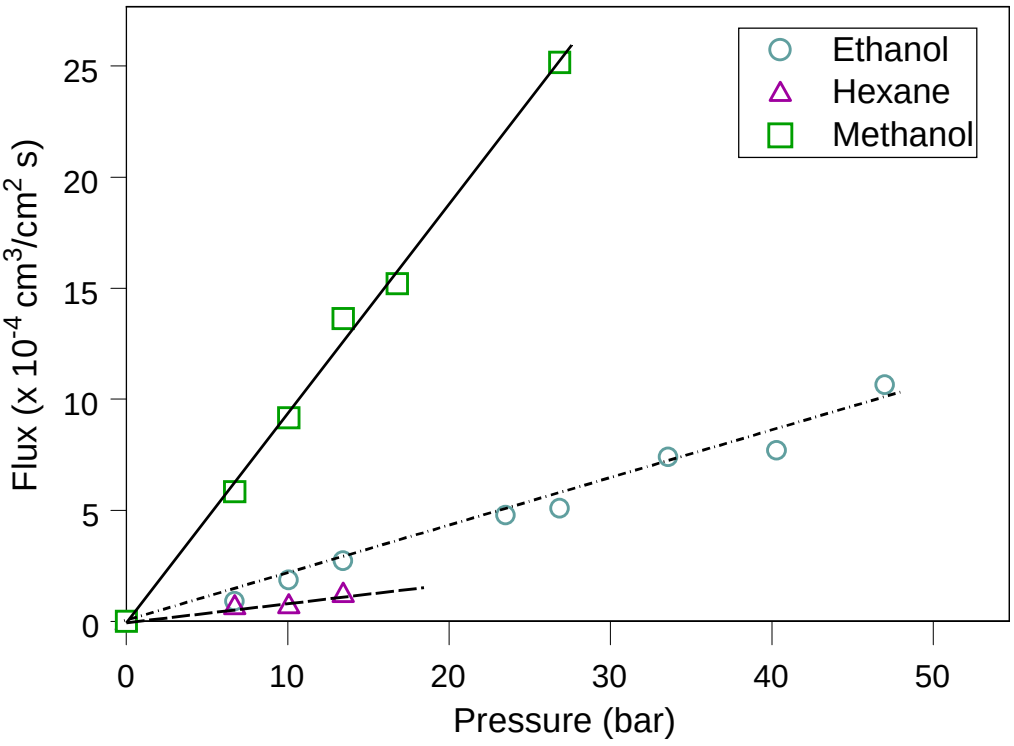

Figure 5.3: Effect of Pressure on the solvent flux through the Osmonics YK membrane (polyamide-based negatively charged NF membrane)

5.1.1.2 Pure Solvent Permeation Studies through Hydrophobic Membranes:

The only hydrophobic membrane tested experimentally for this study is a siloxane-based developmental Membrane D supplied by Osmonics. Studies similar to the hydrophilic membranes were performed with Membrane D. Literature data was available for a similar siloxane-based Koch MPF-50 membrane [Machado *et al*, 1999a] and was used to compare our experimental observations. This literature data reported for the MPF-50 membrane can be shown in Figure 5.4 which compares the pure solvent permeabilities of several solvents. There is a general trend in the permeability behavior indicating that the non-polar solvent transport is much greater than polar solvent transport. Our experimental observations are summarized in Figure 5.5 which shows the effect of pressure on the solvent flux for the hydrophobic silicone based Membrane D. All the experiments were performed at room temperature (23 ^{o}C). It can be clearly seen that the solvent flux increases linearly with applied pressure which is consistent with the observations for the hydrophilic DS-11 AG and the YK membranes discussed above. Typical flux values for solvents through Membrane D are as follows: at ~ 13 bar flux of methanol was ~ 3 x 10^{-4} cm^3/ cm^2 s as opposed to the hexane flux of ~ 6 x 10^{-4} cm^3/ cm^2 s. The measured solvent permeabilities at 23 °C for Membrane D are: Hexane = 0.45 (± 0.03) × 10^{-4} cm^3/cm^2 s bar; octane = 0.41 (± 0.01) × 10^{-4} cm^3/cm^2 s bar; methanol = 0.25 (± 0.03) × 10^{-4} cm^3/cm^2 s bar; ethanol = 0.085 (± 0.004) × 10^{-4} cm^3/cm^2 s bar. As expected, the non-polar solvent flux is much greater than polar solvent flux through the hydrophobic Membrane D and these observations are similar to the Koch MPF-50 data shown in Figure 5.4.

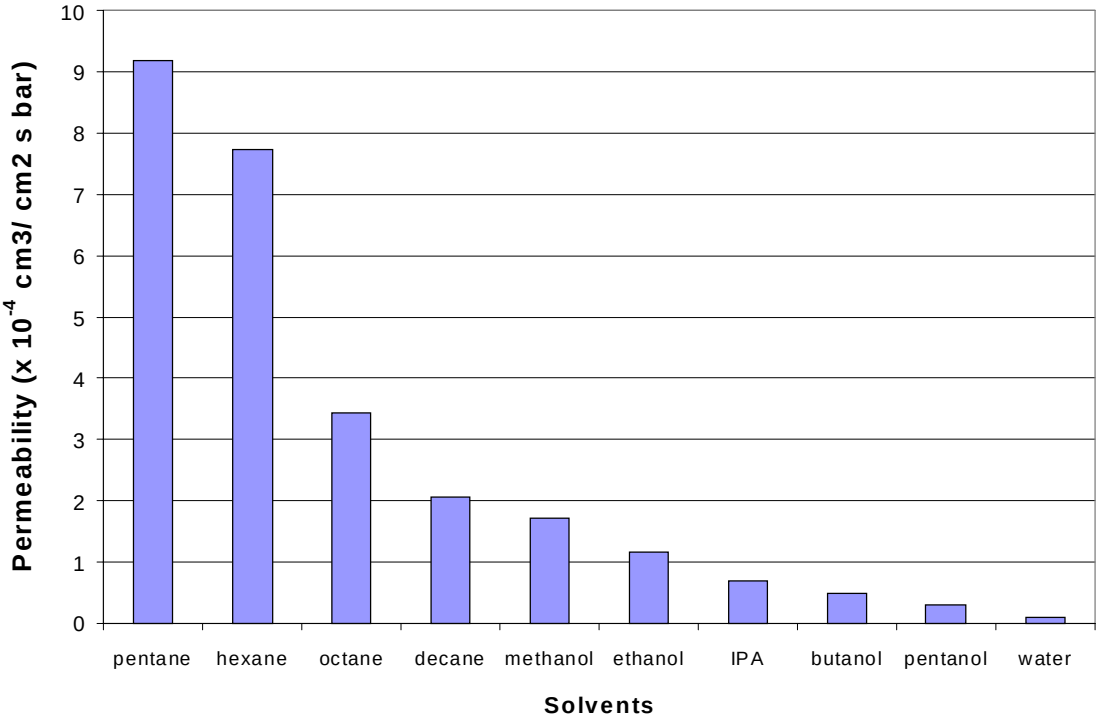

Figure 5.4: Permeabilities of polar and non-polar solvents through hydrophobic Koch MPF-50 membrane using literature data (data taken from [Machado et al, 1999a])

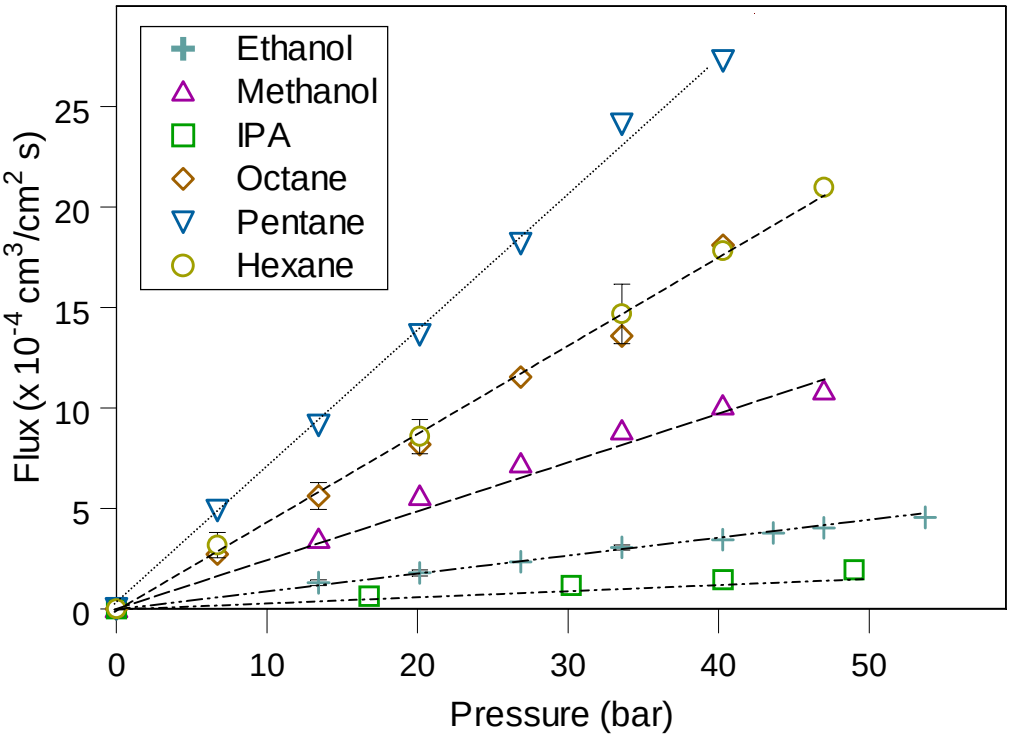

Figure 5.5: Variation of the Solvent Flux with Pressure for the hydrophobic silicone-Based Membrane D

Although the membrane performance trends for various solvents can easily be predicted, the relative flux values for solvents in the same homologous series was quite different. In the alcohol homologous series, the methanol flux is about five times that of ethanol flux and almost 10 times that of the IPA flux through the hydrophilic DS 11 AG membrane. However, for the silicone-based membrane MPF 50, the methanol flux is about 1.5 times that of ethanol flux and about two times that of the IPA flux through the membrane. However, among each homologous series of solvents, the dependence of the flux on molecular size is always true. For example for the alcohol series, methanol flux > ethanol > isopropanol. The above comments readily address the importance of polymer-solvent interactions in selection of membrane material and also prediction of the permeation properties. The key, however, is to obtain a qualitative understanding that will direct future efforts in membrane material selection. Sorption data available in literature for elastomeric materials like PDMS also corroborate the above comments. For example, two groups [Aminabhavi *et al*, 1993 and 1995; Unnikrishnan *et al*, 1997] have reported sorption values for natural rubber for various polar and non-polar solvents. Aminabhavi *et al* [1995, 1997] report about 0.48 mole % uptake of methanol and 0.28 mole % uptake of ethanol at 25 ^{o}C. Unnikrishnan *et al* [1997] studied the effect of different vulcanization techniques (conventional versus efficient) on the sorption capacities of natural rubber. They report about 3.4 mole % uptake of n-hexane for conventionally vulcanized natural rubber and for the efficient vulcanization techniques, a value of 1.4 mole % uptake for n-hexane has been reported as against the low sorption values for the polar solvents. The role of polar solvent will be further discussed in a later

section in order to understand permeation behavior through different membrane materials.

5.1.1.3 Membrane Pretreatment:

Comparison of literature data in non-aqueous medium for different membranes can be difficult because of the variability of treatment protocols and solvents used. In order to eliminate such variability and also to eliminate variability from one membrane coupon to another, it becomes essential to use normalized flux values. This is one of the key limitations of understanding solvent transport and will be briefly discussed here. It is customary in case of aqueous systems to soak the membrane in water before use to remove unreacted glycerine and other residual solvents. However, for non-aqueous systems, several membrane manufacturers prescribe pretreatment techniques for optimal performance. One can easily visualize that miscibility of the solvent phases can be critical when organics are permeated through NF membranes. A quick illustration of this can be given by considering a membrane saturated with a methanol solution when used for hexane permeation would immediately form a two-phase system in the membrane pore structure causing dramatic reduction in the permeability.

The type of pretreatment can also have a tremendous impact on the membrane characteristics. The Koch MPF-50 membrane, for example, gives varying results when exposed to different conditioning techniques. Figure 5.6 shows the impact of such treatment strategies on the pure solvent flux for alcohols and alkanes through the MPF-50 membrane.

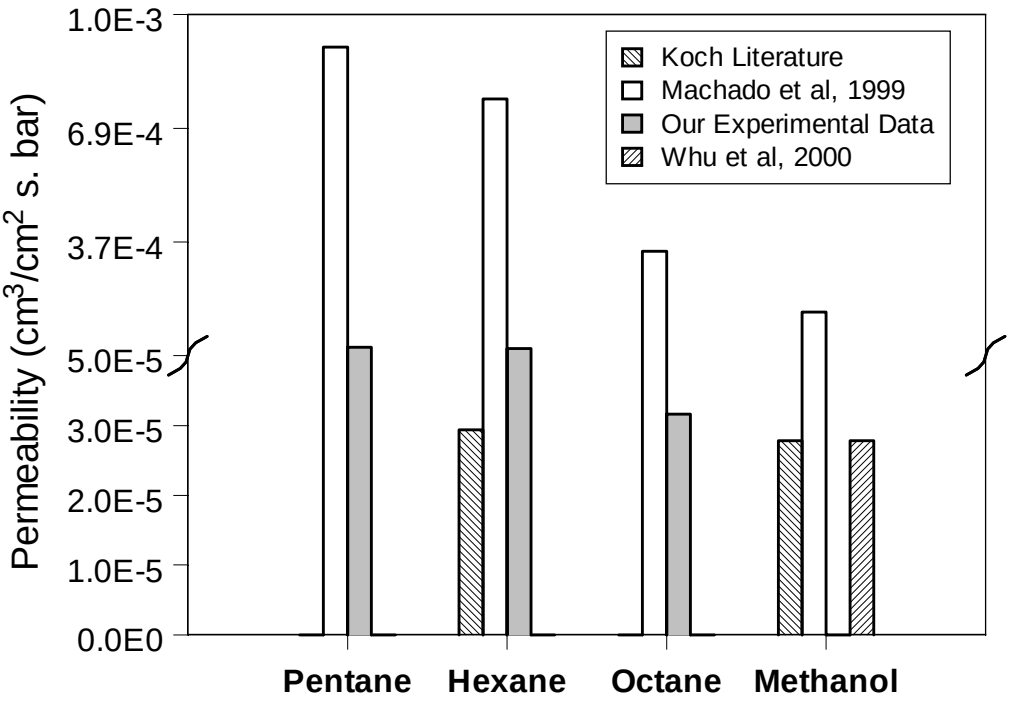

Figure 5.6: Effect of MPF-50 membrane pretreatment techniques on the solvent permeabilities

a) Koch Membrane System Literature:

The manufacturer prescribed pretreatment strategy suggested the membrane (originally in ethanol-water medium) be soaked in methanol followed by soaking the membrane in methylene chloride. The permeability of methanol, for example, is 0.3×10^{-4} cm^3/cm^2 s bar reported in the Koch literature.

b) Whu *et al* (2000):

Whu *et al* [2000] have reported receiving the Koch MPF-50 membrane originally in 0.1% sodium metabisulfite and 10% glycerol. They rinsed the membrane thoroughly by immersion in deinonized water overnight, followed by membrane activation by flushing with ethanol at 440 psi for 60 to 80 min. The treated membranes were soaked in ethanol at room temperature. The permeability of methanol observed was very similar to that reported by Koch Membrane Systems, however, the flux reached steady state after several hours of solvent permeation.

c) Machado *et al* [1999a]:

Machado *et al* immersed MPF-50 membranes in distilled water followed by soaking in ethanol solution overnight and acetone was the first solvent used for permeation studies. The observed flux of methanol was about one order of magnitude higher than what was reported by Koch Membrane Systems.

d) Our Experimental Data:

Our experiments with the MPF-50 membrane followed the same pretreatment procedure as prescribed by the Koch Membrane literature. The membranes were shipped in a 50% ethanol - water system. The permeation results observed are slightly different

from those reported by Koch Membranes and are dramatically different from Machado *et al* [1999a].

These observations suggest that suitable pretreatment protocols need to be established for efficient performance of the membrane. Also, when more than one solvent is used for transport studies, suitable solvent-exchange procedures need to be employed to ensure proper miscibility and to prevent two-phase formation. Tsuru *et al* [2001] have observed the importance of membrane history towards permeation character for their silica-zirconia membranes. They have reported that after solvent-exchange, it requires several hours for the membrane to reach a steady performance. Whu *et al* [2000] have also reported significant delay in reaching steady performance for the MPF-series of membranes in methanol and water medium. In order to completely understand the transport behavior, it becomes essential to normalize the flux values for suitable comparison of data with different membrane materials.

5.1.2 Correlations for Pure Solvent Transport using our Proposed Semi-empirical Model:

Solvent and membrane selection was suitably made in order to understand the effect of solvent and membrane properties on the transport. Molar volume was used as a measure of the solvent size. As has been discussed before, the solvent diffusivity through the membrane can be related to the solvent viscosity indirectly (Equation 3.3). The solvents chosen had reasonable spread in the viscosity and molar volume. For example, the alcohols chosen for the study (methanol to isopropanol) had a viscosity range of 0.54 cP (for methanol) to 2 cP (for isopropanol) and the molar volumes varied from 40.7

cm^3/mole (methanol) to 76.9 cm^3/mole (isopropanol). The alkanes chosen for the study (pentane, hexane, octane and decane) had a viscosity range of 0.23 cP (pentane) to 0.9 cP (decane) and the molar volume range was 116.2 cm^3/mole (pentane) to 195.5 cm^3/mole (decane).

5.1.2.1 Normalization of Solvent Permeability:

To eliminate variability from one membrane coupon to another and also to compare different membrane types, a normalized permeability approach has been used. Several researchers have observed effects of membrane hysterisis after exposure to certain organic solvents. The above section on membrane pretreatment also suggests that different pretreatment protocols lead to large variability in the solvent flux behavior. Machado *et al* [1999a] have used a flux normalization approach for their Koch-MPF50 data. Some sample flux variations reported by them can be illustrated as follows:

(a) Koch MPF-50 Membrane 1: at 30 atm, Acetone flux = 182×10^{-4} cm^3/cm^2 s; Ethanol flux = 43.6×10^{-4} cm^3/cm^2 s; Ratio = 0.239

(b) Koch MPF-50 Membrane 2: at 30 atm, Acetone flux = 133×10^{-4} cm^3/cm^2 s; Ethanol flux = 31.6×10^{-4} cm^3/cm^2 s; Ratio = 0.237

Thus, it can be seen that although two separate membrane coupons had different absolute values of acetone and ethanol flux, the ratios are approximately the same. Since ethanol permeability data is available for most of the membranes of interest, ethanol permeability at 23 ^oC is chosen as the basis to normalize the solvent permeabilities through different membranes. Although a normalized permeability has been used for the correlation purposes, the x-axis which uses the solvent properties has not been

normalized because there are several parameters (e.g. solvent sorption) which would be different for ethanol and the solvent of interest. The goal is to correlate the observed variation in the solvent flux with respect to ethanol as a function of solvent and membrane properties.

5.1.2.2 Correlations for Hydrophobic Membranes:

The goal of this section is to use solvent physical properties to explain permeation behavior through hydrophobic siloxane-based Membrane D. In order to understand the transport mechanism through dense RO/NF type membranes, it becomes essential to understand the transport through porous MF/UF type membranes. As a result, this section will illustrate the key parameters used to explain pure solvent transport through porous membranes (MF/UF) with a simple Hagen-Poiseuille equation and illustrate the controlling parameters. Further discussion outlining why such a model cannot be used to explain transport in dense RO/NF type membranes will also be presented. Our experimental data obtained at room temperature will be used with Equation 3.4 which is a semi-empirical correlation proposed for RO/NF type membranes. In order to verify this correlation, literature data already available for a similar siloxane-based membrane will be used with Equation 3.4 along with experimental data at higher temperature.

5.1.2.2.1 Correlation for Pure Solvent Transport Using Our Experimental Data:

As has been clearly explained, Membrane D is a siloxane-based membrane and has a non-polar solvent flux >> polar solvent flux. The flux relationship with the applied pressure for Membrane D is shown in Figure 5.5. It can be seen that at moderate levels

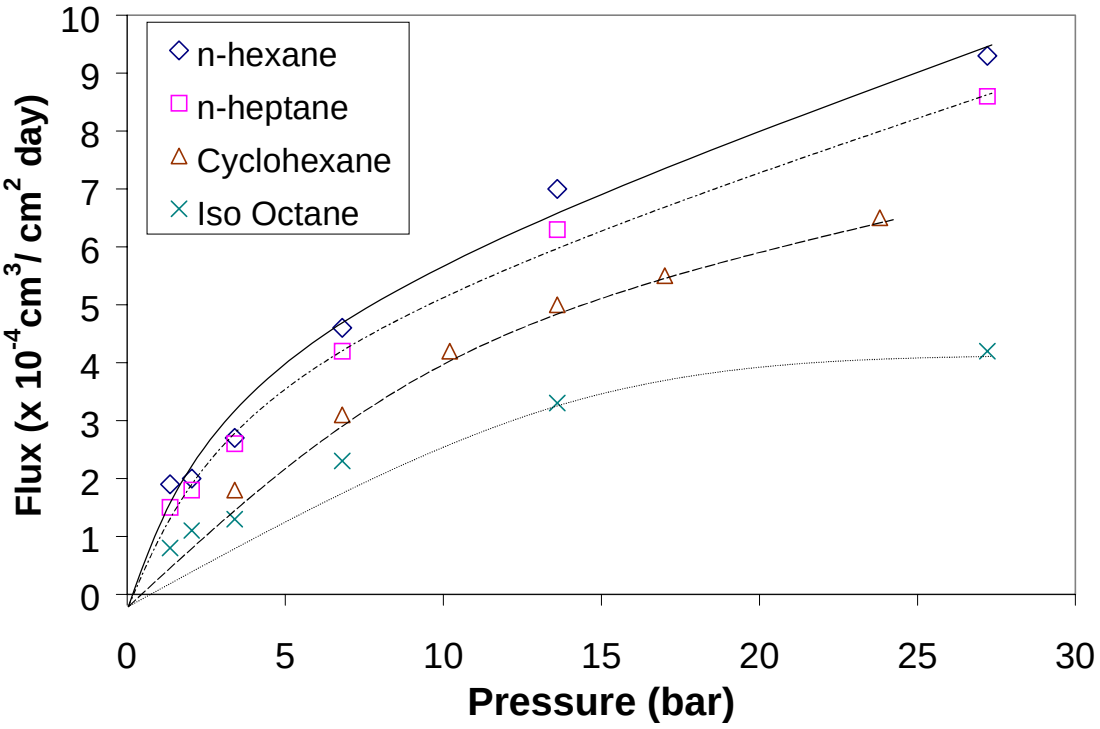

Figure 5.7: Variation of the Solvent Flux with Pressure for a lightly crosslinked natural rubber membrane [data taken from Paul et al, 1970]

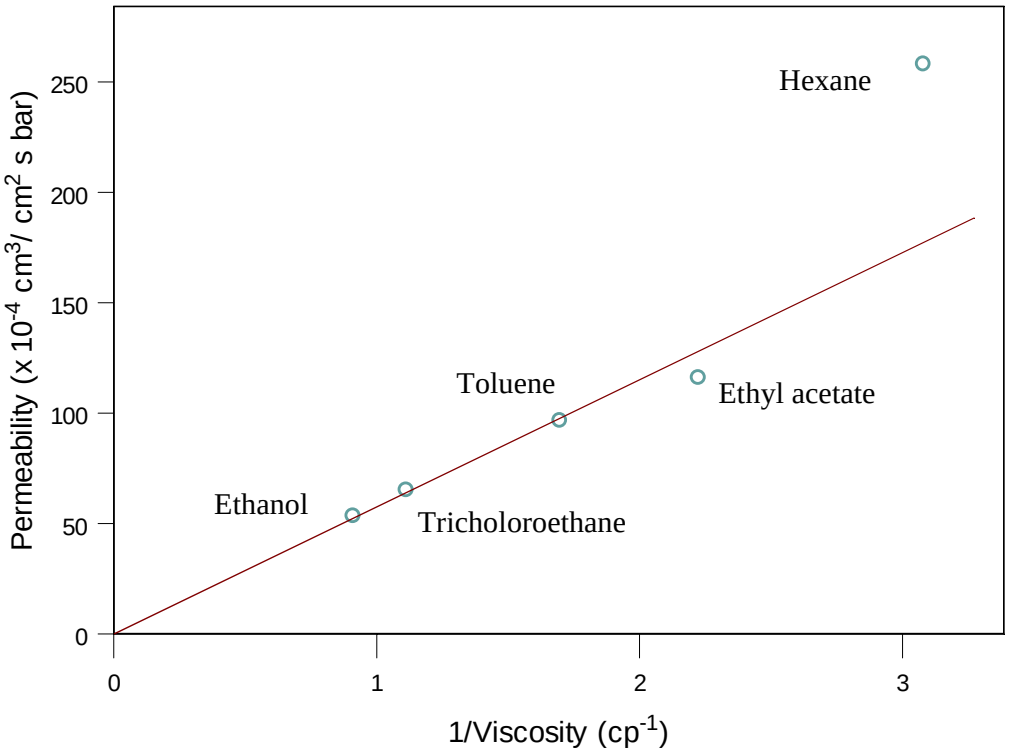

Figure 5.8: Variation of solvent Permeability of a 20,000 MWCO UF membrane for various solvents (data taken from Iwama et al, [1982])

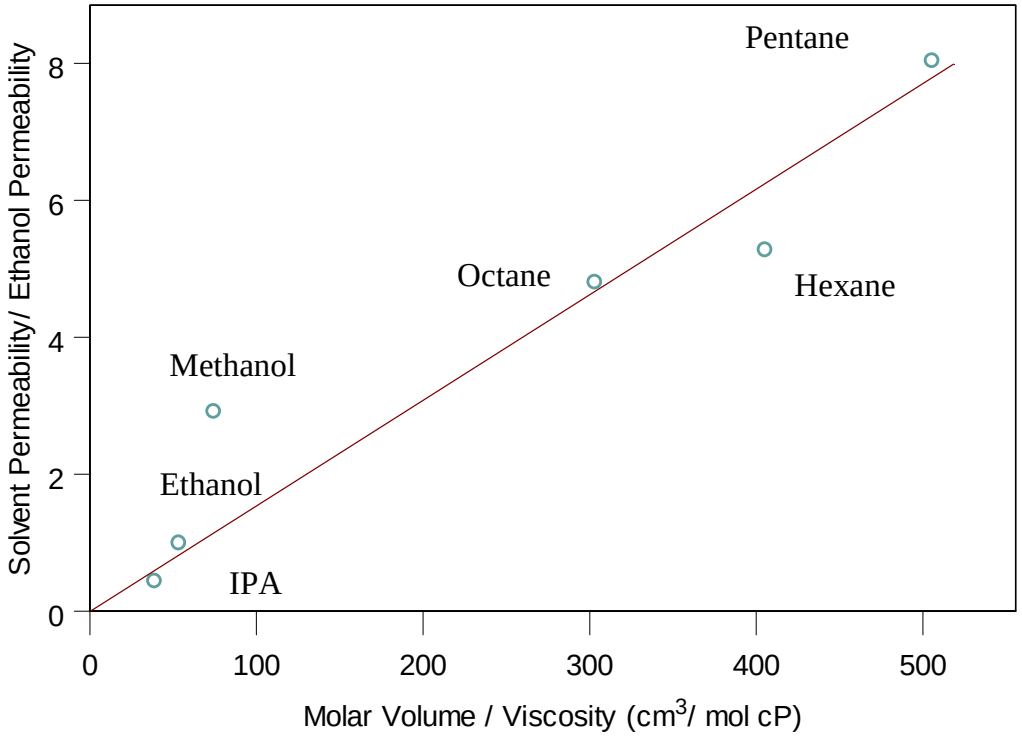

Figure 5.9: Correlation of solvent Normalized Flux (using Ethanol Flux) of polar and non-polar solvents with ratio of molar volume and viscosity for Membrane D (hydrophobic silicone based NF membrane).

of pressure (40 bar) the flux behavior for the solvent is linear with respect to the applied pressure. This linearity of flux obtained with respect to the applied pressure is unlike that obtained by Paul *et al* [1970] for lightly crosslinked rubbery membranes, where severe effects of compaction were observed as shown in Figure 5.7. The saturation flux values and the corresponding pressures were dependent on the type of solvent used. Also, it can be seen from the flux data in Figure 5.5 that for solvents even with relatively high molar volume (hexane, octane), the approximation of the exponential term using a Taylor series (Equation 2.21) is still valid for moderate pressures. Non-linear behavior may be observed at higher pressures (> 68 bar), but such high pressures were not used in our experimental set-up.

As discussed above, to illustrate the transport mechanisms prevalent in RO/NF membranes, a brief discussion of the permeation mechanism in the UF/MF membrane processes is needed. In case of UF/MF membranes the flow is convective in nature and can be predicted by the Hagen-Poiseuille equation for convective flow, which can be represented as:

$$J_{solvent} = \frac{\varepsilon d^2}{32\mu\tau}\frac{\Delta P}{l} \qquad 5.1$$

Where, ΔP is the pressure drop across the pore, l is the length of the pore, d is the diameter of the pore, ε is the surface porosity and τ is the pore tortuosity. Typically, for UF/MF membranes, one can safely assume that the pore size is much greater than solvent molecule size. The factor that controls the transport through a given membrane is the viscosity of the solvent. Figure 5.8 validates the above comments showing the variation of the permeability of the solvents as a function of viscosity for a 20,000 MWCO

polyimide UF membrane (data from Iwama *et al*, [1982]). From the data, one can see that although hexane has the largest molar volume (131.6 cm^3/mol), it has the lowest viscosity (0.32 cP) which causes it to penetrate the fastest through the membrane. A good correlation exists between the permeability and the inverse of the solvent viscosity (if hexane is considered as an outlier) corroborating the transport mechanism being viscous (convective) in nature.

For the case of RO/NF processes, the membranes are dense and do not have a well-defined pore structure. Conventional water permeating NF membranes are typically charged and thus in the case of aqueous systems, the electrical potential is an important factor for permeation of water, other than diffusion. However, in organic medium, the charge is considerably suppressed and thus the transport occurs primarily because of diffusion. In general for RO/NF composite membranes, the active layer is the rate limiting permeation step. The highly porous support membranes used to make DS-11 AG and membrane D have permeabilities that are more than 50 times greater than the permeability of the final composite membrane, so the support layer resistance is insignificant. Both Membranes D and DS 11 AG have backing material of non-woven polyester and the support membrane polymer is polysulfone. It is assumed that the Koch membrane supports have similar characteristics as most composite membranes. Model correlations developed for the membrane active layer can be suitably used to characterize the membrane material.

Figure 5.9 shows the correlation plots for the experimental data for Membrane D, a silicone based hydrophobic membrane, with the parameter molar volume/viscosity (Equation 3.4). It can be seen that a reasonable correlation (R^2 = 0.89) can be obtained

for the experimental data. Thus the following equation can be used for the prediction of the solvent flux:

$$\frac{Solvent\ Permeability}{Ethanol\ Permeability} = k \times \left(\frac{V_m}{\mu} \right) \qquad 5.2$$

If the viscosity of the solvent would be the controlling factor then the methanol flux and the octane flux would be identical because of identical viscosities. Similar comments would also apply for water and decane as the viscosities are very similar at ambient temperatures (0.85 cP and 0.9 cP, respectively). However, it is evident from both the literature [Machado *et al*, 1999a] and our experimental data for the hydrophobic silicone based membranes that the decane and water fluxes are dramatically different, and thus the role of interactions (sorption) becomes important.

5.1.2.2.2 Model Verification using Our Experimental High Temperature Data and Literature Data with Hydrophobic Membranes:

The above mentioned semi-empirical model can be validated by varying the temperature (thus viscosity of the solvents) during the permeation experiments and by using literature data published for the siloxane-based Koch MPF-50 membrane. To corroborate the above comments and thus verify the model, high temperature experiments were performed with methanol, ethanol, isopropanol and hexane. For the alcohols, experiments were performed at 45 ^{o}C. For hexane, experiments were performed at 31 ^{o}C and at 45 ^{o}C. Suitable viscosity corrections [Viswanath *et al*, 1989] were applied for calculating the parameter used for the correlation. The flux behavior with applied pressure at high temperature for the solvents studied are shown in Figure 5.10. It can be clearly seen that the flux behavior is linear with applied pressure as seen for the room

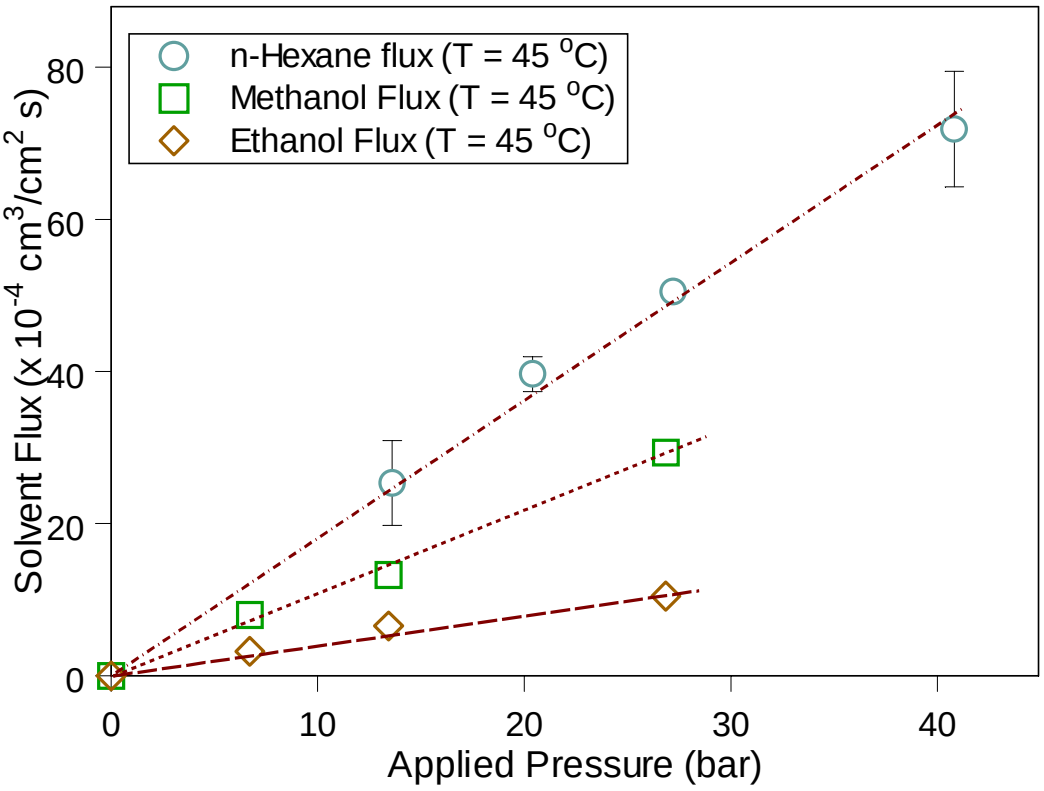

Figure 5.10: Variation of Solvent fluxes with applied pressure at higher operating temperatures (45 °C) through Membrane D.

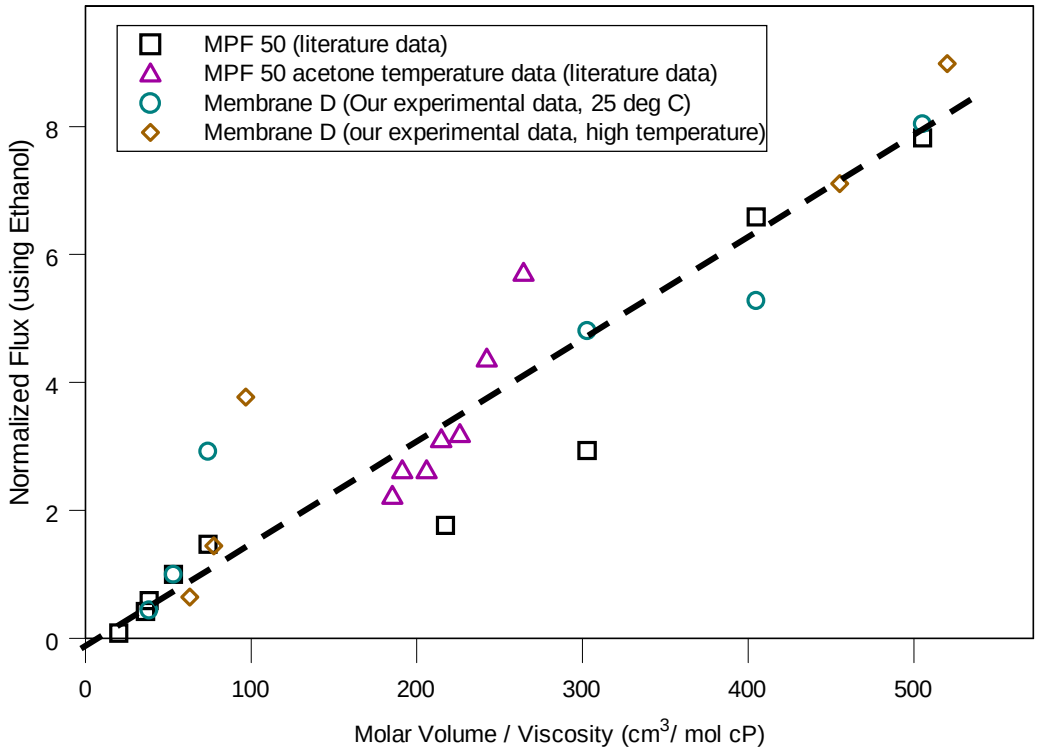

Figure 5.11: Verification of the existing model using literature data (MPF-50 [Machado et al, 1999a]) and our experimental data (Membrane D) at high temperature for hydrophobic membranes

temperature cases. Solvent permeation data for silicone based MPF-50 was obtained from literature [Machado *et al,* 1999a]. Acetone permeation data was also reported in the same work at different temperatures. This literature solvent permeation data including the different temperature runs with acetone have been normalized using ethanol permeability and suitable temperature correction was applied to the viscosity of the solvents used. Figure 5.11 shows the correlation plot for the above data along with the ambient temperature data for the Membrane D. It can be seen that the data (both literature and experimental) agree reasonably well (R^2 = 0.9 with 22 points) thus validating the correlation between the two variables for hydrophobic membranes. The standard error for the prediction of the slope using a 95% confidence limit is ~ 4% if methanol permeability for our experimental data is neglected in the alcohol series (with the methanol data considered, the standard error is ~ 4.3%). Thus, the existing model can be used effectively for hydrophobic non-polar membranes where the transport mechanism is primarily solvent diffusion through the membranes. The proposed model predicts the flux of non-polar compounds, primarily alkanes and also some polar compounds like the higher alcohols (ethanol, isopropanol, etc.) and acetone reasonably well through hydrophobic membranes.

5.1.2.3 Generalized Solvent Permeation Model for Polymeric Membranes:

The model discussed above reasonably predicts solvent permeabilities for hydrophobic membranes (e.g., PDMS type). However, to extend the model to different types of membranes, it becomes imperative to include measurable membrane and solvent properties along with some interaction terms to correct the transport parameter. One

could qualitatively argue that for aqueous solutions, as the membrane hydrophobicity increases, the water permeability would reduce. Rosa *et al* [1997] comment on the use of surface energies for characterization of nanofiltration membrane materials. Their studies involved the use of two commercial nanofiltration membranes, CD-NF-50 (poly(trans-2, 5-dimethyl)piperazinthiofurazanamide cast on PES backing) and HR-98-PP (polyamide active layer cast on a polysulfone backing) and three cellulose acetate nanofiltration membranes made in their laboratories. From their findings they concluded that membranes with equivalent pore radii (obtained using an integrated transport model) but more hydrophilicity (characterized by surface energy) do tend to have higher hydraulic permeabilities. Since contact angle and surface energy are related through Young's equation, contact angles can also be indirectly correlated to the solvent permeability through the membrane dense layer. To illustrate this, contact angle data for a model solvent (water in this case) and several polymers was taken from literature [Kwok *et al*, 1999]. Figure 5.12 shows a clear relationship between the contact angle of water and surfaces with different surface energies. The surface energy axis was obtained by data [Kwok *et al*, 1999] for fluorochemical-coated mica (FC-722 coating from 3M) on the low energy side (hydrophobic) and poly(methyl methacrylate) for the high energy (hydrophilic). On comparison with the contact angle data of hexane with a low surface energy material (FC-722 coated silicon wafer) [Kwok *et al*, 1999], one could qualitatively conclude that there is an indirect relationship between the contact angle and the permeation properties of the polymeric material.

With the above methodology, an attempt has been made here to correct for the solvent permeability using the surface energy and the solvent sorption values to account

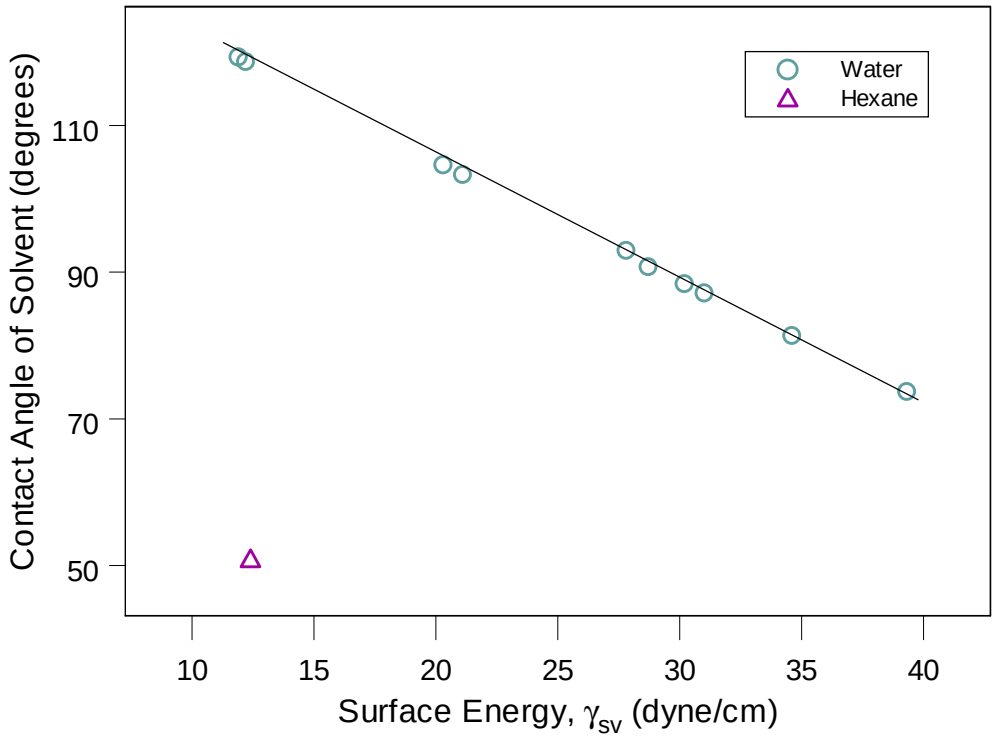

Figure 5.12: Relation between the contact angle made by water and hexane on surfaces with different surface energies (data taken from [Kwok et al, 1999])

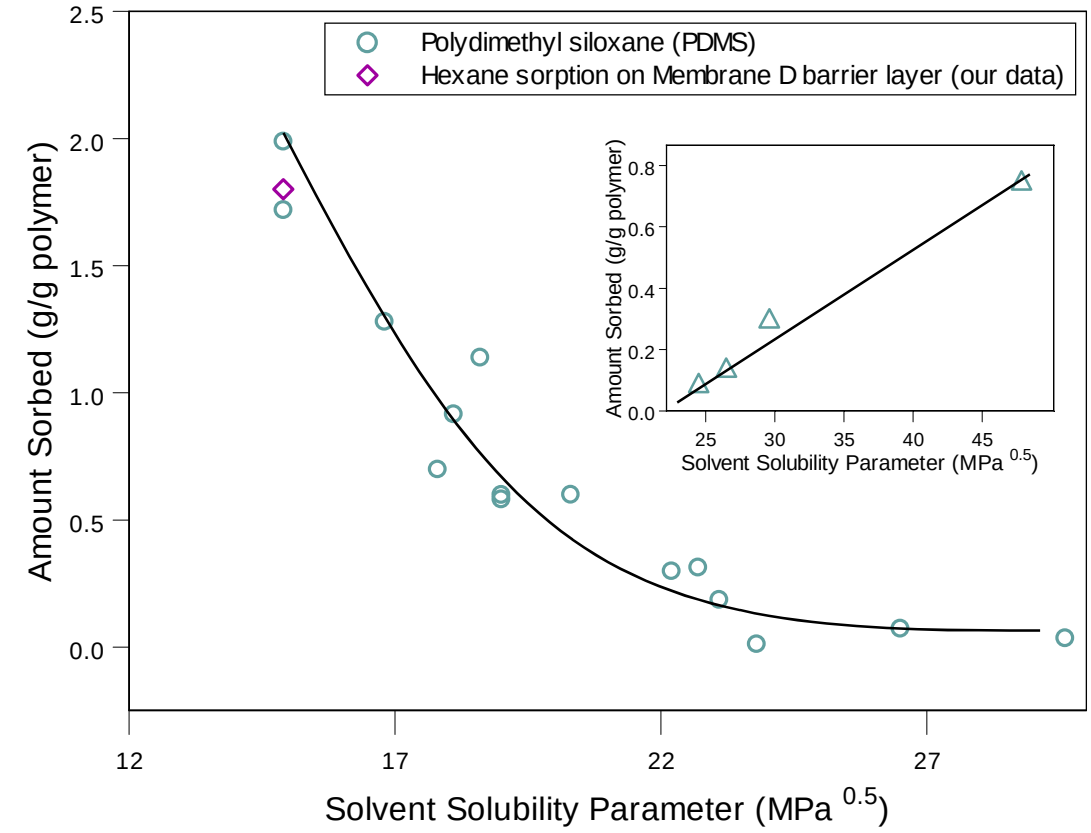

Figure 5.13: Literature and experimental solvent sorption data for Polydimethyl siloxane (PDMS) [Favre et al, 1993a; 1993b and Yang et al, 2000] Insert: Polyvinyl alcohol (PVA) [Will et al, 1992; Hauser et al, 1989] and various solvents

for specific interactions for various membranes (hydrophilic and hydrophobic). Since some of the solvents of interest wet the membrane significantly (for ex. Hexane with Membrane D), their contact angles with the membrane could not be accurately determined. As a result, to account for specific interactions, sorption values need to be incorporated. Surface free energy γ_{sv} values for membrane D and for DS 11 AG were calculated from our contact angle measurement data using the average γ_{sv} values obtained from Geometric Mean and Harmonic Mean methods [illustrated in Kwok et al, 1999] for estimating this parameter. The liquid pairs of methylene iodide and glycerine (for DS 11 AG and membrane D) and methylene iodide and ethylene glycol (for membrane D) were used. The values used for Membrane D and for DS 11 AG membranes were 16.6 dyne/cm and 52 dyne/cm respectively. A brief discussion of the sorption values obtained from literature will be presented here.

5.1.2.3.1 Role of Sorption of the solvent:

Sorption of organic solvents by polymeric membranes is an important aspect and can be used as a good measure of the interaction between the polymer and the solvent. Figure 5.13 shows sorption values for PDMS [Favre *et al*, 1993a; 1993b and Yang *et al*, 2000] and PVA [Will *et al*, 1992; Hauser *et al*, 1989] (as an insert). From the Figure, the reverse trends for the sorption characteristics of hydrophobic vs. hydrophilic materials can be easily visualized. Sorption values for various solvents and Cellulose Acetate were also obtained from literature [Sanopolou *et al*, 1997; Laatikainen *et al*, 1986]. A value of 0.33 g/g polymer was obtained for methanol-cellulose acetate system [Sanopolou *et al*, 1997; Laatikainen *et al*, 1986] as opposed to a value of 0.03 g/g polymer for the n-

heptane-cellulose acetate system [Laatikainen *et al*, 1986]. Figure 5.13 also shows the sorption data obtained for hexane sorption on the Membrane D barrier layer. It can be seen that the observed sorption value is in good agreement with the literature data.

Another aspect of the sorption of polar compounds (water and alcohols) is their clustering tendency. Favre *et al* [1993a and 1993b] have provided proof using FTIR-ATR measurements that water forms clusters when the polymer in contact with it is hydrophobic in nature [Nguyen *et al*, 1996]. They have also expressed the possibility of a similar behavior from other polar compounds like alcohols when they are in contact with hydrophobic polymers like PDMS. It is hypothesized that the type of polymer, which is in contact with the organic solvent, will control this cluster formation. If the solvent and the polymer were compatible then one would not expect cluster formation. Thus, sorption values have been used here not in the conventional term, but as a parameter for taking into account such polymer-solvent interactions. Equation 3.6 can thus be modified to consider such interactions using the sorption value, ϕ. An exponent (n) has been used as an empirical constant to obtain the best possible fit for this correction. Thus,

$$J_{solvent} \propto A \propto \left(\frac{Vm}{\mu}\right)\left(\frac{1}{\phi^{n} \times \gamma_{sv}}\right) \qquad 5.3$$

Although it might be misleading to conclude from the above correlation that the solvent flux is inversely proportional to the solvent sorption value (ϕ), it needs to be reiterated that the solvent sorption value is "LUMPED" with the membrane surface energy to account for specific polymer-solvent interactions. For example, it has been demonstrated by Favre et al [1993a, 1993b] that polar solvents tend to form clusters when

exposed to PDMS-type membranes. As a result, the surface orientation effects might be different for different solvent-polymer systems. Such effects cannot be completely explained by the absolute surface energy which is a bulk property of the membrane. Obviously, the ideal parameter for use would be the γ_{sl} (solid-liquid surface energy) values which would incorporate any sort of surface orientation/clustering effects which are neglected by the use of the absolute membrane surface energy values (γ_{sv}). Also, for a given membrane, the surface energy values would not be needed and as a result, the lumped parameter ($\phi^n \times \gamma_{sv}$) would be eliminated from the semi-empirical correlation. A correlation of the normalized solvent flux for three membranes (Membrane D, MPF-50 and the DS 11 AG hydrophilic RO membrane) with the ratio of molar volume and viscosity (as has been used earlier for hydrophobic membranes) showed large scatter in the data (R^2 = 0.61 with 26 points, standard error ~ 16%). However, on incorporation of the surface energy and the sorption values, the correlation improves. This can be seen from Figure 5.14 which shows the correlation using the above parameter (R^2 = 0.78 with 26 points, standard error = ~ 9%) [Bhanushali *et al*, 2002]. It was assumed that the MPF-50 membrane which is also a siloxane-based membrane had the same surface energy as that for Membrane D (16.6 dyne/cm). For the DS 11 AG and the cellulose actetate membranes, the surface energy values used were 52 dyne/cm and 40 dyne/cm respectively. All standard errors for the prediction of the slope are obtained using a 95% confidence limit. A value of n = 0.25 gave the best fit for the data. Since n is an empirical constant used to obtain the best fit, its value is the same for all the organic solvents and membranes used for the study. The correlation also includes literature data for methanol permeation through a cellulose acetate membrane [Sourirajan *et al*, 1985].

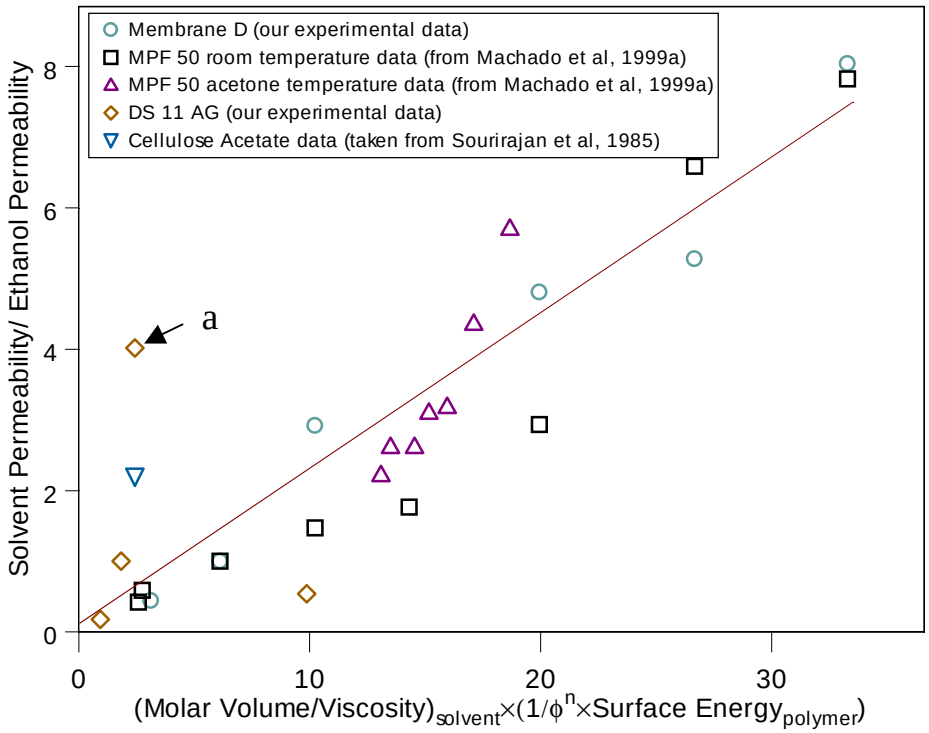

Figure 5.14: Correlation of solvent Normalized Flux (using Ethanol Flux) of polar and non-polar solvents for several hydrophilic and hydrophobic membranes.

On inclusion of surface energy of the membrane and some sorption parameters to correct for the interactions, the model can be expanded to different membranes as well as different organic solvents. The standard error reduces to 7% with R^2 = 0.87 if one methanol-DS11 AG data point (shown as point "a" in Figure 5.14) is excluded. The basicity induced (particularly with highly polar methanol) by the amide groups may account [Rosa *et al*, 1997] for higher permeability of methanol as shown in Figure 5.14.

5.2 Solute Transport:

Solvent transport through polymeric membranes has been explained using solvent and membrane physical properties. This section will concentrate on obtaining a general understanding of the transport behavior of organic solutes in non-aqueous systems experimentally. On the theoretical level, this section will explore the possibility of extension of the existing transport models (e.g., Solution-Diffusion, Spiegler-Kedem and Pore Flow) to such systems. In order to understand the solute transport behavior, it becomes essential to outline the essential variables of the system as follows:

a) Solute Size

b) Solute solubility in organic solvents

c) Solvent type (polarity, molar volume)

d) Membrane type (hydrophobic/hydrophilic, which affects the solubility of the species)

The solubility of the solutes in organic solvents limited the choice to a select few solutes. Table 4.3 and Table 4.4 from the chapter on Experimental Methods and Analysis clearly outline our experiments performed with Membrane D and the YK membrane. It should be noted that all experiments with the solutes were conducted at low concentrations and thus the solvent permeability was independent of solutes used. Permeation results for each solute will be discussed separately.

5.2.1 Experimental Results for Solute Transport:

As discussed above, solute selection was made with the idea of understanding the effect of the above mentioned parameters on solute separation behavior. The organic dye, Sudan IV was chosen because it had a wide range of solubility in organic solvents

(alcohols to alkanes). The triglycerides were chosen to establish the effect of the molecular weight on solute transport. Rejection of the solute (Equation 2.2) is the most commonly used parameter to assess the solute separation and is used in this study for non-aqueous medium. The goal of the experimental study was to obtain a general understanding of the separation behavior in non-aqueous systems and establish the effect of pressure and temperature on the solute rejection. In classical RO/NF membranes for aqueous systems, the rejection is lower at low pressures of operation and reaches an asymptotic value as more solvent passes through the membrane. It is desired to establish this effect of pressure on the rejection behavior and to suitably compare the separation behavior of aqueous and non-aqueous systems. Each solute studied will be now discussed in a separate section.

5.2.1.1 Triglycerides:

Triglycerides (TG) are esters of glycerol and are available in different molecular weights. Thus, dependence of size of the solute molecule on its transport mechanism can be studied very effectively. Also, triglycerides are used to simulate oil in hexane system since one of the potential applications of this work is the separation of hexane from vegetable oil. Effect of temperature was also determined by performing permeation studies at higher temperatures. The rejection behavior of the triglycerides in n-hexane with respect to the applied pressure and temperature is shown in Figure 5.15. It can be seen that the rejection of Tripalmitin (807 MW triglyceride) through the Membrane D is about 92% and that of Tricaprin (554 MW triglyceride) is about 72% at an applied pressure of 41 bar and at 45 °C. Figure 5.15 also shows the effect of temperature and

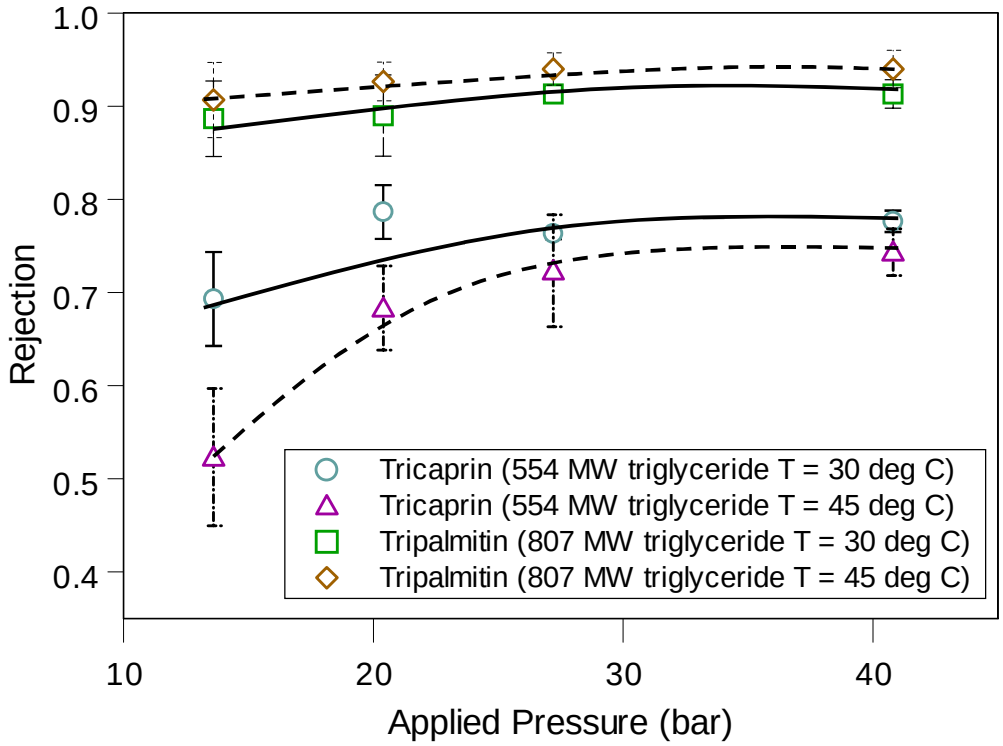

Figure 5.15: Effect of temperature and pressure on the rejection characteristics of Tripalmitin (807 MW) and Tricaprin (554 MW) in n-hexane by Membrane D

pressure on the rejection behavior of Tripalmitin and Tricaprin. It can be seen that the effect of temperature (30 °C and 45 °C) on the asymptotic rejection is not very significant although it must be pointed out that the hexane flux increased to 1.5 times its value at 30 °C. Other triglycerides were also studied for their rejection characteristics in n-hexane medium. The asymptotic rejections of Trilaurin (639 MW), Trimyristin (723 MW) and Tristearin (890 MW) are 81%, 83% and 93% at 41 bar and at 45 °C, respectively. As expected, the rejection behavior of the triglycerides increased with molecular weight. In terms of traditional NF definitions this membrane has an approximate MW cut-off of 900 in n-hexane. From Figure 5.15, it can be seen that the effect of pressure on the solute rejection behavior in hexane medium is similar to that observed in aqueous systems. In aqueous systems, typically, lower rejections are observed at lower operating pressures, however, the rejection increases and reaches an asymptotic value at higher pressures. From general material balance considerations, it can be explained that since more solvent passes through the membrane, the separation efficiency of the membrane increases.

5.2.1.2 Hexaphenyl Benzene:

Solute structure and conformation can have a significant impact on its separation behavior. Thus, hexaphenyl benzene was chosen for separation study because of its rigid aromatic structure. Also, the molecular weight of hexaphenyl benzene is about 534 and one can easily compare the separation behavior with that of Tricaprin (554 MW TG) to understand the role of the solute type on its separation. The rejection of hexaphenyl benzene in n-hexane by Membrane D is about 42 % at about 14 bar applied pressure. It is interesting to compare the rejection of this organic with the 554 MW triglyceride

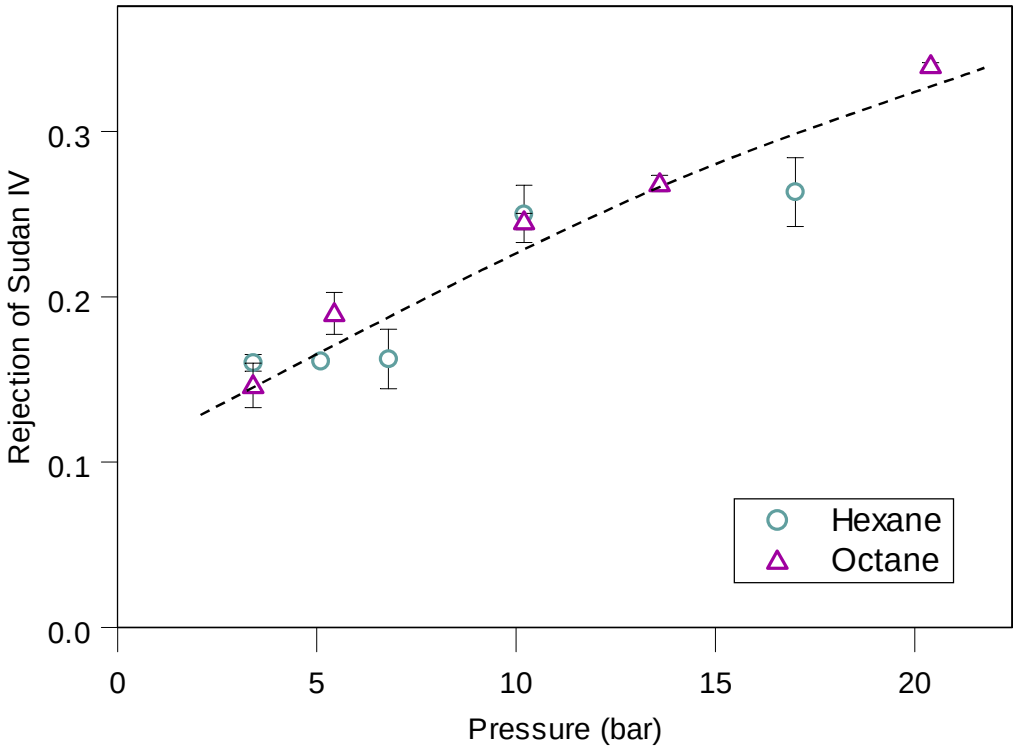

Figure 5.16: Rejection of Sudan IV by Membrane D in n-Hexane and n-Octane

(Tricaprin, 72% at 41 bar, 30 ^{o}C). Although the molecular weights of these two compounds are about the same, the rejection behavior is completely different. Although the solubility parameters for hexaphenyl benzene (534 MW) and Tricaprin (554 MW triglyceride) are 19.2 and 19.4 $(MPa)^{0.5}$ are similar, the triglyceride molecule also has polar carbonyl groups unlike hexaphenyl benzene which has aromatic groups and thus, solute-membrane interactions may also be important.

5.2.1.3 Sudan IV dye:

Solute solubility in a variety of solvents is an important aspect of establishing the separation behavior in non-aqueous medium. Since triglycerides and hexaphenyl benzene are soluble only in non-polar solvents (e.g. hexane), it was decided to use an organic dye, Sudan IV (384 MW) which has solubility in a wider range of solvents, both polar and non-polar. Sudan IV has also been used by Paul *et al* [1976] for diffusion studies through lightly crosslinked natural rubber membranes and the reason for the dye selection was the solubility in various solvents. Separation studies of Sudan IV were conducted in non-polar solvents (hexane and octane) and polar solvents (methanol and ethanol). Because of the wide range of solubility in organic solvents, the effect of membrane type on the solute separation behavior is also investigated in this study. Separation studies have been conducted using the hydrophobic siloxane-based Membrane D and the hydrophilic polyamide-based YK membrane.

For non-polar solvents, the rejection behavior of Sudan IV through siloxane-based hydrophobic Membrane D has been shown in Figure 5.16. It can be seen that the rejection of a 384 MW compound by the Membrane D is about 25% at 15 bar for both n-

hexane and n-octane. Although the separation of Sudan IV does not reach an asymptotic value, it can be seen that the effect of pressure on the separation of Sudan IV is similar to that observed for aqueous systems. Experiments for Sudan IV were typically performed in the Sepa ST© cell. The asymptotic value for Sudan IV could not be established for hexane because the permeability of hexane was high and that would not permit for sufficient time to reach steady state without changing the feed concentration. The interesting behavior of Sudan IV is its transport characteristics in polar solvent medium through Membrane D. Figure 5.17 shows the separation behavior of Sudan IV in methanol and ethanol through Membrane D. Negative rejections have been observed with low concentrations of Sudan IV in methanol and ethanol by Membrane D. For example, the rejection of Sudan IV in methanol at 40 bar is about -18% and that in ethanol at the same pressure is about – 8%. Negative rejections have been observed in literature with phenols and cellulose acetate RO membranes [Matsuura *et al*, 1972, 1973, 1974 and Burghoff *et al*, 1980]. The negative rejections for phenol (unionized) by the cellulose acetate membrane have been attributed to the high interaction with the membrane material and consequently preferential transport. Qualitatively, our experimental observations indicated higher sorption of Sudan IV on Membrane D when in methanol medium than when in hexane medium indicating the role of preferential transport clearly.

On the contrary, positive separations were obtained for Sudan IV with conventional hydrophilic membrane (YK, polyamide based) in methanol and n-hexane and the results are shown in Figure 5.18. The dye rejection at a pressure of 10 bar in methanol medium is about 86% and that in n-hexane medium is about 43%. Flux

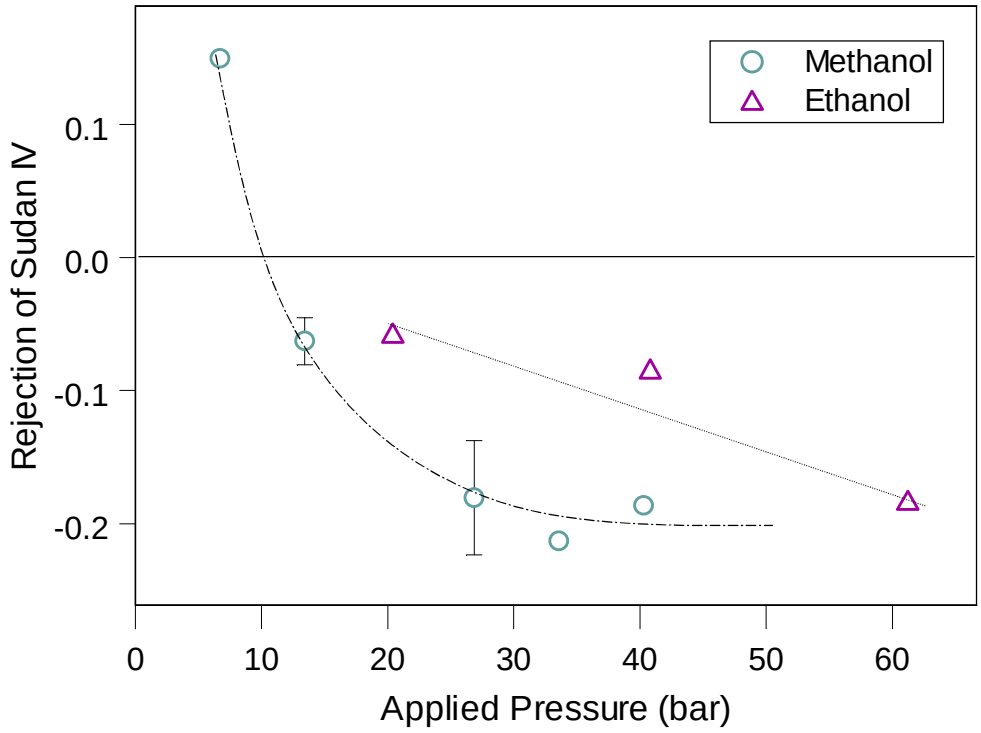

Figure 5.17: Rejection of Sudan IV in methanol and ethanol as a function of applied pressure through Membrane D.

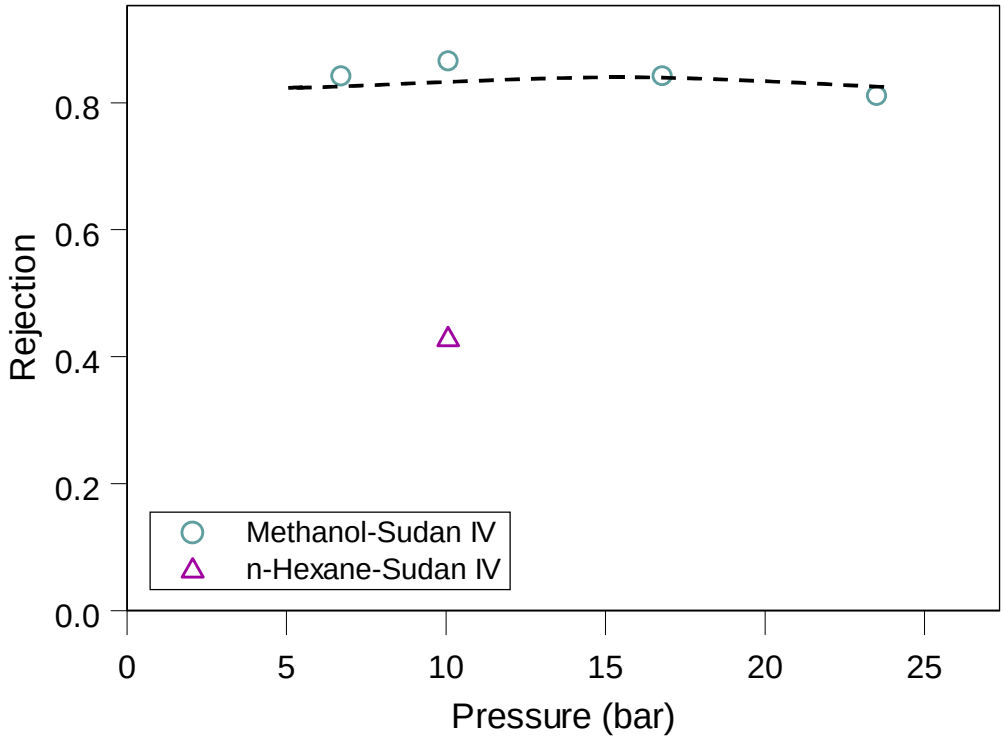

Figure 5.18: Rejection behavior of Sudan IV in methanol and n-hexane medium by the polyamide-based YK membrane

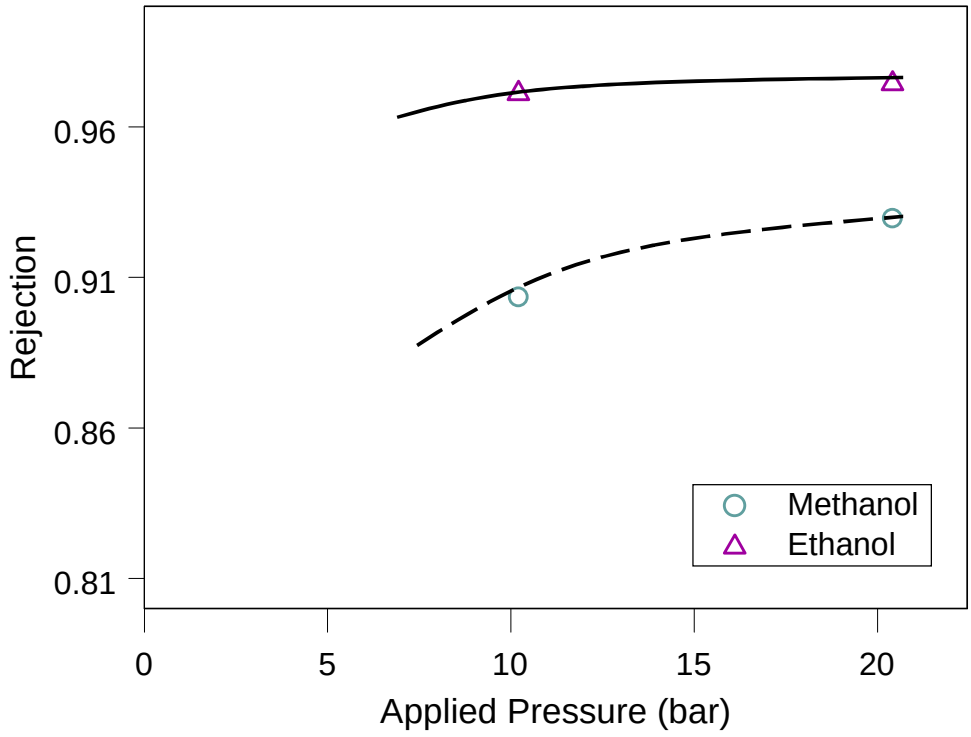

Figure 5.19: Rejection of 800 MW dye Fast Green FCF by Membrane D in alcohols

behavior with respect to pressure for this membrane has been shown as Figure 5.3 in the earlier section. As expected, the flux of n-hexane is considerably lower than that of methanol for the YK membrane, which is a negatively charged polyamide based membrane. Thus, type of membrane material and type of solvent has a significant impact on the transport characteristics of the dye molecule.

5.2.1.4 Fast Green FCF dye:

Fast Green FCF was chosen for transport studies as it is a high-molecular weight dye soluble in polar solvents. This 800 MW dye has extremely high solubility in polar solvents like methanol, ethanol etc. Figure 5.19 shows the rejection characteristics of the dye in alcohol medium. The rejection of the dye by the Membrane D is about 98% in ethanol and about 93 % in methanol at a pressure of about 20 bar. In a separate study, the rejection of the same dye by Membrane D in water was measured. Almost 100% rejections were obtained throughout the pressure range. Obviously, sieving effect is the dominating factor here. It should also be noted that the solvent permeability is in the order methanol > ethanol >> water.

From the above experimental observations, it can be clearly seen that the solvent and membrane type can significantly impact the solute separation behavior. Also qualitative experimental observations indicate the importance of preferential transport (indicated by physical examination of the membrane). One common observation outlining the above results is the effect of pressure on the solute separation behavior. The observed behavior is similar to that reported in aqueous systems, thus indicating that the

mechanisms of transport through dense membranes may be similar to those reported for aqueous systems. In order to establish this effect, further comparisons of the separation behavior for aqueous and non-aqueous systems is essential.

5.2.2 Comparison between Rejection Behavior for Aqueous and Non-aqueous Systems (Dependence of solute size):

As mentioned above, in order to establish a unified transport theory for non-aqueous systems, it is important to understand the role of size of the solvent and solute species. Useful information can be extracted from the vast literature available in aqueous medium for separation of a variety of solute-membrane systems. In an attempt to do that, this section will compare the significance of the relative size of the solvent and solute species towards its asymptotic separation behavior. Since most of the membranes developed for aqueous systems had a high water flux, this section will concentrate on comparing literature data with our experimental data obtained with Membrane D which has a high flux for non-polar solvents (e.g., hexane). Figure 5.20 summarizes our experimental results obtained in n-hexane through siloxane-based Membrane D. It can be clearly seen that for hexaphenyl benzene (534 MW) and Tricaprin (554 MW), the rejection behavior is completely different. This strongly implies that solute size is not the only governing factor for separation in non-aqueous medium and solute-membrane interactions can become critical in the prediction of the separation behavior. Several membrane materials have been developed for purification of aqueous streams. These materials have unique characteristics for the rejection behavior of organic solutes. It is widely known in literature that the mechanism of separation in dense RO/NF membranes

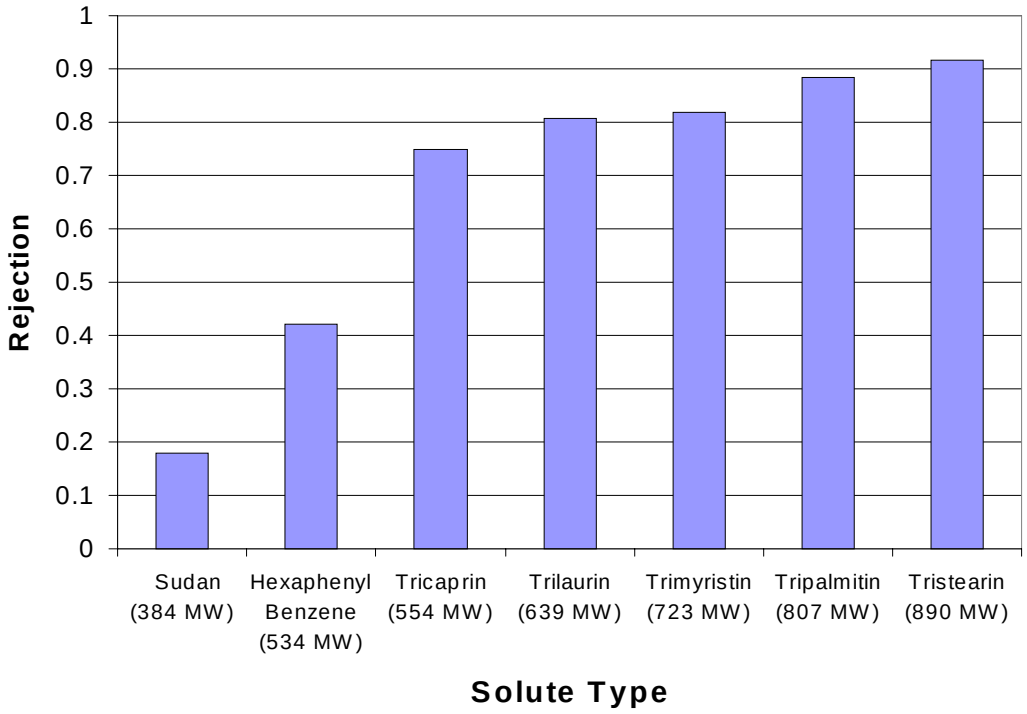

Figure 5.20: Summary of separation results obtained in n-hexane medium through Membrane D.

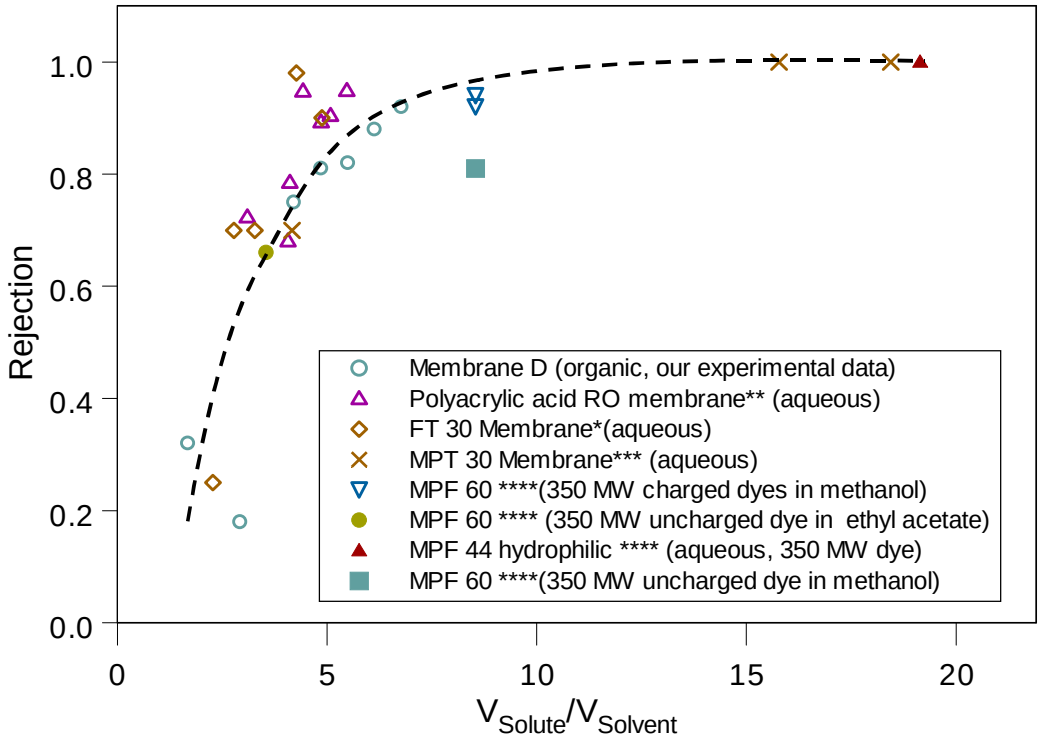

Figure 5.21: Comparison of rejection behavior for aqueous and non-aqueous systems as a function of the ratio of molar volumes of minor and major component
*Data taken from Sirkar et al [1993], ** Data taken from Huang et al [1998], *** Data taken from Perry and Linder [1989], **** Data taken from Yang et al [2001]

is not size exclusion. Figure 5.21 shows a striking similarity between the rejection behavior for aqueous and non-aqueous systems. The figure contains data for water permeating hydrophilic membranes FT-30 [Sirkar *et al*, 1993], a cross-linked polyacrylic acid based RO membrane [Huang *et al*, 1998], a pH stable membrane MPT 30 [Perry and Linder, 1989] and MPF 44 hydrophilic membrane [Yang *et al*, 2001]. The figure also contains our experimental data for Membrane D which is a high solvent (non-polar) permeating membrane and MPF 60 hydrophobic membrane [Yang *et al*, 2001]. The data for Membrane D (summarized in Figure 5.20) consists of solute permeation with n-hexane and Sudan IV and various triglycerides. It also contains data with n-octane and Sudan IV. The solute molar volume was calculated using the ratio of the molecular weight and density of the solute. In cases where the solute density was not known, molecular weight was used as the molar volume. For Sudan IV, molar volume was reported in [Paul *et al*, 1976b] and that value was used (275 cm^3/mol.). It can be seen that for high solvent permeating dense membranes, there is a definite correlation between the asymptotic rejection and the ratio of the molar volume (size) of the solute and that of the solvent. This can be illustrated by considering the rejection characteristics of the triglycerides in hexane by Membrane D. The nature of interaction would remain same as the molecular weight of the triglyceride increases.

When considering different solvents, solutes and membrane materials, however, other factors need to be considered. For example, Figure 5.21 shows the data for hydrophobic MPF 60 membrane [Yang *et al*, 2001]. In methanol medium, for instance, it can be seen that the presence of charge of the solute affects the rejection behavior. The rejection of the neutral solute (Solvent Blue 35, 350 MW) is lower than the positively

(Safranine O, 350 MW) and negatively (Orange II dye, 350 MW) charged solutes. Another interesting observation is that the rejection of the neutral solute changes dramatically when in ethyl acetate as compared to methanol. Importance of solute-membrane affinity is further illustrated. Also, solute conformation in different solvents is an important issue. Bartowiak *et al* [1998] have studied the influence of solvent on the optical properties of some betaine dyes. Ghanadzadeh *et al* [2000] have studied the influence on molecular structure of Sudan dyes in several solvents. Both the above groups point out the importance of the solvent/solute interactions affecting the molecular conformation of the solute. They especially focus on dye molecules where there are both electron-donating and accepting groups. The primary goal, however, in both the studies was to understand the change in optical properties of the system. As a result, conformational aspects due to solute-solvent interactions also need to be addressed.

Thus it can be clearly seen that although there is a striking similarity between the rejection behavior in aqueous and non-aqueous medium. Some critical aspects/variables have been identified which need to be addressed further. Some of the variables include the consideration of solute-membrane, solute-solvent interactions, solute conformation in different solvents, solute effective charge, membrane effective charge, etc. For the purpose of this study, it is not possible to address all of the identified variables. However, one clear conclusion that can be drawn from the experimental observations and the above comparison is that the solvent-solute coupling is predominant in non-aqueous systems. The first attempt to address the issue of solvent-solute coupling is to use theories proposed in literature for aqueous systems which consider the possibility of solute-

solvent coupling. These traditional transport theories will thus be evaluated in the next section to explain the experimental observations.

5.2.3 Solute Transport Mechanism:

A brief discussion of the models developed in the literature for aqueous systems has been presented in the Chapter on Theory and Background. Certain conclusions were drawn based on the comparison of the solute rejection behavior with aqueous systems. The conclusions drawn apply to our experimental data also, for example, the Membrane D rejection of Sudan IV (384 MW) in three different polar solvents followed the order of solvent polarity: hexane >> isopropanol > ethanol > methanol. As pointed above, solvent-solute coupling aspects need to be considered for non-aqueous systems. Thus, in this section, the results obtained by using existing literature models will be presented with special emphasis on the Spiegler-Kedem model and the SFPF model will be discussed briefly with respect to the solute-membrane interactions. Both the models consider the possibility of coupling of the species flux and thus have been used to explain the solute transport mechanism based on our experimental observations in non-aqueous systems.

5.2.3.1 Spiegler-Kedem Model Calculations:

Transport of solute through dense RO membranes in aqueous systems is typically by diffusion and is independent of pressure. For nanofiltration membranes, however, researchers have included convective contributions to the diffusive flux to incorporate solvent-solute coupling. The Spiegler-Kedem model is based on the irreversible thermodynamics theory and is an extension of the Kedem-Katchalsky model. This model

treats the membrane as a black box and interprets coupling of the species flux by using a simple additive contribution of the diffusion and convection. Typically, convection is synonymous with pressure dependence and is used for porous membranes but the Spiegler-Kedem model incorporates this transport mechanism to explain coupling through dense membranes. It needs to be clearly pointed out that the calculations and measurements merely indicate the "physical interpretation" of the model and must not be considered universal. Such a model merely serves to explain the permeation/separation behavior. In order to interpret our experimental results using the Spiegler-Kedem model, it becomes essential to obtain the parameters and the relative contributions shown in Equation 2.27. There are two ways to obtain the diffusive and convective contributions of the solute flux: permeation experiments and independent diffusive flux measurements. Both these methods have been used for determining the solute transport characteristics and the results will be discussed in this section.

Traditionally, the Spiegler-Kedem model has been used [Jagur-Grodzinski and Kedem, 1966; Burghoff *et al*, 1980] to consider such convective coupling between the solute and the solvent species. For example, Gilron *et al* [2001] have used the Spiegler-Kedem analysis (Equation 2.27) to include convective transport of the solute along with the diffusive flux. The solute permeability coefficient, $\overline{P}$ and the reflection coefficient, σ can be obtained from the experimental permeation data. The σ values have been obtained traditionally from the plot of the inverse of rejection vs. the inverse of flux. A sample calculation of σ is shown in Figure 5.22 for the system: Sudan IV-hexane-Membrane D. The σ value is defined as the asymptotic rejection (at infinite solvent flux) and can be obtained from the intercept (1/flux = 0 and thus flux = ∞) of the best-fit

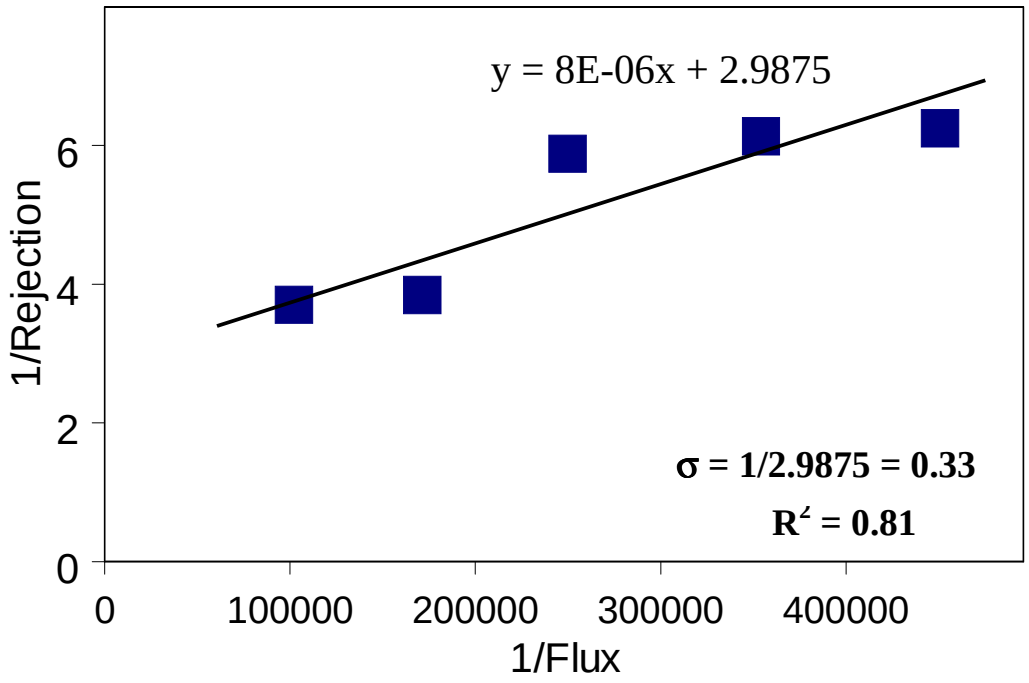

Figure 5.22: Computation of the reflection coefficient in the Spiegler-Kedem model using the membrane permeation data for Sudan IV-hexane-Membrane D system.

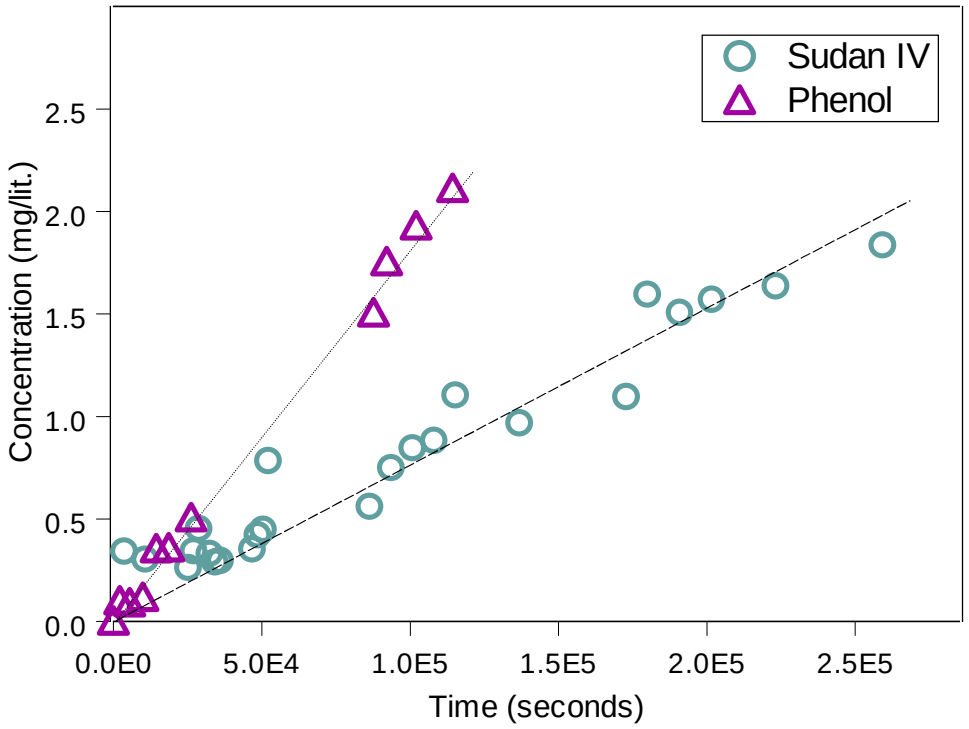

Figure 5.23: Comparison of diffusion data (Concentration Vs. time) obtained from Diffusion Cell Apparatus for Phenol and Sudan IV in n-hexane through Membrane D.

equation of the inverse of flux vs. inverse of rejection plot. $\overline{P}$ on the contrary can also be obtained from independent experiments using a Diffusion Cell apparatus. The results obtained with the diffusion measurements will be summarized in the next subsection.

5.2.3.1.1 Diffusion Measurements:

Diffusion measurements were performed with several solutes and solvents with the idea of getting quantitative insight into the transport mechanism through the Spiegler-Kedem analysis and in general to understand the role of diffusion in solute transport. The solutes, solvents and the membranes with which diffusion studies were carried out are summarized in Section 4.2.2 of Experimental Methods and Analysis Chapter. The results of these diffusion experiments will be summarized here. The standard pretreatment protocols used for membrane permeation studies were also used to pretreat the membranes used for diffusion studies. Diffusion measurements were conducted with Sudan IV, phenol and hexaphenyl benzene in hexane, methanol and ethanol medium for membrane D and YK membrane. It needs to be reiterated that membrane D is a siloxane-based hydrophobic membrane and YK is a negatively charged polyamide-based hydrophilic solvent-resistant NF membrane. Figure 5.23 shows the variation of concentration of Sudan IV and phenol in hexane medium through Membrane D. As expected, the diffusive flux (slope of the concentration vs. time curve) depends on the solute size. The diffusive flux of phenol (92MW) is three times higher than that for Sudan IV (384 MW, 0.8×10^{-8} mol/m^2 s). However, diffusion of the molecule also depends on the level of interaction of the molecule with the solvent and the membrane. As has already been established, the interaction of hexane with membrane D is

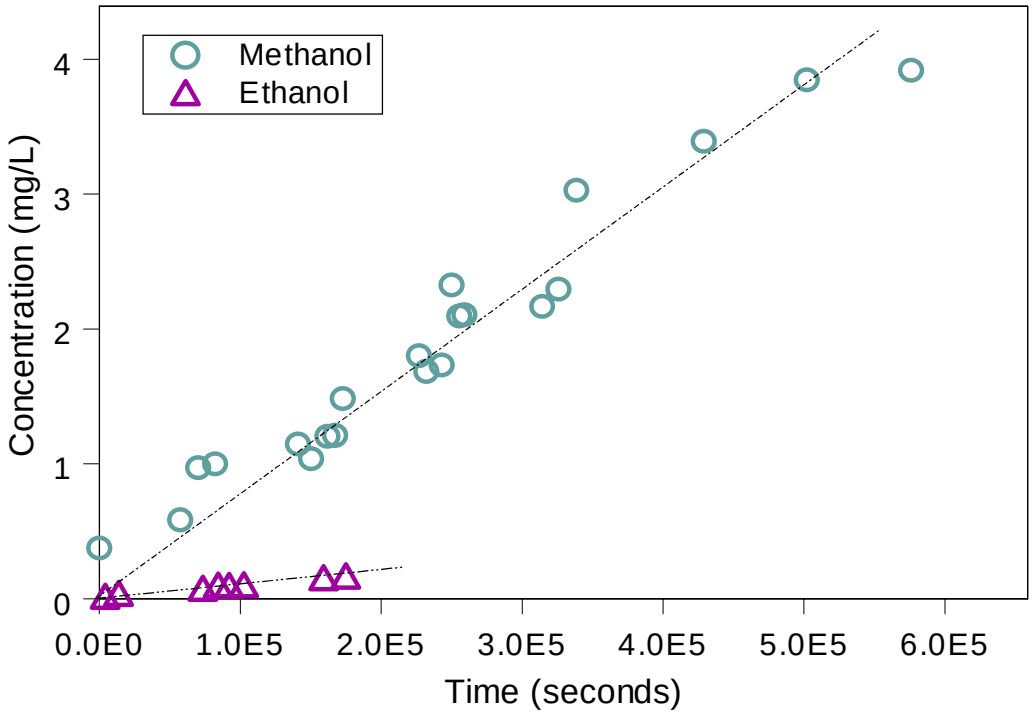

Figure 5.24: Effect of type of solvent on the diffusive flux of Sudan IV in methanol and ethanol medium through Membrane D.

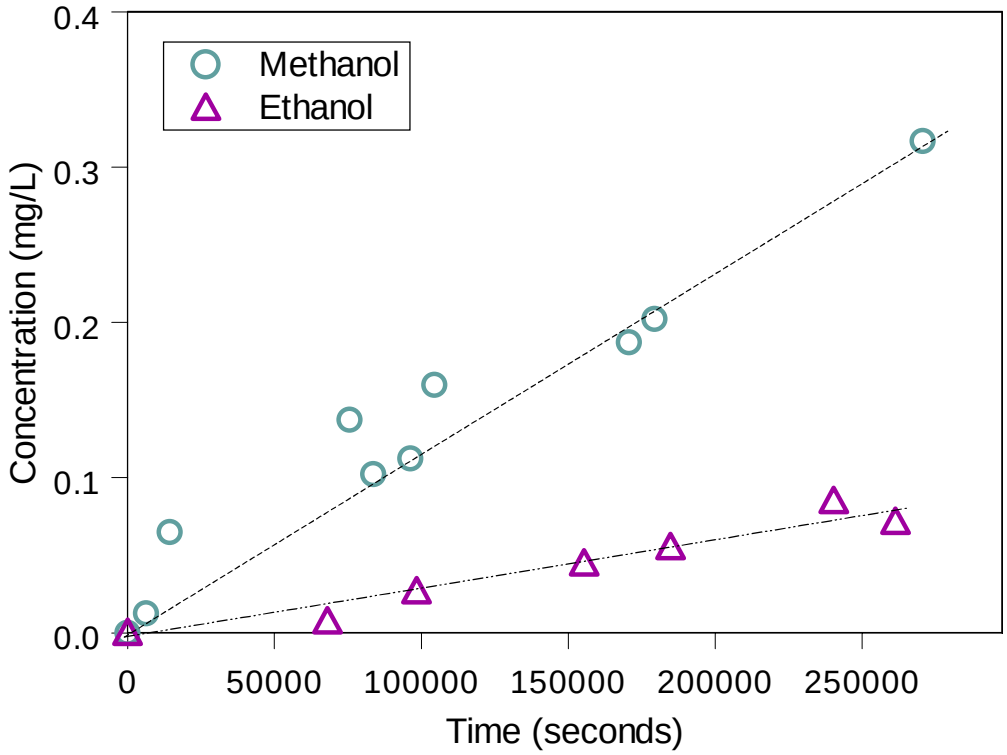

Figure 5.25: Effect of type of solvent on the diffusive flux of Sudan IV in methanol and ethanol medium through YK Membrane.

considerably higher as compared to methanol or ethanol. Within a given homologous solvent series, the diffusive flux does show dependence on solvent size. This can be readily demonstrated by Figure 5.24 which compares the diffusive flux of Sudan IV in methanol and ethanol medium through Membrane D. Figure 5.25 shows a similar dependence of the solute diffusive flux on solvent molecular size, but through the hydrophilic YK membrane. It can be clearly seen that the diffusion of Sudan IV is faster in methanol medium that in ethanol medium. One can qualitatively argue that the solute molecule is moving through the solvent layer formed due to preferential wetting of the membrane by the solvent.

Membrane hydrophilicity/hydrophobicity can also affect the solute diffusion significantly. For example, a hydrophilic membrane will have a lower partitioning for a non-polar solvent (e.g., hexane) as compared to a hydrophobic membrane. Thus, the ability of the solute molecule to diffuse through the membrane would be significantly impacted by the type of solvent-membrane interactions. In order to illustrate this effect, diffusion measurements of phenol in hexane medium were carried out with Membrane D and the YK membrane. It has been clearly shown that hexane would preferentially wet the membrane D more than the YK membrane and thus the diffusion of phenol through the membrane would be higher for Membrane D in hexane medium. This is indeed the case as shown in Figure 5.26, which clearly compares the diffusive flux contributions of phenol through the two membranes of interest.

Membrane morphology and crosslinking can play a critical role in determining the contributions of diffusion to the overall solute transport. For example, the PS-18 membrane supplied by Osmonics has been reported to be a siloxane-based membrane

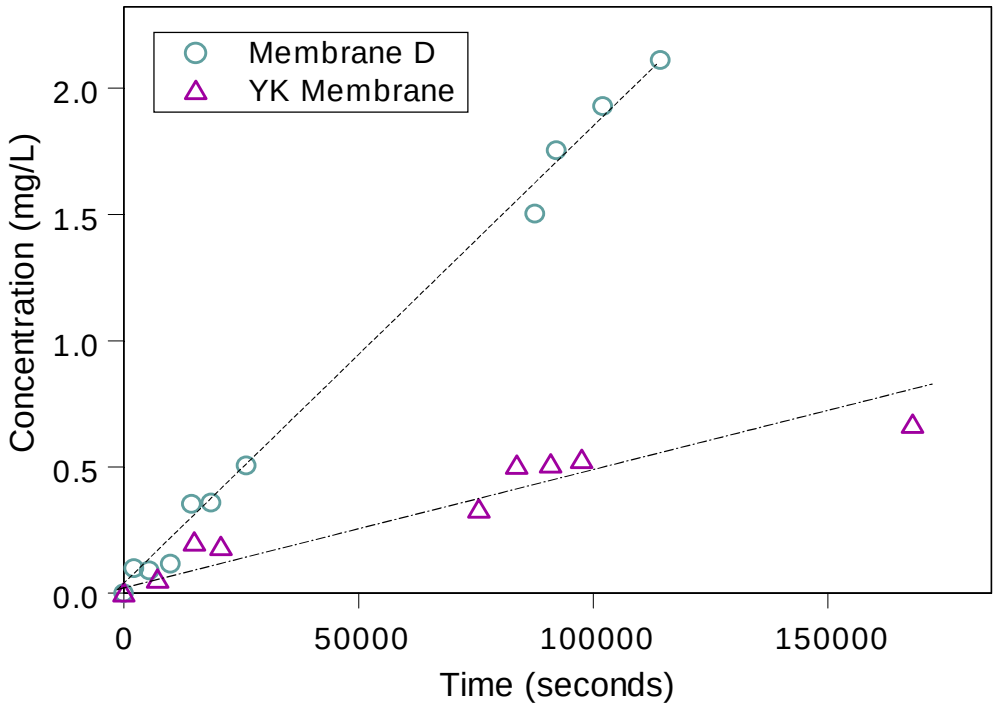

Figure 5.26: Effect of type of membrane on the diffusive flux of Phenol in hexane medium through Membrane D and YK Membrane.

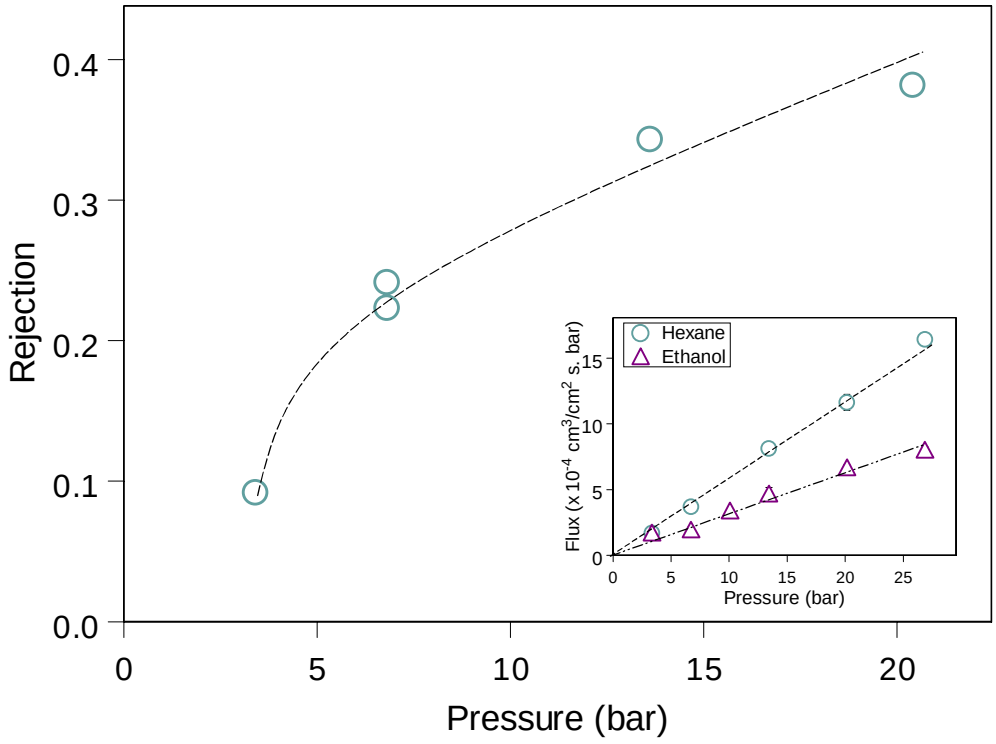

Figure 5.27: Effect of applied pressure on the separation of Sudan IV in n-hexane medium through siloxane-based PS-18 membrane. Inset: Effect of pressure on the solvent flux for siloxane-based PS-18 membrane.

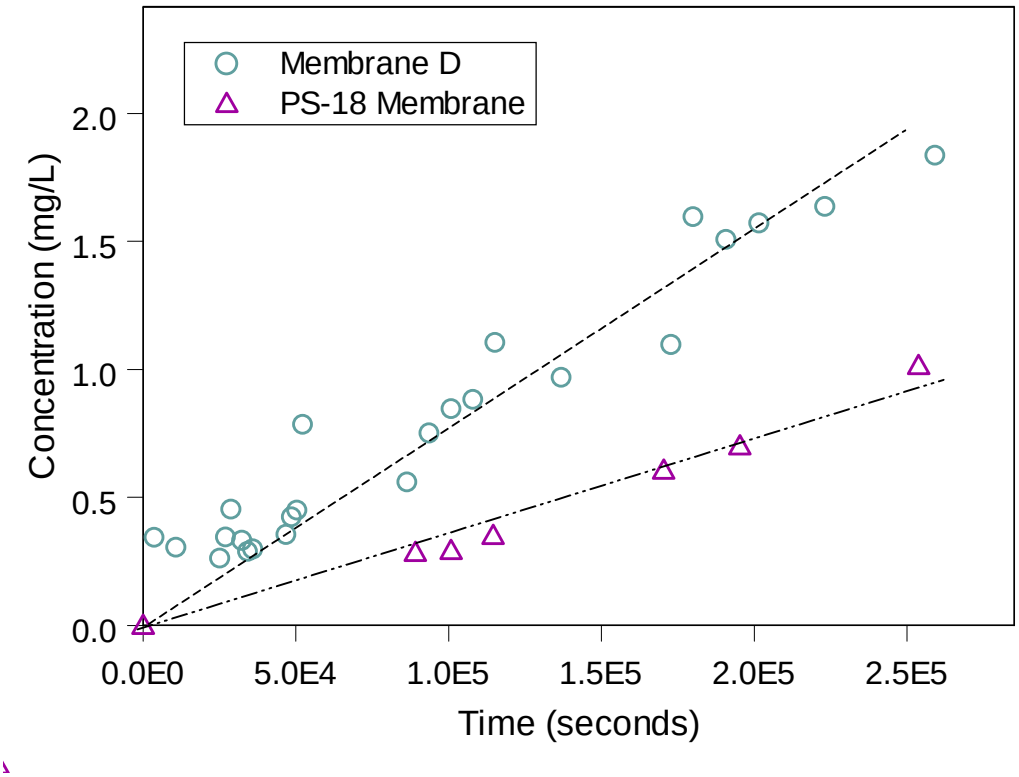

Figure 5.28: Comparison of diffusive flux for Sudan IV-hexane system through PS-18 membrane and Membrane D.

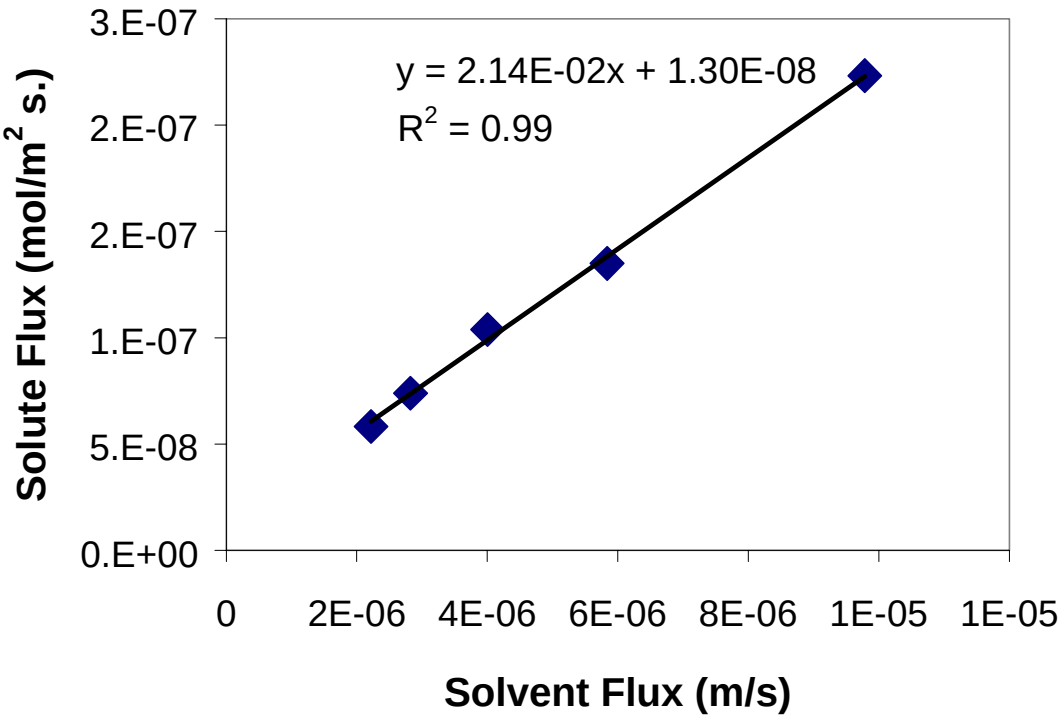

Figure 5.29: Determination of diffusive flux from membrane permeation data for Sudan IV-hexane-Membrane D system.

similar to Membrane D, but with better permeation and separation ability. Permeation and diffusion experiments were carried out with the PS-18 membrane. Figure 5.27 shows the separation results and the flux behavior for the Sudan IV-hexane system obtained with the PS-18 membrane. It can be seen that, for example, at an applied pressure of 13 bar, the hexane flux through the PS-18 membrane is about 8.6×10^{-4} cm^3/cm^2 s as compared to about 6×10^{-4} cm^3/cm^2 s for Membrane D. The separation of Sudan IV at the same pressure is about 34% for PS-18 and about 26% for Membrane D at 13 bar. Thus, the membrane has a higher separation efficiency with a higher solvent flux. As a result, it can be expected that the diffusive flux of Sudan IV must be lower because of the higher separation efficiency of the membrane. This can be seen from a diffusive flux comparison of Sudan IV in hexane through the PS-18 membrane and Membrane D shown in Figure 5.28. The diffusive flux values obtained using the above diffusion experiments can then be used to obtain the relative contributions of convection and diffusion to the total solute flux (Equation 2.27).

5.2.3.1.2 Obtaining diffusive flux values using permeation data:

In the absence of independent diffusion measurements, membrane permeation data can be used to obtain the contribution of the diffusive flux to the total flux. One way to obtain the diffusive flux data is using the classical approach of plotting the solute flux vs. solvent flux and using the Y-intercept of the plot to get the solute flux at zero solvent flux (diffusive flux). A typical plot for the Sudan IV-hexane-Membrane D system can be seen from Figure 5.29. From the plot it can be seen that the calculated diffusive flux is

about 1.3×10^{-8} mol/m^2 s. The Spiegler-Kedem equations can also be utilized to obtain the diffusive contribution. The following equations can be used:

$$R \equiv 1 - \frac{C_p}{C_b} = \frac{(1-F)\sigma}{1-\sigma F} \qquad 2.28$$

where, $F = exp\left[\frac{-J_v(1-\sigma)}{P_s}\right]$ and $P_s = \frac{\overline{P}}{\Delta x}$ = permeance 2.29

Knowing the σ value, the value for the lumped parameter, F, can be calculated using equation 2.29. For a given total flux (J_v), the corresponding rejection is known from membrane permeation data available. Thus, using σ and rejection R, equation 2.28 and equation 2.29 can be solved to obtain a value of P_s. This value of the permeance can now be used with a concentration gradient to obtain the diffusive flux using the following equation:

$$DiffusiveFlux = P_s(c_f - c_p) \qquad 5.4$$

Table 5.2 summarizes the results (i.e. σ and the permeance values) calculated from membrane permeation studies. It includes the parameters obtained from our experimental data as well as literature data [Bhattacharyya *et al*, 1986]. The standard deviations for the permeance values have been obtained by using the different pressure data. The σ values were obtained from the plots of inverse of rejection and inverse of flux (R^2 ranged between 0.89 to 0.99; minimum 3 and maximum 5 points). Since diffusion experiments were carried out for some of the solutes, the results of the diffusion cell will be compared with those obtained from membrane permeation studies. Table 5.3 consists of diffusive fluxes for Sudan IV - Hexane - Membrane D system obtained from membrane permeation data calculations and from independent diffusion cell studies. It

Table 5.2: Solute permeance and sigma parameters from literature [Bhattacharyya et al, 1986] and our experimental data obtained from membrane permeation data

Solute - Solvent	Membrane	σ**	Permeance (m/s)
Formic Acid - Water	FT 30*	0.55	$7.78\ (\pm 0.8) \times 10^{-6}$
Acetic Acid - Water	FT 30*	0.72	$3.23\ (\pm 0.5) \times 10^{-6}$
1-propanol - Water	FT 30*	0.88	$1.18\ (\pm 0.2) \times 10^{-6}$
1-butanol - Water	FT 30*	0.95	$0.62\ (\pm 0.1) \times 10^{-7}$
Sudan IV - hexane	D	0.33	$4.54\ (\pm 0.9) \times 10^{-6}$
Phenol - hexane	D	0.005	$7.78\ (\pm 0.8) \times 10^{-6}$
Sudan IV - octane	D	0.37	$2.69\ (\pm 0.6) \times 10^{-6}$

* Data taken from [Bhattacharyya et al, 1986]
** Equation (2.27)

Table 5.3: Comparison of Diffusive Flux values for Sudan IV - hexane system (our experimental data) obtained from different calculations (all flux values are in mol/m^2 s)

P (bar)	**Using Intercept from plot of Solute Flux Vs. Solvent flux**	**Using Permeance values from Table 5.2 and permeate concentrations**	**Using Diffusion Cell data**
3.35	1.30×10^{-8}	2.27×10^{-8}	0.796×10^{-8}
5.03		2.31×10^{-8}	
6.70		2.41×10^{-8}	
10.05		3.69×10^{-8}	
16.75		3.83×10^{-8}	

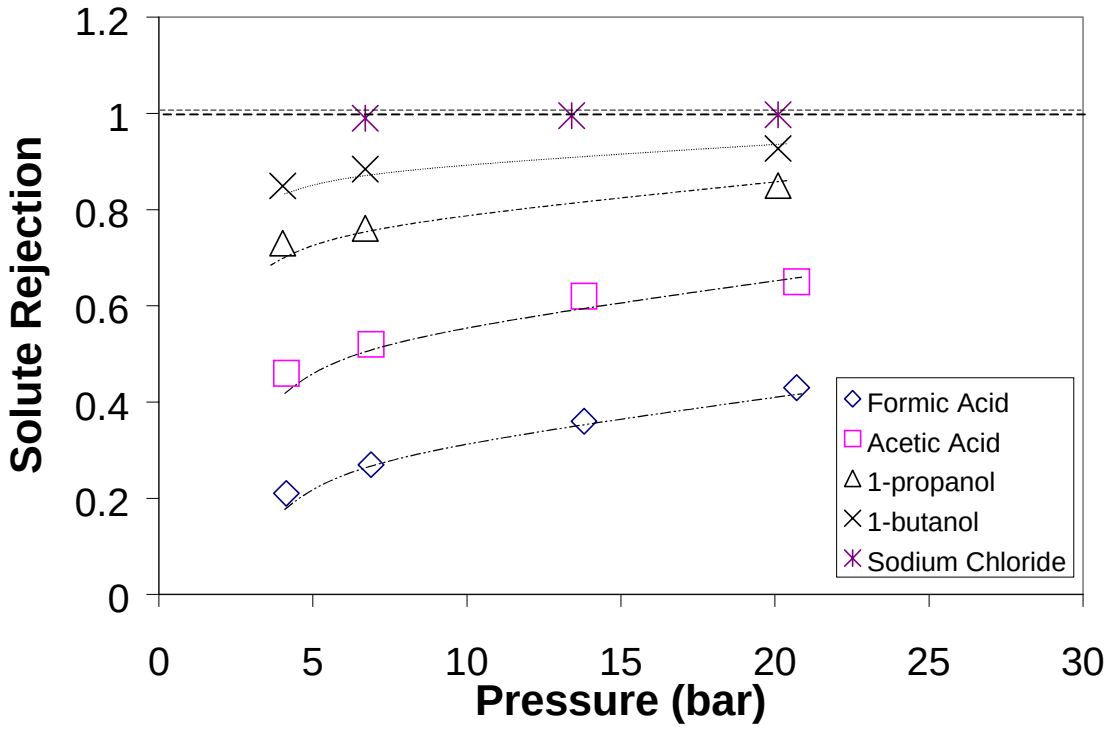

Figure 5.30: Solute separation data as a function of applied pressure for the FT-30 brackish water RO membrane taken from Bhattacharyya et al [1986] for transport analysis.

can be seen that the three values obtained are comparable. For example, the value obtained from intercept of the plot of J_{solute} vs. $J_{solvent}$ is 1.3×10^{-8} mol/m^2 s and that obtained from independent diffusion measurement is 0.796×10^{-8} mol/m^2 s. These two values are of the same order of magnitude as those obtained from permeance calculations. Thus, in absence of independent diffusion cell measurements, the permeance values and the permeation data can be used as reasonable approximations to obtain the diffusive flux.

The above model calculations give insight into the contributions of diffusion and convection to the solute transport. For example, Table 5.4 shows the flux contributions for our experimental data with Membrane D. As expected, the diffusive contributions in hexane medium for Sudan IV (384 MW) are considerably lower than those for the C 10 triglyceride (554 MW). Also, the convective contributions of Sudan IV in methanol dominate the solute flux which can explain the negative rejection behavior. The methanol flux is lower than that of hexane and thus the high convective contribution results in enrichment of Sudan IV in the permeate. In order to examine the validity of the above results, the calculations were performed with membrane permeation data for the classical FT-30 brackish water RO membrane. Figure 5.30 illustrates the data taken from Bhattacharyya *et al* [1986] and Table 5.5 summarizes the results for the FT-30 data. It can be clearly seen from the calculations that the convective contributions reduce significantly with molecular size for a particular homologous series. Figure 5.31 shows a comparison of the convective flux contributions for the systems mentioned above. The convective flux has been normalized with the total solute flux at 10 bar as reference to compare the different solute-solvent-membrane systems. Normalizing the flux eliminates

Table 5.4: Diffusive and Convective Flux contributions for our experimental data with Membrane D

P (bar)	Solute Flux (mol/m^2 s.)	Convective Flux (%)
1. Sudan IV- Hexane**		
3.35	5.82×10^{-8}	86.33
5.03	7.38×10^{-8}	89.22
6.70	1.04×10^{-7}	92.33
10.05	1.35×10^{-7}	94.10
16.75	2.23×10^{-7}	96.43
2. Sudan IV - Methanol**		
6.7	5.85×10^{-8}	88.07
33.5	2.42×10^{-7}	97.11
50.25	2.81×10^{-7}	97.52
60.3	3.07×10^{-7}	97.73
3. C10 Triglyceride - Hexane*		
13.4	7.38×10^{-6}	21.26
26.8	8.33×10^{-6}	24.46
40.2	1.12×10^{-5}	30.71

* Diffusive flux calculated from membrane permeation data
** Diffusive Flux measured from Diffusion Cell Apparatus

Table 5.5: Diffusive and Convective flux contributions for literature data (FT 30 membrane data taken from [Bhattacharyya et al, 1986]

P (bar)	Solute Flux (mol/m^2 s.)	Convective Flux (%)
1. Formic Acid		
4.02	2.84×10^{-5}	46.96
6.7	4.38×10^{-5}	52.50
13.4	7.68×10^{-5}	60.92
20.1	1.02×10^{-4}	64.86
2. Acetic Acid		
4.02	1.56×10^{-5}	33.54
6.7	2.30×10^{-5}	41.39
13.4	3.65×10^{-5}	51.72
20.1	5.01×10^{-5}	59.56
3. 1-Propanol		
4.02	7.78×10^{-6}	22.42
6.7	1.15×10^{-5}	30.58
20.1	2.15×10^{-5}	49.79
4. 1-Butanol		
4.02	5.44×10^{-6}	13.71
6.7	6.96×10^{-6}	18.86
20.1	1.31×10^{-5}	36.34

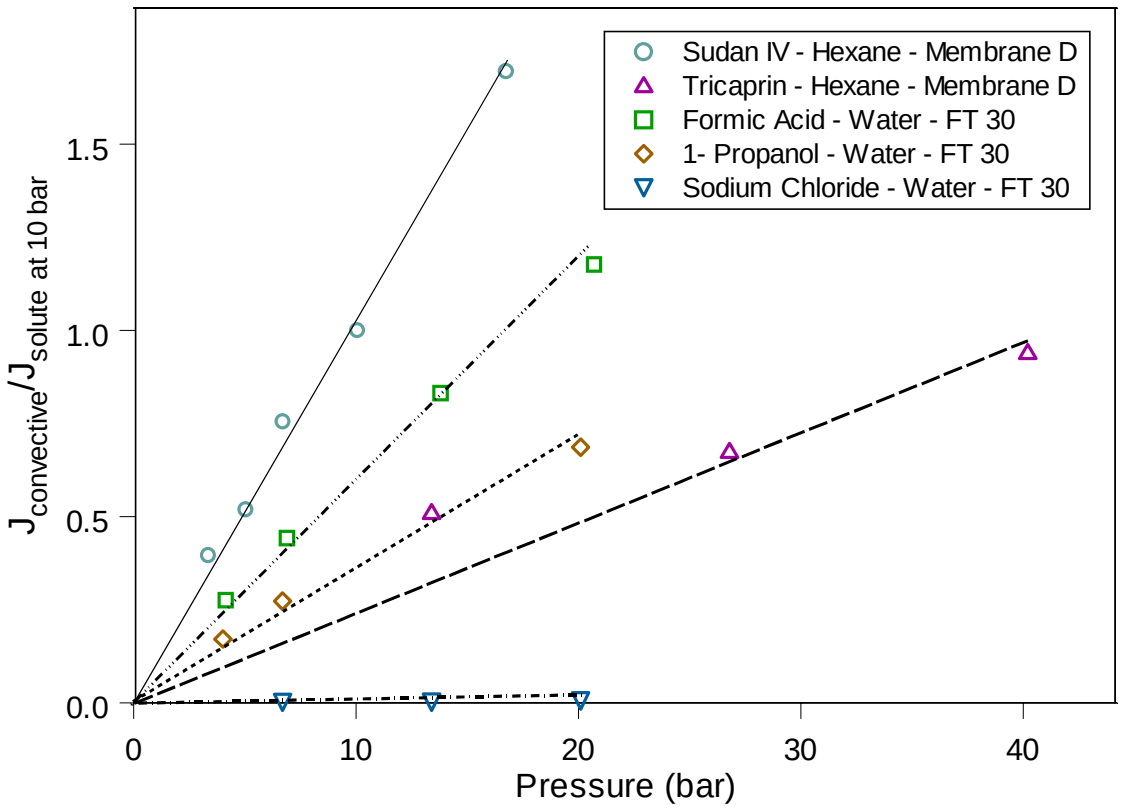

Figure 5.31: Comparison of normalized convective flux contribution to the total solute flux for literature and our experimental data using Spiegler-Kedem analysis (FT 30 data taken from [Bhattacharyya et al, 1986]).

the differences in the feed concentrations and the affinity for the membrane material. It can be seen that in all the cases (FT-30 and Membrane D), the convective flux contribution is linear with respect to pressure. The similarity between the FT-30 data and our experimental data suggests that the principles of convective transport apply to both the systems according to the Spiegler-Kedem Analysis. A similar plot for sodium chloride -water-FT 30 reverse osmosis membrane as expected shows the extremely low contribution of the convective flux to the solute flux. As expected, for sodium chloride there is minimal coupling between the solvent and the solute fluxes. For the same size ratios (i.e. molar volume of the solute to the solvent), the slopes are different indicating that membrane material and cross-linking may be important factors to be considered to obtain a unified theory. Also, as expected the convective contributions to the total solute flux reduce as the size ratio increases as can be seen from the Figure 5.31 clearly. Of course, above a particular molecular size, sieving becomes a dominant mechanism.

From the above calculations, it can be seen that the Spiegler-Kedem model serves merely as a mode of interpreting the experimental observations. It is difficult to use the model as a predictive tool since it considers the membrane as a black box and solvent and solute physical properties are not incorporated into the model.

5.2.3.2 Pore Model Calculations:

The pore flow models assume the membrane to be made of angstrom-diameter pores and transport occurs through these pores. The basic assumption is that the solvent preferentially wets the pore, thus reducing its "effective pore diameter". The solute transports through this reduced diameter and thus the dependence of solute separation on

the solvent type has been incorporated into the theory. The Spiegler-Kedem analysis considers the convective coupling aspects, however, the model does not have parameters to consider specific interactions between the solute and the membrane. The SFPF (Surface Force-Pore Flow) model considers the convective coupling aspects of transport and also has the B_{SFPF} parameter in the potential function which can be used as a measure of the solute-membrane interaction. Several research groups have used the SFPF model for their experimental results. Farnand *et al* [1983] have used organic and inorganic solutes in methanol medium and have determined the values of B_{SFPF}. Table 5.6 summarizes their findings for organic solutes in both aqueous and methanol medium through cellulose acetate membranes. The table also contains the rejection values for these organic solutes in both solvents. It can be clearly seen that the B_{SFPF} values for all the solutes are dependent on the solvent type. This is expected because the basic premise of the model is that the solvent preferentially wets the membrane and thus reduces the effective diameter of the pore available for transport of the solute. As can be seen from Table 5.6, there is a general trend in the B_{SFPF} values. For example, the B_{SFPF} value in methanol medium is more than that in the aqueous medium (except for dimethyl aniline). Also, the rejection values in water are slightly higher than in methanol. The positive B_{SFPF} values also imply that there is an attractive van der Waals force between the solutes and the membrane (cellulose acetate in this case).

The FT-30 results analyzed by the Spiegler-Kedem model in the previous section will now be analyzed using the pore-flow model assumption. Table 5.7 shows B_{SFPF} values for two RO membranes with solutes in aqueous medium. For the FT-30 membrane (adapted from Bhattacharyya *et al*, [1986]), it can be clearly seen that there is

Table 5.6: B_{SFPF} values and rejection behavior of some organic solutes in water and methanol medium through cellulose acetate membrane [Sourirajan et al, 1985; Farnand et al, 1983]

Solute	$B_{SFPF,methanol} \times 10^{30}$ m^3	$R_{methanol}$	$B_{SFPF,water} \times 10^{30}$ m^3	R_{water}
Acetonitrile	79.76	0.034	28.49	0.062
Propionitrile	50.04	0.001	34.2	0.048
Propionamide	26.57	0.074	19.13	0.062
Aniline	76.41	-0.052	48.98	-0.052
Dimethyl Aniline	61.21	-0.001	125.8	0.162

Table 5.7: Solute radius and B_{SFPF} value for FT 30 membrane in aqueous medium [Bhattacharyya et al, 1986] and Cellulose Acetate Membranes [Sourirajan et al, 1985]

Solute	**$B_{SFPF,water} \times 10^{30}$ m^3 (Cellulose Acetate)**	**$B_{SFPF,water} \times 10^{30}$ m^3 (FT-30)**	**Solute Radius $\times 10^{10}$ m**
Butyric Acid	--	-830	2.65
Propionic Acid	--	-400	2.42
Acetic Acid	--	-230	2.05
Formic Acid	--	-105	1.60
1-Butanol	47.27	-820	2.49
1-propanol	38.40	-591	2.21

Table 5.8: SFPF parameters and asymptotic rejections for our experimental data with Membrane D.

System	$B_{SFPF} \times 10^{30}$ m^3	Asymptotic Rejection (%)
Sudan IV – n-hexane (T = 23 °C)	-944 ± 37	27 ± 0.3
Sudan IV – Methanol (T = 23 °C)	-860 ± 14	-13 ± 1.1
C10 TG (T = 30 °C)	-491 ± 10.4	78 ± 0.8
C16 TG (T = 30 °C)	-320 ± 53	94 ± 2

a strong size dependence of the B_{SFPF} value in a homologous series. The FT-30 membrane is an aromatic polyamide based membrane. Thus according to the B_{SFPF} values, there is a repulsive force between the membrane material and the solute. Similar is the case with the alcohols. However, for the cellulose acetate membrane, the B_{SFPF} value is slightly positive for the alcohols, which means that there is an attractive force acting between the solute and the membrane. Thus, the B_{SFPF} values predict the right nature of interaction between the solutes and different membrane materials.

For our experimental data, the following assumptions are made to calculate the B_{SFPF} values for the system of organic solvents and solutes using the SFPF model. These assumptions were made to get an estimate of the B_{SFPF} values and how they agree with existing literature data for aqueous systems. The assumptions made are:

a) Parabolic Velocity Profile for the solution
b) Radius of the pores (R_b) is assumed to be 10 Å [similar to the radius taken for the dense FT-30 RO membrane by Bhattacharyya et al, 1986]
c) Stoke's Radius used for calculating solute radius
d) Wilke-Chang Equation used to obtain D_{ab}
e) Faxen Equations used for calculation of b [Sourirajan and Matsuura, 1985]
f) No concentration polarization (Observed Rejection = Intrinsic Rejection)
g) Solvent Molecule radius ($r_{solvent}$) obtained assuming spherical molecule and from Avogadro Number calculations using Molar Volume

Table 5.8 summarizes the results obtained for our experimental data using the SFPF model. The table contains the asymptotic rejection values for the systems studied and the calculated B_{SFPF} values. The experimental results are all for Membrane D, which

is a siloxane-based membrane. It can be seen that the B_{SFPF} value for the dye Sudan IV depends on the solvent type, which is consistent with the observations in literature for cellulose acetate membranes. The higher B_{SFPF} value of Sudan IV in methanol also suggests that there is a higher attractive force between the dye and the membrane material as compared to that in n-hexane. This higher attractive force can be used to explain the lower rejections in methanol. Also, the B_{SFPF} values for the triglycerides are significantly higher (more positive) than the Sudan IV value which is expected since the triglycerides have a hydrophobic nature as compared to Sudan IV.

5.3 Proposed Diffusion-based Model for Solute Transport:

From the above treatment of results, it can be seen that several literature models fail to be predictive models and serve as mere interpretations of the observed data. Thus, an attempt is made here to develop a transport model which uses the solvent, solute and membrane interactions to explain permeation behavior. The model uses the traditional chemical potential gradient-based approach to explain solute transport. It needs to be pointed out that this proposed model will initially serve as an interpretation of the experimental results and using the information, can be used as a predictive model to calculate solute separation behavior for additional systems. The relevant equations and assumptions used for the proposed model have been highlighted in Chapter Three. Some disadvantages of the literature models discussed above are as follows:

a) Literature models use adjustable parameters which are usually lumped to explain the transport mechanism. The adjustable parameters are typically used to fit experimental data and have little physical significance. Also, it is difficult to measure these parameters experimentally. The Spiegler-Kedem model, for example, requires the permeance, reflection coefficient and the phenomenological constants for predicting transport. It is difficult to measure these parameters from independent experiments.

b) Some models (e.g. Solution-Diffusion Model) fail to incorporate the species coupling aspects which are essential towards any unified theory to explain transport. The Solution-Diffusion-Imperfection model incorporates coupling by introducing an additional parameter which has little physical significance and requires further data fitting.

c) Few literature models incorporate the solvent/solute physical properties (e.g. solvent viscosity, solvent size, solvent/solute molar volume) and membrane properties. Such parameters are essential for any model to be applicable to a wide range of components.

The proposed model considers the interactions by using two activity coefficient theories: Flory-Huggins theory and the sophisticated UNIFAC theory. Although the model uses two adjustable parameters, both these parameters have a strong physical significance: solute and solvent diffusion coefficients through the membrane. The goal is to develop a correlation based on these adjustable parameters to enable prediction of separation behavior for other solutes. Effect of pressure and that of solute size on the separation behavior will be two key issues which will be addressed in this section. The Flory-Huggins and the UNIFAC theories will also be compared for possible advantages and disadvantages. A brief comparison of the diffusion coefficients obtained from the calculation will be presented with some literature values to validate the obtained parameters. A sensitivity analysis section will also be presented which will vary some key parameters to understand their impact on the calculations. This analysis will provide useful guidelines about the applicability of this model to other systems. Throughout the discussion, the following numbering will be used for species i: 1-solvent; 2-solute and 3-membrane.

5.3.1 Input Parameters:

The first step is to obtain the boundary conditions that need to be employed for the calculations, and the input parameters needed for the same. It needs to be reiterated

Table 5.9: Input Parameters used for Flory-Huggins approach (1-solvent; 2-solute)

Parameter	Trilaurin	Trimyristin
δ_1 $(MPa)^{0.5}$	14.90	14.90
δ_2 $(MPa)^{0.5}$	18.98	18.81
δ_3 $(MPa)^{0.5}$	15.50	15.50
V_1 (cm^3/mol)	131.60	131.60
V_2 (cm^3/mol)	639.00	723.00

Table 5.10: Input Parameters used for UNIFAC approach (1-solvent; 2-solute; 3-membrane)

Parameter	Trilaurin	Trimyristin	Tripalmitin	Tristearin
R_{CH3}	0.9011	0.9011	0.9011	0.9011
R_{CH2}	0.6744	0.6744	0.6744	0.6744
R_{CH}	0.4469	0.4469	0.4469	0.4469
R_{CH2COO}	1.6724	1.6724	1.6724	1.6724
R_{SiO}	1.1044	1.1044	1.1044	1.1044
Q_{CH3}	0.8480	0.8480	0.8480	0.8480
Q_{CH2}	0.5400	0.5400	0.5400	0.5400
Q_{CH}	0.2280	0.2280	0.2280	0.2280
Q_{CH2COO}	1.4200	1.4200	1.4200	1.4200
Q_{SiO}	0.4660	0.4660	0.4660	0.4660
ν_{CH2}	31	37	43	49
$\nu^{(2)}_{CH2}$	27	33	39	45
a(1,11)	232.1	232.1	232.1	232.1
a(11,1)	114.8	114.8	114.8	114.8
a(1,43)	252.7	252.7	252.7	252.7
a(43,1)	110.2	110.2	110.2	110.2
a(11,43)	0	0	0	0
a(43,11)	0	0	0	0

* Calculated using our experimental sorption data for hexane and Membrane D active layer of 1.89 gm/gm membrane

** Calculated using Flory-Rehner approach from known $\chi_{2,3}$ values (Equation 2.5)

Note: All R_k, Q_k and a (m,n) values obtained from Poling et al, 1997;

ν_k : Total number of groups of type k in the system ($\nu_{CH3} = 7$; $\nu_{CH} = 1$; $\nu_{CH2COO} = 3$; $\nu_{SiO} = 1$)

$\nu^{(i)}_k$: Number of groups of type k present in species I ($\nu^{(1)}_{CH3} = 2$; $\nu^{(1)}_{CH2} = 4$; $\nu^{(2)}_{CH3} = 3$; $\nu^{(2)}_{CH} = 1$; $\nu^{(2)}_{CH2COO} = 3$; $\nu^{(3)}_{CH3} = 2$; $\nu^{(3)}_{SiO} = 1$)

a(m,n): Interaction parameters between main groups m and n.

that the discontinuous pressure condition on the permeate side induces an activity gradient for the species within the membrane which acts as the driving force for the transport. Table 5.9 summarizes the values of the input parameters used for the Trilaurin-hexane-Membrane D and Trimyristin-Hexane-Membrane D system with the FH treatment. The parameters are the solubility parameters (δ_i 's) and the molar volumes (V_i's). The chi ($\chi_{m,n}$) values for the solute-membrane and the solvent-solute system have been obtained using the Hildebrand solubility parameter approach (Equation 2.4) and the solute and solvent solubility parameters. Although some inherent flaws of the Hildebrand approach have been pointed out, it has been used here due to lack of availability of other techniques to determine the chi parameters. Experimental values for the chi parameter have been used where available. For example, the solvent-membrane (hexane-PDMS in this case) chi parameter ($\chi_{1,3}$=0.45) has been reported by Gundert *et al*, [1997] and has been used directly. Calculations could not be performed with MATLAB for the Tripalmitin-Hexane and the Tristrearin-Hexane case with the Flory-Huggins approach since the equations become stiff for numerical solution. Table 5.10 shows the values of the input parameters used for the systems studied using the UNIFAC approach. The thermodynamic input parameters were obtained from Poling *et al* [1997]. The advantage of the UNIFAC approach is that most of the groups encountered have values tabulated and can be directly used. However, simulations could not be performed with Sudan IV since group contribution parameters were unavailable for the azo group present in the dye structure.

5.3.2 Calculation of Boundary Conditions:

The algorithms for the calculation of the boundary conditions have been outlined in Chapter 3. The solvent partitioning values, i.e., the solvent volume fraction, ϕ_{if} were obtained as follows. The solvent volume fraction has been obtained from partitioning data for hexane. Experimentally, this value was determined as 1.89 gm/gm polymer. Recall that Figure 5.13 shows the variation of the sorption of solvents as a function of the corresponding solubility parameters. Good agreement can be clearly observed from the reported and measured values for the hexane-PDMS system. Converting this value of 1.89 gm/gm into a volume fraction yields a value of $\phi_{1f} = 0.73$. For the case of the solute, such partitioning data was unavailable and thus the Flory-Rehner approach (Equation 2.5) has been used to obtain the volume fraction, ϕ_{2f} as follows. The solute solubility parameter is used to calculate the chi parameter between the solute and the membrane ($\chi_{2,3}$) and using this chi value in Equation 2.5 the polymer volume fraction is calculated. It is assumed that the system is binary in nature during this calculation. Once the polymer volume fraction is calculated to match the $\chi_{2,3}$ value, the solute volume fraction, ϕ_{2f} is obtained and used for further calculation. Additional sample calculations along with the computer programs have been compiled in the Appendix section.

Figure 5.32 and Figure 5.33 show the variation of the boundary condition on the permeate side with applied pressure using Flory-Huggins and UNIFAC theories for the solvent (hexane) and the solute (Trilaurin, 639 MW TG). As expected, the volume fractions of the solute and solvent on the permeate side reduce with increasing applied pressure thus explaining the increase in the solvent flux (and thus the solute flux) with pressure. It can be clearly observed that the variation of the boundary conditions with

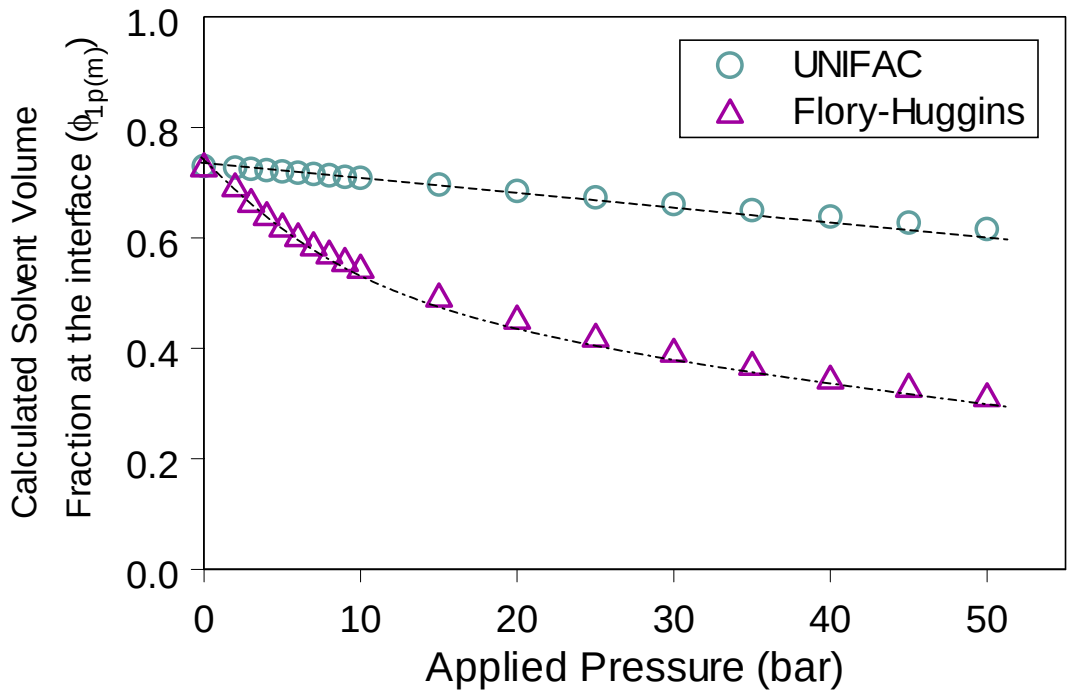

Figure 5.32: Effect of pressure on the calculated hexane volume fraction at the interface ($\phi_{1p(m)}$) for hexane-Trilaurin (639 MW TG)-Membrane D system (T=315 K)

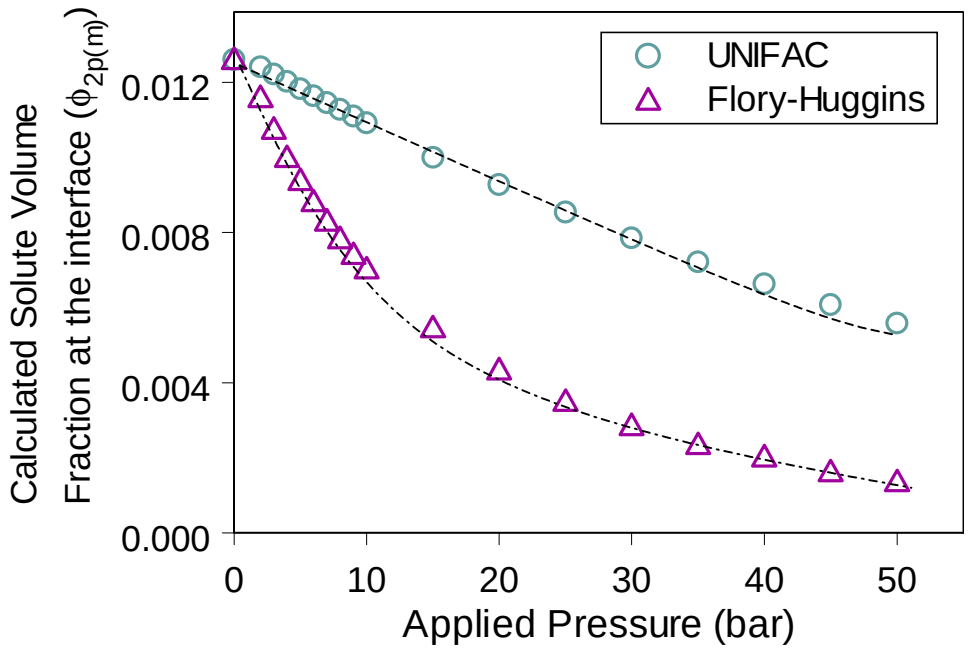

Figure 5.33: Effect of pressure on the solute (Trilaurin, 639 MW TG) volume fraction at the interface ($\phi_{2p(m)}$) for hexane-Trilaurin-Membrane D system (T=315 K)

pressure is not significant for the UNIFAC-based model, however, the FH theory does show a significant variation. This is an inherent flaw of the UNIFAC model and further comment on this will be made in a later section which will illustrate the effect of several parameters on the boundary conditions.

5.3.3 Using Experimental Data to Calculate the Species Diffusion Coefficients:

Once the boundary conditions have been obtained, Equation 3.12 and Equation 3.13 can be solved simultaneously using experimental permeation data (J_1 and J_2) to obtain the solute and solvent diffusion coefficients (D_1 and D_2). The experimental solvent and solute fluxes are used as input parameters and the corresponding applied pressures are used to obtain the boundary conditions. The solute and solvent diffusion coefficients, D_1 and D_2, are then varied to match the boundary conditions with those calculated from the previous section. Since the diffusion coefficients are independent of pressure, the experimental data is used to obtain the standard deviations of the calculated values. Table 5.11 shows the solvent and solute diffusion coefficients obtained using the membrane permeation data for Trilaurin (639 MW TG) and Trimyristin (723 MW TG) in hexane through Membrane D with the Flory-Huggins (FH) treatment. The diffusion coefficient of Trilaurin (639 MW; $2.04 \pm 0.72 \times 10^{-13}$ m^2/s) is higher than Trimyristin (723 MW; $0.78 \pm 0.14 \times 10^{-13}$ m^2/s). Also, the hexane diffusion coefficient is three orders of magnitude higher than the solute diffusion coefficient. Table 5.12 summarizes similar values for the UNIFAC treatment. The dependence of the solute diffusion coefficient on the molecular weight is clearer using the UNIFAC treatment. Comparison of the solute diffusion coefficients with the FH and UNIFAC treatment has been shown

Table 5.11: Solute and Solvent Diffusion Coefficients obtained from membrane permeation data using the Flory-Huggins (FH) theory

Solute Type	Temperature (K)	Solvent Diffusivity		Solute Diffusivity	
		Value (m^2/s)	SD*	Value (m^2/s)	SD*
Trilaurin	320	5.40×10^{-10}	45.4×10^{-12}	2.04×10^{-13}	7.1×10^{-14}
Trimyristin	315	2.26×10^{-10}	9.6×10^{-12}	0.78×10^{-13}	1.3×10^{-14}

* SD = Standard Deviation: Obtained using pressure data

Table 5.12: Solute and Solvent Diffusion Coefficients obtained from membrane permeation data using the UNIFAC theory

Solute Type	Temperature (K)	Solvent Diffusivity		Solute Diffusivity	
		Value (m^2/s)	SD*	Value (m^2/s)	SD*
Trilaurin	320	1.47×10^{-10}	28.7×10^{-12}	1.57×10^{-13}	63.8×10^{-15}
Trimyristin	315	1.39×10^{-10}	8.2×10^{-12}	1.33×10^{-13}	4.3×10^{-15}
Tripalmitin	304	0.93×10^{-10}	8.0×10^{-12}	0.33×10^{-13}	5.1×10^{-15}
Tripalmitin	318	1.32×10^{-10}	3.3×10^{-12}	0.77×10^{-13}	29.5×10^{-15}
Tristearin	320	1.63×10^{-10}	7.1×10^{-12}	0.81×10^{-13}	8.8×10^{-15}

* SD = Standard Deviation: Obtained using pressure data

in Figure 5.34. Also, the triglyceride diffusion coefficients calculated using the UNIFAC treatment and the FH treatment agree reasonably well. It needs to be pointed out that the FH and the UNIFAC theories have drastically different assumptions. Table 5.11 and Table 5.12 also show the predicted hexane diffusivity for the FH and the UNIFAC approaches. It can be seen that the values predicted for the hexane diffusivity are slightly higher than those predicted by the UNIFAC theory, although they are of the same order of magnitude. Comparison of our calculated solvent and solute diffusion coefficients with those from literature will be discussed in the next subsection. Since more calculations were performed with the UNIFAC-based theory, the calculated solute and solvent diffusion coefficients obtained using the UNIFAC theory will be further analyzed with literature data.

5.3.4 Discussion:

Diffusion studies through polymer films/membranes have been reported in literature for several solvents and polymer systems. As has been mentioned in the discussion of the Spiegler-Kedem model, diffusion is obviously a strong function of the polymer type and cross-linking. The dependence of solvent/solute diffusion coefficient on temperature and species size have been established, both experimentally and theoretically. For example, it is a well-known fact that for species of the same homologous series, the diffusion coefficient reduces as the species size increases at the same temperature. Also, for a particular species, the diffusion coefficient increases with increase in temperature and this temperature-dependence is typically obtained using an Arrhenius-type plot. This discussion is aimed at comparing and validating our diffusivity

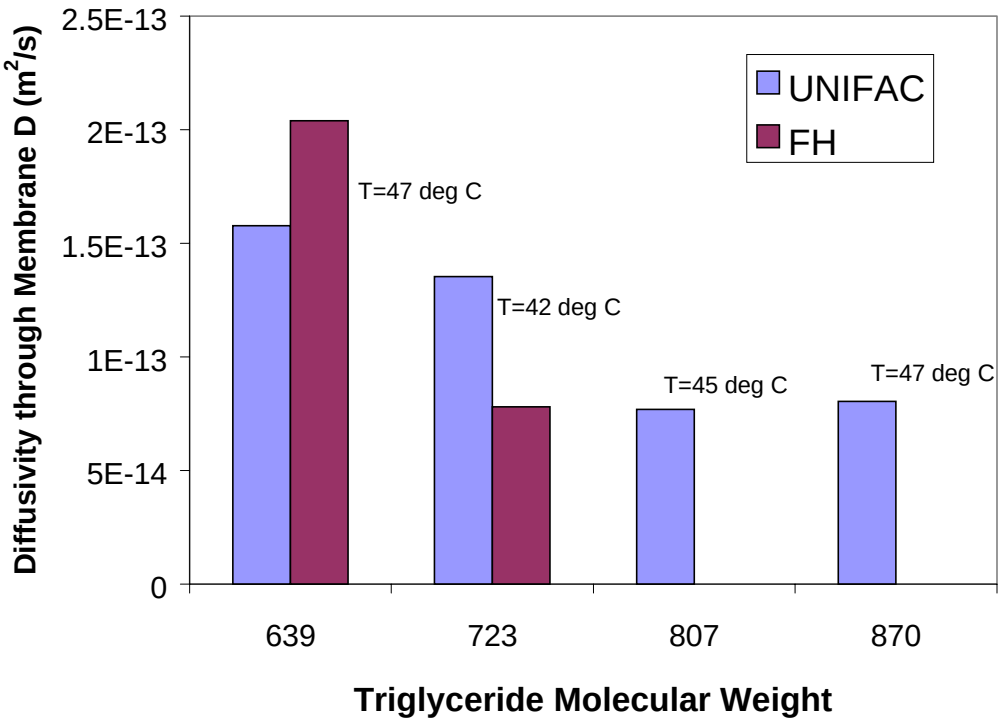

Figure 5.34: Comparison of calculated diffusion coefficients of triglycerides with molecular weight using the FH and UNIFAC theories.

data obtained using the proposed model with that from literature reported by independent investigators.

5.3.4.1 Solvent Diffusion:

Harogoppad and Aminabhavi [1991] have performed sorption and diffusion studies with alkanes in elastomeric membrane materials (Neoprene, SBR, EPDM, Nitrile Rubber). They have also measured the dependence of diffusion coefficients of alkanes (hexane-decane) as a function of temperature (25 to 60 ^{o}C). Figure 5.35 shows a typical Arrhenius-type plot that compares the behavior obtained for our data (from the calculation) with that reported for hexane and several elastomeric materials [Harogoppad and Aminabhavi, 1991]. The activation energies reported in their work for hexane with the elastomeric membranes used are shown in Table 5.13 along with activation energy obtained from Figure 5.35. It can be clearly seen that the magnitude of the activation energy obtained from our calculation is of the same order as that obtained with hexane for similar rubbery materials. Also, the order of magnitude of the hexane diffusion coefficient reported for elastomeric materials is similar to the values obtained from our calculations for siloxane-based Membrane D. This validates our calculated results for solvent diffusion coefficient and thus the plot can be effectively used to calculate hexane diffusion coefficients at other temperatures for simulation purposes.

5.3.4.2 Solute Diffusion:

Solute diffusion studies reported by Paul *et al* [1976b] in the mid-70s have indicated that the solute diffusion coefficient through a crosslinked rubbery membrane is

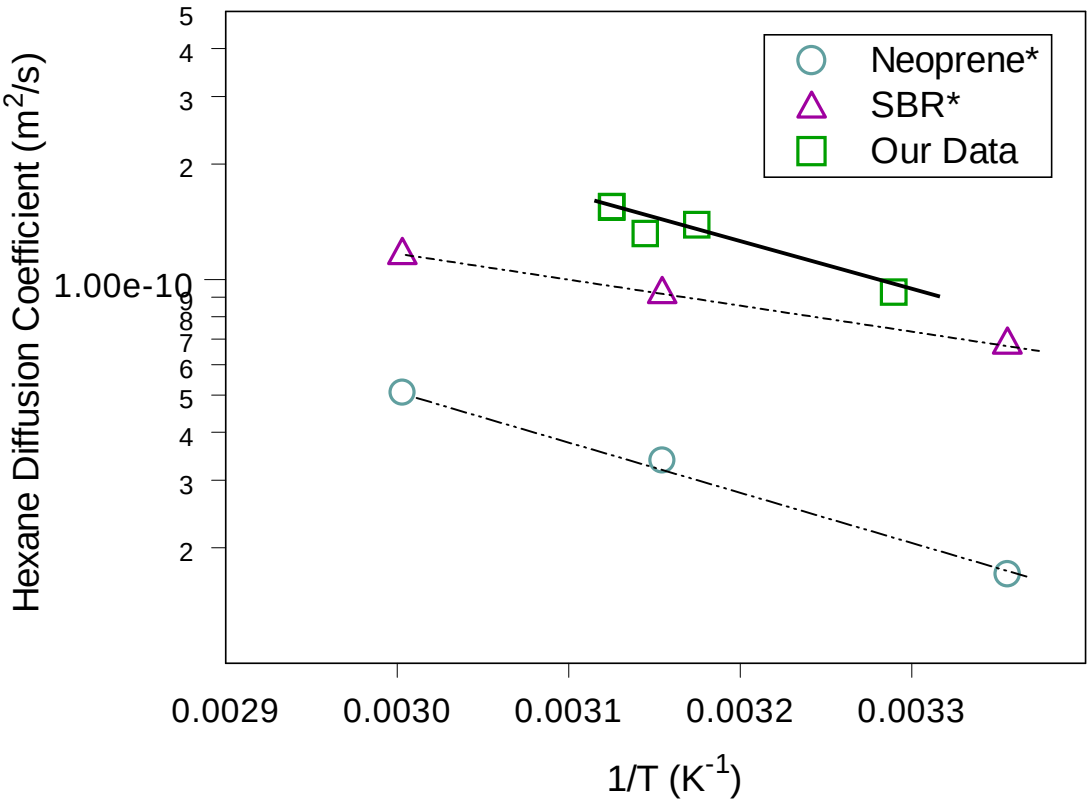

Figure 5.35: Arrhenius-type plot comparing the calculated hexane diffusivity through Membrane D using UNIFAC treatment with that reported in literature for elastomeric materials for hexane (*Harogoppad and Aminabhavi, [1991]).

Table 5.13:Activation Energy for hexane in different polymeric films and comparison with our experimental data

Material	Activation Energy (kJ/mol)
Neoprene*	25.93
Styrene-butadiene Rubber*	12.64
EPDM*	13.58
Nitrile Rubber*	10.16
Membrane D	**24.57**

* data taken from Harogoppad and Aminabhavi, [1991]

a strong function of the solvent-uptake capacity of the membrane material (swelling). They studied the diffusion coefficient of Sudan IV (384 MW) in several solvents (polar and non-polar). For example, they have reported the diffusion coefficient of Sudan IV in hexane to be 3.8×10^{-10} m^2/s which is two orders of magnitude higher than that reported through methanol. The corresponding solvent volume fractions in the polymer were 0.7 for hexane and 0.002 for methanol. Although the authors were not successful in developing a comprehensive correlation for solute diffusion, they proposed the following hypothesis. For solvents which swell the membrane to the same extent (similar solvent volume fractions), the solute diffusivity through the membrane in a particular solvent is directly related to the solute diffusivity in the bulk solution of the same solvent. One interpretation of this hypothesis can be explained using the free-volume theory which suggests that the free volume available for diffusion is a function of the solvent-membrane interactions. Doig *et al* [1999] have also reported the variation of solute diffusion as a function of solvent type through a non-porous silicone rubber membrane and have arrived at a similar conclusion. Their findings can be illustrated by Figure 5.36 which shows the diffusivity data of phenol in 1-decanol and ethyldecanoate solvents. It can be clearly seen that solute diffusion coefficient for phenol (92 MW) is 4.6×10^{-11} m^2/s in 1-decanol (3% swelling) vs. 16×10^{-11} m^2/s (54% swelling) in ethyldecanoate. The authors have also reported a significant increase in the diffusion coefficient of hydroxyprogesterone (330 MW organic) in 1-decanol (0.39×10^{-11} m^2/s) to than in toluene (12×10^{-11} m^2/s). Our experimental diffusive flux measurements also indicate that the solute diffusion depends on solvent and membrane type. For example, Figure 5.26 shows the diffusive flux of phenol in hexane medium for a siloxane-based

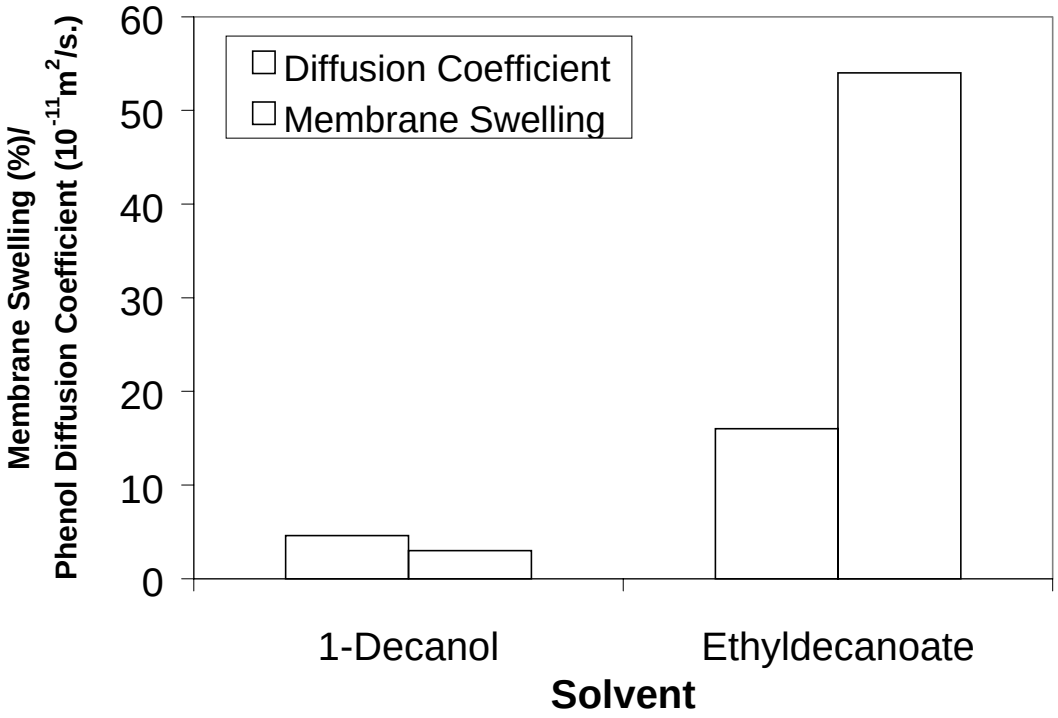

Figure 5.36: Phenol Diffusion coefficient as a function of % membrane swelling (thus solvent type) through a non-porous silicone rubber membrane (data taken from Doig et al, [1999]).

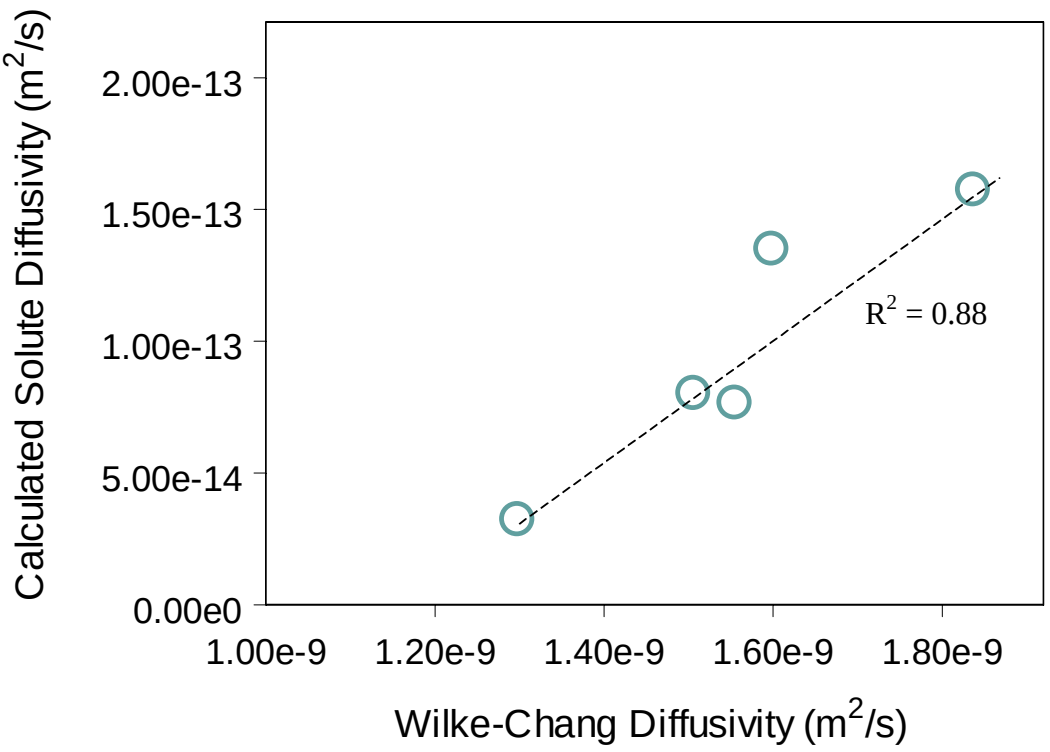

Figure 5.37: Correlation between the calculated triglyceride diffusivity in hexane through Membrane D with the triglyceride diffusivity in bulk hexane (Wilke-Chang Diffusivity)

Membrane D and YK (polyamide-based) membrane. It can be clearly seen that the phenol diffusive flux is higher through Membrane D (higher hexane partitioning) than the polyamide-based YK membrane. The diffusion coefficients for triglycerides obtained from our calculation show that for a single solvent (hexane in this case), the diffusivity values are a function of molecular weight as expected. Also the magnitude of the diffusion coefficients obtained for Trilaurin (639 MW, 2.04×10^{-13} m^2/s) is comparable to that obtained by Doig *et al* [1999] for the same class of membrane material (silicone rubber). Using the hypothesis presented by Paul *et al* [1976b], one can correlate the triglyceride diffusion coefficients in hexane saturated membrane with their corresponding bulk-diffusion values (Figure 5.37). The Wilke-Chang equation has been used for the calculation of the bulk diffusion values. Since the solvent is the same for our calculations, we could have just used the dependence of molecular size on the diffusion coefficient, however, since there are a few temperature variations (which change the viscosity of the solvent), the Wilke-Chang equation has been chosen. As can be seen, the correlation is reasonable and can be used to obtain solute diffusion coefficients in hexane medium to predict their separation behavior. Few simulations of separation behavior will be shown in the following section.

5.3.5 Calculation of Separation data for Selected Solutes using the Correlation:

Using the correlation shown in Figure 5.37, the solute diffusion coefficients for the triglycerides can be calculated and used in the model equations to generate solute separation data. In an attempt to compare the calculated and experimental values, the results for Tricaprin (C10, 554 MW TG) were not used. Using the above correlation, the

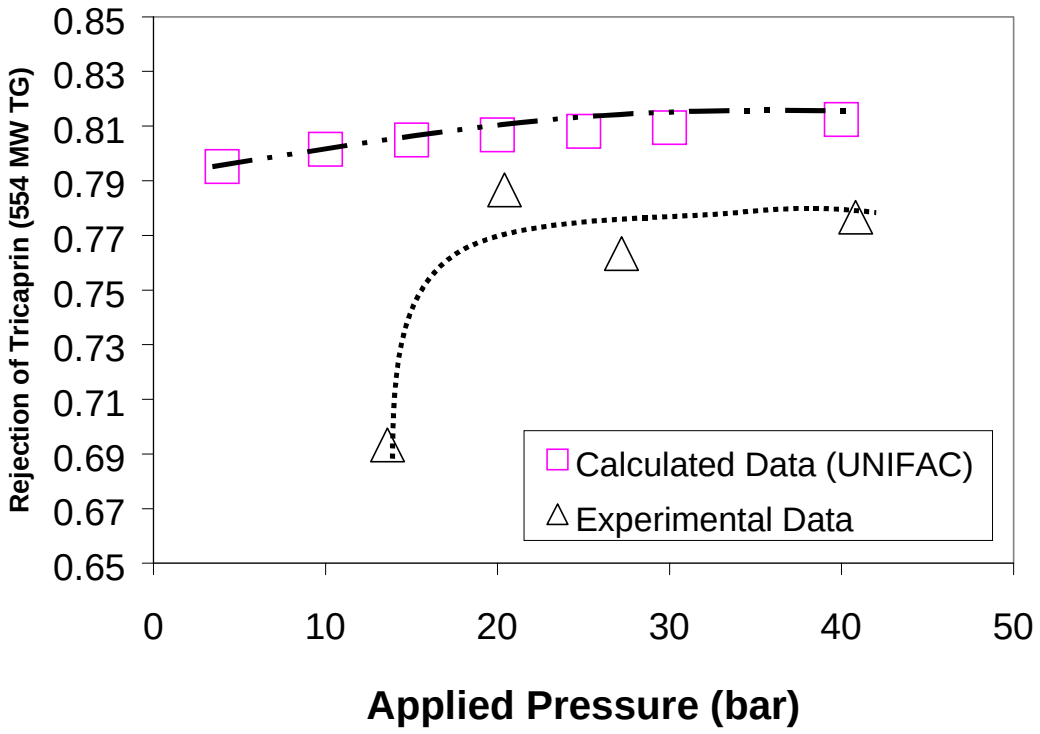

Calculated Diffusion Coefficients

$D_{hexane} = 9.35 \times 10^{-11}$ m^2/s

$D_{C10} = 1.13 \times 10^{-13}$ m^2/s

Figure 5.38: Comparison of calculated and experimental solute separation data for Tricaprin (C10 Triglyceride) in hexane through hydrophobic Membrane D at 31 ^{o}C (Calculated Values obtained using the UNIFAC approach).

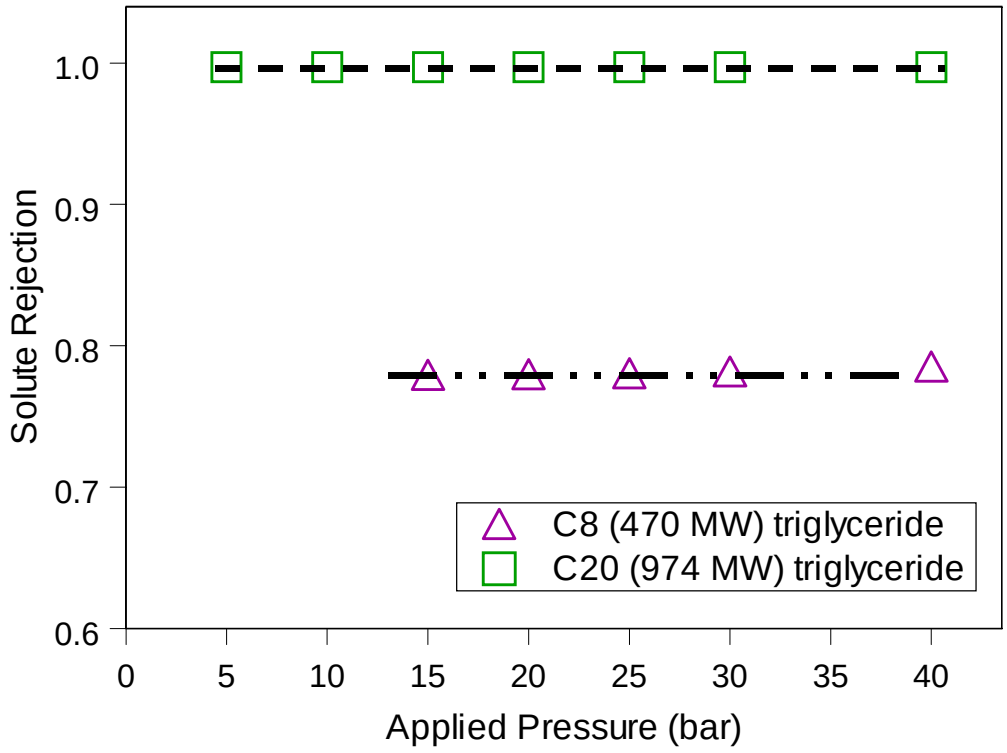

Figure 5.39: Calculated values for the triglyceride solute separation in hexane through Membrane D at 31 ^{o}C obtained using the UNIFAC approach.

diffusion coefficient for Tricaprin was extrapolated and used for calculation of its separation. Figure 5.38 shows a comparison between the calculated and experimental rejection of Tricaprin (C10, 554 MW) in hexane through Membrane D. It can be clearly seen that there is good agreement between the asymptotic values. One distinct observation that can be made from the comparison is that the solute separation is not a strong function of the applied pressure. The pressure effect is significant for the experimental data which is in line with observations in aqueous systems. Recall that the boundary conditions of the solvent and solute calculated using the UNIFAC approach were not a strong function of applied pressure. Additional calculations were performed to generate the separation of different molecular weight triglycerides for which experimental data was not available. The triglycerides chosen for the calculation include C8 (470 MW) and C20 (974 MW) in hexane medium through siloxane-based Membrane D at 31 ^{o}C and are shown in Figure 5.39. The model clearly predicts the dependence of separation on the solute molecular weight however, similar to the C10 TG, the pressure dependence is not significant. It also needs to be pointed out that the model predicts that the C20 (974 MW) triglyceride rejection in hexane is close to 100%. Experimentally, that was one of the key challenges to determine what molecular weight compound truly does not transport through the membrane. This information can be used effectively for the purposes of membrane characterization.

5.3.6 Sensitivity Analysis:

In order to validate the model, certain key input parameters have been varied to understand their impact on the calculated separation behavior. The calculation of the

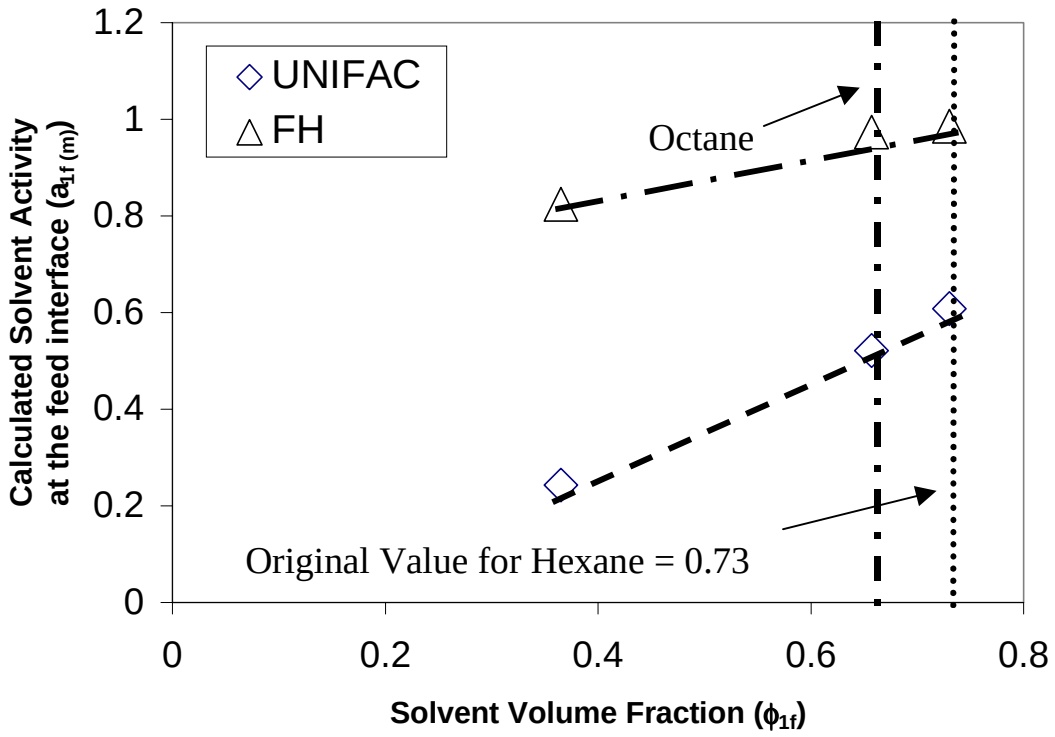

Figure 5.40: Comparison of the effect of solvent volume fraction (ϕ_{1f}) on the calculated solvent activity at the interface ($a_{1f\,(m)}$) using UNIFAC and Flory-Huggins theories.

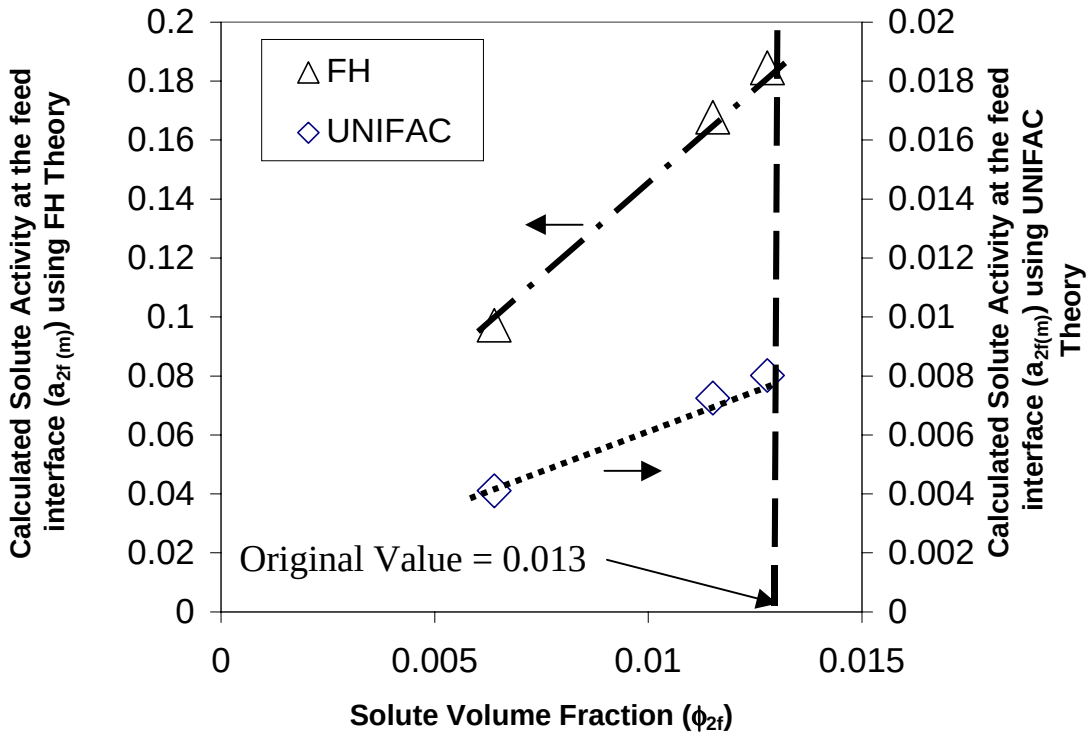

Figure 5.41: Comparison of the effect of solute volume fraction (ϕ_{2f}) on the calculated solvent activity at the feed interface ($a_{2f\,(m)}$) using UNIFAC and Flory-Huggins theories (Tricaprin, C10 TG chosen as target solute)

boundary conditions is one of the key aspects of this model and thus, certain parameters which affect these boundary conditions will be considered in this section. The parameters that will be discussed are the species volume fractions (ϕ_{if}), the applied pressure (P_f) and the species diffusion coefficients obtained from the above calculations. The concentration profiles for the species across the membrane thickness will also be discussed followed by a summary of the observed effects of this sensitivity analysis. Throughout this section, the analysis has been performed with Tricaprin (C10 554 MW TG)-hexane-Membrane D as the system. All the variations will be with respect to the base values of this system. Also, since the correlation for the diffusion coefficients was obtained using the UNIFAC-based calculations, these values will be further used for analysis. The hexane diffusion coefficient used for the analysis is obtained from the Arrhenius plot illustrated in Figure 5.35. All calculations are at 31 ^{o}C.

5.3.6.1 Effect of Solvent and Solute Partitioning Values (Volume Fractions):

The partitioning of the solvent and the solute from the bulk phase to the membrane interface is an important aspect of species transport across the membrane. For example, lower partitioning of the species would imply smaller driving forces which in turn imply lower transport rates through the membrane. The solvent and solute volume fractions were lowered by 10% and 50% individually to establish their impact on the species activity. Figure 5.40 and Figure 5.41 compares the effect of the solvent and solute volume fraction on their respective activities at the membrane interface on the permeate side respectively using both the FH and UNIFAC theories. It can be clearly seen that as expected, species activity decreases with a decrease in the species volume

fraction (partitioning) regardless of the activity coefficient theory used. The reduction in activity with the solvent volume fraction is more significant for the UNIFAC theory (about 60%) as compared to the FH theory (about 18%) for a 50% decrease in the solvent volume fraction which is clearly shown in Figure 5.40. On the other hand, the reduction in the solute volume fraction is the same (about 50%) for both the FH and UNIFAC based theories as is clear from Figure 5.41. The activity variation consequently varies the boundary conditions which in turn affects the separation behavior. Figure 5.40 also shows where the partitioning value for octane would be (ϕ_{1f} = 0.657). This value for octane would change the driving force within the membrane and result in variation of the separation behavior. The calculations have been shown in Appendix B (Figure B1) and the calculated separation value for Tricaprin (C10 554 MW TG) at 40 bar reduces from 0.81 to 0.79 for hexane and octane, respectively. It needs to be pointed out that for simplicity, the same diffusion coefficient values were used for the two calculations. In reality, the octane diffusion coefficient would be lower than that for hexane which would lower the separation of the triglyceride. Thus, it can be clearly seen that as the solvent activity reduces, the solvent flux would reduce and consequently, the solute separation would be lower. Similar is the case for the solute volume fraction also. For example, a reduction in the solute volume fraction (lower membrane affinity) implies reduction in the activity of the solute which translates into a lower solute flux and consequently a higher separation. Thus, from the species volume fraction point-of-view, the model makes clear physical sense and predicts the separation behavior in the correct direction.

5.3.6.2 Effect of Applied Pressure:

The effect of pressure on the species activity and the corresponding volume fractions will be discussed in a little more detail in this section. Pressure affects the species activities and volume fractions at the permeate side interface ($a_{ip(m)}$ and $\phi_{ip(m)}$). It is the objective of this section to clearly demonstrate why the UNIFAC theory does not explain the pressure effect on the separation. Again, the variation in pressure will explain the variation in the activities of the species and consequently the separation.

Figure 5.42 and Figure 5.43 show the effect of pressure on the calculated species activity ($a_{ip(m)}$) and the corresponding species volume fraction using the UNIFAC theory. As can be clearly seen, the effect of pressure is not significant on the species activity. For example, the solvent and solute activities at an applied pressure of 40 bar are 17 % and 56% lower than at no applied pressure. This variation in activities translates into a species volume fraction decrease of 15% and 46% for the solvent and solute respectively at 40 bar. Figure 5.44 and Figure 5.45, on the other hand show similar calculations with the Flory-Huggins theory. The solvent and solute activity reductions are 20% and 55% lower at 40 bar. The corresponding volume fraction variations are 52% and 83% lower for the solvent and solute values respectively. Thus, it can be clearly seen that the effect of pressure on the FH based calculations are more significant than the UNIFAC-based calculations. This explains the reason for the separation behavior of the solutes calculated using UNIFAC not being a strong function of the applied pressure. To illustrate the pressure effect, calculations were performed using the FH theory to obtain separation behavior for Tricaprin (554 MW C10 TG) and the results can be shown in Figure 5.46. It can be seen that the pressure effect is explained by the FH theory,

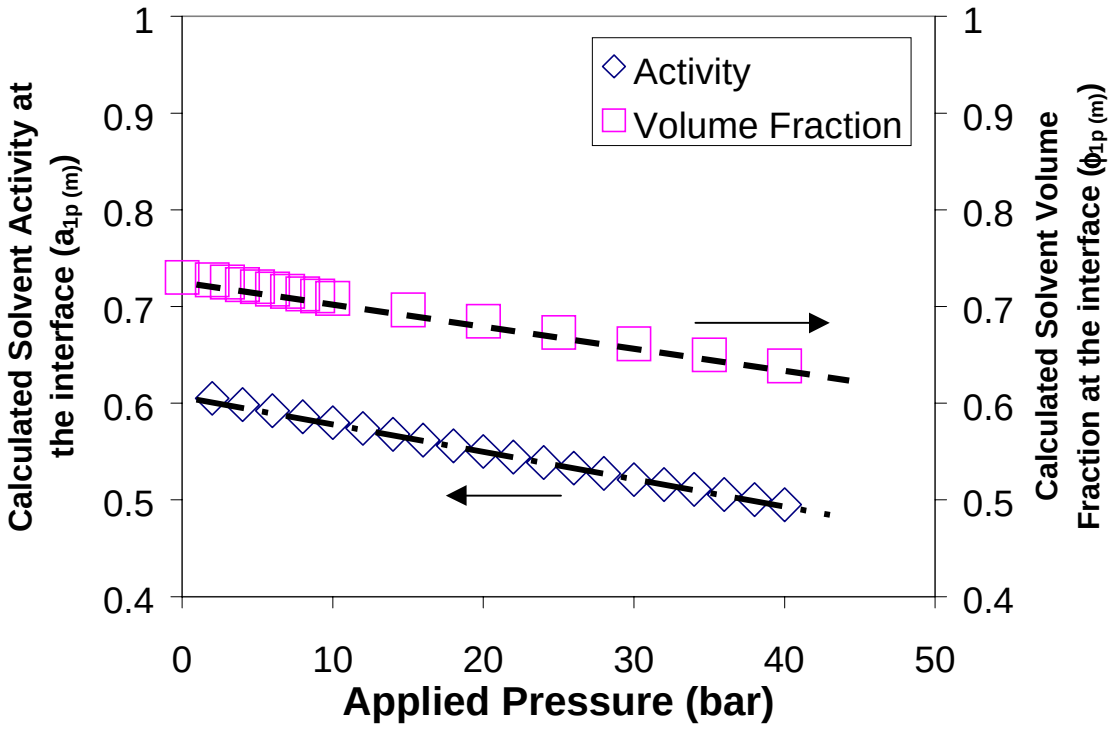

Figure 5.42: Effect of applied pressure on the calculated hexane activity ($a_{1p\,(m)}$) and the corresponding calculated volume fraction ($\phi_{1p\,(m)}$) using the UNIFAC theory.

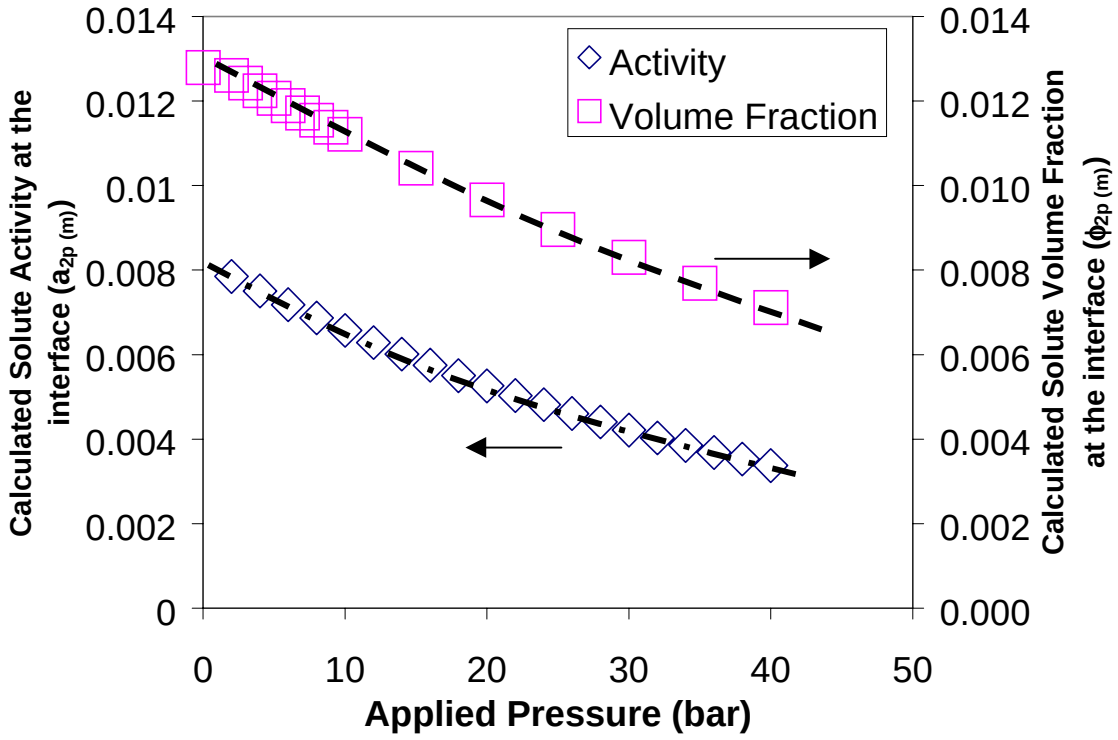

Figure 5.43: Effect of applied pressure on the calculated solute activity ($a_{2p\ (m)}$) and the corresponding calculated volume fraction ($\phi_{2p\ (m)}$) using the UNIFAC theory (Tricaprin, C10 TG chosen as target solute).

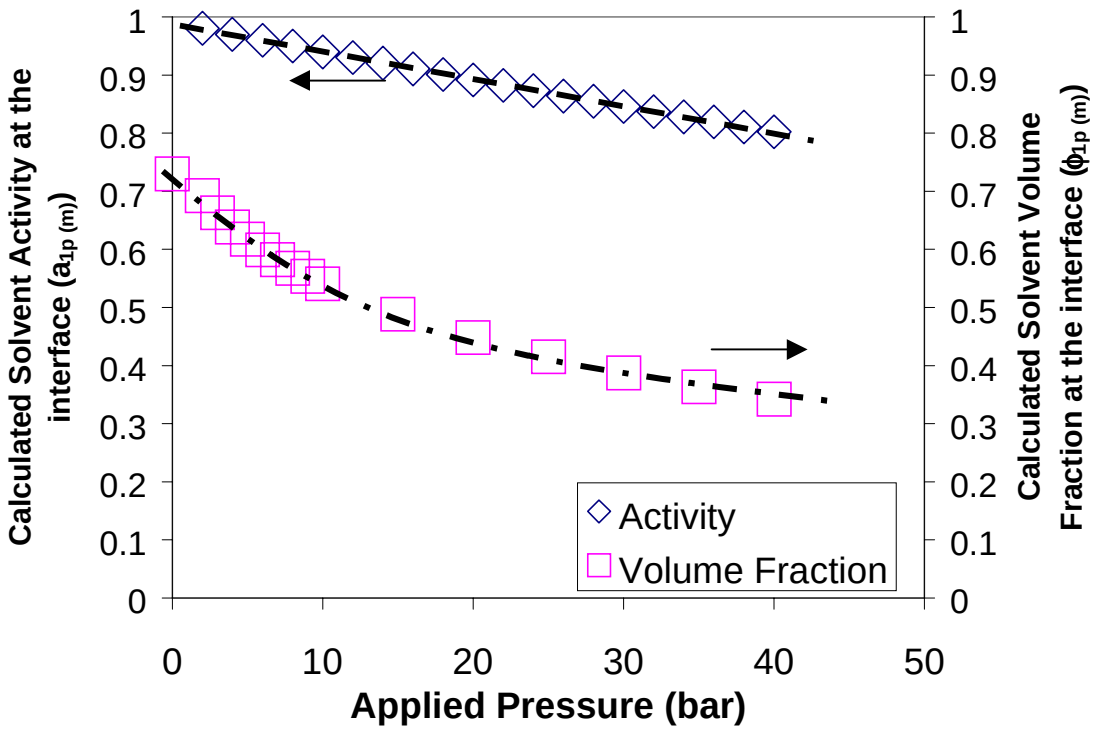

Figure 5.44: Effect of applied pressure on the calculated hexane activity ($a_{1p\,(m)}$)and the corresponding calculated volume fraction ($\phi_{1p\,(m)}$) using the Flory-Huggins theory.

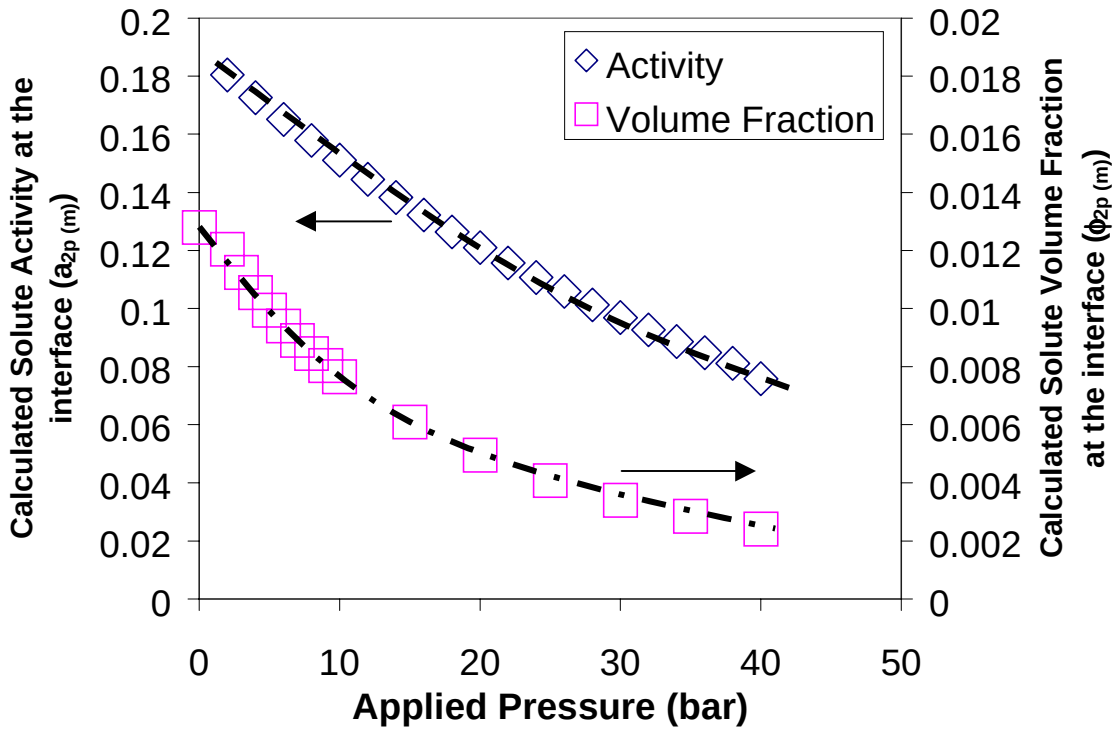

Figure 5.45: Effect of applied pressure on the calculated solute activity ($a_{2p\ (m)}$)and the corresponding calculated volume fraction ($\phi_{2p\ (m)}$) using the Flory-Huggins theory (Tricaprin, C10 TG chosen as target solute).

however, the asymptotic values calculated using the FH theory do not agree well with the experimental data. Since the UNIFAC model is a well-established and well-accepted activity coefficient model, the diffusion coefficients obtained using the UNIFAC model are assumed to be the correct values. It can be clearly seen that the FH theory under-predicts the solute separation behavior. A few reasons that can be used to explain this lower solute separation are as follows:

a. The FH model uses binary interaction parameters in order to explain the activity variation. It might be possible that specific ternary interactions need to incorporated into the theory in order for it to predict the right magnitude of solute separation.
b. Also, these binary interaction parameters have been obtained from the one-parameter Hildebrand approach. This may hinder the activity calculation which eventually results in lower prediction of the solute separation.

Thus, it was decided to mathematically impose the experimental separation value and find out the corresponding species activity on the permeate side at a given pressure. A pressure of 30 bar was chosen for this calculation. The original value at 30 bar for the solute activity using the FH calculation was $a_{2p\ (m)} = 0.134$. In order to match the experimental data, the new solute activity would have to be $a_{2p\ (m)} = 0.063$. Using this modified condition, the calculations have been performed and the results and the behavior is clearly illustrated in Figure 5.47 which compares the values obtained using these imposed activities for the FH theory with those obtained from the UNIFAC theory and our experimental data. It can be seen that there is good agreement in the calculated values and the experimental values using the imposed activities. Since the proposed

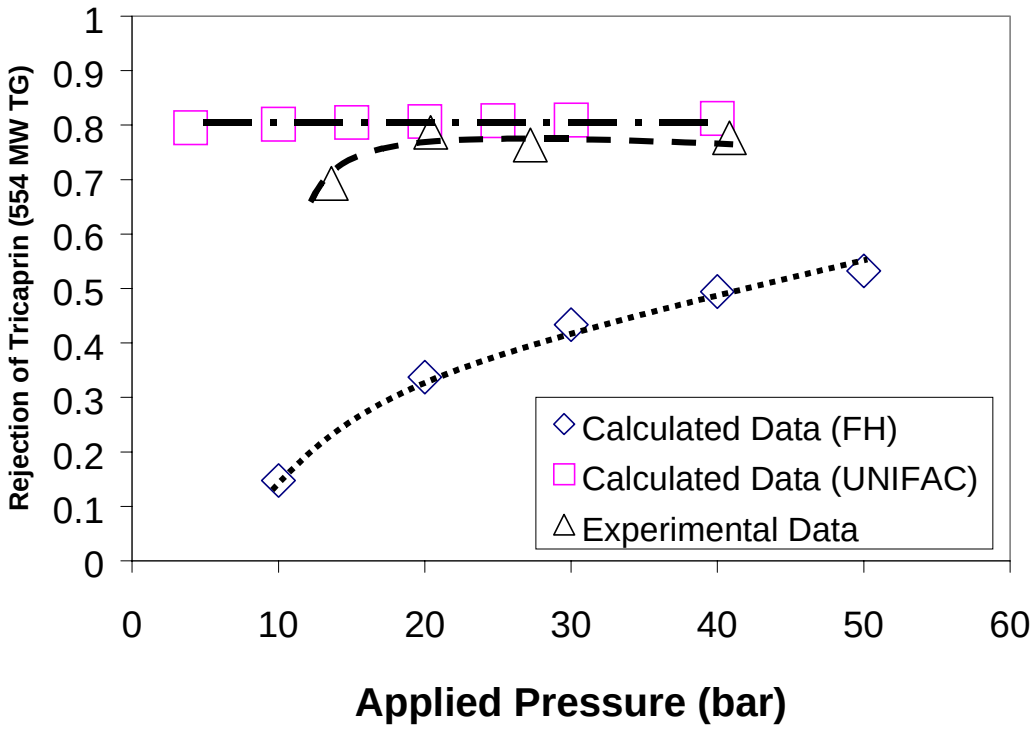

Figure 5.46: Effect of applied pressure on the calculated solute separation using the FH and UNIFAC approach and comparison with experimental solute separation data for Tricaprin (C10 554 MW TG).

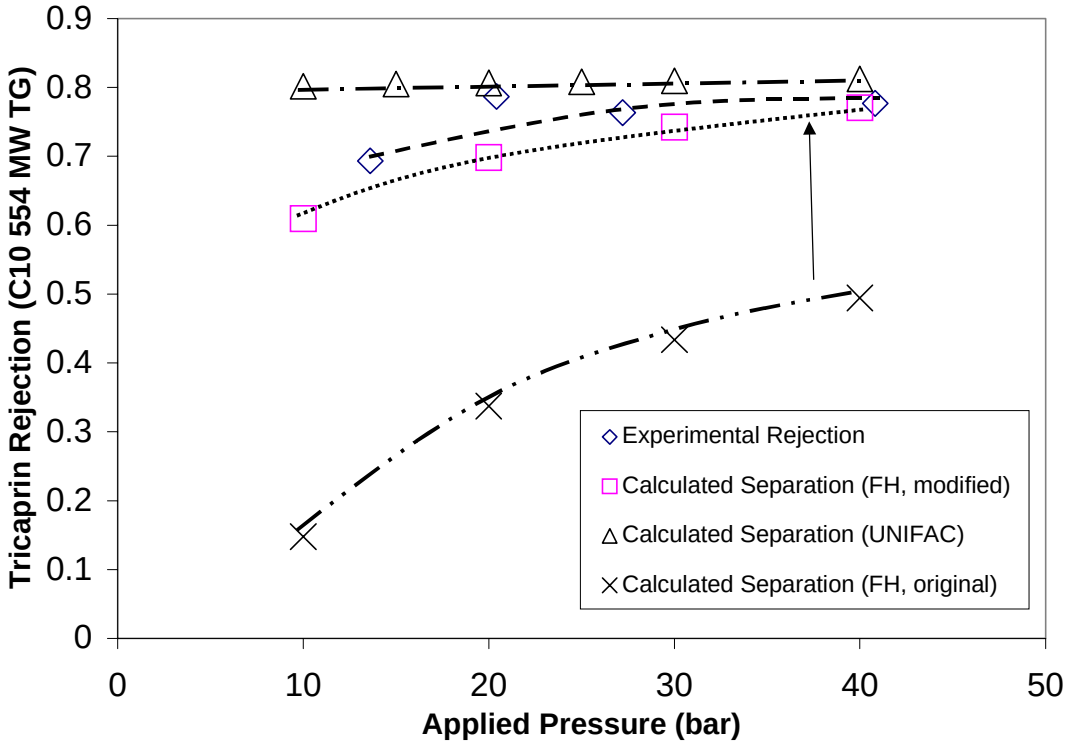

Figure 5.47: Effect of applied pressure on the calculated solute separation using the UNIFAC approach and the modified driving force for the FH theory and comparison with experimental solute separation data for Tricaprin (C10 554 MW TG).

model is a diffusion-based model, the next section will consider the sensitivity of the calculated separation on the solute and solvent diffusion coefficients.

5.3.6.3 Effect of Solute and Solvent Diffusion Coefficients:

The effect of applied pressure and species partitioning has been established using both the UNIFAC and the FH approach. Further discussion will concentrate on understanding the impact of the two adjustable parameters, the solute and solvent diffusion coefficients, on the separation behavior. The solute and solvent diffusion coefficients have been lowered by 10% and 50% individually to understand their effect on the rejection behavior. Figure 5.48 shows the effect of diffusion coefficient on the calculated solute rejection behavior using the FH theory. It can be clearly seen that the solute rejection behavior depends on the solvent diffusion coefficient. This proves an important aspect of the proposed model: the solvent-solute coupling. It needs to be pointed out that the base value for the separation of the Tricaprin-hexane system is about 50% at 40 bar which has been calculated using the FH approach. From the figure it can be seen that the solute rejection at 40 bar is about 45% and -5% which correspond to a 10% and 50% reduction in the solvent diffusion coefficient. On the other hand, the calculated solute separation increases to 55% and 75% when the solute diffusion coefficient is lowered by 10% and 50% respectively. As expected, lowering the solute diffusion coefficient would lower the solute flux and thus improve the rejection. Figure 5.49 shows similar comparisons for the UNIFAC-based calculations. The calculations for the UNIFAC-based theory show that the solute rejection at 40 bar is 79% and 62% when the solvent diffusion coefficient is lowered by 10% and 50% respectively. The

solute separation increases to 83% and 90% when the solute diffusion coefficient is lowered by 10% and 50% respectively. Also, the impact of varying the solvent diffusion has a stronger influence on the solute separation behavior for both the FH and UNIFAC based theories.

5.3.6.4 Species Concentration Profiles Across Membrane Thickness:

Calculations for all the systems described in the above sections were performed by dimensionalizing the membrane thickness. Since all the calculations have been performed with the siloxane-based Membrane D, the membrane thickness has been normalized with this value. From the SEM picture of this membrane (Figure 4.2), the thickness was determined as about 0.6 μm. Typical concentration profiles across the membrane thickness were then obtained for the solvent-Tricaprin system using the FH and UNIFAC approaches. Figure 5.50 and Figure 5.51 show the variation of the solvent and solute volume fraction respectively across the membrane thickness using the FH approach. The solvent volume fraction reduces across the membrane thickness in a slightly non-linear fashion. The solute volume fraction, on the other hand, shows an anomaly in the calculation and the variation before a certain membrane thickness must be neglected since under no condition, the solute volume fraction can go through a maximum. Since the magnitude of the solute volume fractions is low, small variations during numerical calculation can cause erroneous results. The pressure effect, similar to the solvent case is quite pronounced. Figure 5.52 and Figure 5.53 illustrate the variation in the volume fractions as a function of membrane thickness using the UNIFAC theory.

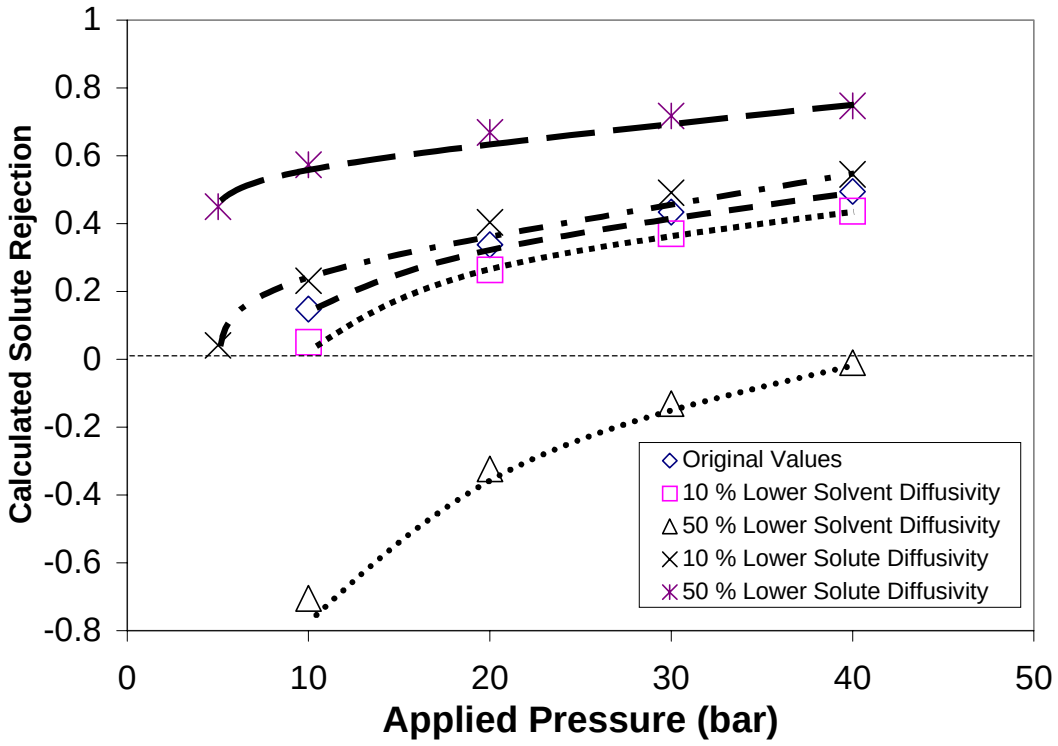

Original Diffusion Coefficients

$D_{hexane} = 9.35 \times 10^{-11}$ m^2/s

$D_{C10} = 1.13 \times 10^{-13}$ m^2/s

Figure 5.48: Effect of solute and solvent diffusion coefficient variations on the calculated solute rejection behavior with applied pressure (Original values for Hexane-Tricaprin system) using the FH approach

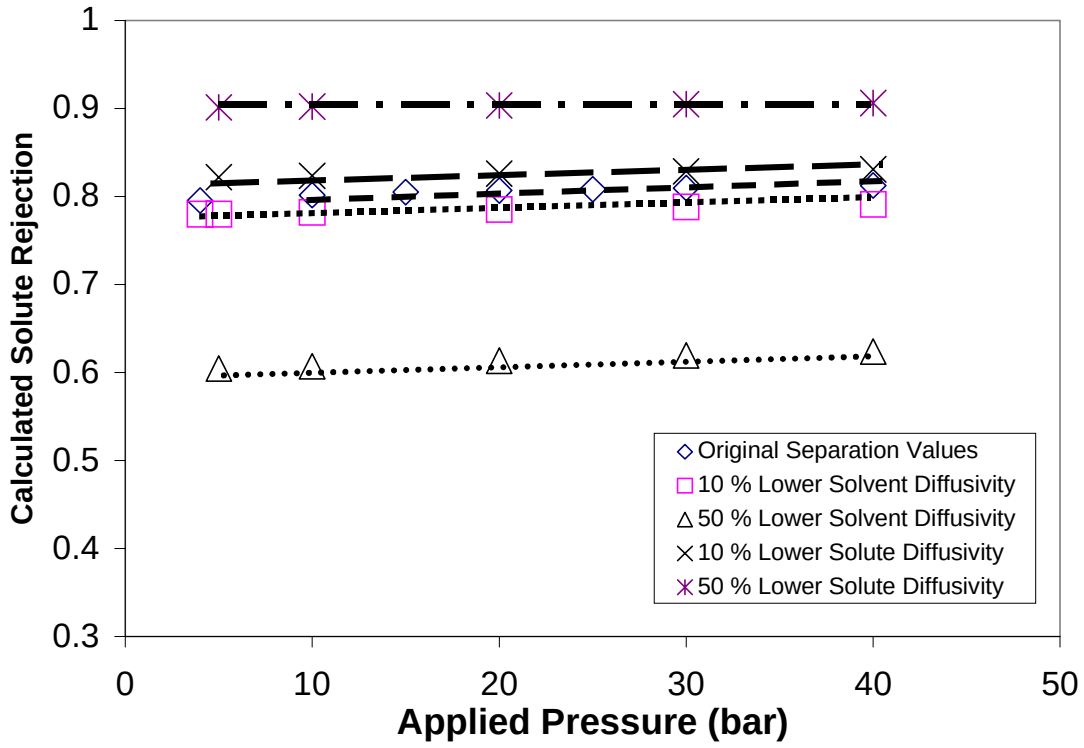

Original Diffusion Coefficients
$D_{hexane} = 9.35 \times 10^{-11}$ m^2/s
$D_{C10} = 1.13 \times 10^{-13}$ m^2/s

Figure 5.49: Effect of solute and solvent diffusion coefficient variations on the calculated solute rejection behavior with applied pressure (Original values for Hexane-Tricaprin system) using the UNIFAC approach

The variations in the solute and solvent volume fractions is quite linear across the membrane unlike the FH theory. The effect of pressure on the variation in the boundary condition with the UNIFAC method is not significant and is further substantiated by the comparisons shown.

5.3.6.5 Extension of the model to other systems:

The sensitivity analysis has been performed on the results to ensure a sound physical basis for the model. In order to extend the model to other systems, the following information is necessary:

a. Single membrane separation data, viz. applied pressure, corresponding solute and solvent flux values.
b. Solute and Solvent partitioning values from membrane independent experiments. If these values are unavailable, then theoretical correlations can be used.
c. Structures of the solvent, solute and membrane to compile the UNIFAC parameters.

Knowledge of the solvent, solute and membrane structures would enable determination of the UNIFAC group surface area and volume parameters and also the interaction parameters. Knowing the volume fractions from the partitioning experiments, the boundary conditions can be obtained. Using the single membrane permeation data, the solvent and solute diffusion coefficient can be calculated. Using the solvent and solute diffusion coefficients, further extension can be made for a given membrane material.

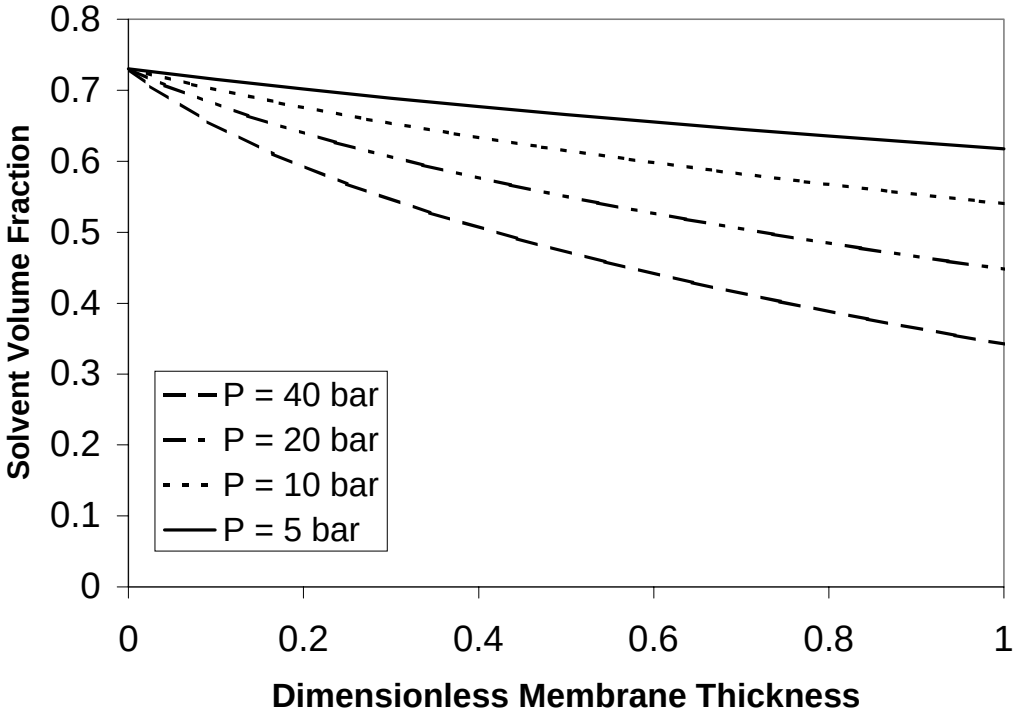

Figure 5.50: Calculated Concentration Profiles of hexane across the membrane thickness as a function of pressure using the FH approach.

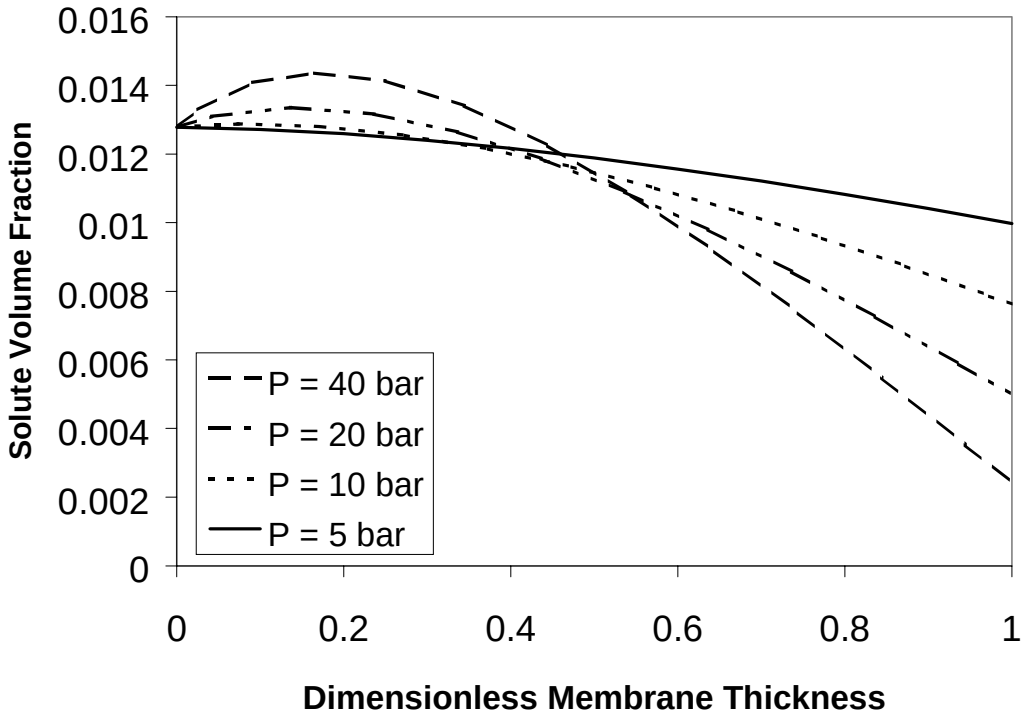

Figure 5.51: Calculated Concentration Profiles of the solute (Tricaprin, C10 554 MW TG) across the membrane thickness as a function of pressure using the FH approach.

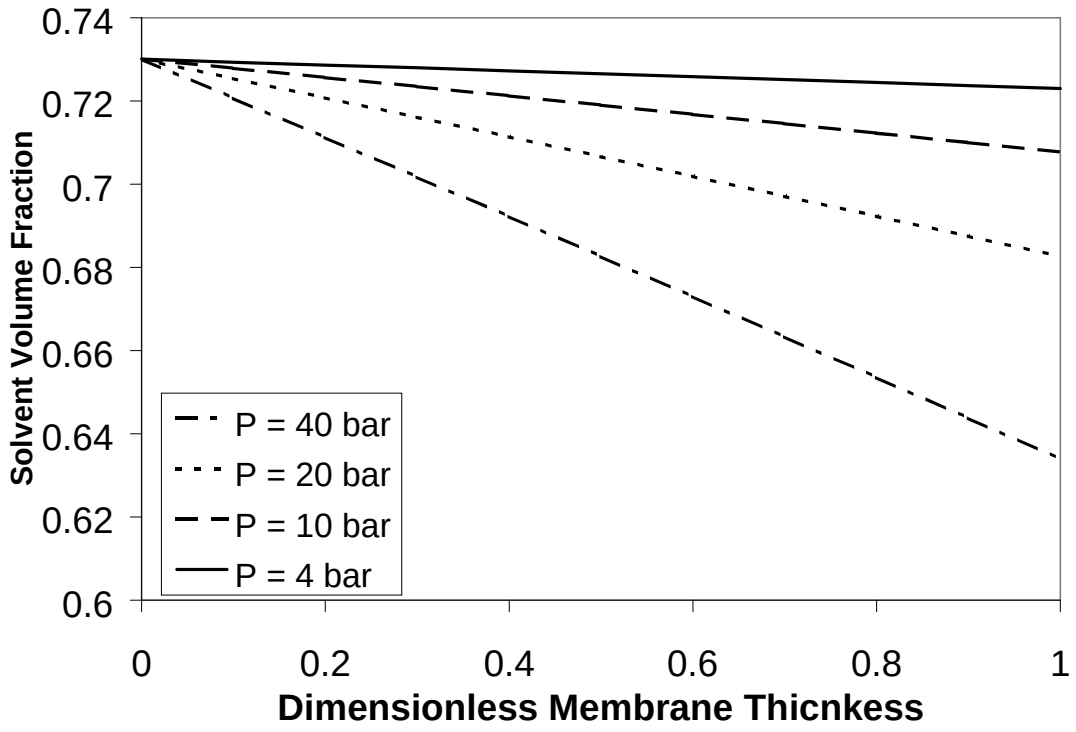

Figure 5.52: Calculated Concentration Profiles of hexane across the membrane thickness as a function of pressure using the UNIFAC approach.

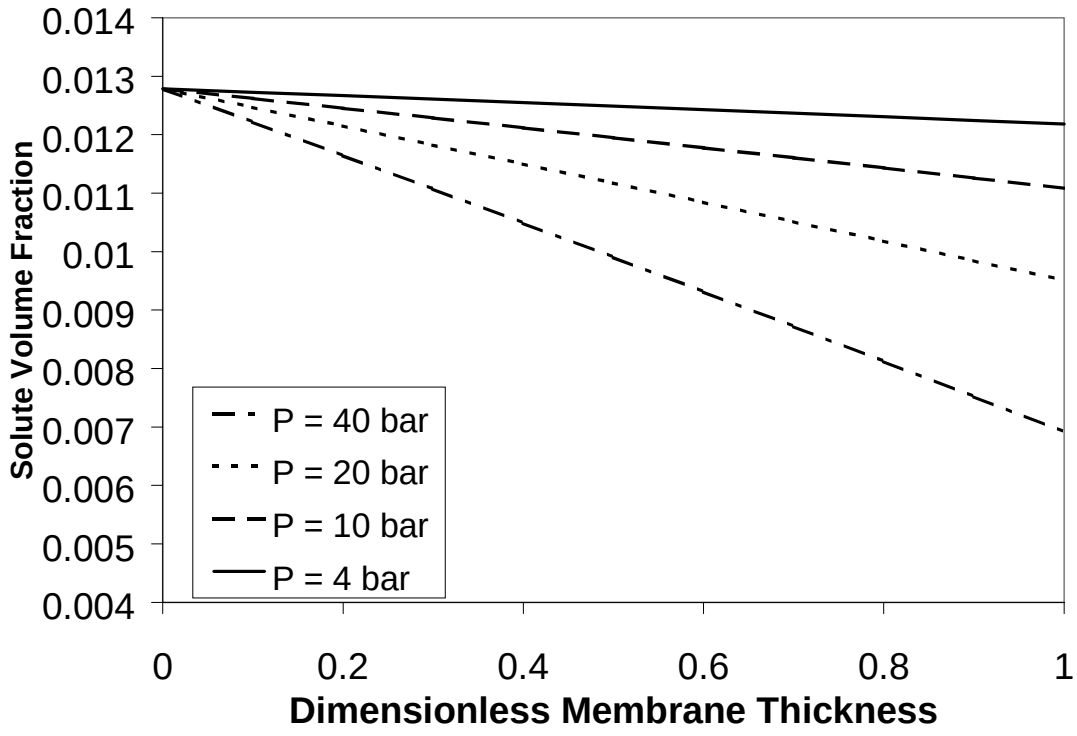

Figure 5.53: Calculated Concentration Profiles of the solute (Tricaprin, C10 554 MW TG) across the membrane thickness as a function of pressure using the UNIFAC approach.

5.3.6.6 Comparison of the Transport Models Discussed:

Solute separation behavior has been rationalized using literature models and our proposed model for solvent-resistant polymeric RO/NF membranes. Soltanieh and Gill [1981] have pointed out in their classical review of Reverse Osmosis that the “actual mechanism of membrane transport is not known and it is both useful and practical to use the term 'permeability' to specify the membrane”. Permeability is obviously a combined effect of solubility and diffusivity. It has been widely accepted that solubility and diffusivity are both critical for the separation ability of dense membranes. The relative contributions of these two parameters can change with different solute-solvent-membrane system. Although most of the models differ in the physical interpretation of the transport mechanism, they are successful in part to rationalize the experimental observations in non-aqueous medium. For example, the Surface Force-Pore Flow model assumes not only “convection” but also includes Lennard-Jones type potential functions to account for solute-membrane interactions to explain solute transport through polymeric membranes. The diffusion-based model proposed in this work considers the interactions possible in the system through classical and modern activity-coefficient theories (Flory-Huggins and UNIFAC) to explain the solute separation. The Spiegler-Kedem model assumes a contribution of both convection and diffusion to explain solute transport. Despite the different physical interpretations of the models discussed, each of the three models discussed in detail in the previous sections take into account solute separation as a function of solvent type, which is commonly referred to in membrane literature as "coupling" of the species fluxes. Some additional advantages/disadvantages of the models is discussed further.

a. Solution-Diffusion Models:

The traditional Solution Diffusion model fails to consider the solvent and solute coupling aspects which are prevalent in non-aqueous medium and thus cannot be applied directly to non-aqueous systems. Also, the model uses a "lumped" parameter to incorporate the sorption and diffusion properties of dense membranes. The Solution-Diffusion-Imperfection model considers coupling aspects, however, it introduces an additional parameter which has little physical significance and is merely used to fit the experimental data. As a result, it is difficult to use this model as a predictive tool.

b. Spiegler-Kedem model:

The Spiegler-Kedem model interprets the dependence of solute flux on the solvent and membrane type by considering convection and diffusion contributions and merely offers insight into their relative contributions. Our experimental data was analyzed using the Spiegler-Kedem model and the results were similar to those obtained from aqueous systems as was shown by adequate comparison. However, several researchers have pointed out that convection cannot be prevalent for such dense polymeric membranes. Also, the Spiegler-Kedem model does not contain any solute-solvent-membrane properties which would enable prediction of separation data. The model uses parameters such as the reflection coefficient (σ) and the permeance which can be obtained only from permeation data. Thus, prediction of separation behavior using the model becomes difficult since the model considers the membrane as a black-box.

c. Surface Force-Pore Flow Model:

The pore model assumes that the membrane is made of "angstrom diameter pores". Such interpretations, however, contradict the original definitions of RO/NF

membranes which define the membrane as a dense film with no well-defined pore structure with the separation mechanism primarily being that of diffusion. Thus, it needs to be pointed out clearly, that the above mentioned models were merely used as interpretations of experimental data. In case of the pore flow models, the SFPF model uses experimental data to obtain the B_{SFPF} parameter. Sourirajan et al [1985] expressed the scope for measuring these parameters experimentally using liquid chromatography. Using such techniques, one can visualize development of a correlation between solute and polymer properties which can further be employed to predict separation behavior. A distinct disadvantage of the SFPF model is that if the assumption of a laminar velocity profile is discarded, it requires complex computer programming to solve the necessary equations. Also, one of the inherent flaws of the SFPF model is that it assumes preferential sorption of the solvent regardless of the solvent-membrane interactions. For example, according to the SFPF model, methanol would preferentially wet a siloxane-based membrane although it has been established clearly that methanol-siloxane interactions are low. Although the SFPF model explains the solute separation by pure convection and interaction with the membrane wall, the controversy arises with respect to the assumption of 8-10 angstrom dimension pores for transport.

d. Diffusion-based Model:

The diffusion-based model for solute separation behavior proposed in this work uses a simple chemical potential gradient approach. The model uses physical properties of the solvent, solute and membrane to calculate solute separation behavior. A major advantage of the proposed theory is the fact that both the adjustable parameters have a distinct physical significance unlike traditional transport theories where the parameters

are essentially lumped. One distinct disadvantage of the proposed transport theory is that it initially serves as another interpretation of the experimental data. However, it has been demonstrated that very few experimental values need to be supplied to generate solute separation behavior for other systems. Another advantage of the model is that it considers the solute-solvent coupling along with the possible interactions of the solute-solvent-membrane ternary system by using activity coefficient theories. The UNIFAC theory, which is a well-established group-contribution theory, can be used for complex systems with the knowledge of the structures of the species. An inherent disadvantage of using the UNIFAC theory is the fact that it does not predict the solute separation as a function of applied pressure. The Flory-Huggins model was also evaluated for the separation behavior and it was concluded that consideration of binary interaction parameters for activity calculations can affect the predictive ability of the transport theory.

From the results obtained using the diffusion-based model, it becomes clear that for systems where the solute separation values are not close to 100%, convective contributions may be important. This can be illustrated from the results obtained for both the UNIFAC and the Flory-Huggins based calculations for the Tricaprin-Hexane-Membrane D system (Figure 5.47). It is apparent that the UNIFAC-based approach is unable to explain the pressure effect of solute separation. This pressure effect is shown predominantly by the Spiegler-Kedem calculations (Figure 5.31) where it can be clearly seen that the solute convective contribution increases linearly with the upstream pressure. For the sodium-chloride FT-30 data, on the other hand, it can be seen that the dependence of the convective flux on the applied pressure is negligible. Thus, for cases where the

asymptotic rejection (σ in the Spiegler-Kedem model) is not close to unity, the convective contributions to solute transport cannot be neglected. In addition, several researchers have argued about the assumption of constant pressure across the membrane for dense membranes. Kataoka et al [1991] have shown in their calculations that even if the assumption of constant pressure is dropped, the system would need to be operated at greater than 100 bar for any substantial difference in its contribution to separation. Most of our experimental results were obtained at pressures less than 50 bar and thus, the assumption of constant pressure across the membrane is valid. The diffusion based model can be used in conjunction with the Spiegler-Kedem model to explain the solute separation to obtain a more comprehensive theory. It can be used to obtain the contribution of diffusion to the total solute separation since the model incorporates interactions between the solute-solvent-polymer system in a comprehensive fashion. Obviously, for solutes which approach the 100% separation value, diffusion contribution is predominant and thus, this diffusion-based model can be used to completely explain the solute separation behavior.

5.4 Applications:

Solvent-resistant membranes have a strong potential for a variety of applications ranging from pharmaceutical to chemical to food industries. Some selected examples for the need of solvent-resistant membranes for material recovery and recycle of solvents are shown in Figure 5.54. An immediate application that can be identified is the separation of vegetable oil/soybean oil from hexane [Koseoglu *et al*, 1990; Raman *et al*, 1996a; 1996b]. With the increasing energy costs, industries are looking into alternate processes

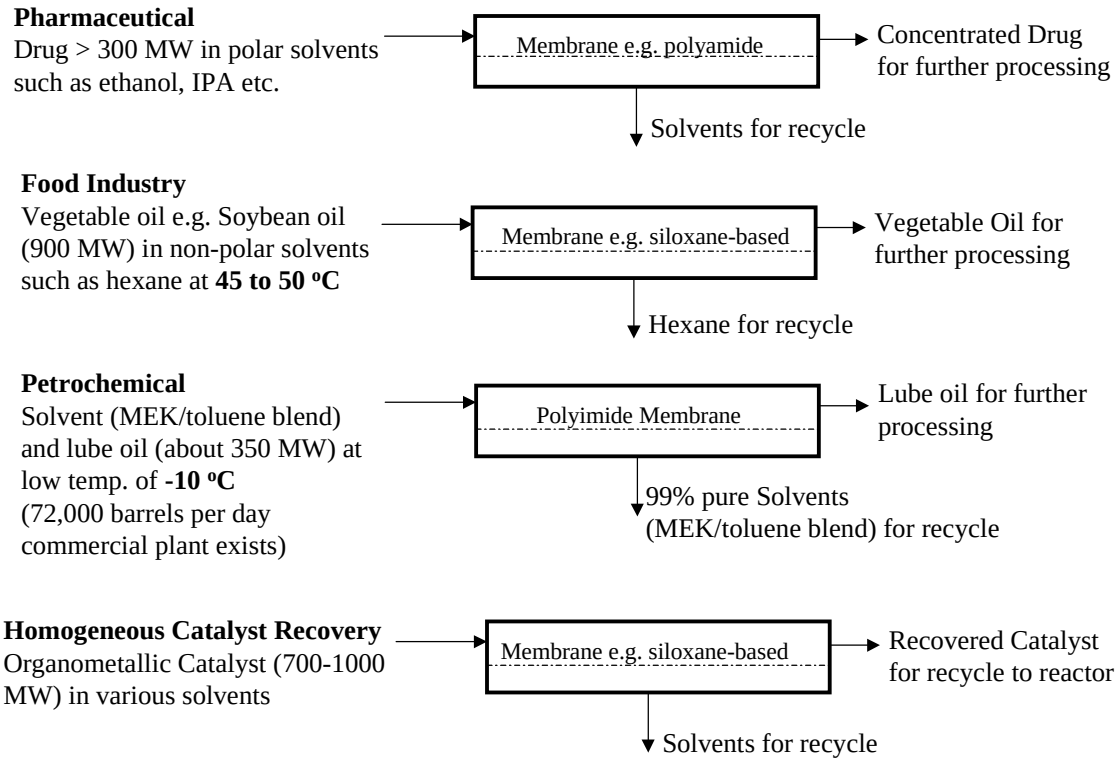

Figure 5.54: Selected examples of solvent-resistant membranes for material recovery and solvent recycle

for recovery of valuable chemicals. Pharmaceutical industries, for example, spend most of their research efforts in downstream processing to recover valuable drugs. Membranes and membrane processes offer an excellent avenue in downstream processing with their versatility and low energy costs.

Solvent lube oil dewaxing [White *et al*, 2000; Gould *et al*, 2001] processes are commonly used in refinery operations. Current recovery processes employ dissolution in solvent blends followed by precipitation of the wax by cooling. ExxonMobil in conjunction with W. R. Grace Company have developed a membrane-based process where the membrane reduces the residence time for the solvent mixtures which allows faster processing of the solvent [White *et al*, 2000; Gould *et al*, 2001]. The membrane was typically operated at -10 ^{o}C (14 ^{o}F) and a pressure of 600 psi (41 bar) with 20 wt % lube oil in the feed. The cold solvent was directly recovered from the permeate and recycled back into the process. The membrane used in this process was a developmental asymmetric polyimide-based membrane which can withstand the corrosive solvent blend (methyl-ethyl-ketone and toluene) used in the application. The authors have reported better-than-expected flux and rejection behavior. The initial data gives better than 95 % rejection of lube oil and better than 99% pure solvent at the operating conditions stated above. The process has been scaled-up from the lab scale to the commercial scale by ExxonMobil in Beaumont, Texas and is called as the MAX-DEWAX process. The authors also report the increase in the base oil production by 25 vol% and the energy consumption per unit volume of product was reduced by about 20%.

Homogeneous catalyst recovery is another important area in chemical/pharmaceutical industries. Use of organometallic catalysts is extremely

common in such industries and their recovery is essential because of their high costs. Membrane processes like NF can be used in such applications to recover the catalyst which can then be reused without sacrificing activity and product quality. This would also enable wide use of homogeneous catalysis (such as Ru or Pd containing organometallic catalysts) which eliminates mass-transfer limitations for the reaction rate. Several researchers [Scarpello *et al*, 2002; Nair *et al*, 2001; Luthra *et al*, 2001; Smet *et al*, 2001; Brinkmann *et al*, 1999; Giffels *et al*, 1998] have ventured into this area to recover these valuable organometallic catalysts.

Nair *et al* [2001], for example, studied the reaction of styrene and iodobenzene to form trans-stilbene with a palladium-based Heck-catalyst. They used developmental polyimide membranes (SR NF, W. R. Grace and Company) and studied the reaction in 3 different organic solvents (Ethyl acetate, MTBE and THF) in order to match catalyst and membrane properties. The authors have also reported that these developmental membranes were preferred to the MPF-series of membranes because of better flux and separation capabilities. Luthra *et al* [2001] have used a similar approach but for a phase-transfer catalyst (PTC) system involving the reaction of bromoheptane and potassium iodide to form iodoheptane. In this reaction, tetraoctylammonium bromide (TOABr) was used as the PTC and toluene was used as the organic solvent. After the reaction, the iodoheptane and the bromoheptane partition into the organic phase and this organic phase is the feed to the NF membrane (142A, polyimide-based 220 Da cut-off, W. R. Grace and Company) which concentrates the catalyst in the retentate.

CHAPTER SIX

Summary and Conclusions

This research dealt with the extension of the principles of Reverse Osmosis/ Nanofiltration to non-aqueous systems. RO/NF studies were conducted on some commercial and developmental membranes, hydrophilic and hydrophobic, with organic solvents. Solvent resistance of the membranes is a critical aspect of extending such membrane processes to non-aqueous systems. Also, the type of membrane, hydrophilic or hydrophobic plays a crucial role in the transport of organic solvents. Thus understanding polymer-solvent interactions is important. For example, for a silicone based NF membrane (Membrane D), the hexane flux at ~ 13 bar was ~ 6 x 10^{-4} cm^3/ cm^2 s (Permeability = 4.6 x 10^{-5} cm^3/ cm^2 s bar) as opposed to methanol flux being ~ 3 x 10^{-4} cm^3/ cm^2 s at the same pressure. On the contrary, for a hydrophilic brackish water RO membrane, the methanol flux obtained at ~ 13 bar was ~ 5 x 10^{-4} cm^3/ cm^2 s as opposed to the hexane flux through the same membrane being ~ 0.7 x 10^{-4} cm^3/ cm^2 s at the same pressure. Thus one can conclude that for the transport of non-polar solvents, the membrane material must be chosen accordingly. A simple model based on the solution-diffusion approach has been developed for predicting the pure solvent fluxes through polymeric hydrophobic membranes. The model uses physical properties of the solvent such as the solvent viscosity and its molar volume for predicting the flux. For hydrophobic membranes, a reasonable correlation has been obtained for both alcohols and alkanes. For a comprehensive model explaining the pure solvent (polar and non-polar) through various membranes, incorporation of surface energies and the use of

solvent sorption values to account for the polymer-solvent interactions gives a reasonable fit for solvent flux prediction.

Solute separation is the overall goal for any membrane process and this study also examined the solute permeation characteristics in non-aqueous medium. Solubility characteristics limited the choice of the solute molecules to some organic dyes and different molecular weight triglycerides. Experiments were performed under a variety of conditions with Membrane D (PDMS based NF membrane) and YK membrane (aromatic polyamide based membrane). From the experimental observations and literature data it was established that the solute rejection was dependent strongly on both the type of solvent and the membrane. This is evident from the results obtained with the Sudan IV organic dye. The rejection of Sudan IV in n-hexane medium is about 25 % at 15 bar and that in methanol is about –10 % at about 20 bar. The negative rejections imply preferential sorption and transport of the organic dye over methanol. Such negative rejections have been observed in literature with phenols (in aqueous systems) and cellulose acetate membranes and the behavior again has been attributed to strong solute-membrane interactions. The research also examined the analogy between the rejection behavior of aqueous and non-aqueous systems where the major component wets the membrane. Six different membranes were compared, four being membranes used for aqueous solutions (literature data) and two hydrophobic membranes (one being our experimental data with Membrane D). There is definitely a striking similarity in the transport mechanisms of the aqueous and non-aqueous systems based on the relative size ratios, however, this simple theory does not account for solute-solvent-membrane interactions. For example, it has been established in literature that water transports

through dense membranes through an additional mechanism of activated diffusion. In non-aqueous medium, this mechanism is not present. Thus, the separation mechanism, although showing considerable similarity with respect to the species relative size, is different for aqueous and non-aqueous systems.

Several literature models have been proposed for aqueous systems, however, there is little consensus in the universal applicability of a single theory. The models predominantly propose a physical and mathematical translation of the observed phenomena. Three traditional transport theories have been evaluated to explain the permeation characteristics in non-aqueous systems. Based on the experimental observations it becomes evident that coupling of the solute and solvent fluxes cannot be neglected. Thus the Solution-Diffusion model cannot be used without modifying it to consider coupling effects. The well-established Spiegler - Kedem and the pore models both consider coupling effects and were thus evaluated to explain the transport mechanisms for our experimental data. The diffusive transport contribution (Spiegler - Kedem model) was obtained by independent diffusion measurements for some of our systems (Sudan IV - n-hexane - Membrane D system) and these values were compared with indirect techniques based on membrane permeation data to obtain the diffusive flux. It was concluded that in the absence of independent diffusive flux measurements, the indirect techniques could be used as a reasonable approximation. The importance of the role of "convective flow" according to the Spiegler-Kedem analysis is also clearly demonstrated. As expected, the convective contribution reduces with increase in the solute molecular weight for both our experimental and data taken from literature. The literature-based models typically use lumped parameters to "fit" the experimental data.

The Spiegler-Kedem model, for example, does not consider physical properties of the solvent-solute-membrane system. It considers the membrane as a black-box and serves as a mere interpretation of the data in terms of convective and diffusive contributions. This limits its applicability to predict separation behavior. The SFPF model considers the physical properties of the system, however, independent measurements of parameters is required along with complex computer programming in order to predict rejection characteristics. For example, the interaction parameters (B_{SFPF}) can be obtained from independent experiments and can be used to predict separation behavior. In view of the above disadvantages of the literature-based models, a new model based on a chemical-potential gradient has been proposed. The model uses two adjustable parameters to fit the data, however, both the adjustable parameters have a very strong physical significance. The parameters are the solvent and solute diffusion coefficients. In order to consider the interactions and coupling effects, the simplified Flory-Huggins theory and the sophisticated UNIFAC theories have been evaluated. Since the UNIFAC theory is a well-established activity coefficient theory, it was used to obtain a correlation between the solvent and solute diffusion coefficients and their respective properties. The calculated diffusion coefficients have been validated by comparison with literature data for similar types of membrane materials. The developed correlation allows for extrapolation of solute and solvent diffusion coefficients as a function of temperature and size which has been used to predict separation behavior. Certain drawbacks of the UNIFAC and FH theories were also determined from the treatment. One distinct disadvantage of the UNIFAC model, is that the species activity is not a strong function of pressure which precludes the prediction of the pressure dependence of the separation

behavior. The Flory-Huggins theory, on the other hand predicts the pressure effect successfully, however, the solute separation predictions are lower by about 40 %. It was concluded that since the FH theory is simplified and uses just binary interaction parameters for the activity calculations, it under-predicts the separation data. The UNIFAC theory considers interactions between all the functional groups present in the system and thus is expected to be more accurate in its activity calculations.

From the above experimental observations and theoretical calculations, it becomes clear that the two literature models and the diffusion-based model proposed in this work are successful in partly rationalizing the separation behavior in non-aqueous medium. For dense RO membranes, the solute separation values are typically close to unity. Thus the convective contribution to transport is negligible (as shown by Figure 5.31 with the NaCl-FT-30 data) for such dense RO membranes. In case of NF membranes and especially in non-aqueous medium because of the swelling issues, convection cannot be ruled out as a mechanism of transport. Although our proposed model is a diffusion-based model, the effects of convective transport as demonstrated by the Spiegler-Kedem calculations (Figure 5.31) cannot be neglected. For solute transport both convection and diffusion become important for cases where the asymptotic rejection (σ) is significantly lower than unity. The diffusion-based model proposed in this work can be used to obtain the diffusive contribution in the Spiegler-Kedem model for such cases to account for convective transport.

Specific achievements of the research can be outlined as follows:

1. Established the importance of polymer-solvent interactions for non-aqueous systems. Evaluated several parameters such as the Flory-Huggins interaction parameter and membrane surface energy which can be used for quantifying such interactions.
2. Experimentally established pure solvent transport through polymeric membranes, both hydrophilic and hydrophobic using polar and non-polar solvents.
3. Developed and verified a simple model based on a Solution-Diffusion approach to explain pure solvent transport through polymeric membranes. The model uses physical properties of the solvent (such as molar volume and viscosity) and those of the membrane (Surface energy) to explain permeation behavior. The developed correlation can be used predict solvent transport through other membrane materials.
4. Experimentally established solute separation behavior in polar and non-polar solvents through polymeric membranes. These experimental studies clearly indicate that solute and solvent fluxes are not independent of each other, i.e. coupling of the species fluxes is critical for non-aqueous systems.
5. Traditional transport theories (e.g. Spiegler-Kedem and Surface Force-Pore Flow models) have been extended to non-aqueous systems to explain separation behavior, however, they only impart a physical interpretation of the transport mechanism.
6. Developed a diffusion-based transport theory using a fundamental chemical potential gradient approach to rationalize solute transport. This theory considers solute-solvent coupling and uses solvent, solute and membrane physical properties to explain separation behavior. Evaluated the model using the Flory-Huggins activity coefficient theory for ternary systems and the sophisticated UNIFAC group-

contribution theory to rationalize the separation characteristics for the triglyceride-hexane system through a hydrophobic membrane.

7. Developed a correlation using the UNIFAC approach for the temperature effect on the hexane diffusion coefficients and size effect for solute diffusion coefficients through hydrophobic Membrane D. These correlations can be further used to predict the separation behavior of solutes in hexane medium for the hydrophobic Membrane D. Extension of the model to other systems has also been addressed with respect to the information needed to carry out the calculations.

This research contributed to fundamental understanding of the membrane processes that are well-established for aqueous systems to non-aqueous systems, both experimentally and theoretically.

APPENDIX A (NOMENCLATURE)

a_i	Activity of species i
a_{if}	Activity of species i on the feed side at the feed-membrane interface (partitioning values)
a_{ip}	Activity of species i on the permeate side at the permeate-membrane interface (partitioning values)
$a_{if,m}$	Activity of species i on the membrane at the feed-membrane interface
$a_{ip,m}$	Activity of species i on the membrane at the permeate-membrane interface
$a_{if,bulk}$	Activity of species i in the bulk solution on the feed side
$a_{ip,bulk}$	Activity of species i in the bulk solution on the permeate side
A_i	Pure solvent permeability of species i
a_{mn}	Group interaction parameters used in the UNIFAC equation.
b(r)	Overall friction coefficient
B	Proportionality Constant (Equation 2.9, Reddy et al [1996])
B_i	Mobility of species i (UNIFAC Analysis)
B_{SD}	Simplified solute transport parameter for the Solution-Diffusion Model
B_{SFPF}	Adjustable Parameter used in the potential function of SFPF model
C	Average solute concentration in the membrane (Spiegler-Kedem Model)
C_f	Solute concentration in feed
c_i	Concentration of species i
c_{if}	Concentration of species i on the feed side
$c_{if(m)}$	Concentration of species i on the feed side membrane interface

c_{ip}	Concentration of species i on the permeate side
$c_{ip(m)}$	Concentration of species i on the permeate side membrane interface
C_p	Solute concentration in permeate
d	Diameter of the pore (UF Membranes)
D_i	Diffusion coefficient of species i
D_{ab}	Mutual diffusion coefficient for the solute (B) in solvent (A) according to the SFPF model
D_{solute}	Solute diffusion coefficient
F	Lumped parameter in Spiegler-Kedem equations
f_1	Solvent-independent adjustable parameter characterizing the NF skin layer (Equation 3.2)
f_2	Solvent-independent adjustable parameter characterizing the UF skin layer (Equation 3.2)
$F_A(r,z)$	Driving force for solute A used in the SFPF model
$F_{AB}(r,z)$	Friction force between the solute A and solvent B used in the SFPF model
$F_{AM}(r,z)$	Friction force between solute A and the membrane wall M used in the SFPF model
g^E	Excess Gibbs Free Energy
J_i	Flux of the species i
J_{solute}	Solute Flux
$J_{solvent}$	Solvent Flux
J_v	Total solution flux
k_1	Solvent parameter used in Equation 3.2 (Machado et al, [1999b])

K_i	Partition coefficient of species i used in the Solution-Diffusion model
$k_{m,n}$	Lumped parameters used in the proposed model for solute transport
K_{solute}	Solute partition coefficient used in the Solution-Diffusion model
l	membrane thickness
L_i	Proportionality constant used in the Solution-Diffusion model
L_p	Phenomenological Coefficient used in the IT-based models
P^0	Reference pressure
P_f	Pressure on feed side
P_p	Pressure on permeate side
$\overline{P}$	Solute Permeability Coefficient
ΔP	Transmembrane applied pressure
q_i	Measure of molecular surface area (UNIQUAC/UNIFAC model)
Q_k	Group area parameter used in UNIFAC theory
r	Radial dimension
R_μ^1	Resistance to flow through the NF skin layer (Machado et al, 1999b)
R_μ^2	Resistance to flow through the UF sublayer (Machado et al, 1999b)
R’	Rejection based on wall concentration used in SFPF model
R_b	Radius of the pore used in SFPF model
R_g	Universal gas constant
r_i	Measure of van der Waals volume used in the UNIQUAC/UNIFAC model
R_k	Group volume parameter used in UNIFAC theory
R_s^0	Resistance to flow at the NF skin layer (Machado et al, 1999b)
$r_{solvent}$	Radius of the solvent

S_i	solubility of the penetrant molecule in the membrane (Reddy et al, 1996)
T	Temperature
$u_B(r)$	Velocity of the solvent B as a function of radius r used in SFPF model
V_i	partial molar volume of the species i
V_m	molar volume of the solvent
x	Dimensionless radius
x_i	Mole fraction of species i
X	Hansen dispersion solubility parameter for membrane material (Reddy et al, 1996)
X_{AB}	Proportionality constant relating the friction force to the velocity gradient.
Y	Hansen hydrogen-bonding solubility parameter for membrane material (Reddy et al, 1996)
Z	Hansen polar solubility parameters for membrane material (Reddy et al, 1996)
z	Length dimension

Greek Symbols:

$\alpha(x)$	Dimensionless velocity used in SFPF model
β_1	Dimensionless solution viscosity used in SFPF model
β_2	Dimensionless operating pressure used in SFPF model
χ_{ij}	Flory-Huggins binary interaction parameter between species i and j
χ_s	entropic contribution of the chi parameter
δ_d	Hansen polar solubility parameters for solvent

δ_h	Hansen hydrogen-bonding solubility parameter for solvent
δ_p	Hansen dispersion solubility parameter for solvent
δ_i	Total solubility parameter of species i
ε	Surface porosity
ϕ_i	Volume fraction of species i
ϕ_{if}	Volume fraction of species i on the feed side (partitioning values)
ϕ_{ip}	Volume fraction of species i on the permeate side (partitioning values)
$\phi_{if,\,m}$	Volume fraction of species i on the feed side membrane interface
$\phi_{ip,m}$	Volume fraction of species i on the permeate side membrane interface
$\phi_{if,\,bulk}$	Volume fraction of species i in the bulk solution on the feed side
$\phi_{ip,bulk}$	Volume fraction of species i in the bulk solution on the permeate side
γ_i	Activity Coefficient of species i
γ_c	Critical surface tension of the membrane (Machado et al, 1999b)
γ_i^C	Combinatorial part of the activity Coefficient of species i
γ_i^R	Residual part of the activity Coefficient of species i
γ_{lv}	Liquid-vapor surface tension
γ_{sl}	Solid-liquid surface tension
γ_{sv}	Solid-vapor surface tension
Γ_k	Group residual activity coefficient used in UNIFAC theory
$\Gamma_k^{(i)}$	Residual activity coefficient of group k in a reference solution containing molecules of type i used in UNIFAC theory
$\varphi(r)$	Potential function used in SFPF model

$\varphi(x)$	Dimensionless potential function used in SFPF model
μ	Solvent viscosity
μ_i	Chemical potential of species i
μ_i^0	standard chemical potential of species i
μ_{if}	Chemical potential of species i on the feed side
$\mu_{if\,(m)}$	Chemical potential of species i at the membrane interface on feed side
μ_{ip}	Chemical potential of species i on the permeate side
$\mu_{ip\,(m)}$	Chemical potential of species i at the membrane interface on permeate side
ν_p	Volume fraction of the polymer used in Flory-Rehner Approach
$\nu_k^{(i)}$	Number of groups of type k in species i used in UNIFAC model
ν_k	Total number of groups of type k present in the system used in UNIFAC model
$\Delta\pi$	Osmotic pressure
θ	Advancing contact angle between the solid and the liquid.
Θ_i	Surface fraction of species i used in UNIQUAC/UNIFAC analysis
σ	Staverman reflection coefficient used in Spiegler-Kedem Analysis
τ	Pore tortuosity.
τ_{ij}	Binary interaction parameters between species i and j used in UNIQUAC/UNIFAC analysis
ω	Phenomenological coefficient used in Kedem-Katchalsky model
Ψ_{mn}	Group interaction parameter used in UNIFAC model

Abbreviations:

CA	Cellulose Acetate
FH	Flory-Huggins
IT	Irreversible Thermodynamics
MF	Microfiltration
NF	Nanofiltration
NRTL	Non-Random Two Liquid
PDMS	Polydimethylsiloxane
PVDF	Polyvinylidene fluoride
RO	Reverse Osmosis
S-D	Solution-Diffusion
SFPF	Surface Force-Pore Flow
UF	Ultrafiltration
UNIQUAC	Universal Quasi Chemical
UNIFAC	UNIQUAC Functional-group Activity Coefficient

APPENDIX B (SAMPLE CALCULATIONS)

Impact of variation of the solvent partitioning on the calculated solute rejection. Values shown here for octane. The diffusion coefficient used for the calculation is the same as that used for hexane, thus the calculation shows the impact of the solvent volume fraction on solute separation.

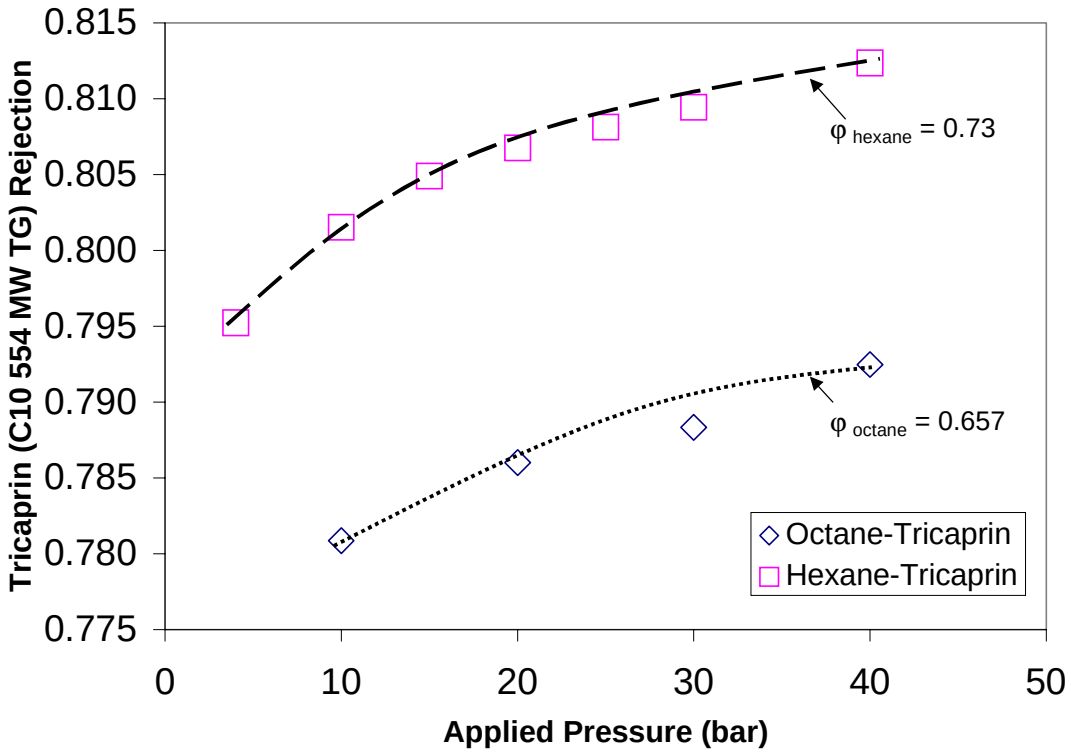

Diffusion Coefficients used:
$D_{solvent} = 9.35 \times 10^{-11}$ m^2/s
$D_{C10} = 1.13 \times 10^{-13}$ m^2/s

Figure B1: Impact of the variation of solvent volume fraction (partitioning) on the calculated solute separation of Tricaprin (C10 554 MW TG) in hexane and octane through Membrane D at 31 ^{o}C using the UNIFAC approach

Sample Calculation of the Separation behavior of Tricaprin (C10 554 MW TG) in hexane through siloxane-based Membrane D. The boundary conditions and the separations will be calculated at an applied pressure of 40 bar and at 31 ^{o}C

STEP 1: Obtaining the Boundary Conditions using the UNIFAC method

MATLAB Program to obtain boundary conditions using UNIFAC approach

```
function f=BC(x)
f=zeros(2,1);
% User INPUT PARAMETERS
V(1)=131.6;          % molar volume in cc/mole
V(2)=554;            % molar volume in cc/mole
Rg=82.06;            % R units = cc-atm/g-mole K
T=304;               % temperature in Kelvin for C10 triglyceride

phi(1)=0.73;         % Using value of 1.89 gm/gm PDMS sorption value
phi(2)=0.012787;     % Using chi(2,3) value and using Flory-Rehner approach
phi(3)=1-(phi(1)+phi(2));

rCH3=0.9011;         % r and q values are the group surface area and volume parameters
qCH3=0.848;          % These parameters are obtained from the UNIFAC tables
rCH2=0.6744;
qCH2=0.540;
rCH=0.4469;
qCH=0.228;
rCH2COO=1.6764;
qCH2COO=1.420;
rSiO=1.1044;
qSiO=0.466;

% For hexane
nuCH3=2;             % Number of CH3 groups in hexane
nuCH2=4;             % Number of CH2 groups in hexane

% For triglyceride
N=10;                % For C10 triglyceride
nuCH3=3;
nuCH2=3*(N-3);
nuCH=1;
nuCH2COO=3;

% For PDMS
nuCH3=2;
```

```
nuSiO=1;

% q and r calculation
q(1)=2*qCH3+4*qCH2;
q(2)=3*qCH3+3*(N-3)*qCH2+1*qCH+3*qCH2COO;
r(1)=2*rCH3+4*rCH2;
r(2)=3*rCH3+3*(N-3)*rCH2+1*rCH+3*rCH2COO;
q(3)=2*qCH3+1*qSiO;
r(3)=2*rCH3+1*rSiO;

Z=10;  % Co-ordination number = 10 mostly

for i=1:3
  l(i)=5*(r(i)-q(i))-(r(i)-1);
end

theta(1)=((phi(1))*(q(1)/r(1)))/((phi(1))*(q(1)/r(1))+(phi(2))*(q(2)/r(2))+(1-
(phi(1)+phi(2)))*(q(3)/r(3)));
theta(2)=((phi(2))*(q(2)/r(2)))/((phi(1))*(q(1)/r(1))+(phi(2))*(q(2)/r(2))+(1-
(phi(1)+phi(2)))*(q(3)/r(3)));

theta(1);
theta(2);

Nu(1,1)=2;     % Nu(m,n) means no. of groups of type m in component n
Nu(2,1)=4;     % m=1=CH3; m=2=CH2; m=3=CH; m=11=Ch2COO; m=43=SiO
Nu(1,2)=3;     % n=1=hexane; n=2=triglyceride; n=3=PDMS
Nu(2,2)=21;    % will change with triglyceride
Nu(3,2)=1;
Nu(11,2)=3;
Nu(1,3)=2;
Nu(43,3)=1;
Q(1,1)=0.848;
Q(2,1)=0.540;
Q(1,2)=0.848;
Q(2,2)=0.540;
Q(3,2)=0.228;
Q(11,2)=1.420;
Q(43,3)=0.466;
R(1,1)=0.9011;
R(2,1)=0.6744;
R(1,2)=0.9011;
R(2,2)=0.6744;
R(3,2)=0.4469;
R(11,2)=1.6764;
R(43,3)=1.1044;
```

% phig(m) means volume fraction of group m. m is the secondary number of group in UNIFAC table.

```
phig(1)=(phi(1)*Nu(1,1)+phi(2)*Nu(1,2)+phi(3)*Nu(1,3))/(phi(1)*(Nu(1,1)+Nu(2,1))+p
hi(2)*(Nu(1,2)+Nu(2,2)+Nu(3,2)+Nu(11,2))+phi(3)*(Nu(1,3)+Nu(43,3)));
phig(2)=(phi(1)*Nu(2,1)+phi(2)*Nu(2,2))/(phi(1)*(Nu(1,1)+Nu(2,1))+phi(2)*(Nu(1,2)+
Nu(2,2)+Nu(3,2)+Nu(11,2))+phi(3)*(Nu(1,3)+Nu(43,3)));
phig(3)=(phi(2)*Nu(3,2))/(phi(1)*(Nu(1,1)+Nu(2,1))+phi(2)*(Nu(1,2)+Nu(2,2)+Nu(3,2)
+Nu(11,2))+phi(3)*(Nu(1,3)+Nu(43,3)));
phig(11)=(phi(2)*Nu(11,2))/(phi(1)*(Nu(1,1)+Nu(2,1))+phi(2)*(Nu(1,2)+Nu(2,2)+Nu(3,
2)+Nu(11,2))+phi(3)*(Nu(1,3)+Nu(43,3)));
phig(43)=(phi(3)*Nu(43,3))/(phi(1)*(Nu(1,1)+Nu(2,1))+phi(2)*(Nu(1,2)+Nu(2,2)+Nu(3,
2)+Nu(11,2))+phi(3)*(Nu(1,3)+Nu(43,3)));
```

% theta(m,n) means the theta for main group "m" and secondary group "n"

```
thetag(1,1)=(phig(1)*(Q(1,1)/R(1,1)))/(phig(1)*(Q(1,1)/R(1,1))+phig(2)*(Q(2,1)/R(2,1))
+phig(3)*(Q(3,2)/R(3,2))+phig(11)*(Q(11,2)/R(11,2))+phig(43)*(Q(43,3)/R(43,3)));
thetag(1,2)=(phig(2)*(Q(2,1)/R(2,1)))/(phig(1)*(Q(1,1)/R(1,1))+phig(2)*(Q(2,1)/R(2,1))
+phig(3)*(Q(3,2)/R(3,2)) +phig(11)*(Q(11,2)/R(11,2))+phig(43)*(Q(43,3)/R(43,3)));
thetag(1,3)=(phig(3)*(Q(3,2)/R(3,2)))/(phig(1)*(Q(1,1)/R(1,1))+phig(2)*(Q(2,1)/R(2,1))
+phig(3)*(Q(3,2)/R(3,2))+phig(11)*(Q(11,2)/R(11,2))+phig(43)*(Q(43,3)/R(43,3)));
thetag(11,22)=(phig(11)*(Q(11,2)/R(11,2)))/(phig(1)*(Q(1,1)/R(1,1))+phig(2)*(Q(2,1)/R
(2,1))+phig(3)*(Q(3,2)/R(3,2))+phig(11)*(Q(11,2)/R(11,2))+phig(43)*(Q(43,3)/R(43,3))
);
thetag(43,84)=(phig(43)*(Q(43,3)/R(43,3)))/(phig(1)*(Q(1,1)/R(1,1))+phig(2)*(Q(2,1)/R
(2,1))+phig(3)*(Q(3,2)/R(3,2))+phig(11)*(Q(11,2)/R(11,2))+phig(43)*(Q(43,3)/R(43,3))
);
```

% Psi values obtained from MAIN GROUP CONTRIBUTIONS ONLY. THERE ARE INTERACTIONS BETWEEN ONLY 1,11 AND 1,43 GROUPS.
% a(m,n) values obtained from UNIFAC table

```
a(1,11)=232.1;
a(11,1)=114.8;
a(1,43)=252.7;
a(43,1)=110.2;
```

% psi values calculated from psi(m,n)=exp(-a(m,n)/T) where T is temperature in deg Kelvin.

```
psi(11,1)=exp(-a(11,1)/T);
psi(1,11)=exp(-a(1,11)/T);
psi(43,1)=exp(-a(43,1)/T);
psi(1,43)=exp(-a(1,43)/T);
```

% Calculation of the activity of Species 1

```
ap(1)=exp(log(phi(1))+(z/2)*q(1)*log((theta(1))/(phi(1)))+l(1)-
((phi(1))*l(1)+(phi(2))*(r(1)/r(2))*l(2)+(phi(3))*(r(1)/r(3))*l(3))+Nu(1,1)*Q(1,1)*((1-
log(thetag(1,1)+thetag(1,2)+thetag(1,3)+psi(11,1)*thetag(11,22)+psi(43,1)*thetag(43,84)
))-
((((thetag(1,1)+thetag(1,2)+thetag(1,3))/(thetag(1,1)+thetag(1,2)+thetag(1,3)+psi(43,1)*t
hetag(43,84)+psi(11,1)*thetag(11,22)))+
((psi(11,1)*thetag(11,22))/(psi(1,11)*(thetag(1,1)+thetag(1,2)+thetag(1,3))+thetag(11,22)
))+
((psi(43,1)*thetag(43,84))/(psi(1,43)*(thetag(1,1)+thetag(1,2)+thetag(1,3))+thetag(43,84)
)))))+                                                    Nu(2,1)*Q(2,1)*((1-
log(thetag(1,1)+thetag(1,2)+thetag(1,3)+psi(11,1)*thetag(11,22)+psi(43,1)*thetag(43,84)
))-
((((thetag(1,1)+thetag(1,2)+thetag(1,3))/(thetag(1,1)+thetag(1,2)+thetag(1,3)+psi(43,1)*t
hetag(43,84)+psi(11,1)*thetag(11,22)))+
((psi(11,1)*thetag(11,22))/(psi(1,11)*(thetag(1,1)+thetag(1,2)+thetag(1,3))+thetag(11,22)
))+((psi(43,1)*thetag(43,84))/(psi(1,43)*(thetag(1,1)+thetag(1,2)+thetag(1,3))+thetag(43,
84)))))));
```

% Calculation of the activity of Species 2

```
ap(2)=exp(log(phi(2))+(z/2)*q(2)*log((theta(2))/(phi(2)))+l(2)-
((phi(2))*l(2)+(phi(1))*(r(2)/r(1))*l(1)+(phi(3))*(r(2)/r(3))*l(3))+...
   Nu(1,2)*(Q(1,2)*((1-
log(thetag(1,1)+thetag(1,2)+thetag(1,3)+psi(11,1)*thetag(11,22)+psi(43,1)*thetag(43,84)
))-
(((thetag(1,1)+thetag(1,2)+thetag(1,3))/(thetag(1,1)+thetag(1,2)+thetag(1,3)+psi(43,1)*th
etag(43,84)+psi(11,1)*thetag(11,22)))+
((psi(11,1)*thetag(11,22))/(psi(1,11)*(thetag(1,1)+thetag(1,2)+thetag(1,3))+thetag(11,22)
))+
((psi(43,1)*thetag(43,84))/(psi(1,43)*(thetag(1,1)+thetag(1,2)+thetag(1,3))+thetag(43,84)
))))-(-0.0258))+Nu(2,2)*(Q(2,2)*((1-
log(thetag(1,1)+thetag(1,2)+thetag(1,3)+psi(11,1)*thetag(11,22)+psi(43,1)*thetag(43,84)
))                                                                                    -
(((thetag(1,1)+thetag(1,2)+thetag(1,3))/(thetag(1,1)+thetag(1,2)+thetag(1,3)+psi(43,1)*th
etag(43,84)+psi(11,1)*thetag(11,22)))+((psi(11,1)*thetag(11,22))/(psi(1,11)*(thetag(1,1)
+thetag(1,2)+thetag(1,3))+thetag(11,22)))+((psi(43,1)*thetag(43,84))/(psi(1,43)*(thetag(
1,1)+thetag(1,2)+thetag(1,3))+thetag(43,84)))))-(-0.0164))+Nu(3,2)*(Q(3,2)*((1-
log(thetag(1,1)+thetag(1,2)+thetag(1,3)+psi(11,1)*thetag(11,22)+psi(43,1)*thetag(43,84)
))-
(((thetag(1,1)+thetag(1,2)+thetag(1,3))/(thetag(1,1)+thetag(1,2)+thetag(1,3)+psi(43,1)*th
etag(43,84)+psi(11,1)*thetag(11,22)))+((psi(11,1)*thetag(11,22))/(psi(1,11)*(thetag(1,1)
+thetag(1,2)+thetag(1,3))+thetag(11,22)))+((psi(43,1)*thetag(43,84))/(psi(1,43)*(thetag(
1,1)+thetag(1,2)+thetag(1,3))+thetag(43,84)))))-(-0.069))+Nu(11,2)*(Q(11,2)*((1-
log((psi(1,11))*(thetag(1,1)+thetag(1,2)+thetag(1,3))+thetag(11,22))-
```

((((psi(1,11))*(thetag(1,1)+thetag(1,2)+thetag(1,3)))/(thetag(1,1)+thetag(1,2)+thetag(1,3)
+psi(43,1)*thetag(43,84)+psi(11,1)*thetag(11,22)))+((thetag(11,22))/(psi(1,11)*(thetag(1
,1)+thetag(1,2)+thetag(1,3))+thetag(11,22))))))-0.5607));

% Variation of the Applied Pressure

```
for j=1:1
  Papp(j)=j*40;                    % Sample Calculation at 40 bar
for i=1:2
  am(i,j)=exp(log(ap(i))+(V(i)/(Rg*T))*(1-Papp(j)));
end
end

thetax(1)=((x(1))*(q(1)/r(1)))/((x(1))*(q(1)/r(1))+(x(2))*(q(2)/r(2))+((1-x(1)-
x(2)))*(q(3)/r(3)));
thetax(2)=((x(2))*(q(2)/r(2)))/((x(1))*(q(1)/r(1))+(x(2))*(q(2)/r(2))+((1-x(1)-
x(2)))*(q(3)/r(3)));

phigx(1)=(x(1)*Nu(1,1)+x(2)*Nu(1,2)+(1-x(1)-
x(2))*Nu(1,3))/(x(1)*(Nu(1,1)+Nu(2,1))+x(2)*(Nu(1,2)+Nu(2,2)+Nu(3,2)+Nu(11,2))+(1
-x(1)-x(2))*(Nu(1,3)+Nu(43,3)));
phigx(2)=(x(1)*Nu(2,1)+x(2)*Nu(2,2))/(x(1)*(Nu(1,1)+Nu(2,1))+x(2)*(Nu(1,2)+Nu(2,2
)+Nu(3,2)+Nu(11,2))+(1-x(1)-x(2))*(Nu(1,3)+Nu(43,3)));
phigx(3)=(x(2)*Nu(3,2))/(x(1)*(Nu(1,1)+Nu(2,1))+x(2)*(Nu(1,2)+Nu(2,2)+Nu(3,2)+Nu(
11,2))+(1-x(1)-x(2))*(Nu(1,3)+Nu(43,3)));
phigx(11)=(x(2)*Nu(11,2))/(x(1)*(Nu(1,1)+Nu(2,1))+x(2)*(Nu(1,2)+Nu(2,2)+Nu(3,2)+
Nu(11,2))+(1-x(1)-x(2))*(Nu(1,3)+Nu(43,3)));
phigx(43)=((1-x(1)-
x(2))*Nu(43,3))/(x(1)*(Nu(1,1)+Nu(2,1))+x(2)*(Nu(1,2)+Nu(2,2)+Nu(3,2)+Nu(11,2))+(
1-x(1)-x(2))*(Nu(1,3)+Nu(43,3)));

% theta(m,n) means the theta for main group "m" and secondary group "n"

thetagx(1,1)=(phigx(1)*(Q(1,1)/R(1,1)))/(phigx(1)*(Q(1,1)/R(1,1))+phigx(2)*(Q(2,1)/R(
2,1))+phigx(3)*(Q(3,2)/R(3,2))...
   +phigx(11)*(Q(11,2)/R(11,2))+phigx(43)*(Q(43,3)/R(43,3)));
thetagx(1,2)=(phigx(2)*(Q(2,1)/R(2,1)))/(phigx(1)*(Q(1,1)/R(1,1))+phigx(2)*(Q(2,1)/R(
2,1))+phigx(3)*(Q(3,2)/R(3,2))...
   +phigx(11)*(Q(11,2)/R(11,2))+phigx(43)*(Q(43,3)/R(43,3)));
thetagx(1,3)=(phigx(3)*(Q(3,2)/R(3,2)))/(phigx(1)*(Q(1,1)/R(1,1))+phigx(2)*(Q(2,1)/R(
2,1))+phigx(3)*(Q(3,2)/R(3,2))...
   +phigx(11)*(Q(11,2)/R(11,2))+phigx(43)*(Q(43,3)/R(43,3)));
thetagx(11,22)=(phigx(11)*(Q(11,2)/R(11,2)))/(phigx(1)*(Q(1,1)/R(1,1))+phigx(2)*(Q(2
,1)/R(2,1))+phigx(3)*(Q(3,2)/R(3,2))...
   +phigx(11)*(Q(11,2)/R(11,2))+phigx(43)*(Q(43,3)/R(43,3)));
```

thetagx(43,84)=(phigx(43)*(Q(43,3)/R(43,3)))/(phigx(1)*(Q(1,1)/R(1,1))+phigx(2)*(Q(2
,1)/R(2,1))+phigx(3)*(Q(3,2)/R(3,2))...
+phigx(11)*(Q(11,2)/R(11,2))+phigx(43)*(Q(43,3)/R(43,3)));

% Equations for the Simultaneous Solution to obtain the Volume Fractions on the Permeate side ($\phi_{ip\ (m)}$). The species volume fractions are named as x(1) and x(2)

%Equation 1

e1=(log(x(1))+(z/2)*q(1)*log((thetax(1))/(x(1)))+l(1)-
((x(1))*l(1)+(x(2))*(r(1)/r(2))*l(2)+((1-x(1)-x(2)))*(r(1)/r(3))*l(3))+...
Nu(1,1)*Q(1,1)*((1-
log(thetagx(1,1)+thetagx(1,2)+thetagx(1,3)+psi(11,1)*thetagx(11,22)+psi(43,1)*thetagx(
43,84)))-
((((thetagx(1,1)+thetagx(1,2)+thetagx(1,3))/(thetagx(1,1)+thetagx(1,2)+thetagx(1,3)+psi(
43,1)*thetagx(43,84)+psi(11,1)*thetagx(11,22)))+((psi(11,1)*thetagx(11,22))/(psi(1,11)*
(thetagx(1,1)+thetagx(1,2)+thetagx(1,3))+thetagx(11,22)))+((psi(43,1)*thetagx(43,84))/(
psi(1,43)*(thetagx(1,1)+thetagx(1,2)+thetagx(1,3))+thetagx(43,84))))))+Nu(2,1)*Q(2,1)*
((1-
log(thetagx(1,1)+thetagx(1,2)+thetagx(1,3)+psi(11,1)*thetagx(11,22)+psi(43,1)*thetagx(
43,84)))-
((((thetagx(1,1)+thetagx(1,2)+thetagx(1,3))/(thetagx(1,1)+thetagx(1,2)+thetagx(1,3)+psi(
43,1)*thetagx(43,84)+psi(11,1)*thetagx(11,22)))+((psi(11,1)*thetagx(11,22))/(psi(1,11)*
(thetagx(1,1)+thetagx(1,2)+thetagx(1,3))+thetagx(11,22)))+((psi(43,1)*thetagx(43,84))/(
psi(1,43)*(thetagx(1,1)+thetagx(1,2)+thetagx(1,3))+thetagx(43,84)))))))-log(am(1,j));

%Equation 2

e2=log(x(2))+(z/2)*q(2)*log((thetax(2))/(x(2)))+l(2)-
((x(2))*l(2)+(x(1))*(r(2)/r(1))*l(1)+((1-x(1)-x(2)))*(r(2)/r(3))*l(3))+...
Nu(1,2)*(Q(1,2)*((1-
log(thetagx(1,1)+thetagx(1,2)+thetagx(1,3)+psi(11,1)*thetagx(11,22)+psi(43,1)*thetagx(
43,84))) -
(((thetagx(1,1)+thetagx(1,2)+thetagx(1,3))/(thetagx(1,1)+thetagx(1,2)+thetagx(1,3)+psi(4
3,1)*thetagx(43,84)+psi(11,1)*thetagx(11,22)))+((psi(11,1)*thetagx(11,22))/(psi(1,11)*(t
hetagx(1,1)+thetagx(1,2)+thetagx(1,3))+thetagx(11,22)))+((psi(43,1)*thetagx(43,84))/(ps
i(1,43)*(thetagx(1,1)+thetagx(1,2)+thetagx(1,3))+thetagx(43,84)))))-(-
0.0258))+Nu(2,2)*(Q(2,2)*((1-
log(thetagx(1,1)+thetagx(1,2)+thetagx(1,3)+psi(11,1)*thetagx(11,22)+psi(43,1)*thetagx(
43,84)))-
(((thetagx(1,1)+thetagx(1,2)+thetagx(1,3))/(thetagx(1,1)+thetagx(1,2)+thetagx(1,3)+psi(4
3,1)*thetagx(43,84)+psi(11,1)*thetagx(11,22)))+((psi(11,1)*thetagx(11,22))/(psi(1,11)*(t
hetagx(1,1)+thetagx(1,2)+thetagx(1,3))+thetagx(11,22)))+((psi(43,1)*thetagx(43,84))/(ps
i(1,43)*(thetagx(1,1)+thetagx(1,2)+thetagx(1,3))+thetagx(43,84)))))-(-
0.0164))+Nu(3,2)*(Q(3,2)*((1-
log(thetagx(1,1)+thetagx(1,2)+thetagx(1,3)+psi(11,1)*thetagx(11,22)+psi(43,1)*thetagx(
43,84)))-
(((thetagx(1,1)+thetagx(1,2)+thetagx(1,3))/(thetagx(1,1)+thetagx(1,2)+thetagx(1,3)+psi(4

```
3,1)*thetagx(43,84)+psi(11,1)*thetagx(11,22)))+((psi(11,1)*thetagx(11,22))/(psi(1,11)*(t
hetagx(1,1)+thetagx(1,2)+thetagx(1,3))+thetagx(11,22)))+((psi(43,1)*thetagx(43,84))/(ps
i(1,43)*(thetagx(1,1)+thetagx(1,2)+thetagx(1,3))+thetagx(43,84)))))-(-
0.069))+Nu(11,2)*(Q(11,2)*((1-
log((psi(1,11))*(thetagx(1,1)+thetagx(1,2)+thetagx(1,3))+thetagx(11,22))-
((((psi(1,11))*(thetagx(1,1)+thetagx(1,2)+thetag(1,3)))/(thetagx(1,1)+thetagx(1,2)+thetag
x(1,3)+psi(43,1)*thetagx(43,84)+psi(11,1)*thetagx(11,22)))+((thetagx(11,22))/(psi(1,11)
*(thetagx(1,1)+thetagx(1,2)+thetagx(1,3))+thetagx(11,22))))))-0.5607)-log(am(2,j));

f(1)=e1;
f(2)=e2;
```

% Command used to solve the program
%x=fsolve('FILENAME',[x1(0);x2(0)])

TYPICAL MATLAB OUTPUT FOR THE ABOVE COMMAND AND PROGRAM WHICH GIVES THE SPECIES BOUNDARY CONDITIONS FOR THE GIVEN PRESSURE

```
> In C:\MATLABR12\toolbox\optim\fsolve.m (parse_call) at line 346
  In C:\MATLABR12\toolbox\optim\fsolve.m at line 100
Optimization terminated successfully:
 Relative function value changing by less than OPTIONS.TolFun

x =

   0.63400          % This is the value for ϕ1p (m) at 40 bar (SOLVENT)
   0.00692          % This is the value for ϕ2p (m) at 40 bar (SOLUTE)
```

The program needs to be solved by changing the pressure individually and obtaining the boundary condition variation with pressure.

STEP 2: Solving the differential equations simultaneously to satisfy the Boundary Conditions using the UNIFAC method

MATLAB Program for solving the simultaneous differential equations using the UNIFAC Approach

```
function xdot=UNIFAC_C12(z,x)
xdot=zeros(2,1);

x(1)=0.73;              % Using value of 1.89 gm/gm PDMS sorption value
x(2)=0.012787;          % Using chi(2,3) value and using Flory-Rehner approach

rCH3=0.9011;
qCH3=0.848;
rCH2=0.6744;
qCH2=0.540;
rCH=0.4469;
qCH=0.228;
rCH2COO=1.6764;
qCH2COO=1.420;
rSiO=1.1044;
qSiO=0.466;

% For hexane
nuCH3=2;
nuCH2=4;

% For triglyceride
N=10;                   % For C10 triglyceride
nuCH3=3;
nuCH2=3*(N-3);
nuCH=1;
nuCH2COO=3;

% For PDMS
nuCH3=2;
nuSiO=1;

% q and r calculation
q(1)=2*qCH3+4*qCH2;
q(2)=3*qCH3+3*(N-3)*qCH2+1*qCH+3*qCH2COO;
r(1)=2*rCH3+4*rCH2;
r(2)=3*rCH3+3*(N-3)*rCH2+1*rCH+3*rCH2COO;
q(3)=2*qCH3+1*qSiO;
r(3)=2*rCH3+1*rSiO;
```

```
Z=10;            % Co-ordination number = 10 mostly

for i=1:3
  l(i)=5*(r(i)-q(i))-(r(i)-1);
end

Nu(1,1)=2;     % Nu(m,n) means no. of groups of type m in component n
Nu(2,1)=4;     % m=1=CH3; m=2=CH2; m=3=CH; m=11=Ch2COO; m=43=SiO
Nu(1,2)=3;     % n=1=hexane; n=2=triglyceride; n=3=PDMS
Nu(2,2)=21;    % will change with triglyceride
Nu(3,2)=1;
Nu(11,2)=3;
Nu(1,3)=2;
Nu(43,3)=1;
Q(1,1)=0.848;
Q(2,1)=0.540;
Q(1,2)=0.848;
Q(2,2)=0.540;
Q(3,2)=0.228;
Q(11,2)=1.420;
Q(43,3)=0.466;
R(1,1)=0.9011;
R(2,1)=0.6744;
R(1,2)=0.9011;
R(2,2)=0.6744;
R(3,2)=0.4469;
R(11,2)=1.6764;
R(43,3)=1.1044;
```

% Psi values obtained from MAIN GROUP CONTRIBUTIONS ONLY. THERE ARE INTERACTIONS BETWEEN ONLY 1,11 AND 1,43 GROUPS.
% a(m,n) values obtained from UNIFAC table

```
a(1,11)=232.1;
a(11,1)=114.8;
a(1,43)=252.7;
a(43,1)=110.2;
```

% psi values calculated from psi(m,n)=exp(-a(m,n)/T) where T is temperature in deg Kelvin.

```
T=304;           % temperature in kelvin for C10 triglyceride

psi(11,1)=exp(-a(11,1)/T);
psi(1,11)=exp(-a(1,11)/T);
psi(43,1)=exp(-a(43,1)/T);
psi(1,43)=exp(-a(1,43)/T);
```

```
thetax(1)=((x(1))*(q(1)/r(1)))/((x(1))*(q(1)/r(1))+(x(2))*(q(2)/r(2))+((1-x(1)-
x(2)))*(q(3)/r(3)));
thetax(2)=((x(2))*(q(2)/r(2)))/((x(1))*(q(1)/r(1))+(x(2))*(q(2)/r(2))+((1-x(1)-
x(2)))*(q(3)/r(3)));

phigx(1)=(x(1)*Nu(1,1)+x(2)*Nu(1,2)+(1-x(1)-
x(2))*Nu(1,3))/(x(1)*(Nu(1,1)+Nu(2,1))+x(2)*(Nu(1,2)+Nu(2,2)+Nu(3,2)+Nu(11,2))...
   +(1-x(1)-x(2))*(Nu(1,3)+Nu(43,3)));
phigx(2)=(x(1)*Nu(2,1)+x(2)*Nu(2,2))/(x(1)*(Nu(1,1)+Nu(2,1))+x(2)*(Nu(1,2)+Nu(2,2
)+Nu(3,2)+Nu(11,2))+(1-x(1)-x(2))*(Nu(1,3)+Nu(43,3)));
phigx(3)=(x(2)*Nu(3,2))/(x(1)*(Nu(1,1)+Nu(2,1))+x(2)*(Nu(1,2)+Nu(2,2)+Nu(3,2)+Nu(
11,2))+(1-x(1)-x(2))*(Nu(1,3)+Nu(43,3)));
phigx(11)=(x(2)*Nu(11,2))/(x(1)*(Nu(1,1)+Nu(2,1))+x(2)*(Nu(1,2)+Nu(2,2)+Nu(3,2)+
Nu(11,2))+(1-x(1)-x(2))*(Nu(1,3)+Nu(43,3)));
phigx(43)=((1-x(1)-
x(2))*Nu(43,3))/(x(1)*(Nu(1,1)+Nu(2,1))+x(2)*(Nu(1,2)+Nu(2,2)+Nu(3,2)+Nu(11,2))+(
1-x(1)-x(2))*(Nu(1,3)+Nu(43,3)));

% theta(m,n) means the theta for main group "m" and secondary group "n"

thetagx(1,1)=(phigx(1)*(Q(1,1)/R(1,1)))/(phigx(1)*(Q(1,1)/R(1,1))+phigx(2)*(Q(2,1)/R(
2,1))+phigx(3)*(Q(3,2)/R(3,2))...
   +phigx(11)*(Q(11,2)/R(11,2))+phigx(43)*(Q(43,3)/R(43,3)));
thetagx(1,2)=(phigx(2)*(Q(2,1)/R(2,1)))/(phigx(1)*(Q(1,1)/R(1,1))+phigx(2)*(Q(2,1)/R(
2,1))+phigx(3)*(Q(3,2)/R(3,2))...
   +phigx(11)*(Q(11,2)/R(11,2))+phigx(43)*(Q(43,3)/R(43,3)));
thetagx(1,3)=(phigx(3)*(Q(3,2)/R(3,2)))/(phigx(1)*(Q(1,1)/R(1,1))+phigx(2)*(Q(2,1)/R(
2,1))+phigx(3)*(Q(3,2)/R(3,2))...
   +phigx(11)*(Q(11,2)/R(11,2))+phigx(43)*(Q(43,3)/R(43,3)));
thetagx(11,22)=(phigx(11)*(Q(11,2)/R(11,2)))/(phigx(1)*(Q(1,1)/R(1,1))+phigx(2)*(Q(2
,1)/R(2,1))+phigx(3)*(Q(3,2)/R(3,2))...
   +phigx(11)*(Q(11,2)/R(11,2))+phigx(43)*(Q(43,3)/R(43,3)));
thetagx(43,84)=(phigx(43)*(Q(43,3)/R(43,3)))/(phigx(1)*(Q(1,1)/R(1,1))+phigx(2)*(Q(2
,1)/R(2,1))+phigx(3)*(Q(3,2)/R(3,2))...
   +phigx(11)*(Q(11,2)/R(11,2))+phigx(43)*(Q(43,3)/R(43,3)));

% Calculation of dln a1/dphi(1)

A=((qCH3/rCH3)*(2*x(1)+3*x(2)+2*(1-x(1)-
x(2)))+(qCH2/rCH2)*(4*x(1)+21*x(2))+(qCH/rCH)*x(2)+(qCH2COO/rCH2COO)*(3*x
(2))+(qSiO/rSiO)*(1-x(1)-x(2)));
B=(qCH2/rCH2)*4-(qSiO/rSiO);
C=(qCH3/rCH3)+21*(qCH2/rCH2)+(qCH/rCH)+(qCH2COO/rCH2COO)*3-
(qSiO/rSiO);

dtd1(1,1)=(-(qCH3/rCH3)*(2*x(1)+3*x(2)+2*(1-x(1)-x(2)))*B)/A^2;
```

```
dtd2(1,1)=(A*(qCH3/rCH3)-(qCH3/rCH3)*(2*x(1)+3*x(2)+2*(1-x(1)-x(2)))*C)/A^2;

dtd1(1,2)=(A*(qCH2/rCH2)*4-(qCH2/rCH2)*(4*x(1)+21*x(2))*B)/A^2;
dtd2(1,2)=(A*(qCH2/rCH2)*21-(qCH2/rCH2)*(4*x(1)+21*x(2))*C)/A^2;

dtd1(1,3)=(-(qCH/rCH)*x(2)*B)/A^2;
dtd2(1,3)=(A*(qCH/rCH)-(qCH/rCH)*x(2)*C)/A^2;

dtd1(11,22)=((qCH2COO/rCH2COO)*3*x(2)*B)/A^2;
dtd2(11,22)=(-A*(qCH2COO/rCH2COO)*3-(qCH2COO/rCH2COO)*3*x(2)*C)/A^2;

dtd1(43,84)=(-A*(qSiO/rSiO)-B*(1-x(1)-x(2))*(qSiO/rSiO))/A^2;
dtd2(43,84)=(-A*(qSiO/rSiO)-C*(1-x(1)-x(2))*(qSiO/rSiO))/A^2;
```

% to calculate dthetax(1)/dt1

```
D=((x(1))*(q(1)/r(1))+(x(2))*(q(2)/r(2))+((1-x(1)-x(2)))*(q(3)/r(3)));

dthetaxd1(1)=(D*(q(1)/r(1))-(x(1)*(q(1)/r(1))*((q(1)/r(1))-(q(3)/r(3)))))/D^2;
dthetaxd2(1)=(-(x(1)*(q(1)/r(1))*((q(2)/r(2))-(q(3)/r(3)))))/D^2;
dthetaxd1(2)=(-(x(2)*(q(2)/r(2))*((q(1)/r(1))-(q(3)/r(3)))))/D^2;
dthetaxd2(2)=(D*(q(2)/r(2))-(x(2)*(q(2)/r(2))*((q(2)/r(2))-(q(3)/r(3)))))/D^2;

E=thetagx(1,1)+thetagx(1,2)+thetagx(1,3)+psi(11,1)*thetagx(11,22)+psi(43,1)*thetagx(4
3,84);

G=psi(1,11)*(thetagx(1,1)+thetagx(1,2)+thetagx(1,3))+thetagx(11,22);

H=psi(1,43)*(thetagx(1,1)+thetagx(1,2)+thetagx(1,3))+thetagx(43,84);

dEd1=dtd1(1,1)+dtd1(1,2)+dtd1(1,3)+psi(11,1)*dtd1(11,22)+psi(43,1)*dtd1(43,84);
dGd1=psi(1,11)*(dtd1(1,1)+dtd1(1,2)+dtd1(1,3))+dtd1(11,22);
dHd1=psi(1,43)*(dtd1(1,1)+dtd1(1,2)+dtd1(1,3))+dtd1(43,84);
dEd2=dtd2(1,1)+dtd2(1,2)+dtd2(1,3)+psi(11,1)*dtd2(11,22)+psi(43,1)*dtd2(43,84);
dGd2=psi(1,11)*(dtd2(1,1)+dtd2(1,2)+dtd2(1,3))+dtd2(11,22);
dHd2=psi(1,43)*(dtd2(1,1)+dtd2(1,2)+dtd2(1,3))+dtd2(43,84);
```

% to calculate the activity dlna(1)/dphi(1)

```
dlna1d1=(1/(x(1)))+(z/2)*q(1)*((x(1))/thetax(1))*(((x(1))*dthetaxd1(1)-
thetax(1))/(x(1))^2)-(l(1)-(r(1)/r(3))*l(3))+Nu(1,1)*Q(1,1)*((-
1/E)*(dtd1(1,1)+dtd1(1,2)+dtd1(1,3)+psi(11,1)*dtd1(11,22)+psi(43,1)*dtd1(43,84))-...
   (((E*(dtd1(1,1)+dtd1(1,2)+dtd1(1,3))-
(thetagx(1,1)+thetagx(1,2)+thetagx(1,3))*dEd1)/E^2)+((G*psi(11,1)*dtd1(11,22)-
psi(11,1)*thetagx(11,22)*dGd1)/G^2)+((H*psi(43,1)*dtd1(43,84)-
```

```
psi(43,1)*thetagx(43,84)*dHd1)/H^2)))+Nu(2,1)*Q(2,1)*((-
1/E)*(dtd1(1,1)+dtd1(1,2)+dtd1(1,3)+psi(11,1)*dtd1(11,22)+psi(43,1)*dtd1(43,84))-...
   (((E*(dtd1(1,1)+dtd1(1,2)+dtd1(1,3))-
(thetagx(1,1)+thetagx(1,2)+thetagx(1,3))*dEd1)/E^2)+...
   ((G*psi(11,1)*dtd1(11,22)-
psi(11,1)*thetagx(11,22)*dGd1)/G^2)+((H*psi(43,1)*dtd1(43,84)-
psi(43,1)*thetagx(43,84)*dHd1)/H^2)));


dlna1d2=(z/2)*q(1)*((x(1))/thetax(1))*(1/x(1))*dthetaxd2(1)-((r(1)/r(2))*l(2)-
(r(1)/r(3))*l(3))+...
   Nu(1,1)*Q(1,1)*((-
1/E)*(dtd2(1,1)+dtd2(1,2)+dtd2(1,3)+psi(11,1)*dtd2(11,22)+psi(43,1)*dtd2(43,84))-...
   (((E*(dtd2(1,1)+dtd2(1,2)+dtd2(1,3))-
(thetagx(1,1)+thetagx(1,2)+thetagx(1,3))*dEd2)/E^2)+...
   ((G*psi(11,1)*dtd2(11,22)-
psi(11,1)*thetagx(11,22)*dGd2)/G^2)+((H*psi(43,1)*dtd2(43,84)-
psi(43,1)*thetagx(43,84)*dHd2)/H^2)))+...
   Nu(2,1)*Q(2,1)*((-
1/E)*(dtd2(1,1)+dtd2(1,2)+dtd2(1,3)+psi(11,1)*dtd2(11,22)+psi(43,1)*dtd2(43,84))-...
   (((E*(dtd2(1,1)+dtd2(1,2)+dtd2(1,3))-
(thetagx(1,1)+thetagx(1,2)+thetagx(1,3))*dEd2)/E^2)+((G*psi(11,1)*dtd2(11,22)-
psi(11,1)*thetagx(11,22)*dGd2)/G^2)+((H*psi(43,1)*dtd2(43,84)-
psi(43,1)*thetagx(43,84)*dHd2)/H^2)));

dlna2d1=(z/2)*q(2)*((x(2))/thetax(2))*(1/x(2))*dthetaxd1(2)-((r(2)/r(1))*l(1)-
(r(2)/r(3))*l(3))+...
   Nu(1,2)*Q(1,2)*((-
1/E)*(dtd1(1,1)+dtd1(1,2)+dtd1(1,3)+psi(11,1)*dtd1(11,22)+psi(43,1)*dtd1(43,84))-...
   (((E*(dtd1(1,1)+dtd1(1,2)+dtd1(1,3))-
(thetagx(1,1)+thetagx(1,2)+thetagx(1,3))*dEd1)/E^2)+...
   ((G*psi(11,1)*dtd1(11,22)-
psi(11,1)*thetagx(11,22)*dGd1)/G^2)+((H*psi(43,1)*dtd1(43,84)-
psi(43,1)*thetagx(43,84)*dHd1)/H^2)))+...
   Nu(2,2)*Q(2,2)*((-
1/E)*(dtd1(1,1)+dtd1(1,2)+dtd1(1,3)+psi(11,1)*dtd1(11,22)+psi(43,1)*dtd1(43,84))-...
   (((E*(dtd1(1,1)+dtd1(1,2)+dtd1(1,3))-
(thetagx(1,1)+thetagx(1,2)+thetagx(1,3))*dEd1)/E^2)+...
   ((G*psi(11,1)*dtd1(11,22)-
psi(11,1)*thetagx(11,22)*dGd1)/G^2)+((H*psi(43,1)*dtd1(43,84)-
psi(43,1)*thetagx(43,84)*dHd1)/H^2)))+Nu(3,2)*Q(3,2)*((-
1/E)*(dtd1(1,1)+dtd1(1,2)+dtd1(1,3)+psi(11,1)*dtd1(11,22)+psi(43,1)*dtd1(43,84))-...
   (((E*(dtd1(1,1)+dtd1(1,2)+dtd1(1,3))-
(thetagx(1,1)+thetagx(1,2)+thetagx(1,3))*dEd1)/E^2)+...
```

```
   ((G*psi(11,1)*dtd1(11,22)-
psi(11,1)*thetagx(11,22)*dGd1)/G^2)+((H*psi(43,1)*dtd1(43,84)-
psi(43,1)*thetagx(43,84)*dHd1)/H^2)))+...
   Nu(11,2)*Q(11,2)*((-1/G)*(psi(1,11)*(dtd1(1,1)+dtd1(1,2)+dtd1(1,3))+dtd1(11,22))-
...(((E*psi(1,11)*(dtd1(1,1)+dtd1(1,2)+dtd1(1,3))-
psi(1,11)*(thetagx(1,1)+thetagx(1,2)+thetagx(1,3))*dEd1)/E^2)+((G*dtd1(11,22)-
thetagx(11,22)*dGd1)/G^2)));


dlna2d2=(1/(x(2)))+(z/2)*q(2)*((x(2))/thetax(2))*(((x(2))*dthetaxd2(2)-
thetax(2))/(x(2))^2)-(l(2)-(r(2)/r(3))*l(3))+...
   Nu(1,2)*Q(1,2)*((-
1/E)*(dtd2(1,1)+dtd2(1,2)+dtd2(1,3)+psi(11,1)*dtd2(11,22)+psi(43,1)*dtd2(43,84))-...
   (((E*(dtd2(1,1)+dtd2(1,2)+dtd2(1,3))-
(thetagx(1,1)+thetagx(1,2)+thetagx(1,3))*dEd2)/E^2)+...
   ((G*psi(11,1)*dtd2(11,22)-
psi(11,1)*thetagx(11,22)*dGd2)/G^2)+((H*psi(43,1)*dtd2(43,84)-
psi(43,1)*thetagx(43,84)*dHd2)/H^2)))+...
   Nu(2,2)*Q(2,2)*((-
1/E)*(dtd2(1,1)+dtd2(1,2)+dtd2(1,3)+psi(11,1)*dtd2(11,22)+psi(43,1)*dtd2(43,84))-...
   (((E*(dtd2(1,1)+dtd2(1,2)+dtd2(1,3))-
(thetagx(1,1)+thetagx(1,2)+thetagx(1,3))*dEd2)/E^2)+...
   ((G*psi(11,1)*dtd2(11,22)-
psi(11,1)*thetagx(11,22)*dGd2)/G^2)+((H*psi(43,1)*dtd2(43,84)-
psi(43,1)*thetagx(43,84)*dHd2)/H^2)))+...
   Nu(3,2)*Q(3,2)*((-
1/E)*(dtd2(1,1)+dtd2(1,2)+dtd2(1,3)+psi(11,1)*dtd2(11,22)+psi(43,1)*dtd2(43,84))-...
   (((E*(dtd2(1,1)+dtd2(1,2)+dtd2(1,3))-
(thetagx(1,1)+thetagx(1,2)+thetagx(1,3))*dEd2)/E^2)+...
   ((G*psi(11,1)*dtd2(11,22)-
psi(11,1)*thetagx(11,22)*dGd2)/G^2)+((H*psi(43,1)*dtd2(43,84)-
psi(43,1)*thetagx(43,84)*dHd2)/H^2)))+...
   Nu(11,2)*Q(11,2)*((-1/G)*(psi(1,11)*(dtd2(1,1)+dtd2(1,2)+dtd2(1,3))+dtd2(11,22))-
...(((E*psi(1,11)*(dtd2(1,1)+dtd2(1,2)+dtd2(1,3))-
psi(1,11)*(thetagx(1,1)+thetagx(1,2)+thetagx(1,3))*dEd2)/E^2)+...
   ((G*dtd2(11,22)-thetagx(11,22)*dGd2)/G^2)));

J(1)=5.5e-5;          % Calculated Flux of Solvent
J(2)=5.16e-9;         % Calculated Flux of Solute

D(1)=9.35e-11;        % Diffusion Coefficient of Solvent (From Correlation)
D(2)=1.13e-13;        % Diffusion Coefficient of Solute (From Correlation)
```

% Equations used for Simultaneous Solution to calculate the Solute and Solvent Flux values. The Flux values are varied till the boundary conditions match with those calculated from the previous graph

% Equation 1

```
e1=(6e-7)*((x(1)*D(1)*J(2)*dlna1d2-
x(2)*D(2)*J(1)*dlna2d2)/(x(1)*x(2)*D(1)*D(2)*(dlna1d1*dlna2d2-dlna1d1d2*dlna2d1)));
```

% Equation 2

```
e2=(6e-7)*((x(2)*D(2)*J(1)*dlna2d1-
x(1)*D(1)*J(2)*dlna1d1)/(x(1)*x(2)*D(1)*D(2)*(dlna1d1*dlna2d2-dlna1d1d2*dlna2d1)));
xdot(1)=e1;
xdot(2)=e2;
```

% Command used to solve this equation
%[z,x]=ode23s('FILENAME',[0;1],[x1(0);x2(0)]

TYPICAL MATLAB OUTPUT FOR THE ABOVE PROGRAM AND COMMAND

```
z =
            0
   0.10000000000000
   0.20000000000000
   0.30000000000000
   0.40000000000000
   0.50000000000000
   0.60000000000000
   0.70000000000000
   0.80000000000000
   0.90000000000000
   1.00000000000000                    % z=1 corresponds to the permeate side
x =
   0.73000000000000   0.01278700000000
   0.72061522533319   0.01221801041658
   0.71118186257322   0.01164507891909
   0.70169939904755   0.01106816391480
   0.69216731392652   0.01048722314921
   0.68258507804931   0.00990221369191
   0.67295215374535   0.00931309192212
   0.66326799465082   0.00871981351375
   0.65353204552030   0.00812233342018
   0.64374374203316   0.00752060585852
   0.63390251059470   0.00691458429349 %Boundary Conditions on Permeate Side
```

The Calculated Solvent and Solute fluxes that match the boundary conditions are:
J1 = 5.5×10^{-5} m/s; J2 = 5.16×10^{-9} m/s
The Solute concentration in the bulk phase = 500 mg/l.
The solute density is taken as = 1 gm/cc
This gives a rejection of solute = 0.812
This value corresponds to the point shown in Figure 5.46 for the UNIFAC series

STEP 1: Obtaining the Boundary Conditions using the Flory-Huggins method

MATLAB Program for calculation of boundary conditions using the Flory-Huggins Approach

```
function f=BC_COUP(x)
f=zeros(2,1);

phi(1)=0.73;          % using value of 1.89 gm/gm PDMS sorption value
phi(2)=0.012787;      % Using chi(2,3) value and using Flory-Rehner approach
V(1)=131.6;           % molar volume of n-hexane in cc/mole
V(2)=554;             % molar volume of C10 TG in cc/mole
R=82.06;              % R units = cc-atm/g-mole K
T=304;                % Temperature in deg K
chi(1,3)=0.45;        % interaction parameter taken from literature for Hexane-PDMS
chi(2,3)=3.46;        % interaction parameter calculated using the Solubility Parameters
chi(1,2)=1.35;        % interaction parameter calculated using the Solubility Parameters

phi(3)=1-(phi(1)+phi(2));

% Calculation of the activity of species 1
ap(1)=exp(log(phi(1))+(1-phi(1))-
phi(2)*(V(1)/V(2))+(phi(2)+phi(3))*(chi(1,2)*phi(2)+chi(1,3)*phi(3))-
chi(2,3)*(V(1)/V(2))*phi(2)*phi(3));

% Calculation of the activity of species 2
ap(2)=exp(log(phi(2))+(1-phi(2))-
phi(1)*(V(2)/V(1))+(phi(1)+phi(3))*((chi(1,2)*phi(1)*(V(2)/V(1)))+chi(2,3)*phi(3))-
chi(1,3)*(V(2)/V(1))*phi(1)*phi(3));

% Applied Pressure Variation

for j=1:1
  Papp(j)=j*40;       % Sample Calculation done at 40 bar
for i=1:2
  am(i,j)=exp(log(ap(i))+(V(i)/(R*T))*(1-Papp(j)));
end
end
```

% Equations for the Simultaneous Solution to obtain the Volume Fractions on the Permeate side ($\phi_{ip\ (m)}$). The species volume fractions are named as x(1) and x(2)

%Equation 1

```
e1=log(x(1))+(1-x(1))-x(2)*(V(1)/V(2))+(x(2)+(1-
(x(1)+x(2))))*(chi(1,2)*x(2)+chi(1,3)*(1-(x(1)+x(2)))-chi(2,3)*(V(1)/V(2))*x(2)*(1-
(x(1)+x(2)))-log(am(1,j));
```

%Equation 2

```
e2=log(x(2))+(1-x(2))-x(1)*(V(2)/V(1))+(x(1)+(1-
(x(1)+x(2))))*((chi(1,2)*x(1)*(V(2)/V(1)))+chi(2,3)*(1-(x(1)+x(2))))-
chi(1,3)*(V(2)/V(1))*x(1)*(1-(x(1)+x(2)))-log(am(2,j));

f(1)=e1;
f(2)=e2;
```

% Command used to solve the program
%x=fsolve('FILENAME',[x1(0);x2(0)])

TYPICAL MATLAB OUTPUT OBTAINED FOR THE ABOVE SYSTEM:

```
> In C:\MATLABR12\toolbox\optim\fsolve.m (parse_call) at line 346
  In C:\MATLABR12\toolbox\optim\fsolve.m at line 100
Optimization terminated successfully:
 Relative function value changing by less than OPTIONS.TolFun
```

The Boundary Conditions can be shown as follows:

```
x =

   0.34200        % This is the value for φ1p (m) at 40 bar (SOLVENT)
   0.00237        % This is the value for φ2p (m) at 40 bar (SOLUTE)
```

STEP 2: Solving the differential equations simultaneously to satisfy the Boundary Conditions using the Flory-Huggins method

MATLAB Program used for solving the simultaneous differential equations using the Flory-Huggins Approach

```
function xdot=FH_COUP(z,x)
xdot=zeros(2,1);

chi(1,3)=0.45;
chi(2,3)=3.473;
chi(1,2)=1.234;
V(1)=131.6;     % molar volume of hexane in cc/mole
V(2)=554;       % molar volume of C10 TG in cc/mole
```

% Flux and Diffusion Values

```
J(1)=1.51e-5;          % Calculated Flux of Solvent
J(2)=3.81e-9;          % Calculated Flux of Solute

D(1)=9.35e-11;         % Diffusion Coefficient of Solvent (From Correlation)
D(2)=1.13e-13;         % Diffusion Coefficient of Solute (From Correlation)
```

% Equations used for Simultaneous Solution to calculate the Solute and Solvent Flux values. The Flux values are varied till the boundary conditions match with those calculated from the previous graph

```
k(1,1)=-x(1)*D(1)*((1/x(1))+(2*chi(1,3))*x(1)+(chi(1,3)-
chi(1,2)+chi(2,3)*(V(1)/V(2)))*x(2)-1-2*chi(1,3));
k(1,2)=-x(1)*D(1)*((chi(1,3)-
chi(1,2)+chi(2,3)*(V(1)/V(2)))*x(1)+2*chi(2,3)*(V(1)/V(2))*x(2)+chi(1,2)-chi(1,3)-
chi(2,3)*(V(1)/V(2))-(V(1)/V(2)));
k(2,2)=-x(2)*D(2)*((chi(2,3)+chi(1,3)*(V(2)/V(1))-
chi(1,2)*(V(2)/V(1)))*x(1)+2*chi(2,3)*x(2)-1-2*chi(2,3)-(V(2)/V(1))+(1/x(2)));
k(2,1)=-x(2)*D(2)*((2*chi(1,3)*(V(2)/V(1)))*x(1)+(chi(2,3)+chi(1,3)*(V(2)/V(1))-
chi(1,2)*(V(2)/V(1)))*x(2)+chi(1,2)*(V(2)/V(1))-chi(2,3)-chi(1,3)*(V(2)/V(1)));
```

%Equation 1

```
e1=(6e-7)*(k(2,2)*J(1)-k(1,2)*J(2))/(k(1,1)*k(2,2)-k(2,1)*k(1,2));
```

%Equation 2

```
e2=(6e-7)*(k(2,1)*J(1)-k(1,1)*J(2))/(k(2,1)*k(1,2)-k(1,1)*k(2,2));

xdot(1)=e1;
xdot(2)=e2;
```

% Command used to solve this equation
%[z,x]=ode23s('FILENAME',[0;1],[x1(0);x2(0)]

TYPICAL MATLAB OUTPUT OBTAINED FOR THE ABOVE SYSTEM:

```
z =
            0
   0.02556168751845
   0.09084321338888
   0.16482367958453
   0.24899503689678
   0.34372796589643
   0.44372796589643
   0.54372796589643
   0.64372796589643
   0.74372796589643
   0.84372796589643
   0.94372796589643
   1.00000000000000                    % z=1 corresponds to the permeate side

x =
   0.73000000000000   0.01278700000000
   0.70578064812214   0.01330083990452
   0.65534916498804   0.01409024411491
   0.61011027671644   0.01436830367121
   0.56769160574011   0.01414879089681
   0.52732303865272   0.01342290497348
   0.49047572376405   0.01226572801365
   0.45788805568910   0.01082240110066
   0.42852134665525   0.00917519758905
   0.40169045619863   0.00738399027544
   0.37691671650722   0.00549323734183
   0.35385093754467   0.00353630991452
   0.34152018589908   0.00241604920910 %Boundary Conditions on permeate side
```

The Calculated Solvent and Solute fluxes that match the boundary conditions are:
J1 = 1.51 × 10^{-5} m/s; J2 = 3.81 × 10^{-9} m/s
The Solute concentration in the bulk phase = 500 mg/l.
The solute density is taken as = 1 gm/cc
This gives a rejection of solute = 0.494
This value corresponds to the point shown in Figure 5.46 for the FH model

MATLAB Program for calculating the B_{SFPF} values for C10 Triglyceride system

```
function f=sfpf(x)

% for C10 Triglyceride in n-hexane

R=82.06;        % cc-atm/gmole K
T=298;          % K
P=40.8;         % operating pressure in atm
Rb=10e-10;      % m
Visc=0.325;     % Viscosity of n-Hexane in cP

%Input Parameters for Radius of Solvent

NAv=6.023e23;       % Avogadro Number
Vm=131;             % Molar Volume of Solvent (n-hexane) in cc/gmole

% Input Parameters for Dab

psi=1;          % psi=assosication constant for solvents
                % psi=1 for unassosciating solvents (e.g. hexane, heptane)
                % Psi=2.6 for Water, =1.9 for MeOH, =1.5 for EtOH
Mb=86;          % Molecular Weight of the Solvent
Va=554;         % for C 10 Triglyceride

% Input Parameters for Solute Concn.

Ca=500;         % in mg/liter of solution
Ma=554;         % Molecular Weight of Solute (Sudan IV)
k=1.38e-16;     % Boltzmann Constant (dyne.cm/K)
```

%Part 1: Calculation of Ra, D(Stokes Radius) and b

% Calculation of Ra:

```
% Assume Spherical Molecule
% 1 mole = 6.023e23 molecules
% Thus 1 molecule = (1/6.023e23) moles
% Also 1 mole occupies volume = Molar Volume of the solvent
% Thus Molar Volume = 6.023e23 molecules
% Thus 1 molecule = Molar volume / 6.023e23 cc
% Using Volume of a Sphere = 4/3*pi*R^3, calculate the radius of the solvent molecule
```

% Calculation of Radius of solvent

```
r=0.01*((Vm/NAv)*(3/(4*pi)))^(1/3);
```

```
% Rb is the mean radius of the pores. Can be obtained from N2 sorption
% Using Rb = 8.5 Angstroms (for FT30 BW membrane used by Mike Jevtitch)

Ra=Rb-r;

% Calculation of b

% Use Faxen equations for estimating b
% Need to obtain the radius of the Solute molecule
% Assume Stokes' Radius is valid
% D=k*T/(6*pi*Visc*Dab)
% k=Boltzmann Constant=1.38e-16 (dyne.cm/K)
% Dab= Solute Diffusivity, can be obtained from Wilke-Chang Equation

% Calculation of Dab from Wilke Chang Equation

% Dab=7.4e-8*(psi*Mb)^0.5*T/(Visc*Va^0.6)
% Dab=Solute Diffusivity, cm2/s
% psi=assosication constant for solvents
% psi=1 for unassosciating solvents (e.g. hexane, heptane)
% Psi=2.6 for Water, =1.9 for MeOH, =1.5 for EtOH
% Mb=Molecular Weight of the Solvent
% T=Temperature (K)
% Visc= viscosity of the solvent (cP)
% Va=molar volume of solute (cc/gmole)


Dab=7.4e-8*((psi*Mb)^0.5)*T/(Visc*Va^0.6);

% Calculation of Stokes Radius

Dstok=k*T/(6*pi*Visc*0.01*Dab);    % in cm, Viscosity is multiplied by 0.01 to match the units

% to convert Stokes radius to meters:

D=Dstok*1e-2;                      % in m

% Calculation of Lamda

Lamda=D/Rb;

if Lamda <= 0.22
   b=1/(1-2.104*Lamda+2.09*Lamda^3-0.95*Lamda^5);
else
```

```
   b=44.57-416.2*Lamda+934.9*Lamda^2+302.4*Lamda^3;
end
```

% Concentration of Solute if feed (converted to gmole/cc)

```
Ca2=(Ca*1e-6)/Ma;
```

% Part 2: Numerical Integration for the calculation of Rejection

```
Rc=Ra.*1e10;

B=-490;

Beta1=Visc*0.98e-8*Dab/(R*T*Ca2*(Ra*1e2)^2);

Beta2=P/(R*T*Ca2);

%b=quad('test',0,1);

%b1=1/b

f=4.52*(Beta2.*(1-x.^2)./(4*Beta1)).*exp(Beta2.*(1-x.^2)./(4*Beta1)).*x./(1+(b./exp((-
B./(Rc.^3))./((Rb./Ra)-x).^3)));
```

% Command used to solve this
% f=quad('FILENAME',0,1)

Subroutine for calculation of velocity

```
function f=test(x)

Visc=0.325;          % Viscosity of n-Hexane in cP
Dab=1.42e-5;         % cm2/sec  Diffusivity of Sudan IV in hexane using Wilke Chang
R=82.06;             % cc-atm/gmole K
T=298;               % K
Ca2=9.025e-7;        % gmole/cc
P=40.8;              % atm
Ra=6.26;             % Angstroms
Beta1=Visc*0.98e-8*Dab/(R*T*Ca2*(Ra*1e-8)^2);
Beta2=P/(R*T*Ca2);

f=Beta2.*x.*(1-x.^2)./(4*Beta1);
```

REFERENCES

Abrams, D. S. and Prausnitz, J. M.: "Statistical Thermodynamics of Liquid Mixtures: A New Expression for the Excess Gibbs Energy of Partly or Completely Miscible Systems", *AIChE Journal*, **21**, 116, (1975).

Aminabhavi, T. M.; Harogoppad, S. B. & Khinnavar, R. S., "Rubber-Solvent Interactions", *Journal of Macromolecular Science-Reviews In Macromolecular Chemistry And Physics*, **C31(4)**, 433-498 (1991).

Aminabhavi, T. M. & Khinnavar, R. S., "Diffusion and Sorption of organic liquids through polymer membranes: 10. Polyurethane, nitrile-butadiene rubber and epichlorohydrin versus aliphatic alcohols (C1-C5)", *Polymer*, **34**(5), 1006-1018 (1993).

Aminabhavi, T. M. & Phayde, H. T. S., "Sorption, Desorption, Diffusion and Permeation of Aliphatic Alkanes into Santoprene Thermoplastic Rubber", *J. Applied Polymer Science*, **55**, 17-37 (1995).

Barton, A. F. M.: "CRC Handbook of Solubility Parameters and other Cohesion Parameters" 2nd Edition, CRC Press (1991)

Bartowiak, W and Lipinski, J: "Conformation and Solvent Dependence of the first Molecular Hyperpolarizability of Pyridinium-N-Phenoxide Betaine Dyes. Quantum Chemical Calculations", *J. Phys. Chem. A*, **102**, 5236-5240 (1998).

Bhanushali, D., Bhattacharyya, D, Kloos S. D. and Kurth, C. J. "Performance of solvent-resistant membranes for non-aqueous systems: Solvent permeation results and modeling", *J. Membrane Science*, **189**, 1-21 (2001)

Bhanushali, D., Bhattacharyya, D, Kloos S. D.: "Solute transport in solvent-resistant nanofiltration membranes for non-aqueous systems: experimental results and the role of solute-solvent coupling", *J. Membrane Science*, **208 (1-2)**, 343-359 (2002)

Bhattacharyya, D; Jevtitch, M, Schrodt, J. T. and Fairweather, G.: "Prediction of Membrane Separation Characteristics by Pore Distribution Measurements and Surface Force-Pore Flow Model", C*hemical Engineering Communications*, **42**, 111-128 (1986)

Burghoff; H. G.; Lee, K. L. and Pusch, W.: "Characterization of Transport Across Cellulose Acetate Membrane in the Presence of Strong Solute-Membrane Interactions", *J. Applied Polymer Science*, **25**, 323-347 (1980).

Capelle, N.; Moulin, P.; Charbit, F. and Gallo, R.: "Purification of heterocyclic drug derivatives by nanofiltration", *J. Membrane Science*, **196**, 125-141 (2002)

Danner, R. P. & High, M. S.: "Handbook of Polymer Solution Thermodynamics", Design Institute For Physical property data, AIChE (1993).

Doig, S. D.; Boam, A. T.; Livingston, A. G. and Stuckey, D. C.: "Mass transfer of hydrophobic solutes in solvent swollen silicone rubber membranes", *J. Membrane Sci.*, **154**, 127-140 (1999).

Farnand, B. A.; Talbot, F. D. F.; Matsuura, T. & Sourirajan S.: "Reverse Osmosis Separations of Some Organic and Inorganic Solutes in Methanol Solutions using Cellulose Acetate Membranes", *Ind. Eng. Chem. Process Design and Development*, **22**, 179-187 (1983).

Favre, E; Clement, R; Nguyen, Q. T.; Schaetzel, P and Neel, J: "Sorption of Organic Solvents into Dense Silicone Membranes: Part 1- Validity and Limitations of Flory-Huggins and Related Theories", *J. Chemical Society Faraday Transactions,* **89** (24), 4339-4346 (1993a).

Favre, E; Clement, R; Nguyen, Q. T.; Schaetzel, P and Neel, J: "Sorption of Organic Solvents into Dense Silicone Membranes: Part 2- Development of a New Approach based on a Clustering Hypothesis for Associated Solvents", *J. Chemical Society Faraday Transactions*, **89** (24), 4347-4353 (1993b).

Fredenslund, A.; Jones, R. L. and Prausnitz, J. M.: "Group-Contribution Estimation of Activity Coefficients in Nonideal Liquid Mixtures", *AIChE Journal*, **21**, 1086, (1975).

Fredenslund, A.: "UNIFAC and Related Group-Contribution Models for Phase Equilibria", *Fluid Phase Equilibria*, **52**, 135-150 (1989)

Ghanadzadeh, A; Ghanadzdeh, H and Ghasmi, G.: "On the Molecular Structure and Aggregative Properties of Sudan Dyes in the Anisotropic Host", *J. Molecular Liquids,* **88**, 299-308 (2000).

Gilron, J; Gara, N and Kedem, O: "Experimental Analysis of Negative Salt Rejection in Nanofiltration Membranes", *J. Membrane Science*, **185**, 223-236 (2001)

Gould, R. M.; White S. L. and Wildemuth, C. R.: "Membrane Separation in Solvent Lube Dewaxing", *Environmental Progress*, **20** (1), 12-16 (2001)

Gundert, F. & Wolf, B. A.: "Polymer-Solvent Interaction Parameters", *Polymer Handbook*, 3rd edition (1991).

Hance, D. E.: Masters' Thesis, Department of Chemical and Materials Engineering, University of Kentucky, Lexington (1987)

Harogoppad, S. B. and Aminabhavi, T. M.: “Diffusion and Sorption of Organic Liquids through Polymer Membranes. II. Neoprene, SBR, EPDM, NBR, and Natural Rubber versus n-Alkanes”, *J. Appl. Pol. Sci.*, **42**, 2329-2336 (1991).

Hauser, J; Heintz, A.; Schmittecker, B. and Lichtenthaler, R. N.: "Sorption Equilibria and Diffusion in Polymeric Membranes", *Fluid Phase Equilibria*, **51**, 369-381 (1989)

Heintz, A. and Stephan, W.: “A Generalized Solution-Diffusion Model of the Pervaporaiton Process through Composite Membranes. Part I. Prediction of Mixture Solubilitites in the Dense Active Layer using the UNIQUAC Model”, *J. Membrane Sci.*, **89**, 143 (1994).

Iwama, A. and Kazuse, Y.: “New Polyimide Ultrafiltration Membrane for Organic Use”, *J. Membrane Science*, **11**, 297-309 (1982)

Jagur-Grodzinski, J. and Kedem, O.: “Transport Coefficients and salt rejection in hyperfiltration membranes”, *Desalination*, **1**, 327 (1966)

Kale, V.; Katikaneni, S. P. R. & Cheryan, M., “Deacidifying Rice Bran Oil by Solvent Extraction and Membrane Technology”, *J. Am. Oil Chemists' Soc.*, **76**, 723-727 (1999)

Kataoka, T.; Tsuru, T.; Nakao, S.-I. And Kimura, S.: “Permeation Equations Developed for Prediction of Membrane Performance in Pervaporation, Vapor Permeation and Reverse Osmosis Based on the Solution-Diffusion Model”, *J. Chem. Eng. Japan.*, **24 (3)**, 326-333 (1991)

Kedem, O. and Katchalsky, A.: “Thermodynamic Analysis of the Permeability of Biological Membranes to Non-Electrolytes”, *Biochim. Biophys. Acta*, **27**, 229 (1958).

Kim, J. Y.; Lee, H. K., Baik, K. J. & Kim, S. C.: “Liquid-Liquid Phase Separation in Polysulfone/ Solvent/ Water Systems”, *J. Applied Polymer Science*, **65**, 2643-2653 (1997)

Koops, G. H.; Yamada, S. and Nakao, S. –I.: “Separation of Linear hydrocarbons and carboxylic acids from ethanol and hexane solutions by reverse osmosis”, *J. Membrane Science*, **189**, 241-254 (2001)

Kopecek, J. and Sourirajan, S., “Performance of Porous Cellulose Acetate Membranes for the Reverse Osmosis Separation of Mixtures of Organic Liquids”, *Ind. Eng. Chem. Process Design And Development*, **9**(1), 5-12 (1970).

Koseoglu, S. S.; Lawhon, J. T. & Lusas, E. W., “Membrane Processing of Crude Vegetable Oils: Pilot Plant Scale Removal of Solvent from Oil Miscellas”, *J. Am. Oil Chemists’ Society*, **67**, 315-322 (1990).

Kwok, D. Y. and Neumann, A. W.: “Contact angle measurement and contact angle interpretation”, *Advances in Colloid and Interface Science*, **81**, 167-249 (1999).

Laatikainen, M. and Lindstrom, M.: "Measurement of Sorption in Polymer Membranes with a Quartz Microbalance", *J Membrane Science*, **29** (2), 127-141 (1986)

Lonsdale, H.; Merten, U. and Riley, R.: “Transport of Cellulose Acetate Osmotic Membranes”, *J. Applied Polymer Science*, **9**, 1341 (1965).

Luthra, S. S.; Yang, X.; Freitas dos Santos, L. M.; White, L. S. and Livingston, A. G.: “Phase-transfer catalyst separation and re-use by solvent resistant nanofiltration membranes”, *Chem. Commun*., **(16)**, 1468 - 1469 (2001)

Machado, D. R.; Hasson, D & Semiat, R.: “Effect of Solvent Properties on Permeate flow through nanofiltration membranes. Part 1:investigation of parameters affecting solvent flux”, *J. Membrane Science*, **163**, 93-102 (1999a)

Machado, D. R.; Hasson, D & Semiat, R.: “Effect of solvent properties on permeate flow through nanofiltration membranes Part II. Transport model”, *J. Membrane Science*, **166**, 63-69 (1999b)

Matsuura, T. & Sourirajan S.: “Reverse Osmosis Separation of Phenols in aqueous solutions using porous cellulose acetate membranes”, *J. Applied Polymer Science*, **16**, 2531-2554 (1972).

Matsuura, T. & Sourirajan S.: “Reverse Osmosis Separations of Hydrocarbons in aqueous solutions using porous cellulose acetate membranes”, *J. Applied Polymer Science*, **17**, 3683-3708 (1973).

Matsuura, T.; Blais, P; Dickson, J. M.; & Sourirajan S.: “Reverse Osmosis Separations for some alcohols and phenols in aqueous solutions using Aromatic Polyamide Membranes”, *J. Applied Polymer Science*, **18**, 3671-3684 (1974).

Mehdizadeh, H. and Dickson, J. M.: “Evaluation of Surface Force-Pore Flow Model and Modified Surface Force-Pore Flow Models for Reverse Osmosis Transport”, C*hemical Engineering Communications. Membrane Science*, **103**, 65-82 (1991)

Mehdizadeh, H. and Dickson, J. M.: “Modeling of Reverse Osmosis in the Presence of Strong Solute-Membrane Affinity”, *AIChE J*., **39** (3), 434-445, (1993)

Mulder, M. H. V. and Smolders, C. A., “On the mechanism of separation of ethanol/water mixtures by pervaporation. I. Calculations of concentration profiles”, *J. Membrane Science*, **17**(3), 289-307 (1984)

Mulder, M. H. V.; Franken, A. C. M. and Smolders, C. A., "On the mechanism of separation of ethanol/water mixtures by pervaporation. I. Experimental concentration profiles", *J. Membrane Science*, **23**, 42-58 (1985)

Mulder, M.: Basic Principles of Membrane Technology, Kluwer Academic Publishers, 2nd ed. 1997.

Nair, D; Scarpello, J. T.; White, L. S.; Freitas dos Santos, L.; Vankelecom, I. F. J. and Livingston, A. G.: "Semi-continuous nanofiltration-coupled Heck Reactions as a new approach to improve productivity of homogeneous catalysts", *Tetrahedron Letters*, **42**, 8219-8222 (2001)

Nguyen, Q. T.; Favre, E.; Ping, Z. H. and Neel, J: "Clustering of solvents in membranes and its influence on membrane transport properties", J. Membrane Science, **113**, 137-150 (1996).

Niwa, Masahiro; Ohya, Haruhiko; Kuwahara, E. and Negihshi, Youichi: "Reverse Osmosis concentration of aqueous 2-butanone (MEK), THF and ethyl acetate solutions", *J. Chemical Engineering of Japan*, **21** (2), 164 (1988).

Paul, D. R. & Ebra-Lima, O. M., "The Mechanism of Liquid Transport Through Highly Swollen Polymeric Membranes", *J. Applied Polymer Science*, **15**, 2199-2210 (1970).

Paul, D. R. & Paciotti, J. D., "Driving Force for Hydraulic and Pervaporative Transport in Homogeneous Membranes", *J. Polymer Science*, **13**, 1201-1214 (1975a).

Paul, D. R.; Paciotti, J. D. & Ebra-Lima, O. M., "Hydraulic Permeation of Liquids Through Swollen Polymeric Networks", *J. Applied Polymer Science*, **19**, 1837-1845 (1975b).

Paul, D. R., "The Solution-Diffusion Model for Swollen Membranes", *Separation and Purification Methods*, **5**(1), 33-50 (1976a).

Paul, D. R.; Garcin, M. and Garmon, W. E.: "Solute Diffusion Through Swollen Polymer Membranes", *J. Applied Polymer Science*, **20**, 609-625 (1976b).

Poling, B. E.; Prausnitz, J. M. and O'Connell, J. P.: "The Properties of Gases and Liquids", 5th Edition, McGraw Hill, (2001).

Radovanovic, P.; Theil, S. & Hwang, S.: "Formation of asymmetric polysulfone membranes by immersion precipitation. Part1. Modelling mass transport during gelation", *J. Membrane Science*, **65**, 213-229 (1992)

Raman, L. P.; Cheryan, M. & Rajagopalan, N, "Deacidification of soybean oil by membrane technology", *J. Am. Oil Chemists' Soc.*, **73**, 219-224 (1996a)

Raman, L. P.; Cheryan, M. & Rajagopalan, N, "Solvent Recovery and Partial Deacidification of Vegetable Oils by Membrane Technology", *Lipid*, **98**, 10, (1996b)

Reddy, K. K.; Kawakatsu, T; Snape, J. B. and Nakajima, M.: "Membrane Concentration and Separation of L-Aspartic Acid and L-Phenylalanine Derivatives in Organic Solvents", *Separation Science and Technology*, **31**, 1161-1178 (1996).

Sanopolou, M. and Petropolous, J. H.: "Sorption and longitudinal kinetic behavior in the system cellulose acetate-methanol", *Polymer*, **38** (23), 5761-5768 (1997).

Schmidt, M; Mirza, S; Schunert, R; Rodicker, H; Kattanek, S & Malisz, J., "Nanofiltration Membranes for Separation Problems in Organic Solutions", *Chemie Ingenieur Technik*, **71**, 199 (1998).

Shah, D. S: Ph.D Dissertation, Department of Chemical and Materials Engineering, University of Kentucky, Lexington (2001)

Sherwood, T.; Brian, P. and Fisher, R.: "Desalination by Reverse Osmosis", *Ind. & Eng. Chem. Fundamentals*, **6**, 2 (1967).

Sirkar, K. S. and Ho, W. S.: "Membrane Handbook", Chapman & Hall, 1993.

Smet, K. D.; Aerts, S.; Ceulemans, E.; Vankelecom, I. F. J. and Jacobs, P. A.: "Nanofiltration-coupled catalysis to combine the advantages of homogeneous and heterogeneous catalysis", *Chem. Commun.*, **(7)**, 597 - 598 (2001)

Smith, J. M. and Van Ness, H. C.: "Introduction to Chemical Engineering Thermodynamics", 4th Edition, McGraw Hill, (1987)

Soltanieh, M. and Gill, W.: "Review of Reverse Osmosis Membranes and Transport Models", *Chemical engineering Communications*, **12**, 279 (1981).

Sourirajan, S.: "Separation of Hydrocarbon Liquids by Flow under Pressure through Porous Membranes", *Nature*, **203**, 1348-1349 (1964).

Sourirajan, S. and Matsuura, T.: "Reverse Osmosis/Ultrafiltration Principles", National Research Council of Canada, Ottawa, Canada (1985).

Surana, R. K.; Danner, R. P. & Duda, J. L.: "Diffusion and Equilibrium Measurements in Ternary Polymer-Solvent-Solvent Systems Using Inverse Gas Chromatography", *Ind. & Eng. Chem. Res.*, **37**, 3203-3207 (1998).

Tester, J. W. and Modell, M.: "Thermodynamics and Its Applications", 3rd Edition, Prentice Hall (1996)

Unnikrishnan, G. and Thomas, S.: "Sorption and Diffusion of Aliphatic Hydrocarbons into Crosslinked Natural Rubber", *J. Polymer Science B: Polymer Physics*, **35**, 725-734 (1997)

Viswanath, D. S. and Natarajan, G.: "Data Book on the Viscosity of Liquids", Hemisphere Publishing Corporation (1989).

Wang, D.; Li, K; Sourirajan, S & Teo, W. K.: "Phase-Separation Phenomena of Polysulfone/Solvent/Organic Non-Solvent and polyethersulfone/ solvent/ Organci Nonsolvent Systems", *J. Applied Polymer Science*, **50**, 1693-1700 (1993)

White, S. L. and Nitsch, A. R.: "Solvent Recovery from lube oil filtrates with a polyimide membrane", *J. Membrane Science*, **179**, 267-274 (2000)

Whu, J. A.; Baltzis, B. C. & Sirkar, K. K.: "Modeling of nanofiltration - assisted organic synthesis", *J. Membrane Science*, **163**, 319-331 (1999)

Whu, J. A.; Baltzis, B. C. & Sirkar, K. K.: "Nanofiltration studies of larger organic microsolutes in methanol solutions", *J. Membrane Science*, **170**, 159-172 (2000)

Wijmans, J. G. and Baker, R. W.: "The Solution-Diffusion Model: a review", *J. Membrane Science*, **107**, 1-21 (1995).

Will, B and Lichtenthaler, R. N.: "Comparison of the separation of mixtures by vapor permeation and by pervaporation using PVA composite membranes. I. Binary alcohol-water systems" *J. Membrane Science*, **68**, 119-125 (1992)

Yang, X. J.; Livingston, A. G. and Freitas dos Santos, L.: "Experimental Observations of nanofiltration with organic solvents", *J. Membrane Science*, **190**, 45-55 (2001)

Yang, H; Nguyen, Q. T.; Ding, Y; Long, Y. and Ping Z: "Investigation of poly(dimethyl siloxane) (PDMS)-solvent interactions by DSC", *J. Membrane Science*, **164**, 37-43 (2000)

Zwijnenberg, H. J.; Krosse, A. M.; Ebert, K.; Peinemann, K. –V. and Cuperus, F. P.: "Acetone-stable Nanofiltration Membranes in Deacidifying Vegetable Oil", *J. American Oil Chemists Society*, **76** (1), 83-87 (1999)

VITA

Dharmesh S. Bhanushali was born on April 20th 1976 in Mumbai, India. He received his B.S. degree in Chemical Engineering in 1998 from University of Bombay, Department of Chemical Technology (U.D.C.T.), India. He joined the Ph.D. program at University of Kentucky in Fall 1998.

Dharmesh S. Bhanushali

Publications

1. Bhanushali, D., Bhattacharyya, D, Kloos S. D. and Kurth, C. J. "Performance of solvent-resistant membranes for non-aqueous systems: Solvent permeation results and modeling", *Journal of Membrane Science*, **189**, 1-21 (2001)

2. Bhanushali, D., Bhattacharyya, D, Kloos S. D.: "Solute transport in solvent-resistant nanofiltration membranes for non-aqueous systems: experimental results and the role of solute-solvent coupling", *J. Membrane Science*, **208 (1-2)**, 343-359 (2002)

3. Bhanushali, D. and Bhattacharyya, D.: "Advances in Solvent-Resistant Nanofiltration Membranes: Experimental Observations and Applications", Book Chapter for Advanced Membrane Technology, *Annals of the New York Academy of Sciences*, **(IN PRESS, 2002)**.

4. Bhanushali, D., Bhattacharyya, D and Kloos S. D., "Solvent Flux characterization for Reverse Osmosis and Nanofiltration Membranes", Proceedings on Membrane and Extraction Science and Technologies for Environmental Applications; AIChE Topical Conference, Mar. 5-9, Atlanta, (2000).